

**Faunal Change, Paleoecology, and Landscape History in the Middle Miocene Dove Spring Formation, California**

by

Fabian Cerón Hardy

A dissertation submitted in partial fulfillment  
of the requirements for the degree of  
Doctor of Philosophy  
(Earth and Environmental Sciences)  
in the University of Michigan  
2023

Doctoral Committee:

Professor Catherine Badgley, Chair  
Professor Daniel C. Fisher  
Professor John D. Kingston  
Associate Professor Naomi E. Levin  
Professor Nathan A. Niemi  
Dr. Xiaoming Wang, Natural History Museum of Los Angeles County

Fabian Cerón Hardy

hardyf@umich.edu

ORCID iD: 0000-0002-9000-7227

© Fabian Cerón Hardy 2023

## **Dedication**

To those who persevere.

## Acknowledgements

This work has been financially supported by funding from the Geological Society of America, the National Science Foundation, the University of Michigan Rackham Graduate School, and the University of Michigan Department of Earth and Environmental Sciences. In addition to my funding sources, there are countless people who contributed in innumerable ways to the completion of this dissertation. I will attempt to thank as many of them as possible here.

Catherine Badgley has been my advisor and mentor for the past five years. She has shared endless hours of her time in helping me develop as a researcher, writer, and person. She is a wellspring of knowledge who readily shares her experience and insight with those who listen. Her meticulous attention to detail and jubilant drive to push the boundaries of understanding has inspired so many others, and I am forever grateful that she provided me with the opportunity to join her lab as a student.

The members of my committee were selected not only for their expertise in their fields, but also their willingness to collaborate and explore the intersection of geology and ecology. The depth and breadth of their knowledge is extraordinary and is matched by their generosity. Each of them has helped me along the way and I greatly appreciate their guidance. Naomi Levin's boundless energy in tackling the complicated nature of isotopic datasets was always refreshing when I was scratching my head at  $\delta^{13}\text{C}$  charts. Nathan Niemi and his easygoing nature in both the field and the classroom always made conversations about the complexities of tectonics enjoyable. Meetings with John Kingston always felt like speaking with a friend, and his

perspective on faunal assemblages was invaluable. Dan Fisher was always happy to challenge assumptions and delve into the intricate details of any subject, and always in a positive way.

Xiaoming Wang was instrumental in developing this project, and supported me along the way in the museum, in the field, and in many discussions.

Thank you to all of my professors at the University of Michigan. Your mentorship and the examples you set are an inspiration for my own career. Classes, seminars, and all the other events were invaluable opportunities to learn from you and get to see the human side of academia. I would like to thank the staff of the University of Michigan Department of Earth and Environmental Sciences (EARTH): Anne Hudon continually encouraged me to apply for grad school year after year at GSA meetings, and she was an enormous source of support in navigating my first years in EARTH. Nico Spraggins was always ready to assist as I approached the deadline for my defense, and made sure my presentation was the best it could be. Chrissy Zigulis and Paula Frank both made office visits cheerful as well as productive. I also thank the University of Michigan Museum of Paleontology staff for their administrative support: Linda Garcia and Cindy Stauch both kept an eye on the grad students and helped us survive shattered 4<sup>th</sup>-floor window, fire shutters, and our potentially cursed new office space.

Thanks to my friends and colleagues in the Badgley Lab. Bian Wang, Katie Loughney, Mariah Schlis-Elias, Luke Weaver, Kaori Chambers, and Aurelia Allen were all supportive friends and a pleasure to work with. I must extend my gratitude to my field assistants: Mairin Balisi, Brandon Agcopra, Ethan van Valkenburg, Wes Johnston, and Isaiah Newbins, without whom far fewer sections would have been measured and months spent living in a tent in the desert would have been lonely. Өнөөдөр эзэн минь тэнгэр харахыг зөвшөөрөв.

My expeditions to the field were made possible in no small part thanks to the Bureau of Land Management, California State Parks. In particular I thank Jacqueline Boyster, Ranger Damion Laughlin, and Mark Faull of Red Rock Canyon State Park. Their site knowledge and eagerness to discuss anything related to the desert were greatly appreciated. Dave Whistler's storied career of work in the Dove Spring Formation and his generosity in sharing both his time and extensive field notes formed an enormous part of the foundation for this project – without which all of this would not have been possible.

Some of the best experiences I have had while studying here were actually in Wyoming at Camp Davis. I want to thank everyone involved: Thanks to my faculty mentors: Greg Dick, Drew Gronewald, Jena Johnson, Joel Blum, Don Zak, Julia Kelson, and Jen Cotton for sharing the experience and giving me the latitude to really develop my teaching style. Thank you to the camp staff, Chris Malvica and his always cheery disposition (Happy Birthday, Chris)! Thanks to Sarah Katz, a fellow house elf who became one of my best friends. Finally, thanks to the students – you are all the most important part of Camp Davis and I am proud of every one of you!

The past five years have been a whirlwind of learning and struggles. Throughout it all, my friends and colleagues in the EARTH and Paleo departments have helped me survive the ups and downs, and brought levity when it was needed the most. Sarah Katz, Zack Quirk, Rodrigo Figueroa, Rafa Rivero, Cecilia Howard, Meg Veitch, Ethan Shirley, Tariq Abdul Kareem, James Andrews, Lindsey DeHaan, Hadeel Saad, and Sanaa El-Sayed were fantastic friends and officemates. My grad school experience would not have been nearly as enjoyable without the office shenanigans, 12 days of meme-mas, D&D, trivia nights, random lunches and bar visits that you all were happy to accommodate! Thanks also to the Gang: Chris, and Kat.

There are some NARLEE folks who I would like to thank: Brian Yanites, Sam Hopkins, Joshua Samuels, Nora Loughlin, Amanda Peng, and June Grimes. I appreciate our discussions while adventuring in the Basin and Range and Kansas, and look forward to future collaborations!

I found Ann Arbor to be very different from my neon desert origins, but I was lucky to find new friends in my neighbors. Thank you to Mark, Dagmar, and Cooper Ford, Corinne, Tony, and Simba, Shae, Lauren, and Lily Valko, and Bob and Fawn for welcoming me and making this sometimes frozen wasteland feel like home. Clementine and Mojave Jones (Mojo for short), Juliet (3/4 of a cat), and Monty the horse have brought me joy and support as well.

To my family, you have been an endless source of support and comfort from day one. Al and Brenda Cerón, you've seen my journey through life and school, and even helped me move 2000 miles across the continent – thank you! Ashley Cerón and Nick, I'm so glad we stay in touch whenever we can. Connie, Diego, and Britni Cortes, thank you so much for making the time when I drop into town. Jim and Julie Hardy are always encouraging and a great sounding board for complicated thoughts. Jamie and Sean Joiner are always excited to hear about whatever new ideas I've had. My mom and dad (Yvonne and Bill Hardy) truly gave me the experiences and opportunities that circuitously led me to the discipline of paleontology. Thanks to camping trips and adventures in the wilds of Nevada, I am here today because of you.

To absent friends. Jillian Weiner. Jerry Smith. Mark Robbins. You are not forgotten.

My wife, Brianne Catlin, has been by my side through every part of this journey. Grad school encompasses a broad spectrum of emotions and experiences. I often found myself charged

with victory one day and fraught with catastrophe the next. Brianne's exuberant and joyful nature bring me genuine happiness and fulfillment on a daily basis. Her patience and fierce devotion to seeing things through are a constant inspiration to me. She is a firefly in the dark and a lighthouse on the tumultuous sea, the one I can always turn to for comfort, support, and a reminder that the shore was within sight. Wise men say only fools rush in, but I couldn't help falling in love with you. Thank you, thank you very much.

I cannot possibly name everyone who has been a part of this experience. This written document is truly the culmination of years of family, friendship, and camaraderie. The day has finally come where I can step beyond this work and continue a lifelong journey in the pursuit of knowledge, thanks to the communities who have embraced me.



## Table of Contents

Dedication.....	ii
Acknowledgements.....	iii
List of Figures.....	ix
List of Tables.....	xiii
Abstract.....	xiv
Chapter 1 Introduction.....	1
Chapter 2 Mammalian Faunal Change of the Miocene Dove Spring Formation, Mojave Region, in Relation to Tectonic History.....	15
Chapter 3 Stable Isotope Ecology of Miocene Ungulates in the Context of Tectonic History: Insights from the Dove Spring Formation, California, USA.....	63
Chapter 4 Facies Analysis of Depositional Environments at Multiple Scales in the Dove Spring Formation, Southern California.....	119
Chapter 5 Faunal Change and Paleoecology in the Context of Landscape History.....	170
Appendix Stratigraphic Sections of Highly Productive Fossil Localities in the Dove Spring Formation.....	179

## List of Figures

Figure 1.1: Location map of the El Paso Basin, illustrating fault boundaries. ....	14
Figure 2.1: Map of study location, centered on the El Paso Basin. ....	49
Figure 2.2: Stratigraphy of the Dove Spring Formation with updated correlations based on recalibrated radiometric dates. ....	50
Figure 2.3: Temporal distribution of large mammals from the Dove Spring Formation. ....	51
Figure 2.4: Patterns of fossil productivity and sediment accumulation in the Dove Spring Formation. ....	52
Figure 2.5: Standing richness of the Dove Spring Formation, excluding singletons ....	53
Figure 2.6: Taxonomic composition of large mammals in the Dove Spring Formation through time, including singletons. ....	54
Figure 2.7: Diversification of large mammals based on estimated residence times. ....	55
Figure 2.8: Sample-based rarefaction curves for 0.5-Myr time intervals within the Dove Spring Formation. ....	56
Figure 3.1: Composite stratigraphic column for the Dove Spring Formation showing stratigraphic position of samples. ....	99
Figure 3.2: $\delta^{13}\text{C}$ values for tooth enamel in the Dove Spring Formation. ....	100
Figure 3.3: $\delta^{18}\text{O}$ values for ungulates in the Dove Spring Formation ....	101
Figure 3.4: $\delta^{13}\text{C}$ results for three ungulate families in the Dove Spring Formation. ....	102
Figure 3.5: $\delta^{18}\text{O}$ values for ungulate families from the Dove Spring Formation. ....	103
Figure 3.6 Linear measurements of ungulate teeth. ....	104
Figure 3.7: Equid $\delta^{18}\text{O}$ values from the Dove Spring Formation and other regions ....	105
Figure 3.8: Comparison of terrestrial Dove Spring Formation whole assemblage tooth enamel isotopic record with the marine Monterey Formation. ....	106

Figure 3.9: Box and whisker plots illustrating $\delta^{13}\text{C}$ values of individual lineages within the Antilocapridae. ....	107
Figure 3.10: Box and whisker plots illustrating $\delta^{13}\text{C}$ values of individual genera within the Equidae. ....	108
Figure 4.1: Location map of the Dove Spring Formation. ....	148
Figure 4.2: Composite lithostratigraphy of the Dove Spring Formation with dominant macrofacies associations for each member. ....	149
Figure 4.3: Fence diagram illustrating correlations of macrofacies associations throughout meter-scale stratigraphic sections. ....	150
Figure 4.4: Representative stratigraphic columns for each microfacies association. ....	151
Figure 4.5: Correlation of microstratigraphic sections illustrating landscape heterogeneity and fossil horizons within each microfacies sequence. ....	152
Appendix Figure 1: Key to symbols used to denote sedimentary structures and other features within stratigraphic sections. ....	180
Appendix Figure 2: Section 21.01 .....	181
Appendix Figure 3: Section 21.02 .....	182
Appendix Figure 4: Section 21.03 .....	183
Appendix Figure 5: Section 21.04 .....	184
Appendix Figure 6: Section: 21.05 .....	185
Appendix Figure 7: Section 21.06 .....	186
Appendix Figure 8: Section 22.01 .....	187
Appendix Figure 9: Section 22.02 .....	188
Appendix Figure 10: Section 22.03 .....	189
Appendix Figure 11: Section 22.04 .....	190
Appendix Figure 12: Section 22.05 .....	191
Appendix Figure 13: Section 22.06 .....	192
Appendix Figure 14: Section 22.07 .....	193

Appendix Figure 15: Section 22.08 .....	194
Appendix Figure 16: Section 22.09a .....	195
Appendix Figure 17: Section 22.09b .....	196
Appendix Figure 18: Section 22.10 .....	197
Appendix Figure 19: Section 22.11 .....	198
Appendix Figure 20: Section 22.12 .....	199
Appendix Figure 21: Section 22.13 .....	200
Appendix Figure 22: Section 22.14 .....	201
Appendix Figure 23: Section 22.15 .....	202
Appendix Figure 24: Section 22.16 .....	203
Appendix Figure 25: Section 22.17 .....	204
Appendix Figure 26: Section 22.18 .....	205
Appendix Figure 27: Section 22.19 .....	206
Appendix Figure 28: Section 22.20 .....	207
Appendix Figure 29: Section 22.21 .....	208
Appendix Figure 30: Section 22.22 .....	209
Appendix Figure 31: Section 22.33 .....	210
Appendix Figure 32: Section 22.24 .....	211
Appendix Figure 33: Section 22.25 .....	212
Appendix Figure 34: Section 22.26 .....	213
Appendix Figure 35: Section 22.27 .....	214
Appendix Figure 36: Section 22.28 .....	215
Appendix Figure 37: Section 22.29 .....	216
Appendix Figure 38: Section 22.30 .....	217
Appendix Figure 39: Section 22.31 .....	218

Appendix Figure 40: Section 22.32 .....	219
Appendix Figure 41: Section 22.33 .....	220
Appendix Figure 42: Section 22.34 .....	221
Appendix Figure 43: Section 22.35 .....	222
Appendix Figure 44: Section 22.36 .....	223
Appendix Figure 45: Section 22.37 .....	224
Appendix Figure 46: Section 22.38 .....	225
Appendix Figure 47: Section 22.39 .....	226

## List of Tables

Table 2.1: Large mammals of the Dove Spring Formation with observed and estimated first and last occurrences. ....	57
Table 2.2: Radiometric dates of prominent and laterally continuous ash layers within the Dove Spring Formation. ....	60
Table 2.3: Taxon names corresponding to numbers in Figure 2.3. ....	61
Table 3.1: Whole-assemblage enamel $\delta^{13}\text{C}$ and $\delta^{18}\text{O}$ values in the Dove Spring Formation. ....	109
Table 3.2: Tooth enamel bulk samples with $\delta^{13}\text{C}$ and $\delta^{18}\text{O}$ values collected by Hardy (this study) .....	110
Table 3.3: Tooth enamel bulk samples with $\delta^{13}\text{C}$ values collected and measured by Bowman et al. (2017). ....	114
Table 3.4: Published equid tooth enamel $\delta^{18}\text{O}$ values shown in Figure 3.7. ....	116
Table 4.1: Highly productive fossil localities of the Dove Spring Formation. ....	153
Table 4.2: Descriptions of facies within each macrofacies association (FA). ....	155
Table 4.3: Descriptions of facies within each high-resolution microfacies association (FA). ...	156
Table 4.4: Distribution of fossil localities and specimens within macrofacies sequences .....	157
Table 4.5: Distribution of fossil localities and specimens among microfacies associations .....	158
Table 4.6: Comparison of bone elements recovered from 10.2 Ma lateral transect .....	159
Table 4.7: List of localities and specimens from NHM database for 10.2 Ma lateral section correlation in Table 4.6. ....	160

## **Abstract**

The evolution and distribution of mammals have been influenced throughout earth history by tectonic processes that produce regions with varied topography and environmental gradients. Biological responses to these factors are recorded in the fossil record, but the same processes that generate suitable life habitats affect the fossil productivity of depositional environments, confounding interpretations. The goal of this dissertation is to investigate fossil assemblages of terrestrial mammals and determine whether faunal change is influenced by tectonic history. This work has focused on the fossil and geohistorical record of a continental basin at the western edge of the Basin and Range, USA.

The Miocene Dove Spring Formation (12.5–8.5 Ma) has a rich vertebrate fossil record and 1800 m of sediments that hold evidence for three major tectonic episodes. Two phases of extension and a period of shearing are documented through structural and sedimentological evidence. I compiled data from museum specimens, topographic maps, and field notes from the past 60 years. Using this foundation, I integrated field work, geographic information system analysis, and stable isotope analyses to investigate the interactions between tectonic processes and changes in the species richness and faunal composition of mammal assemblages.

I updated radiometric decay constants and incorporated a recent tephrochronological correlation to revise the geochronology of the Dove Spring Formation and provide context for the spatial and stratigraphic distribution of fossil localities. I conducted a diversification analysis for large mammals to estimate residence times and account for the incomplete nature of fossil preservation. Originations were prevalent early in the sequence, during an extensional tectonic

episode. Extinction became the dominant process later, coinciding with the onset of shear tectonic movement. Significant changes in faunal composition correlated with these tectonic episodes. With a connection between tectonics and faunal change established, I conducted additional investigations to determine whether apparent faunal change was driven by the productivity of different lithofacies or was the result of ecological change.

I sampled tooth enamel from three ungulate families (Antilocapridae, Camelidae, and Equidae) for stable isotopes of carbon and oxygen to describe their dietary ecology. The  $\delta^{13}\text{C}$  values indicate that the plant resources consumed by these ungulates remained relatively stable through the formation despite changes in the tectonic setting. The  $\delta^{18}\text{O}$  record exhibits a similar trend to a regional signal, suggesting that conditions in the basin became gradually more arid over time, with little correlation with the tectonic history. The Dove Spring Formation represents an environment that persisted for four million years and has no close modern analogue. Changes in dietary ecology were not the primary drivers of faunal change.

I documented lithofacies associations and inferred depositional environments at two scales. At the basin-scale, large channels are associated with episodes of extension, while floodplains developed during the shear episode. I detected variability across the landscape at the locality scale, recognizing two types of channels, three types of floodplains, pond deposits, and crevasse splays. Changes in depositional environments over time correlate well with the basin's tectonic history, and the shear episode exhibited the highest fossil productivity. However, the area of these environments was not a strong predictor of fossil productivity. The presence of chronically rare taxa, such as carnivores during poorly-sampled intervals indicates that not all faunal change can be attributed to sampling. Investigations of regional patterns are necessary to further our understanding of this phenomenon.



## **Chapter 1**

### **Introduction**

Landscape evolution and climate have high level effects on terrestrial ecosystems. Tectonically driven changes in topography influence the distribution and connectivity of basin habitats, while also affecting the regional and local climates experienced by organisms. The generation of topographically complex landscapes throughout geologic time has had measurable effects on species diversity and its preservation within the fossil record (Badgley et al., 2017). The goal of my dissertation is to investigate potential correlations between mammalian faunal change and periods of tectonic activity by leveraging the rich fossil record and robust geochronology of the Miocene Dove Spring Formation. To accomplish this goal, I employed a suite of methods including analysis of faunal change and diversity dynamics, stable isotope paleoecology, and facies analysis in relation to episodes of tectonic history. My results provide new insight into the complex and often subtle relationships between tectonic processes and the faunal history of a terrestrial basin.

The Miocene is notable for significant environmental change that affected terrestrial ecosystems from the global to local scales. The Middle Miocene Climatic Optimum (MMCO; 16.9-14.7 Ma) was a period of high global temperatures and increasing diversity of terrestrial mammals in North America (Janis et al., 2000; Zachos et al., 2001; Steinthorsdottir et al., 2021). This species-rich interval was followed by the Middle Miocene Climatic Transition (MMCT; 14.7-13.8 Ma), an interval of global cooling that continues today (Steinthorsdottir et al., 2021).

Global climate is modulated at the regional and local scales by elevation and topographic relief driven by tectonic processes such as extension and subsidence (Chamberlain et al., 2012).

The Basin and Range province of western North America underwent significant extension leading to the collapse of major topographic highlands during the Miocene, generating regions with complex topography that significantly influenced the distribution of species (McQuarrie and Wernicke, 2005; Bahadori et al., 2018).

Tectonically driven changes in topography generate climatic and vegetation gradients, open or close corridors to dispersal, and alter habitat space (Körner, 2000; Coblenz and Riitters, 2004; Badgley, 2010). By altering habitat gradients, topographic changes allow for the expansion or contraction of geographic ranges, leading to changes in species richness and faunal composition (Barnosky and Kraatz, 2007; Kent-Corson et al., 2013). Habitats for terrestrial mammals may be connected or interrupted by topographic barriers that develop as the result of tectonic processes, which may lead to the evolution or extinction of species. This last scenario relies on data from the fossil record and investigations of faunal changes that coincide with or closely follow the onset of major tectonic episodes. These principles form the basis for my investigations of faunal change within a terrestrial basin.

Topographically complex regions today host higher species diversity than adjacent lowlands due to the generation of barriers and environmental gradients of climate and vegetation (Badgley et al., 2017). This pattern is seen at the regional scale between the Basin and Range Province when compared to the Great Plains region (Badgley and Finarelli, 2013). Mammals respond to changes in climate and vegetation structure with geographic-range shifts, changes in dietary ecology, body size, and locomotion (Janis, 1993; Davies et al., 2009; Stromberg et al., 2013).

The El Paso Basin of the northwestern Mojave region in southern California records evidence for several well-constrained tectonic episodes. The basin is bounded on two sides by faults and exhibits evidence for both extensional and shear movement (Figure 1.1). Three distinct tectonic episodes are relevant to the Miocene history of faunal change in this location (Loomis and Burbank, 1988). Extension that began between 17.0 and 15.0 Ma contributed to area growth in the basin until it was interrupted around 10.3 Ma by a period of basin rotation and translation along the Garlock Fault to the south. Extension resumed between 9.5 and 9.0 Ma, indicating a new period of basin growth.

The Dove Spring Formation is the middle to late Miocene component of sedimentary fill within the El Paso Basin and contains a rich fossil record. A sequence of 1800 meters of alluvial and lacustrine sediments was deposited between 12.5 and 8.5 Ma, and has yielded over 7,200 vertebrate fossils from more than 750 localities (Whistler et al., 2009). The formation's tectonic history and fossil record have been studied since the early 1900s by geologists and paleontologists, yielding detailed records of stratigraphy and fossil-mammal assemblages (Merriam, 1919; Dibblee, 1952; Loomis and Burbank, 1988; Whistler et al., 2009). Over 100 mammalian species are present in the Dove Spring Formation, and large mammals represent the majority of fossil specimens recovered. Four orders and 15 families of large mammals contain 59 taxa identified to the genus level and 20 are further identified to the species level (Whistler et al., 2009). A series of 18 radiometrically dated ash layers, tephrochronologic correlation, and magnetostratigraphy provide age control on fossil localities. The extensive body of work conducted in the formation makes possible investigations into the timing of tectonically driven landscape changes and patterns of species diversity, faunal composition, and dietary ecology.

In Chapter 2, I present a geochronological framework that establishes the timing of faunal change in the Dove Spring Formation. I first revised the stratigraphy and geochronology to establish a robust chronostratigraphic framework. This involved fieldwork to measure new stratigraphic sections and recalculating published radiometric dates using updated decay constants. I calculated sediment accumulation rates to track changes in accommodation space. I determined the stratigraphic placement of fossil localities within the context of the magnetostratigraphic record, older and newly measured stratigraphic sections, and ash beds with known radiometric dates. For my analysis of faunal change, I focused on large mammals because they are the most abundant component of the fossil assemblages in terms of both specimens recovered and species richness. Large-mammal fossils are also collected in a different way than small mammals, resulting in different taphonomic biases for each size group. I generated a new biochronology of the estimated residence time for large mammals using 80% confidence intervals based on the observed fossil record and the average temporal gap between species occurrences (Marshall, 1990, 2010). I used this biochronology to evaluate change in faunal composition and assessed per-capita rates of origination, extinction, and diversification using methods of Foote (2000).

My findings revealed insight into the patterns of faunal change in the Dove Spring Formation as they relate to its tectonic history. Two phases of faunal change occur through the sequence: early extension is associated with originations, species accumulation and long residence times; basin rotation and translation are associated with a shift towards extinction or extirpation as the dominant process of faunal change. The presence of chronically rare taxa such as carnivores during intervals with low fossil productivity provides compelling evidence for the

authenticity of the signals of faunal change within the formation, despite indications of a strong sampling effect.

Two hypotheses arose from my findings in Chapter 2: either that actual faunal change is linked to the basin's tectonic history through ecological changes, or that apparent faunal change is the result of variations in the fossil productivity of sedimentary facies. There are additional possibilities, such as geographic-range shifts caused by the opening or closing of dispersal corridors, but these require regional data and are beyond the scope of this investigation. In the first scenario, the expectation would be to observe significant changes in dietary ecology that relate to changes in vegetation coinciding with episodes of tectonic activity. In the second scenario, changes in fossil productivity would occur without significant ecological change, and community composition would remain relatively stable throughout the sequence. These hypotheses formed the basis for my subsequent chapters.

In Chapter 3, I address the hypothesis that tectonic episodes contributed to environmental change in the Dove Spring Formation by investigating the dietary paleoecology of selected mammals using stable isotopes of carbon and oxygen. My goal was to determine whether significant change in herbivore diets occurred, and if present, whether it was related to the tectonic and climatic history of the El Paso Basin. I sampled tooth enamel from three ungulate families (Antilocapridae, Camelidae, and Equidae) for stable isotope analysis of carbon and oxygen. The ratio of carbon-13 to carbon-12 ( $\delta^{13}\text{C}$ ) is used to determine the carbon pathway of vegetation consumed by herbivores, and is in turn a reliable indicator of the composition of plant assemblages at the time of fossil deposition (Cerling and Harris, 1999). Oxygen-18 is an indicator of temperature and moisture availability that is affected by a variety of factors, including elevation, distance from the coast, temperature, and latitude (Dansgaard, 1964; Kohn,

1996). Due to the El Paso Basin's low-elevation, midlatitude location less than 200 km from the Pacific coast, the primary control on  $\delta^{18}\text{O}$  in the formation was probably the amount of precipitation. In addition to stable isotope analysis, I measured the hypsodonty index for the three ungulate families. This index is a measure of molar crown height compared to tooth width, which is informative of the ability of herbivores to consume abrasive material (Janis et al., 2000; Jardine et al., 2012). Higher hypsodonty indices have been traditionally interpreted to be a signal of open habitats where dust and grit wear down dentition (Madden, 2014).

I found that there were minor variations in the  $\delta^{13}\text{C}$  signature of large mammals, there were no significant changes in their dietary ecology through the Dove Spring Formation. Instead, the formation contains evidence for an ecosystem with vegetation assemblages that remained relatively stable for four million years. The combination of relatively depleted  $\delta^{13}\text{C}$  values with assemblages of large mammals that no longer exist today indicates that the environments of the Dove Spring Formation do not have exact modern analogues in terms of vegetation that supports such diverse communities of large mammals.  $\delta^{18}\text{O}$  values in the Dove Spring Formation did not vary significantly throughout its history, indicating that the amount of precipitation remained relatively constant. While slight variations in both  $\delta^{13}\text{C}$  and  $\delta^{18}\text{O}$  change from one tectonic episode to the next, changes in vegetation, temperature, and precipitation characteristics were not sufficient enough to be the main drivers of faunal change. In the absence of significant changes in dietary ecology, I rejected the hypothesis that faunal change was primarily a response to tectonically driven changes in vegetation.

In Chapter 4, I test the hypothesis that faunal change in the Dove Spring Formation is primarily related to fossil productivity that varies with changes over time in depositional environments. Heterogeneity across the landscape is driven in part by tectonic and climatic

processes that affect the transport of sediments, as well as autocyclic processes that influence the migration of channels across the floodbasin (Bridge, 2003). The depositional environments associated with evolving landscapes vary in their ability to preserve fossil remains of vertebrates due to differences in energy level, water availability, and sediment supply (Behrensmeier, 1988; Holland, 2016). Low-energy environments, such as floodplains, have a relatively high likelihood to preserve fossils, while high-energy environments, such as active river channels, point bars, and avulsion deposits may be less likely to preserve fossils due to reworking of sediments and erosion (Bridge, 2003; Holland, 2016). Depositional environments can be inferred based on facies characteristics, which are patterns of lithology, sedimentary structures, and stratigraphic relationships that form under specific hydrological and sedimentological conditions (Reading, 1986; Behrensmeier, 1987). My goals were to 1) determine the spatial and temporal extent of major facies associations; 2) evaluate facies changes in relation to the tectonic history of the El Paso Basin; 3) describe the dominant depositional environments of highly productive localities within the Dove Spring Formation; and 4) compare the history of faunal change to the configuration of facies associations.

To address these research topics, I measured stratigraphic sections to characterize lithological facies. Meter-scale sections allowed me to recognize macrofacies associations that occur in broad patterns throughout the entire formation while decimeter-scale sections revealed the depositional environments of fossil assemblages and variation across the landscape and allowed for comparison of fossil productivity between environments. The frequency and spatial extent of facies associations at both scales varied with the basin's tectonic history, leading to a series of inferred depositional environments with differences in fossil productivity.

Changes in the areal extent of macrofacies associations only partially influenced fossil productivity throughout the sequence. Channel and channel-margin macrofacies associations exhibit the greatest differences in fossil productivity in response to tectonically-driven changes in area. As the areal exposure of channel deposits decreased during basin rotation and translation near 10.3 Ma, channel margin deposits increased in area accompanied by a moderate increase in fossil localities. Conversely, localities per area containing large mammals were highest during the initial phase of extension, and dropped by approximately half with the onset of basin rotation. While floodplain deposits increased in area through the whole sequence, the highest numbers of localities per area are found during the shearing tectonic episode.

During a period of tectonic extension early in the sequence, large channels were common and species accumulation was the dominant process of faunal change. Around 10.3 Ma, extinction became the dominant process, coinciding with the increased prevalence of floodplain deposits and the onset of basin rotation and translation. Around 9.5 Ma, local extension resumed and generated more heterogeneous depositional environments that preserved more species despite a trend of extinction. While most fossil localities are found within fine-grained sediments in floodplain sequences, stream channels tend to aggregate specimens from more species. Rare taxa and singletons are most commonly recovered from floodplain deposits, indicating that floodplains have the potential to deliver a more complete view of species richness. My findings indicate that at least some of the faunal change captured in the fossil record is the result of changes in fossil productivity due to the evolution of the landscape. However, the presence of numerous rare taxa from facies associations that do not typically preserve a high number of specimens suggests that faunal changes are not solely the result of changes in depositional environment.



In Chapter 5, I synthesize the results of my studies into the faunal, paleoecological, and depositional history of the Dove Spring Formation. This section is organized into the context of the three major tectonic episodes that drove landscape evolution during the middle to late Miocene. The integration of these datasets builds upon a century of previous research and advances our understanding of the influence of tectonically driven environmental gradients on patterns of faunal change and paleoecology. By combining geological and paleontological information, I investigated the connections between the physical environment, local climate, vegetation, and the history of mammals within a terrestrial basin.

While the fossil record is incomplete by nature, thorough investigation of faunal patterns and stratigraphy reveal insight into factors that contribute to preservational and ecological processes. This work contributes new perspectives on how the dynamic tectonic setting of the El Paso Basin influenced the rich fossil record of the Dove Spring Formation. Extensional and shearing processes altered the distribution of life habitats and environments where mammal remains were likely to be preserved. However, changes in the area of dominant depositional environments were not strong predictors of fossil productivity or species richness. These results suggest that processes other than sampling controlled the observed patterns of faunal change. The Dove Spring Formation is also an example of post-MMCO environmental stability within a terrestrial basin. Despite tectonically-driven changes in the dominant depositional environment and water availability, mammalian communities did not significantly alter their dietary ecology.

These results indicate that other processes must have contributed to faunal change in the Dove Spring Formation. Topographic changes may have led to the expansion of dispersal corridors that allowed large mammals to travel throughout the region, with some populations remaining in the basin. Global or regional climate change may have driven mammals into the

basin due to its moderate local climate and abundant vegetation resources. Further investigations of these factors will require regional data to place the observed faunal patterns into context with the greater Basin and Range. This dissertation advances our understanding of local processes and provides context for future studies of the relationship between faunal change and landscape history.

## References

- Badgley, C., 2010, Tectonics, topography, and mammalian diversity: *Ecography*, v. 33, p. 220-231.
- Badgley, C., and Finarelli, J. A., 2013, Diversity dynamics of mammals in relation to tectonic and climatic history: comparison of three Neogene records from North America: *Paleobiology*, v. 39, no. 3, p. 373-399.
- Badgley, C., Smiley, T. M., Terry, R., Davis, E. B., DeSantis, L. R. G., Fox, D. L., Hopkins, S. S. B., Jezkova, T., Matocq, M. D., Matzke, N., McGuire, J. L., Mulch, A., Riddle, B. R., Roth, V. L., Samuels, J. X., Stromberg, C. A. E., and Yanites, B. J., 2017, Biodiversity and topographic complexity: Modern and geohistorical perspectives: *Trends in Ecology & Evolution*, v. 32, no. 3, p. 211-226.
- Bahadori, A., Holt, W. E., and Rasbury, E. T., 2018, Reconstruction modeling of crustal thickness of western North America since 36 Ma: *Geosphere*, v. 14, no. 3, p. 1207-1231.
- Barnosky, A. D., and Kraatz, B. P., 2007, The role of climatic change in the evolution of mammals: *BioScience*, v. 57, no. 6, p. 523-532.
- Behrensmeyer, A. K., 1987, Miocene fluvial facies and vertebrate taphonomy in northern Pakistan: *Recent Developments in Fluvial Sedimentology*, v. Society of Economic Paleontologists and Mineralogists Recent Developments in Fluvial Sedimentology, no. SP39, p. 169-176.
- , 1988, Vertebrate preservation in fluvial channels: *Palaeogeography, Palaeoclimatology, Palaeoecology*, v. 63, p. 183-199.
- Bridge, J. S., 2003, *Rivers and Floodplains*, Blackwell Science, 491 p.:
- Cerling, T. E., and Harris, J. M., 1999, Carbon isotope fractionation between diet and bioapatite in ungulate mammals and implications for ecological and paleoecological studies: *Oecologia*, v. 120, p. 347-363.
- Chamberlain, C. P., Mix, H. T., Mulch, A., Hren, M. T., Kent-Corson, M. L., Davis, S. J., Horton, T. W., and Graham, S. A., 2012, The Cenozoic climatic and topographic evolution of the western North American Cordillera: *American Journal of Science*, v. 312, p. 213-262.
- Coblentz, D. D., and Riitters, K. H., 2004, Topographic controls on the regional-scale biodiversity of the south-western USA: *Journal of Biogeography*, v. 31, p. 1125-1138.
- Dansgaard, W., 1964, Stable isotopes in precipitation: *Tellus*, v. 16, p. 436-468.
- Davies, T. J., Purvis, A., and Gittleman, John L., 2009, Quaternary Climate Change and the Geographic Ranges of Mammals: *The American Naturalist*, v. 174, no. 3, p. 297-307.
- Dibblee, T. W., 1952, *Geology of the Saltdale quadrangle, California*: State of California Department of Natural Resources Bulletin, v. 160, p. 7-44.

- Foote, M., 2000, Origination and extinction components of taxonomic diversity: general problems: *Paleobiology*, v. 26, p. 74-102.
- Holland, S. M., 2016, The non-uniformity of fossil preservation: *Philosophical Transactions of the Royal Society B: Biological Sciences*, v. 371, p. 11.
- Janis, C. M., 1993, Tertiary mammal evolution in the context of changing climates, vegetation, and tectonic events: *Annual Review of Ecology, Evolution, and Systematics*, v. 24, p. 467-500.
- Janis, C. M., Damuth, J., and Theodor, J. M., 2000, Miocene ungulates and terrestrial primary productivity: Where have all the browsers gone?: *Proceedings of the National Academy of Sciences of the United States of America*, v. 97, no. 14, p. 7899-7904.
- Jardine, P. E., Janis, C. M., Sahney, S., and Benton, M. J., 2012, Grit not grass: Concordant patterns of early origin of hypsodonty in Great Plains ungulates and Glires: *Palaeogeography, Palaeoclimatology, Palaeoecology*, v. 365-366, p. 1-10.
- Kent-Corson, M. L., Barnosky, A. D., Mulch, A., Carrasco, M. A., and Chamberlain, C. P., 2013, Possible regional tectonic controls on mammalian evolution in western North America: *Palaeogeography, Palaeoclimatology, Palaeoecology*, v. 387, p. 17-26.
- Kohn, M. J., 1996, Predicting animal  $\delta^{18}\text{O}$ : Accounting for diet and physiological adaptation: *Geochimica et Cosmochimica Acta*, v. 60, no. 23, p. 4811-4829.
- Körner, C., 2000, Why are there global gradients in species richness? Mountains might hold the answer: *Trends Ecol Evol*, v. 15, no. 12, p. 513-514.
- Loomis, D. P., and Burbank, D. W., 1988, The stratigraphic evolution of the El Paso basin, southern California: Implications for the Miocene development of the Garlock fault and uplift of the Sierra Nevada: *Geological Society of America Bulletin*, v. 100, p. 12-28.
- Madden, R. H., 2014, *Hypsodonty in mammals: Evolution, geomorphology, and the role of earth surface processes*, Cambridge University Press, 423 p.:
- Marshall, C. R., 1990, Confidence intervals on stratigraphic ranges: *Paleobiology*, v. 16, no. 1, p. 1-10.
- , 2010, Using confidence intervals to quantify the uncertainty in the end-points of stratigraphic ranges, *in* Alroy, J., and Hunt, G., eds., *The Paleontological Society Papers*, Volume 16, The Paleontological Society, p. 291-316.
- McQuarrie, N., and Wernicke, B. P., 2005, An animated tectonic reconstruction of southwestern North America since 36 Ma: *Geosphere*, v. 1, no. 3, p. 147-172.
- Merriam, J. C., 1919, *Tertiary mammalian faunas of the Mohave Desert*: University of California Publications. Department of Geology, Bulletin, v. 10, p. 111-127.
- Reading, H. G., 1986, Facies, *in* Reading, H. G., ed., *Sedimentary Environments and Facies*, Department of Earth Sciences University of Oxford, p. 4-19.
- Steinthorsdottir, M., Coxall, H. K., de Boer, A. M., Huber, M., Barbolini, N., Bradshaw, C. D., Burls, N. J., Feakins, S. J., Gasson, E., Henderiks, J., Holbourn, A. E., Kiel, S., Kohn, M.

- J., Knorr, G., Kürschner, W. M., Lear, C. H., Liebrand, D., Lunt, D. J., Mörs, T., Pearson, P. N., Pound, M. J., Stoll, H., and Strömberg, C. A. E., 2021, The Miocene: The Future of the Past: *Paleoceanography and Paleoclimatology*, v. 36, no. 4.
- Stromberg, C., Dunn, R., Madden, R. H., Kohn, M. J., and Carlini, A. A., 2013, Decoupling the spread of grasslands from the evolution of grazer-type herbivores in South America: *Nature Communications*, v. 4, no. 1478, p. 8.
- Whistler, D. P., Tedford, R. H., Takeuchi, G. T., Wang, X., Tseng, Z. J., and Perkins, M. E., 2009, Revised Miocene biostratigraphy and biochronology of the Dove Spring Formation, Mojave Desert, California: *Museum of Northern Arizona Bulletin*, v. 65, p. 331-362.
- Zachos, J., Pagani, M., Sloan, L., Thomas, E., and Billups, K., 2001, Trends, rhythms, and aberrations in global climate 65 Ma to Present: *Science*, v. 292, no. 5517, p. 686-693.

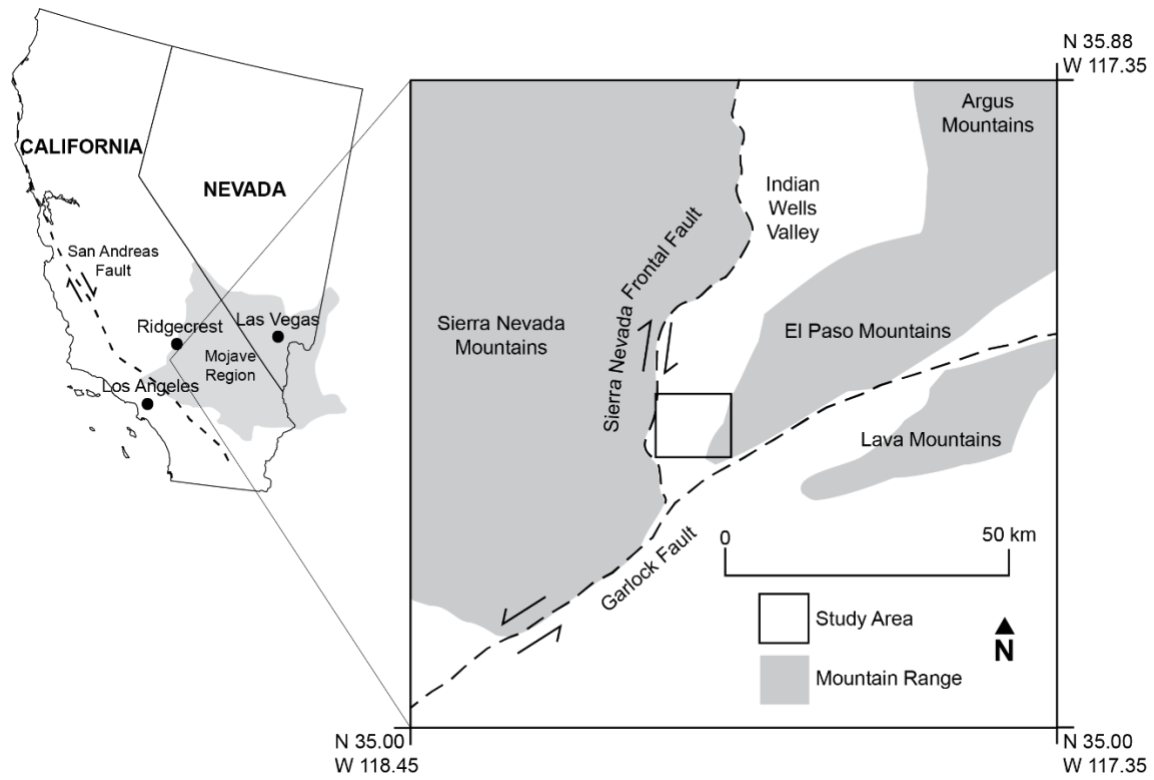


Figure 1.1: Location map of the El Paso Basin, illustrating fault boundaries.

## **Chapter 2**

# **Mammalian Faunal Change of the Miocene Dove Spring Formation, Mojave Region, in Relation to Tectonic History**

### **Abstract**

Tectonic processes drive the evolution of basins through local and regional changes in topographic relief, which has a long-term effect on mammalian richness and distribution. Mammals respond to the resulting changes in landscape and climate through evolution, geographic-range shifts, and by altering their community composition. Studies of these responses rely on the timing of faunal change in relation to changes in topography and climate (Badgley, 2010). Here we evaluate the relationship between tectonic episodes and the diversification history of fossil mammals in the Miocene Dove Spring Formation (12.5-8.5 Ma) of southern California. This formation contains a rich fossil record of mammals and other vertebrates as well as structural and sedimentological evidence for tectonic episodes of basin extension, rotation, and translation. We used several methods to compare the fossil record to the tectonic history of the formation. We updated the geochronology of the stratigraphic sequence to incorporate current radiometric dating standards and measured additional stratigraphic sections to refine the temporal resolution of the fossil localities to 500-kyr (or shorter) intervals. We compiled observed stratigraphic ranges of large mammals (>1 kg), number of fossil localities, and number of catalogued specimens in 500-kyr intervals. Observed species richness over time follows the same trend as the number of localities and specimens, suggesting a strong sampling influence. To acknowledge incomplete fossil preservation, we determined 80% confidence intervals for the

observed stratigraphic ranges of taxa. These estimates of stratigraphic ranges were used to conduct per-capita diversification analysis and a likelihood approach to changes in faunal composition from one time interval to the next. We found that significant changes in faunal composition occurred in three intervals (11.0, 10.0, and 9.5 Ma). The lower portion of the formation is characterized by high origination rates and long residence times until the initiation of basin rotation and westward translation at 10.5 Ma. The upper portion has high per-capita extinction rates that increase in magnitude with a period of basin extension and subsidence near 9.5 Ma. The greatest magnitude of change in faunal composition occurred during basin rotation and translation that interrupted a long-running extensional period. Sampling had only a moderate effect on these patterns, suggesting that tectonics played a key role in the diversity of mammals by shaping the landscapes that they inhabited.

## Introduction

Global changes in climate and regional tectonic episodes that altered elevation and topographic relief led to increased seasonality of temperature and precipitation, which contributed to the emergence and spread of novel biomes throughout western North America during the Middle to Late Miocene (Wing, 1998; Jacobs et al., 1999; Kohn and Fremd, 2008; Chamberlain et al., 2014; Steinthorsdottir et al., 2021). Mammals responded to the appearance of new types of vegetation with significant changes in feeding strategies, body size, and locomotion, forming faunal assemblages that have no modern analogues (Janis, 1993; Webb and Opdyke, 1995; Janis et al., 2000; Finarelli and Badgley, 2010; Samuels and Hopkins, 2017).



Local and regional tectonic processes have a direct influence on climatic gradients and resultant vegetation patterns relevant to animals, which may influence their evolution, distribution, and community composition (Beatley, 1975; Janis, 1993; Kohn and Fremd, 2008). When examined in conjunction with tectonic history, the fossil record can reveal the response of mammalian communities to these environmental influences. If faunal changes (such as changes in species richness, faunal composition, or rates of diversification) coincide with or closely follow tectonic episodes, it suggests a link between tectonically-driven landscape changes and terrestrial mammals. Ecological factors such as the changes in vegetation resources, competition and predation pressure, or character displacement may all be related to changes in topography that contribute to the development of habitat gradients or the expansion of dispersal corridors (Brown and Nicoletto, 1991; Janis, 2004; Maguire and Stigall, 2008). If such changes occur in the absence of tectonic activity, other processes such as global or regional climate change are more likely to be the driving factors.

Here we focus on the Middle to Late Miocene Dove Spring Formation (12.5-8.5 Ma), located in the El Paso Basin of the northwestern Mojave Region in southern California, USA (Figure 2.1). We investigated the links between tectonic history and mammalian species richness through geologic time with three goals: 1) To refine the stratigraphy and geochronology to serve as a temporal framework for evaluating faunal change in relation to tectonic episodes; 2) to identify changes in species richness and composition based on estimated residence time of large mammals; 3) to assess per-capita origination and extinction rates in relation to the timing of tectonic episodes. Our work is part of a broader effort to examine changes in landscape, climate, vegetation and mammalian diversity that are associated with tectonic processes occurring

throughout western North America (Finarelli and Badgley, 2010; Badgley and Finarelli, 2013; Badgley et al., 2017; Loughney and Badgley, 2020).

### **Paleontological Background**

The Dove Spring Formation is located in the El Paso Basin of southern California (35.373° N, 117.991° W). This formation spans Clarendonian (12.5-10.3 Ma) to early Hemphillian (10.3-8.5 Ma) North American Land Mammal Ages, intervals of geologic time characterized in part by decreasing species richness of ungulate taxa (Woodburne, 1987; Janis et al., 2000; Woodburne, 2004). The Dove Spring Formation has been well studied in terms of vertebrate paleontology, lithostratigraphy, tephrochronology, and tectonic setting (Merriam, 1919; Dibblee, 1967; Loomis and Burbank, 1988; Whistler and Burbank, 1992; Perkins et al., 1998; Wang and Barnes, 2008). Over 7,200 vertebrate fossils have been collected and catalogued from more than 750 localities by workers associated with the Natural History Museum of Los Angeles County (NHM) for over a century, leading to a well-documented sequence of mammalian assemblages (Tedford et al., 2004; Whistler et al., 2009). The NHM database recognizes over 100 mammalian species from the Dove Spring Formation, 70 of which are large-mammal lineages (>1 kg in estimated adult body weight) (Whistler et al., 2009). Four orders (Artiodactyla, Carnivora, Perissodactyla, and Proboscidea) and 15 families of large mammals are recognized in the Dove Spring Formation, with 59 taxa identified to the genus level and 20 further identified to the species level. (Here we refer to the taxonomic order “Artiodactyla” due to its priority over “Cetartiodactyla” as a monophyletic group that includes the last common ancestors of all even-toed ungulates in this study; Asher and Helgen, 2010; Prothero et al., 2021).

Ungulates are well represented in the Dove Spring Formation. Artiodactyl families include Antilocapridae (pronghorns), Camelidae (camels), Merycoidodontidae (oreodonts), and

Tayassuidae (peccaries) (Whistler and Burbank, 1992; Whistler et al., 2009). Antilocaprids are represented by six genera and are the most commonly occurring artiodactyls in terms of specimens and localities. Camelids are represented by three genera and numerous specimens. Two merycoidodontid genera are present. Two species of tayassuid are present, though rare. Perissodactyls in the formation belong to the Equidae (horses) and Rhinocerotidae (rhinos), with equids represented by numerous specimens from 14 species, while rhinocerotids are rare and limited to one genus. Seven proboscidean species in five genera are present, all of which are rare. Borophagine canids (bone-crushing dogs) are the most common carnivores with 13 species recognized in the formation (Wang and Barnes, 2008; Tedford and Wang, 2009). Eight species of Felidae are present but their fossils are considerably rarer than those of the Canidae (Whistler et al., 2009; Tseng et al., 2010). Four mustelid species are present (Whistler and Burbank, 1992; Whistler et al., 2009). Tedford (1965) divided the fossil record of the Dove Spring Formation into three superposed faunal assemblages that were later revised with new age interpretations by Whistler et al (2009).

We used the fossil record of large mammals to evaluate potential causes of faunal change, particularly tectonic changes in the basin and regional climate. Changes in per-capita rates of origination and extinction can be detected by analyzing taxonomic richness through a stratigraphic sequence. Using statistical estimates of residence times of lineages, we generated a record of estimated richness and faunal composition that provides a more realistic chronology of faunal history compared to the observed fossil record. We focus on the large mammals of the Dove Spring Formation because they are the most abundant group among the fossil assemblages in terms of specimens recovered and species richness.

## **Geologic Background**

The Dove Spring Formation consists of 1,800 meters of fluvial and lacustrine sediments and ashes deposited between 12.5 and 8.5 Ma (Figure 2.2) (Whistler and Burbank, 1992; Whistler et al., 2009). The sequence mostly consists of sandstones and mudstones interbedded with at least 18 laterally extensive ash units (Loomis and Burbank, 1988; Whistler and Burbank, 1992; Perkins et al., 1998). Dating methods include magnetostratigraphy, tephrochronologic correlation, and radiometric dating (U-Pb, K/Ar, Ar/Ar, and fission-track dating) and provide a temporal resolution of about 500 thousand years to most fossil localities (Evernden et al., 1964; Tedford, 1965; Cox and Diggles, 1986; Loomis and Burbank, 1988; Whistler and Burbank, 1992; Perkins et al., 1998; Perkins and Nash, 2002; Smith et al., 2002; Lourens et al., 2004; Tedford et al., 2004; Bonnicksen et al., 2007; Whistler et al., 2009; Table 2). The lower half of the sequence contains two thick basalt flows, one of which has an Ar/Ar radiometric age of  $10.5 \pm 0.25$  Ma (Loomis and Burbank, 1988; Whistler and Burbank, 1992).

Analysis of faunal and environmental changes requires a well-resolved chronology. The current chronological framework for the Dove Spring Formation is the culmination of decades of work integrating lithostratigraphy, magnetostratigraphy, biostratigraphy, and tephrochronology of the sequence. Improvements to radiometric methods necessitate occasional revisions to age estimates to ensure accuracy and consistency (Begemann et al., 2001; Renne et al., 2010; Carter et al., 2020; Schaen et al., 2020). Ages for many fossil localities are based on the tephrochronology of associated ash layers (Whistler et al. 2009, 2013). In order to further refine the stratigraphic resolution and age estimates of fossil localities, we measured 19 new stratigraphic sections and updated magnetostratigraphic correlations to the 2012 edition of the geomagnetic time scale (Whistler and Burbank, 1992; Hilgen et al., 2012). We updated 18

published radiometric dates for the sequence using current decay-constant standards (Begemann et al., 2001; Renne et al., 2010; Carter et al., 2020).

The El Paso Basin is located within a large fault zone that separates the western Basin and Range from the Sierra Nevada Mountains. The Walker Lane Belt and the Eastern California Shear Zone are right-lateral, strike-slip fault zones separated by the left-lateral Garlock fault (Loomis and Burbank, 1988; Faulds and Henry, 2008; Andrew et al., 2014; Dixon and Xie, 2018). These fault zones accommodate boundary motion between the Pacific and North American tectonic plates (Guest et al. 2007). The fault geometry within the El Paso Basin displays characteristics of both extensional and shear movement. Loomis and Burbank (1988) recognized four episodes of structural development in the basin. Tectonic processes occur over the course of thousands of years, so we allow for uncertainty of up to 0.25 Myr in estimates of their timing. During episode 1, the underlying Paleocene Goler Formation was tilted between the late Paleocene and early Miocene. Episode 2 is a period of north-south extension that began during the deposition of the underlying Cudahy Camp Formation (>18-15 Ma). A series of east-west trending dikes within the Cudahy Camp Formation is associated with the northwest movement of an extensive area of bedrock known as the Sierra Nevada-Great Valley crustal block that began between 17 and 15 Ma (McQuarrie and Wernicke, 2005; Camp et al., 2015). This long episode of extension continued to increase the basin area and created accommodation space for sediment accumulation during the first 2.5 Myr of the Dove Spring Formation. Episode 3 began ~10.5 Ma with counterclockwise rotation of the basin, allowing for westward translation of the entire basin along the Garlock fault up to 64 km closer to the Sierra Nevada. In episode 4, west-northwest tilting and related extension deformed strata as young as 9.0 Ma, increasing subsidence and basin relief relative to the Sierra Nevada Mountains.

As the extension taking place during episode 2 progressed during the early deposition of the Dove Spring Formation, increasing accommodation space allowed for the development of mature southeast-to-northwest drainage networks that transported sediments from the El Paso Mountains into the basin. Lacustrine sediments are present in the northern part of the basin underneath the basalts, and lakes are common features in extensional settings (Gawthorpe and Leeder, 2000). The isotopic signal of a rain shadow east of the Sierra Nevada Mountains documented since 16.0 Ma in several locations throughout the Great Basin indicates that there was significant relief between the southern Sierra Nevada and the northwestern Mojave region during the early deposition of the Dove Spring Formation (Loomis and Burbank, 1988; Poage and Chamberlain, 2002; Crowley et al., 2008; Whistler et al., 2009). This rain shadow began to weaken during episode 2 as regional extension lowered the paleoelevation of the southern Sierra Nevada (Poage and Chamberlain, 2002; Lechler et al., 2013). In addition, pollen and diatom records from the contemporaneous marine Monterey Formation indicate that the regional climate during tectonic episode 2 was becoming cooler and drier since at least 15 Ma (Flower and Kennett, 1993; Heusser et al., 2022).

The rotation and translation of episode 3 coincided with growth of accommodation space throughout the central Basin and Range (Andrew et al., 2014; Loughney et al., 2021). Movement along the Garlock fault during this interval is partially constrained by volcanism in the Summit Range east of the El Paso Basin, with lithological and geochemical correlations that suggest close proximity to the Lava Mountains until approximately 10.3 Ma (Figure 1; Smith et al., 2002; Andrew et al., 2014). The initiation of movement on this segment of the Garlock fault accommodates slip between the Walker Lane belt to the north and the Eastern California Shear Zone to the south. Fault movement is correlated with changes in sediment accumulation rate and

an age of 10.5 Ma allows for uncertainty in estimating the timing of its initiation (Mitchell and Reading, 1978; Loomis and Burbank, 1988; Burbank and Anderson, 2012). The tectonic activities of episode 3 locally interrupted the steady growth of accommodation space within the basin and may have cut off existing drainage channels (Loomis and Burbank, 1988; Gawthorpe and Leeder, 2000). The regional cooling and drying trends observed within the Monterey Formation that began during episode 2 continued into tectonic episode 3 (Flower and Kennett, 1993; Heusser et al., 2022).

Episode 4 represents a new period of east-west extension in the El Paso Basin that began between 9.5 Ma and 9.0 Ma based on cut strata and progressively less rotation observed in beds younger than 10.0 Ma (Loomis and Burbank, 1988). Concurrent regional extension was associated with southward migration of the Rivera triple junction as the San Andreas transform boundary between the Pacific and North American plates shifted towards the current Gulf of California (Dickinson, 2002; McQuarrie and Wernicke, 2005; Bahadori et al., 2018). Dove Spring sediments from episode 4 are increasingly coarse with distinctive clast composition that indicates the Sierra Nevada Mountains to the west as a new sediment source by 9.0 Ma (Loomis & Burbank, 1988; Figure 2). Paleocurrent studies by Loomis & Burbank (1988) demonstrated a shift to a northwest-to-southeast drainage pattern, and the coarser sediments suggest the presence of higher-energy stream channels than during the extension of episode 2. Mean annual precipitation in the region began to increase after 8.9 Ma throughout the region based on macrofossil and pollen records from several nearby basins that indicate the expansion of water-reliant pine forests (Axelrod, 1977; Heusser et al., 2022). Regional extension during episode 4 may have further weakened the rain shadow effect from the southern Sierra Nevada, although

there is debate regarding the precise timing of changes to its paleoelevation (Poage and Chamberlain, 2002; Lechler et al., 2013).

## Data and Methods

Our motivation for this study is to determine relationships between mammalian species richness, faunal composition, and the changes in tectonic and climatic history of the basin. To investigate the potential link between tectonic episodes and fossil preservation, we used a composite stratigraphic column to calculate average sediment accumulation rates throughout the Dove Spring Formation. Variations in sediment accumulation rate are indicators of changes in topography or subsidence that influence the preservation potential of sediments (Rust and Koster, 1984; Paola et al., 1992; Finarelli and Badgley, 2010; Loughney et al., 2021). In terrestrial basins, this rate is controlled by changes in accommodation space driven largely by fault movement resulting in subsidence or changes in relief (Leeder, 1993; Holland, 2016). We utilized data for the stratigraphic thickness of each magnetic polarity interval and the thickness between dated ash deposits to calculate sediment accumulation rates. We omitted the pair of thick basalt flows near the middle of the section from our calculations because these volcanic units are not part of the normal mode of deposition.

We assigned fossil localities to 0.5-Myr time bins and developed a biochronology based on fossil occurrences within these intervals. This interval length captures variation in species richness and fossil productivity with regards to tectonic episodes while allowing for uncertainty in the stratigraphic placement of localities and specimens. We placed fossil localities into accurate geographic and stratigraphic context by reviewing a series of 24 aerial photographs, 15 field notebooks, seven topographic maps, and three geologic maps produced by David Whistler



of the NHM during his extensive work on the Dove Spring Formation. GPS technology did not exist at the original time of collection for many of these localities, so Whistler and colleagues used topographic and geologic maps in conjunction with USGS aerial photographs to document localities on the ground. We georeferenced these maps using the North American Datum of 1983 (NAD 83) as a spatial reference to place localities in Google Earth and ESRI ArcGIS. We measured 19 new stratigraphic sections in the field and used stratigraphic marker units to correlate them to the stratigraphy of Whistler and Burbank (1992), Whistler et al. (2009), and Whistler et al. (2013) to refine the stratigraphic placement of fossil localities throughout the sequence.

The NHM vertebrate paleontology database contains over 7,200 specimens recovered from the Dove Spring Formation. The majority (6,747) of these specimens are fossil mammals, with the remainder consisting of reptiles, amphibians, birds, and fish. We compiled a faunal list of large mammal specimens identified to the species, genus, or family level for a total of 61 taxa that span the 4 million years of stratigraphic record. In some cases, specimens are identified to the genus or family level but cannot be assigned to a single species. These specimens still provide valuable occurrence data so we established criteria for their inclusion in our analyses. When a genus is represented by a single species, specimens identified to the genus level may represent a different species, so we treated them as separate species lineages. When a genus is represented by multiple species, unassigned specimens could belong to any of those species, so we omitted these from further analysis. Family level designations were only included as species lineages when their estimated residence times did not span the entire formation.

The true residence time of any fossil taxon is under-represented by observed specimens due to incomplete preservation. To account for the uncertainty in observed stratigraphic ranges,

we used the method of Marshall (1990) to calculate 80% confidence intervals based on the number of time intervals containing each taxon. We selected this confidence level as a compromise between the sampling density for large mammal specimens in the formation ( $n = 3,648$ ) and a moderate level of confidence. This method assumes a constant probability of recovering a fossil from within a taxon's true stratigraphic range. We calculated the unbiased point estimates of first and last occurrences of each large mammal lineage by adding the average gap size between fossil horizons to the observed first and last occurrences in 0.5 Myr time bins. Most of our analyses are based on the estimated residence times (Figure 3). Confidence intervals and point estimates were not calculated for singletons, as these estimates require multiple horizons. Species recovered from few localities separated by multiple time bins may display  $>1$  Myr range extensions that place their first and last occurrences well outside the formation. We omitted five family-level taxa that had  $>1$  Myr gaps between their observed and estimated first appearances because such poorly constrained residence times do not illuminate patterns of faunal change; their omission did not meaningfully affect such patterns (Table 1).

Following Marshall (1990, 2010), the formula for calculating a stratigraphic range extension using an 80% confidence interval is:

$$r_c = R[(1 - C)^{-1/(H-1)} - 1], \quad (1)$$

where:

$r_c$  = projected stratigraphic range extension,  
 $R$  = observed stratigraphic range, (Observed First Occurrence datum – Observed Last Occurrence datum),  
 $H$  = number of time intervals with occurrence of taxon.

The average gap size between fossil occurrences is given in the following equation:

$$r_{unbiased} = R / (H - 1), \quad (2)$$

where:

$r_{unbiased}$  = average gap size between fossil occurrences,  
 R = observed stratigraphic range, (Observed First Occurrence datum – Observed Last Occurrence datum),  
 H = number of time intervals with occurrence of taxon.

To evaluate change in faunal composition, we used a multinomial likelihood method to compare change between adjacent 0.5-Myr time intervals. Equation 3 is the log-likelihood (LnL) of the multinomial distribution. For each time interval of interest ( $i$ ) and its preceding interval, we calculated the proportion of species in each family from the total assemblage and the likelihood of that proportion.

The equation to calculate the log-likelihood of the multinomial distribution is:

$$\text{LnL}(i) = \sum_j a_j \ln(p_j), \quad (3)$$

where:

$a_j$  = count of species in family  $j$ ,  
 $p_j$  = proportion of total species in interval  $i$  assigned to family  $j$ .

We compared the maximum likelihood of faunal proportions for each time interval to the maximum likelihood estimate based on the preceding interval, by subtracting the latter from the former, to evaluate the difference in log-likelihood values (delta LnL). The results are used to evaluate changes in faunal composition between subsequent time intervals; the magnitude of delta LnL is higher with increasingly divergent proportions between intervals. A delta LnL value of 2.0 is the standard threshold for significant change in maximum-likelihood estimates (Edwards, 1992; Badgley and Finarelli, 2013).

Variations in sampling frequency and preservation contribute to uncertainty in rates of origination and extinction in the fauna, which are based on first and last occurrences of lineages.

We used Foote’s (2000) estimate of preservation rate to evaluate changes in the quality of the fossil record for comparison with rates of origination and extinction. This estimate of preservation rate relies on the difference between the number of range-through taxa and the number observed within a time interval. We calculated preservation rate  $r(i)$  for each 0.5 Myr interval of the fossil record using Foote’s (2000) equation:

$$r(i) = -\ln(1 - N_{bt,samp}(i) / N_{bt}(i) ), \quad (4)$$

where

$N_{bt,samp}$  = number of species present before, during, and after interval ( $i$ ),  
 $N_{bt}$  = equal to  $N_{bt,samp}$  plus range-through taxa.

We compared changes in species richness based on observed and estimated residence times and determined the observed and estimated number of “originations” and “extinctions” that occurred within each time interval. Here, “originations” refer to first appearances and may include endemic speciation events or immigrations, while “extinctions” refer to last appearances including actual extinctions or emigration of species. The majority of species are found elsewhere in the Basin and Range or Great Plains regions before their first appearance in the Dove Spring Formation (Tedford et al., 2004; Pagnac, 2009; Whistler et al., 2009; Priego-Vargas et al., 2016).

We used the per-capita approach to diversification of Foote (2000). This approach recognizes four categories of occurrences: species confined within a single time interval (singletons), bottom-boundary crossers ( $N_b$ ) with a last occurrence during the focal interval, top boundary-crossers ( $N_t$ ) with a first appearance in the focal interval, and taxa that range-through the focal interval and cross both the bottom and top boundaries ( $N_{bt}$ ). We calculated the standing richness and per-capita rates of origination  $p(i)$  and extinction  $q(i)$  for each interval as follows.

$$p(i) = -\ln(N_{bt}(i)/N_t(i)), \quad (4)$$

$$q(i) = -\ln(N_{bt}(i)/N_{bL}(i)), \quad (5)$$

where:

$N_{bt}(i)$  = range-through taxa,  
 $N_t(i)$  = top boundary-crossers,  
 $N_b(i)$  = bottom boundary-crossers.

We determined rates of diversification from the per-capita origination and extinction rates to evaluate the per-capita rate of change in species richness for each interval.

Diversification rate  $d(i)$  is the net change in species richness, expressed as the absolute difference between per-capita rates of extinction and origination (Equation 6; Foote, 2000; Badgley and Finarelli, 2013; Domingo et al., 2014). Diversification rate  $d(i)$  is expressed as:

$$d(i) = ((N_t(i) - N_b(i)) / N_{bt}(i)), \quad (6)$$

where:

$N_{bt}(i)$  = range-through taxa,  
 $N_t(i)$  = top boundary-crossers,  
 $N_b(i)$  = bottom boundary-crossers.

To evaluate the significance of the diversification metrics, we generated 1,000 bootstrap replicates of the estimated temporal durations for each taxon. Each bootstrapped dataset was generated using a random pull of 44 taxa with replacement based on estimated first and last occurrences. For each time interval, we determined confidence intervals of origination rate, extinction rate, and diversification rate as two standard deviations of the mean of the bootstrap distribution. Values of each metric are considered significantly positive or negative when the confidence intervals on the bootstrap distribution do not include zero (Foote, 2000).

To determine whether poorly sampled time intervals originally exhibited similar species richness to well-sampled intervals, we conducted sample-based rarefaction analysis using the observed fossils recovered from each time interval. This method randomly resamples the reference dataset and generates a rarefaction curve based on the average number of species found among time intervals (Chao and Jost, 2012; Colwell et al., 2012; Chao et al., 2014). Rarefaction curves utilize the documented number of specimens for each species to generate the expected number of species in an assemblage for a given number of specimens (Chao and Jost, 2012; Chao et al., 2014).

## Results

In this section, we first present the stratigraphic and geochronologic framework of the Dove Spring Formation. We then describe the biochronology of large-mammals and patterns of change in faunal composition. Finally, we compare the patterns of origination and extinction based on estimated residence times to the tectonic history of the El Paso Basin.

### **Stratigraphic and Geochronologic Framework**

Our new stratigraphic sections provide context for the spatial distribution of fossil localities and their stratigraphic placement within the updated chronology of the Dove Spring Formation, with a stratigraphic resolution of approximately 25 to 50 meters and a temporal resolution of 500 kyr. The chronostratigraphy for most of the sequence is well-resolved based on radiometric ash dates using current decay constants and correlation to the geomagnetic timescale. Based on a new tephrochronologic correlation to the marine Monterey Formation from Knott et al. (2022; Table 2), we revised the age of the top of the sequence to 8.5 Ma and adjusted species'

temporal ranges accordingly. The majority of revised ash dates fall within their original uncertainty estimates ( $\pm 0.03$  Myr; Table 2.2).

We recorded lithological variation in the lower 600 m of the formation, adding information to a sparsely documented section of the stratigraphic sequence (Figure 2.2). We also correlated dated ash layers to additional outcrops throughout the basin. The lithological and geochronological changes that are most relevant to our study occur in the upper half of the Dove Spring Formation due to their association with boundaries between tectonic episodes. Sediments in the upper half of the sequence begin at 900 m in the section W92B (Figure 2) with a thick interval of fine- to medium-grained sandstones interbedded with mudstones extending upward to 1,400 m ( $\sim 10.5$  to 9.0 Ma; Figure 2.2). Sandstones then coarsen significantly and include an increasing proportion of granitic clasts above 1,400 m (9.0 Ma), which signifies a change in source area from the El Paso Mountains to the Sierra Nevada Range (Loomis and Burbank, 1988).

The average sediment accumulation rate for the entire Dove Spring Formation is 383 m/Myr. The rate varies between 100 and 650 m/Myr over time spans of 0.3 Myr to 0.5 Myr for the first two million years of deposition as a series of sandstones and silty sandstones sourced from the El Paso Mountains were deposited in the basin (4B). A moderate peak of 650 m/Myr occurs at 11.8 Ma, driven in part by deposition of tuff breccia associated with regional volcanism, and conglomerates and sandstones from the El Paso Mountains. A moderate peak of 893 m/Myr occurs at 10.3 Ma following at least 1 million years of very slow accumulation of similar sediments. Basin rotation and translation began 0.3 Myr after this peak and coincided with another long period of slow accumulation. Basin extension resumed by 9.5 Ma, shortly

before coarse, granitic clasts from the Sierra Nevada were deposited during a final peak of 1,300 m/Myr at 8.9 Ma.

### **Biochronology and Faunal Composition**

Fossils recovered from the Dove Spring Formation are the basis for initial interpretations of changes in species richness and the quality of the fossil record (Figures 3 & 4). The number of large-mammal specimens per interval closely follows the number of localities per interval ( $r = 0.97$ ,  $p < 0.05$ ). Two exceptions occur prior to 11.5 Ma (Figure 4A). From 12.5 to 12.0 Ma, the number of specimens increases only slightly despite an increase from 10 to 70 localities, and more specimens are recovered from fewer localities by 11.5 Ma. The interval between 10.5 and 9.5 Ma contains the greatest number of localities and specimens, peaking at 9.5 Ma. A significant dip in both localities and specimens occurs at 9.0 Ma, before rising again at 8.5 Ma. The observed species richness of large mammals per time interval generally follows the same pattern as the number of localities ( $r = 0.92$ ,  $p < 0.05$ ) and specimens ( $r = 0.82$ ,  $p < 0.05$ ). A steady increase from 16 species at the base of the section reaches 51 species by 10.0 Ma. Species richness then declines until 9.0 Ma. The plateau in species richness at 10.0 Ma is concurrent with the highest number of localities and specimens, suggesting a strong sampling effect on species richness. Preservation rate is moderate throughout most of the sequence until a sharp decrease at 9.0 Ma. Sample-based rarefaction showed that time intervals 12.0 Ma and 11.5 Ma have rarefaction curves that level off at lower values of species richness compared to later intervals, indicating that the relationships between specimens and species changed at 11.0 Ma (Figure 2.8).



Our analyses of species richness and diversification for large mammals are based on estimated residence times (Figure 2.3). Twenty species occur within the first 0.5 Myr of deposition in the Dove Spring Formation. Equids, rhinocerotids, and mammutids are present at the base of the section and maintain their species richness throughout the sequence, with equids consistently having the highest number of species of all taxa (Figure 6A). Antilocaprids, camelids, and merycoidodontids are present at the base of the section, gain species by 11.0 Ma, and maintain higher richness until 9.0 Ma. Gomphotherids and amebelodontids appear at the base of the section but are rare until 10.5 Ma, when the amebelodontids gain three additional species that persist until 9.5 Ma. Two species of tayassuid appear at 12.0 Ma and persist until 9.0 Ma. At least two species of canids are present throughout the sequence and their species richness increases to a peak of eight at 10.0 Ma. Felids also occur throughout the sequence, with a peak of three species by 9.5 Ma. A single species of nimravid appears at 11.0 Ma and the family has a peak of three species at 9.5 Ma. A single species of mustelid appears at 11.5 Ma and is joined by two additional species at 11.0 Ma that persist through the end of the sequence.

Significant changes in faunal composition, according to the change in log likelihoods ( $\Delta \text{LnL}$ ), occurred in three time intervals (Figure 2.6). Change at 11.0 Ma was driven by the appearance of two additional species each of Canidae, Merycoidodontidae, and Mustelidae. Change at 10.0 Ma was the result of three additional species each of Amebelodontidae and Canidae. The largest influx of new species began at 10.5 Ma, with 14 species (two singletons) appearing at 10.5 Ma and seven (all singletons) at 10.0 Ma. Following this interval, the only additional species to appear are three carnivores and one antilocaprid, all occurring as singletons. The interval with the greatest magnitude of change in faunal composition was 9.5 Ma, when Amebelodontidae and Canidae declined by three and six species, respectively, and the species

richness of Nimravidae increases from one to three. Castoridae, Mustelidae, Nimravidae, Felidae, Equidae, Protoceratidae, and Tayassuidae all declined in species richness following this interval.

## **Diversification**

Per-capita origination and extinction rates depict the proportion of species appearing or disappearing from the sequence, standardized by range-through taxa (Figure 7). Per-capita origination rates are moderate and positive at the base of the sequence and begin to decline after 11.0 Ma (Figure 7B). The per-capita extinction rate is low early in the sequence and displays a gradual increase from 10.0 Ma through the top of the sequence (Figure 7B). Per-capita origination rates are significant at 12.0 Ma, 11.5 Ma, and 11.0 Ma (Figure 7B). Significant per-capita extinction rates occur at 10.5 Ma and in the three youngest intervals between 9.5 Ma and 8.5 Ma. We found statistically non-significant correlations ( $p > 0.05$ ) between preservation rate and per-capita origination rate ( $r = 0.67$ ), per-capita extinction rate ( $r = 0.53$ ), and species richness ( $r = 0.27$ ).

The per-capita diversification rate is positive but non-significant from the base of the sequence until it becomes significantly positive at 11.0 Ma as a result of high origination and low extinction rates (Figure 7C). The diversification rate becomes negative after this interval, reflecting higher extinction rates through the top of the section. Significant negative per-capita diversification rates occur at 9.5 Ma and continue through the end of the sequence (Figures 7C & 7D).

Two extended time intervals showed significant diversification rates that coincide with episodes of tectonic extension: Gradual and significant origination was the dominant trend in the lower half of the formation (12.5-10.5 Ma), coinciding with extension that began in the middle Miocene and continued during the deposition of the Dove Spring Formation. The last million-year interval of the section (9.5-8.5 Ma) exhibited significant extinction rates that coincide with basin rotation and translation.

## Discussion

We used estimated residence times to determine the number and per-capita rates of origination and extinction in order to test whether changes in species richness and faunal composition could have been influenced by changes in tectonic history. The three major stages of landscape evolution recorded in the Dove Spring Formation each correspond with a different phase of faunal change. North-south extension that began in the middle Miocene was the dominant tectonic process early in the formation's history (12.5-10.5 Ma). During this phase of extension, the basin increased in accommodation space and grew in area (Loomis and Burbank, 1988; Gawthorpe and Leeder, 2000). The deposition of fine-grained fluvial and lacustrine sediments suggest that drainage channels had relatively gentle slopes and for a time fed a lake in the northern part of the basin (Gawthorpe and Leeder, 2000). The lowest sediment accumulation rates occur at 11.0 Ma, indicating slow changes in accommodation space or continued basin growth. The first significant peak in per-capita origination also occurs at 11.0 Ma, suggesting that extension opened corridors for an influx of species from outside the basin. Positive origination and diversification rates are often correlated with area (Kisel et al., 2011). Greater

area supports larger population sizes and also promotes increased habitat diversity, with the potential to generate environmental gradients that allow for a higher number of species to coexist. Here, the gradual accumulation of species prior to 10.0 Ma is likely driven by the long-term generation of additional habitat space as the basin grew in area.

Rotation and translation of the El Paso Basin along the Garlock fault began at 10.5 Ma, interrupting the long episode of basin growth. The basin's geometry and relationships to its sediment sources in the El Paso Mountains were altered, triggering changes to drainage patterns and likely the availability of water and vegetation resources. Origination rates became non-significant during this stage of the basin's evolution. While environmental conditions during this episode were conducive to preservation, yielding the highest species richness within the sequence, extinction had already become the dominant pattern of faunal change by 10.5 Ma as origination rates fell (Figures 4, 7). The greatest change in faunal composition coincides with the highest preservation rate at 9.5 Ma and is driven by apparent species loss across multiple families. Preservation rate declined to its lowest rate during this tectonic episode.

East-west extension beginning near 9.5 Ma increased the distance between the basin and its original sediment source area. This episode represents a new stage of basin extension that generated the coarser sediments with a source in the Sierra Nevada. The resulting depositional environments were less likely to preserve fossils as indicated by the low preservation rate (Figure 4B). These higher-energy environments may have disrupted pre-existing vegetation and sources of fresh water. Per-capita extinction rates increased through the top of the section, although a contemporaneous and steep decline in sample size may be partially responsible for this trend. Intervals of significant negative diversification rates coincide with the apparent disappearance of many species from the basin's fossil record.

While the strong relationship between species richness and the productivity of the fossil record (Figure 4A) suggests a sampling effect, there is also evidence for genuine change in richness and composition. Significant origination rates that are coupled with rare species from few localities indicate the likelihood that faunal changes in the lower half of the formation are not the result of sampling alone (Figures 4B, 6 & 7B). For example, carnivores represent only four percent of all taxa within the formation, but canids and mustelids are the main drivers of significant faunal change at 11.0 Ma. Three of the four time intervals in the lower part of the sequence exhibit significant origination and low extinction rates, indicating that new species appeared without displacing resident species (Figures 6 & 7). The upper half of the formation is dominated by high extinction rates and a greater magnitude of faunal change. Significant change in composition occurs from 10.0 Ma to 9.5 Ma and species richness of large mammals reaches its highest value (47 species) at 9.5 Ma (Figure 4A). Subsequent apparent loss in species richness is due to sharply declining preservation rates in the sequence and many of the disappearing species likely persisted through this interval based on estimated residence times. Carnivores and new singletons continue to appear after 9.5 Ma, despite a low preservation rate and a sharp decrease in the number of localities.

An important point to consider is whether the patterns of faunal change in the formation represent real processes or result from fluctuations in sampling. If fossil productivity were the primary control on the record of faunal change, we would expect strong correlations between preservation, sampling, and processes of faunal change. However, we calculated non-significant relationships throughout the sequence between preservation and all other variables. The number of range-through taxa that persist through multiple time intervals is consistently high and the average residence time for large-mammal species was 2.5 Myr. The appearance of chronically

rare taxa in intervals with low preservation potential and few localities is contrary to the expectations of poor sampling (we would expect the common species to persist). While preservation is always a factor when examining the fossil record, our results indicate that the patterns of faunal change within the Dove Spring Formation are not entirely tied to the quality of the fossil record. Additional data about the history of depositional environments are needed in order to evaluate the influence of preservation on the species richness and composition of large-mammal assemblages. Changes in the dominant lithologies from coarse-grained breccia and sandstones in the lower part of the sequence, to fine- to medium-grained silty sandstones in the middle, to coarse conglomerates in the upper part track changes in the preservation potential of the basin.

Ecological factors that may have affected species richness include competition, predation, or character displacement (Brown and Nicoletto, 1991; Janis, 2004). Tectonic processes may have also contributed to the generation of dispersal corridors, allowing species to move freely in and out of the basin (Maguire and Stigall, 2008). Much of the potential evidence for these contributing factors requires a dataset of faunal patterns at the regional scale. However, it is possible to utilize facies analysis and environmental data from local assemblages to investigate potential ecological causes for faunal change, such as changes in vegetation resources, precipitation amount, and paleotemperature.

This additional information in combination with this analysis of taxonomic richness and the timing of tectonic episodes will enable us to test two hypotheses regarding the correlations between the physical environment and changes in the mammalian faunas of the basin. One hypothesis is that tectonic influences on basin topography contributed to significant change in the environments present within the Dove Spring Formation. An independent record of change in

climate or vegetation would provide evidence for testing this hypothesis. Under this scenario, we would expect to observe significant variation in ecological diversity within the mammalian fauna that coincides with the timing of tectonically-driven changes in depositional setting and climate. Mammalian body size is correlated with ecological characteristics such as diet, population density and growth rate, home range size, and behavioral adaptations (Damuth and MacFadden, 1990; Eisenberg, 1990; Janis et al., 2002). Variations in the predominant body size of mammals that coincide with the basin's tectonic history would support this hypothesis by indicating a change in one or more characters was related to habitat-level changes. The stable isotopic ratios of carbon in herbivore teeth also document the composition of vegetation (Quade et al., 1992; Koch et al., 1994; Cerling et al., 1997). Significant change in isotopic values that correlate with tectonic episodes would support this second hypothesis.

An alternative hypothesis is that the tectonic episodes altered the preservation potential of sediments and depositional environments. In this scenario, changes in fossil productivity would occur in the absence of significant ecological change; mammal species would not exhibit marked changes in feeding ecology or body size, and the community composition would change little through the section, regardless of depositional environment. Changes in depositional environments can be identified through facies analysis and correlated with the timing of tectonic activity to evaluate whether changes in preservation affect the fossil record of the Dove Spring Formation.

## Conclusion

Study sites like the El Paso Basin are part of a growing record of basins that are providing insight into the interactions between changing topography and mammalian evolution (Badgley and Finarelli, 2013; Badgley et al., 2017; Loughney and Badgley, 2017; Smiley et al., 2017). The Dove Spring Formation is a record of mammalian faunas preserved in the sediments of a basin that developed during the end of the Middle Miocene Climatic Transition. We reviewed its geochronology using updated decay constants and newly measured stratigraphic sections to place fossil localities within a temporal and stratigraphic framework for the present analysis and to support additional paleoecological research.

We identified two phases of significant change in taxonomic richness: high species accumulation and long residence times early in the section, and steady species loss in the later portion. These changes track fossil productivity but there is also evidence that some of this pattern is genuine. The sequence includes three major tectonic episodes that altered the basin's geometry and topography. Basin extension in the lower part of the section is associated with an increase in basin area, high per-capita origination rates, and a minor but significant change in faunal composition. At 10.5 Ma, the basin underwent a period of rotation and translation away from the El Paso Mountains, disrupting existing drainages and likely affecting connectivity to the surrounding region. High numbers of specimens, localities, and species richness accompany the highest magnitude of change in faunal composition at 10.0 Ma, when per-capita extinction rate became the dominant form of faunal change. Extinction rates continued to increase at 9.0 Ma as basin extension resumed and coarse sediments from the Sierra Nevada became prevalent. New drainage networks began to form and changed the preservation potential of sediments or



generated new environmental settings, either way leading to the apparent or actual disappearance of most species from the El Paso Basin's fossil record.

Time intervals early in the sequence contain faunas with lower species richness that are not simply the result of low sampling. The presence of multiple time intervals with significant per-capita extinction rates and appearances of rare taxa indicates that some aspects of faunal change are authentic despite a strong sampling effect later in the sequence. Distinct episodes of tectonic history coincide with the timing of changes in faunal patterns, suggesting a link between tectonic processes and the basin's mammalian community. The timeline of tectonic and faunal changes in this study provides the framework for further testing of the nature of this link through studies of preservation potential, depositional environments, and vegetation history.

#### Acknowledgements

We received funding for this research from the Rackham Graduate School and the Department of Earth and Environmental Sciences at the University of Michigan. We acknowledge support from the National Science Foundation, Integrated Earth Systems Program award # 1813996 to CB. We thank Xiaoming Wang, Juliet Hook, Sam McCleod, and Vanessa Rhue of the Natural History Museum of Los Angeles County for granting us access to the vertebrate specimen database and for assistance in the field. We thank Dave Whistler for generously donating his original field notes and for conversations that led to a greater understanding of the Dove Spring Formation.

## References

- Andrew, J. E., Walker, J. D., and Monastero, F. C., 2014, Evolution of the central Garlock fault zone, California: A major sinistral fault embedded in a dextral plate margin: *Geological Society of America Bulletin*, v. 127, no. 1/2, p. 227-249.
- Asher, R. J., and Helgen, K. M., 2010, Nomenclature and placental mammal phylogeny: *BMC Evolutionary Biology*, v. 10, no. 102, p. 1-9.
- Axelrod, D., 1977, Outline history of California vegetation, *in* Barbour, M., and Major, J., eds., *Terrestrial vegetation of California*: New York, John Wiley & Sons, p. 139-194.
- Badgley, C., and Finarelli, J. A., 2013, Diversity dynamics of mammals in relation to tectonic and climatic history: comparison of three Neogene records from North America: *Paleobiology*, v. 39, no. 3, p. 373-399.
- Badgley, C., Smiley, T. M., Terry, R., Davis, E. B., DeSantis, L. R. G., Fox, D. L., Hopkins, S. S. B., Jezkova, T., Matocq, M. D., Matzke, N., McGuire, J. L., Mulch, A., Riddle, B. R., Roth, V. L., Samuels, J. X., Stromberg, C. A. E., and Yanites, B. J., 2017, Biodiversity and topographic complexity: Modern and geohistorical perspectives: *Trends in Ecology & Evolution*, v. 32, no. 3, p. 211-226.
- Bahadori, A., Holt, W. E., and Rasbury, E. T., 2018, Reconstruction modeling of crustal thickness of western North America since 36 Ma: *Geosphere*, v. 14, no. 3, p. 1207-1231.
- Beatley, J. C., 1975, Climates and vegetation pattern across the Mojave/Great Basin Desert transition of southern Nevada: *The American Midland Naturalist*, v. 93, no. 1, p. 53-70.
- Begemann, F., Ludwig, K. R., Lugmair, G. W., Min, K., Nyquist, L. E., Pratchett, P. J., Renne, P. R., Shih, C.-Y., Villa, I. M., and Walker, R. J., 2001, Call for an improved set of decay constants for geochronological use: *Geochimica et Cosmochimica Acta*, v. 65, no. 1, p. 111-121.
- Bonnichsen, B., Leeman, W. P., Honjo, N., McIntosh, W. C., and Godchaux, M. M., 2007, Miocene silicic volcanism in southwestern Idaho: geochronology, geochemistry, and evolution of the central Snake River Plain: *Bulletin of Volcanology*, v. 70, no. 3, p. 315-342.
- Brown, J. H., and Nicoletto, P. F., 1991, Spatial scaling of species composition: Body masses of North American land mammals: *The American Naturalist*, v. 138, no. 6, p. 1478-1512.
- Burbank, D. W., and Anderson, R. S., 2012, *Tectonic Geomorphology*, Wiley-Blackwell, 472 p.:
- Camp, V. E., Pierce, K. L., and Morgan, L. A., 2015, Yellowstone plume trigger for Basin and Range extension, and coeval emplacement of the Nevada–Columbia Basin magmatic belt: *Geosphere*, v. 11, no. 2, p. 203-225.

- Carter, J., Ickert, R. B., Mark, D. F., Tremblay, M. M., Cresswell, A. J., and Sanderson, D. C. W., 2020, Production of  $^{40}\text{Ar}$  by an overlooked mode of  $^{40}\text{K}$  decay with implications for K-Ar geochronology: *Geochronology*, v. 2, no. 2, p. 355-365.
- Cerling, T. E., Harris, J. M., Ambrose, S. H., Leakey, M. G., and Solounias, N., 1997, Dietary and environmental reconstruction with stable isotope analyses of herbivore tooth enamel from the Miocene locality of Fort Ternan, Kenya: *Journal of Human Evolution*, v. 33, no. 635-650.
- Chamberlain, C. P., Winnick, M. J., Mix, H. T., Chamberlain, S. D., and Maher, K., 2014, The impact of neogene grassland expansion and aridification on the isotopic composition of continental precipitation: *Global Biogeochemical Cycles*, v. 28, p. 992-1004.
- Chao, A., Gotelli, N. J., Hsieh, T. C., Sander, E. L., Ma, K. H., Colwell, R. K., and Ellison, A. M., 2014, Rarefaction and extrapolation with Hill numbers: a framework for sampling and estimation in species diversity studies: *Ecological Monographs*, v. 84, no. 1, p. 45-67.
- Chao, A., and Jost, L., 2012, Coverage-based rarefaction and extrapolation: standardizing samples by completeness rather than size: *Ecology*, v. 93, no. 12, p. 2533-2547.
- Colwell, R. K., Chao, A., Gotelli, N. J., Lin, S. Y., Mao, C. X., Chazdon, R. L., and Longino, J. T., 2012, Models and estimators linking individual-based and sample-based rarefaction, extrapolation and comparison of assemblages: *Journal of Plant Ecology*, v. 5, no. 1, p. 3-21.
- Cox, B. F., and Diggles, M. F., 1986, Geologic map of the El Paso Mountains Wilderness Study Area, Kern County, California: United States Geological Survey.
- Crowley, B. E., Koch, P. L., and Davis, E. B., 2008, Stable isotope constraints on the elevation history of the Sierra Nevada Mountains, California: *Geological Society of America Bulletin*, v. 120, no. 5-6, p. 588-598.
- Damuth, J., and MacFadden, B. J., 1990, *Body size in mammalian paleobiology: Estimation and biological implications*, Cambridge University Press, 397 p.:
- Dibblee, T. W., 1967, *Areal geology of the western Mojave Desert California*.
- Dickinson, W. R., 2002, The Basin and Range Province as a composite extensional domain: *International Geology Review*, v. 44, p. 1-38.
- Dixon, T. H., and Xie, S., 2018, A kinematic model for the evolution of the Eastern California Shear Zone and Garlock Fault, Mojave Desert, California: *Earth and Planetary Science Letters*, v. 494, p. 60-68.
- Edwards, A. W. F., 1992, *Likelihood*, Baltimore, Johns Hopkins University Press.
- Eisenberg, J. F., 1990, The behavioral/ecological significance of body size in the Mammalia, *in* Damuth, J., and MacFadden, B. J., eds., *Body size in mammalian paleobiology: Estimation and biological implications*, Cambridge University Press, p. 25-37.

- Evernden, J. F., Savage, D. E., Curtis, G. H., and James, G. T., 1964, Potassium-argon dates and the Cenozoic mammalian chronology of North America: *American Journal of Science*, v. 262, p. 145-198.
- Faulds, J. E., and Henry, C. D., 2008, Tectonic influences on the spatial and temporal evolution of the Walker Lane: An incipient transform fault along the evolving Pacific - North American plate boundary: *Arizona Geological Society Digest*, v. 22, p. 437-470.
- Finarelli, J. A., and Badgley, C., 2010, Diversity dynamics of Miocene mammals in relation to the history of tectonism and climate: *Proceedings of the Royal Society B: Biological Sciences*, v. 277, p. 2721-2726.
- Flower, B. P., and Kennett, J. P., 1993, Relations between Monterey Formation deposition and middle Miocene global cooling: Naples Beach section, California: *Geology*, v. 21, p. 877-880.
- Foote, M., 2000, Origination and extinction components of taxonomic diversity: general problems: *Paleobiology*, v. 26, p. 74-102.
- Frigola, A., Prange, M., and Schulz, M., 2018, Boundary conditions for the Middle Miocene Climate Transition (MMCT v1.0): *Geoscientific Model Development*, v. 11, p. 1607-1626.
- Gawthorpe, R. L., and Leeder, M. R., 2000, Tectono-sedimentary evolution of active extensional basins: *Basin Research*, v. 12, p. 195-218.
- Hammer, Ø., Harper, D. A. T., Ryan, P. D., 2001, PAST: Paleontological Statistics software package for education and data analysis. *Palaeontologia Electronica*, v. 4, no. 1, p. 9.
- Heusser, L. E., Barron\*, J. A., Blake, G. H., and Nichols, J., 2022, Miocene terrestrial paleoclimates inferred from pollen in the Monterey Formation, Naples Coastal Bluffs section, California, *Understanding the Monterey Formation and Similar Biosiliceous Units across Space and Time*, p. 215-227.
- Hilgen, F. J., Lourens, L. J., and Dam, J. A. V., 2012, The Neogene Period, *in* Gradstein, F. M., Ogg, J. G., Schmitz, M. D., and Ogg, G. M., eds., *The geologic time scale*: Amsterdam; Boston, Elsevier, p. 923-978.
- Holland, S. M., 2016, The non-uniformity of fossil preservation: *Philosophical Transactions of the Royal Society B: Biological Sciences*, v. 371, p. 11.
- Jacobs, B. F., Kingston, J. D., and Jacobs, L. L., 1999, The origin of grass-dominated ecosystems: *Annals of the Missouri Botanical Garden*, v. 86, no. 2, p. 590-643.
- Janis, C. M., 1993, Tertiary mammal evolution in the context of changing climates, vegetation, and tectonic events: *Annual Review of Ecology, Evolution, and Systematics*, v. 24, p. 467-500.
- , 2004, The species richness of Miocene browsers, and implications for habitat type and primary productivity in the North American grassland biome: *Palaeogeography, Palaeoclimatology, Palaeoecology*, v. 207, no. 3-4, p. 371-398.

- Janis, C. M., Damuth, J., and Theodor, J. M., 2000, Miocene ungulates and terrestrial primary productivity: Where have all the browsers gone?: *Proceedings of the National Academy of Sciences of the United States of America*, v. 97, no. 14, p. 7899-7904.
- , 2002, The origins and evolution of the North American grassland biome: the story from the hoofed mammals: *Palaeogeography, Palaeoclimatology, Palaeoecology*, v. 177, p. 183-198.
- Kisel, Y., McInnes, L., Toomey, N. H., and Orme, C. D., 2011, How diversification rates and diversity limits combine to create large-scale species-area relationships: *Philos Trans R Soc Lond B Biol Sci*, v. 366, no. 1577, p. 2514-2525.
- Knott, J. R., Sarna-Wojcicki, A. M., Barron, J. A., Wan, E., Heizler, L., and Martinez, P., 2022, Tephrochronology of the Miocene Monterey and Modelo Formations, California, Understanding the Monterey Formation and Similar Biosiliceous Units across Space and Time, p. 187-214.
- Koch, P. L., Fogel, M. L., and Tuross, N., 1994, Tracing the diets of fossil animals using stable isotopes, *in* Lajtha, K., and Michener, R., eds., *Stable isotopes in ecology and environmental science*: Boston, Blackwell Scientific, p. 16.
- Kohn, M. J., and Fremd, T. J., 2008, Miocene tectonics and climate forcing of biodiversity, western United States: *Geology*, v. 36, no. 10, p. 783-786.
- Lechler, A. R., Niemi, N. A., Hren, M. T., and Lohmann, K. C., 2013, Paleoelevation estimates for the northern and central proto-Basin and Range from carbonate clumped isotope thermometry: *Tectonics*, v. 32, no. 3, p. 295-316.
- Leeder, M. R., 1993, Tectonic control upon drainage basin development, river channel migration and alluvial architecture: Implications for hydrocarbon reservoir development and characterization, *in* North, C. P., and Prosser, D. J., eds., *Characterization of fluvial and aeolian reservoirs*, Volume 73, Geological Society Special Publications, p. 7-22.
- Loomis, D. P., and Burbank, D. W., 1988, The stratigraphic evolution of the El Paso basin, southern California: Implications for the Miocene development of the Garlock fault and uplift of the Sierra Nevada: *Geological Society of America Bulletin*, v. 100, p. 12-28.
- Loughney, K. M., and Badgley, C., 2017, Facies, environments, and fossil preservation in the Barstow Formation, Mojave Desert, California: *Palaios*, v. 32, p. 396-412.
- , 2020, The Influence of Depositional Environment and Basin History on the Taphonomy of Mammalian Assemblages from the Barstow Formation (Middle Miocene), California: *Palaios*, v. 35, no. 4, p. 175-190.
- Loughney, K. M., Badgley, C., Bahadori, A., Holt, W. E., and Rasbury, E. T., 2021, Tectonic influence on Cenozoic mammal richness and sedimentation history of the Basin and Range, western North America: *Science Advances*, v. 7, p. 13.
- Maguire, K. C., and Stigall, A. L., 2008, Paleobiogeography of Miocene Equinae of North America: A phylogenetic biogeographic analysis of the relative roles of climate, vicariance, and dispersal: *Palaeogeography, Palaeoclimatology, Palaeoecology*, v. 267, no. 3-4, p. 175-184.

- Marshall, C. R., 1990, Confidence intervals on stratigraphic ranges: *Paleobiology*, v. 16, no. 1, p. 1-10.
- , 2010, Using confidence intervals to quantify the uncertainty in the end-points of stratigraphic ranges, *in* Alroy, J., and Hunt, G., eds., *The Paleontological Society Papers*, Volume 16, The Paleontological Society, p. 291-316.
- McQuarrie, N., and Wernicke, B. P., 2005, An animated tectonic reconstruction of southwestern North America since 36 Ma: *Geosphere*, v. 1, no. 3, p. 147-172.
- Merriam, J. C., 1919, Tertiary mammalian faunas of the Mohave Desert: University of California Publications. Department of Geology, Bulletin, v. 10, p. 111-127.
- Mitchell, A. H. G., and Reading, H. G., 1978, Sedimentation and tectonics, *in* Reading, H. G., ed., *Sedimentary environments and facies*: New York, Elsevier, p. 557.
- Pagnac, D., 2009, Revised large mammal biostratigraphy and biochronology of the Barstow Formation (Middle Miocene), California: *PaleoBios*, v. 29, no. 2, p. 48-59.
- Paola, C., Hellert, P. L., and Angevine, C. L., 1992, The large-scale dynamics of grain-size variation in alluvial basins, 1: Theory: *Basin Research*, v. 4, p. 73-90.
- Perkins, M. E., Brown, F. H., Nash, W. P., McIntosh, W., and Williams, S. K., 1998, Sequence, age, and source of silicic fallout tuffs in middle to late Miocene basins of the northern Basin and Range province: *Geological Society of America Bulletin*, v. 110, no. 3, p. 344-360.
- Perkins, M. E., and Nash, B. P., 2002, Explosive silicic volcanisms of the Yellowstone hotspot: the ash fall tuff record: *Geological Society of America Bulletin*, v. 114, no. 3, p. 367-381.
- Poage, M. A., and Chamberlain, C. P., 2002, Stable isotopic evidence for a Pre-Middle Miocene rain shadow in the western Basin and Range: Implications for the paleotopography of the Sierra Nevada: *Tectonics*, v. 21, no. 4, p. 10.
- Priego-Vargas, J., Bravo-Cuevas, V. M., and Jiménez-Hidalgo, E., 2016, The record of Cenozoic horses in Mexico: current knowledge and palaeobiological implications: *Palaeobiodiversity and Palaeoenvironments*, v. 96, no. 2, p. 305-331.
- Prothero, D. R., Domning, D., Fordyce, R. E., Foss, S., Janis, C., Lucas, S., Marriott, K. L., Metais, G., Naish, D., Padian, K., Rössner, G., Solounias, N., Spaulding, M., Stucky, R. M., Theodor, J., and Uhen, M., 2021, On the Unnecessary and Misleading Taxon “Cetartiodactyla”: *Journal of Mammalian Evolution*, v. 29, no. 1, p. 93-97.
- Quade, J., Cerling, T. E., Barry, J. C., Morgan, M. E., Pilbeam, D. R., Chivas, A. R., Lee-Thopr, J. A., and Merwe, N. J. v. d., 1992, A 16-Ma record of paleodiet using carbon and oxygen isotopes in fossil teeth from Pakistan: *Chemical Geology*, v. 94, p. 183-192.
- Renne, P. R., Mundil, R., Balco, G., Min, K., and Ludwig, K. R., 2010, Joint determination of  $^{40}\text{K}$  decay constants and  $^{40}\text{Ar}^*/^{40}\text{K}$  for the Fish Canyon sanidine standard, and improved accuracy for  $^{40}\text{Ar}/^{39}\text{Ar}$  geochronology: *Geochimica et Cosmochimica Acta*, v. 74, p. 5349-6367.

- Rust, B. R., and Koster, E. H., 1984, Coarse alluvial deposits, *in* Walker, R. G., ed., *Facies Models: Canada*, Geosci, p. 53-69.
- Samuels, J. X., and Hopkins, S. S. B., 2017, The impacts of Cenozoic climate and habitat changes on small mammal diversity of North America: *Global and Planetary Change*, v. 149, p. 36-52.
- Schaen, A. J., Jicha, B. R., Hodges, K. V., Vermeesch, P., Stelten, M. E., Mercer, C. M., Phillips, D., Rivera, T. A., Jourdan, F., Matchan, E. L., Hemming, S. R., Morgan, L. E., Kelley, S. P., Cassata, W. S., Heizler, M. T., Vasconcelos, P. M., Benowitz, J. A., Koppers, A. A. P., Mark, D. F., Niespolo, E. M., Sprain, C. J., Hames, W. E., Kuiper, K. F., Turrin, B. D., Renne, P. R., Ross, J., Nomade, S., Guillou, H., Webb, L. E., Cohen, B. A., Calvert, A. T., Joyce, N., Ganerød, M., Wijbrans, J., Ishizuka, O., He, H., Ramirez, A., Pfänder, J. A., Lopez-Martínez, M., Qiu, H., and Singer, B. S., 2020, Interpreting and reporting  $^{40}\text{Ar}/^{39}\text{Ar}$  geochronologic data: *GSA Bulletin*, v. 133, no. 3-4, p. 461-487.
- Smiley, T. M., Hyland, E. G., Cotton, J. M., and Reynolds, R. E., 2017, Evidence of early C4 grasses, habitat heterogeneity, and faunal response during the Miocene Climatic Optimum in the Mojave Region: *Palaeogeography, Palaeoclimatology, Palaeoecology*, v. 490, p. 415-430.
- Smith, E. I., Sánchez, A., Keenan, D. L., and Monastero, F. C., 2002, Stratigraphy and geochemistry of volcanic rocks in the Lava Mountains, California: Implications for the Miocene development of the Garlock fault, *Geologic Evolution of the Mojave Desert and Southwestern Basin and Range*.
- Steinthorsdottir, M., Coxall, H. K., de Boer, A. M., Huber, M., Barbolini, N., Bradshaw, C. D., Burls, N. J., Feakins, S. J., Gasson, E., Henderiks, J., Holbourn, A. E., Kiel, S., Kohn, M. J., Knorr, G., Kürschner, W. M., Lear, C. H., Liebrand, D., Lunt, D. J., Mörs, T., Pearson, P. N., Pound, M. J., Stoll, H., and Strömberg, C. A. E., 2021, The Miocene: The Future of the Past: *Paleoceanography and Paleoclimatology*, v. 36, no. 4.
- Tedford, R. H., 1965, Clarendonian faunal succession, Ricardo Formation, Kern County, California: *Geological Society of America Special Paper*, v. 87, p. 174.
- Tedford, R. H., Albright, L. B., Barnosky, A. D., Ferrusquia-Villafranca, I., Hunt, R. M., Storer, J. E., Swisher, C. C., Voorhes, M. R., Webb, S. D., and Whistler, D. P., 2004, Mammalian biochronology of the Arikareean through Hemphillian intervals (late Oligocene through early Pliocene epochs), *in* Woodburne, M. O., ed., *Late Cretaceous and Cenozoic mammals in North America: Biostratigraphy and Geochronology*: New York, New York, Columbia University Press, p. 169-213.
- Tedford, R. H., and Wang, X., 2009, Phylogenetic systematics of the North American fossil Caninae (Carnivora: Canidae): *Bulletin of the American Museum of Natural History*, v. 325, p. 218.
- Tseng, Z. J., Takeuchi, G. T., and Wang, X., 2010, Discovery of the upper dentition of *Barbourofelis whitfordi* (Nimravidae, Carnivora) and an evaluation of the genus in California: *Journal of Vertebrate Paleontology*, v. 30, no. 1, p. 244-254.

- Wang, X., and Barnes, L. G., 2008, Geology and vertebrate paleontology of western and southern North America: Contributions in honor of David P. Whistler, Volume 41: Los Angeles, Natural History Museum of Los Angeles County, p. 388.
- Webb, S. D., and Opdyke, N. D., 1995, Global Climatic Influence on Cenozoic Land Mammal Faunas, Effects of Past Global Change on Life, National Academies Press, p. 184-208.
- Whistler, D. P., and Burbank, D. W., 1992, Miocene biostratigraphy and biochronology of the Dove Spring Formation, Mojave Desert, California, and characterization of the Clarendonian mammal age (late Miocene) in California: Geological Society of America Bulletin, v. 104, p. 644-658.
- Whistler, D. P., Takeuchi, G. T., Groves, L. T., and Wang, X., 2013, Western Mojave Desert geology and vertebrate paleontology with special emphasis on the Dove Spring Formation, Society of Vertebrate Paleontology, Field Trip Guidebook, 76 p.:
- Whistler, D. P., Tedford, R. H., Takeuchi, G. T., Wang, X., Tseng, Z. J., and Perkins, M. E., 2009, Revised Miocene biostratigraphy and biochronology of the Dove Spring Formation, Mojave Desert, California: Museum of Northern Arizona Bulletin, v. 65, p. 331-362.
- Wing, S. L., 1998, Tertiary vegetation of North America as a context for mammalian evolution, *in* Janis, C. M., Scott, K. M., and Jacobs, L. L., eds., Evolution of Tertiary mammals of North America, p. 37-60.
- Woodburne, M. O., 1987, Cenozoic mammals of North America, University of California Press, 336 p.:
- , 2004, Late Cretaceous and Cenozoic mammals of North America: Biostratigraphy and geochronology, Columbia University Press, 376 p.
- Zachos, J., Pagani, M., Sloan, L., Thomas, E., and Billups, K., 2001, Trends, rhythms, and aberrations in global climate 65 Ma to Present: Science, v. 292, no. 5517, p. 686-693.



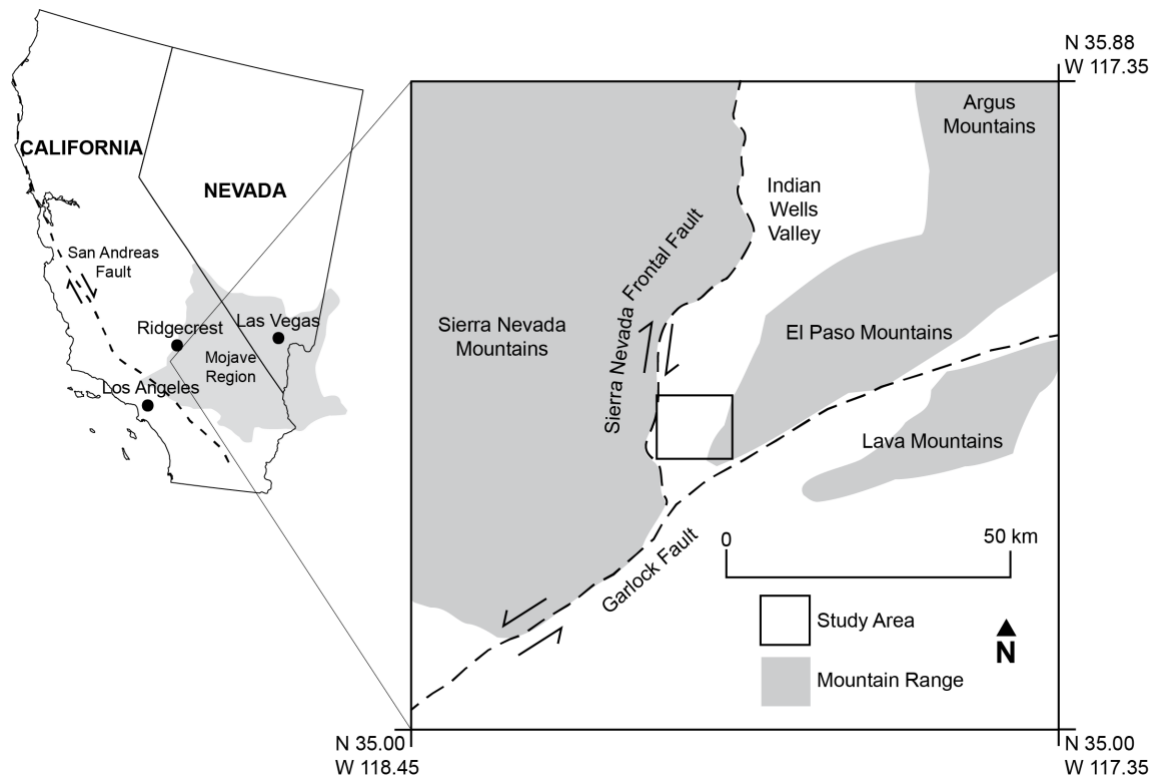


Figure 2.1: Map of study location, centered on the El Paso Basin. The basin's southern boundary is the Garlock fault and the western boundary is the frontal fault of the Sierra Nevada Range.

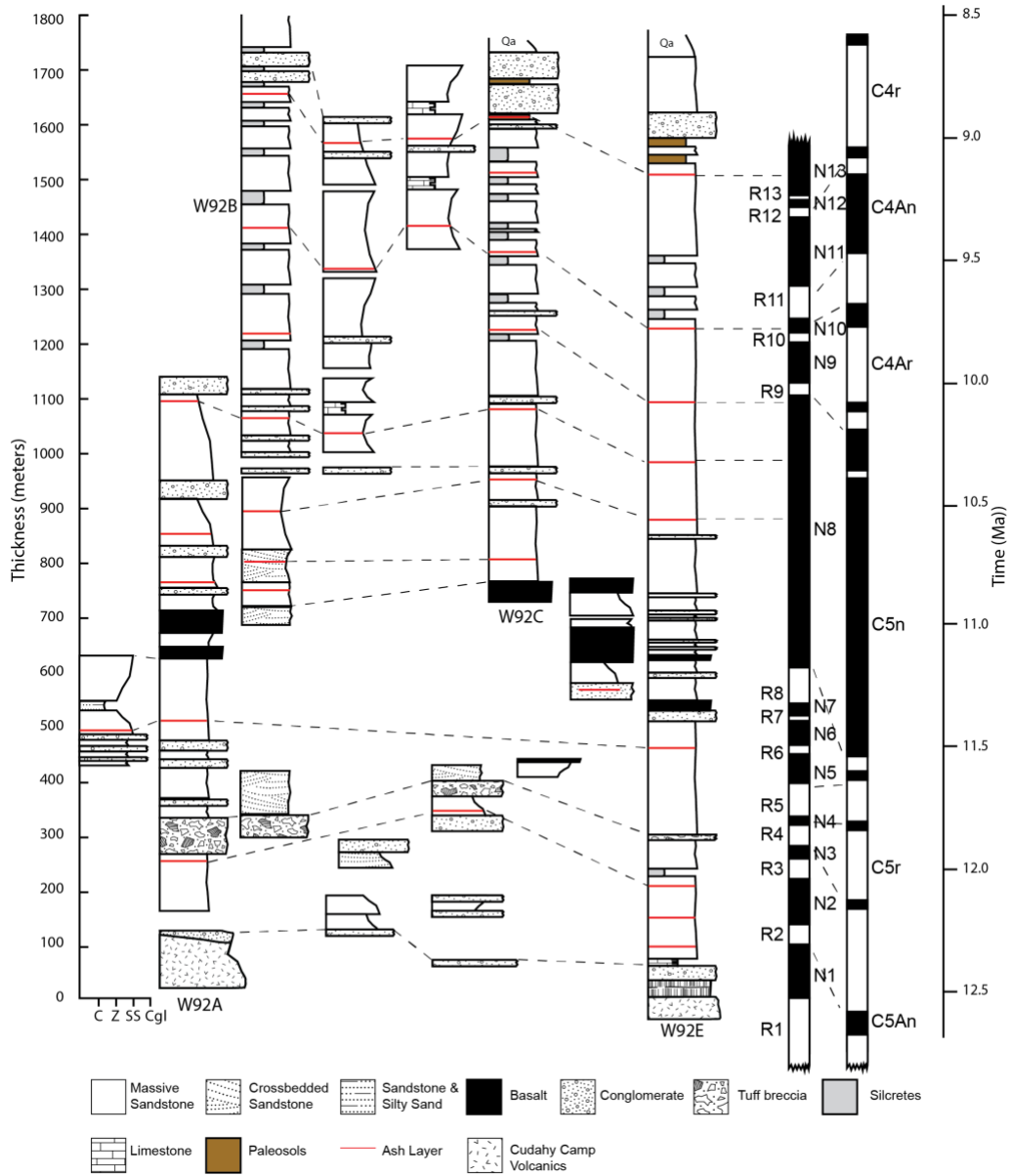


Figure 2.2: Stratigraphy of the Dove Spring Formation with updated correlations based on recalibrated radiometric dates. Top of sequence is based on new tephrochronologic correlation by Knott et al. (2022). Columns labelled W92 are modified from Whistler et al. (1992). Magnetic polarity stratigraphy from Whistler et al. (2009). Magnetic polarity time scale is modified from Hilgen et al. (2012). Lateral distance between first and last columns is approximately 8 km.

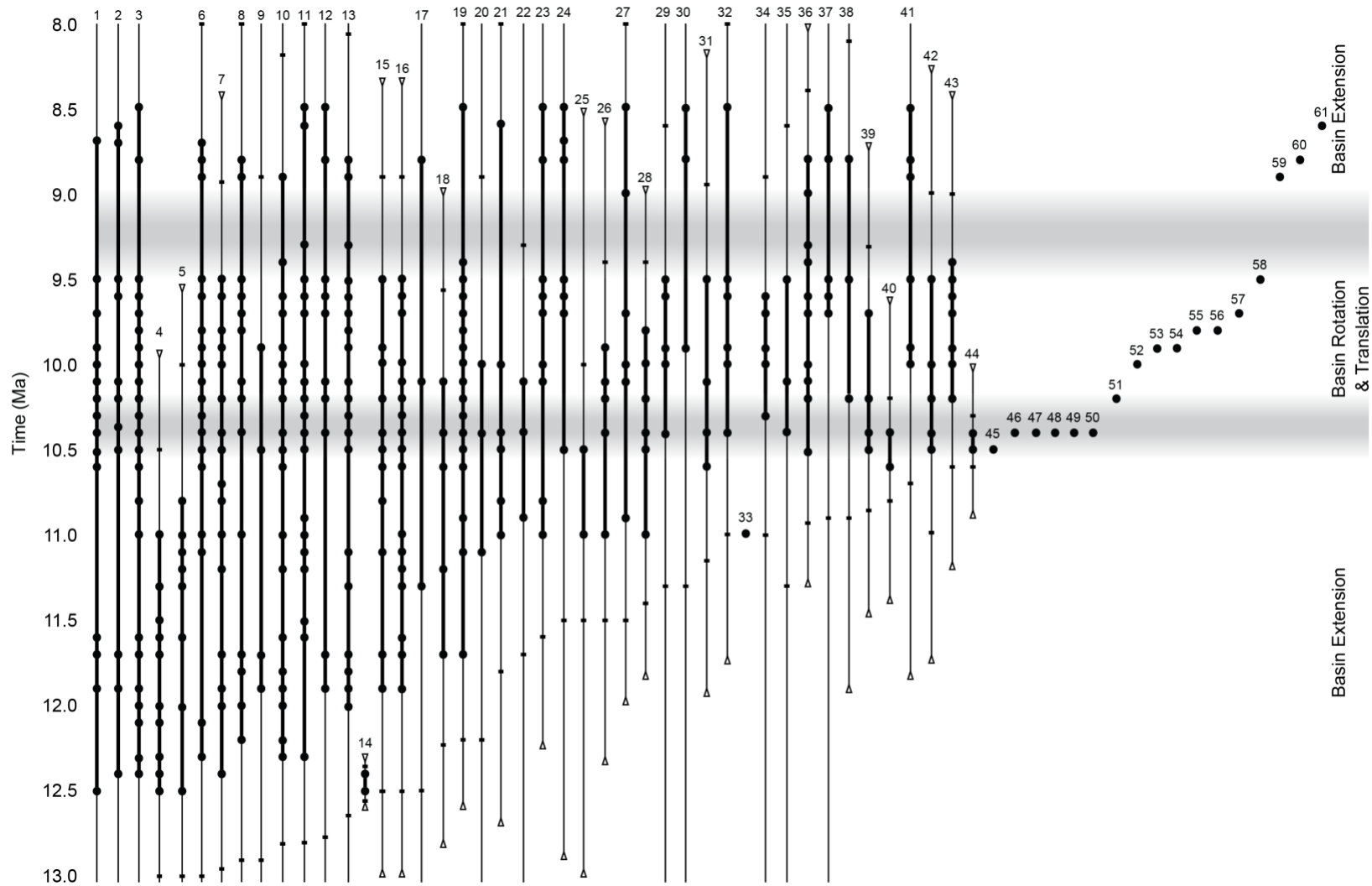


Figure 2.3: Temporal distribution of large mammals from the Dove Spring Formation. Stratigraphic occurrences of fossil taxa are denoted by black points. Thick vertical lines represent observed residence time with thin vertical lines indicating 80% confidence intervals. Unbiased point estimates of first and last occurrences are indicated by horizontal tick marks. Tectonic intervals of basin rotation and extension occur near 10.5 Ma and 9.5 Ma, respectively. Numbers correspond to taxon names listed in Appendix 1.

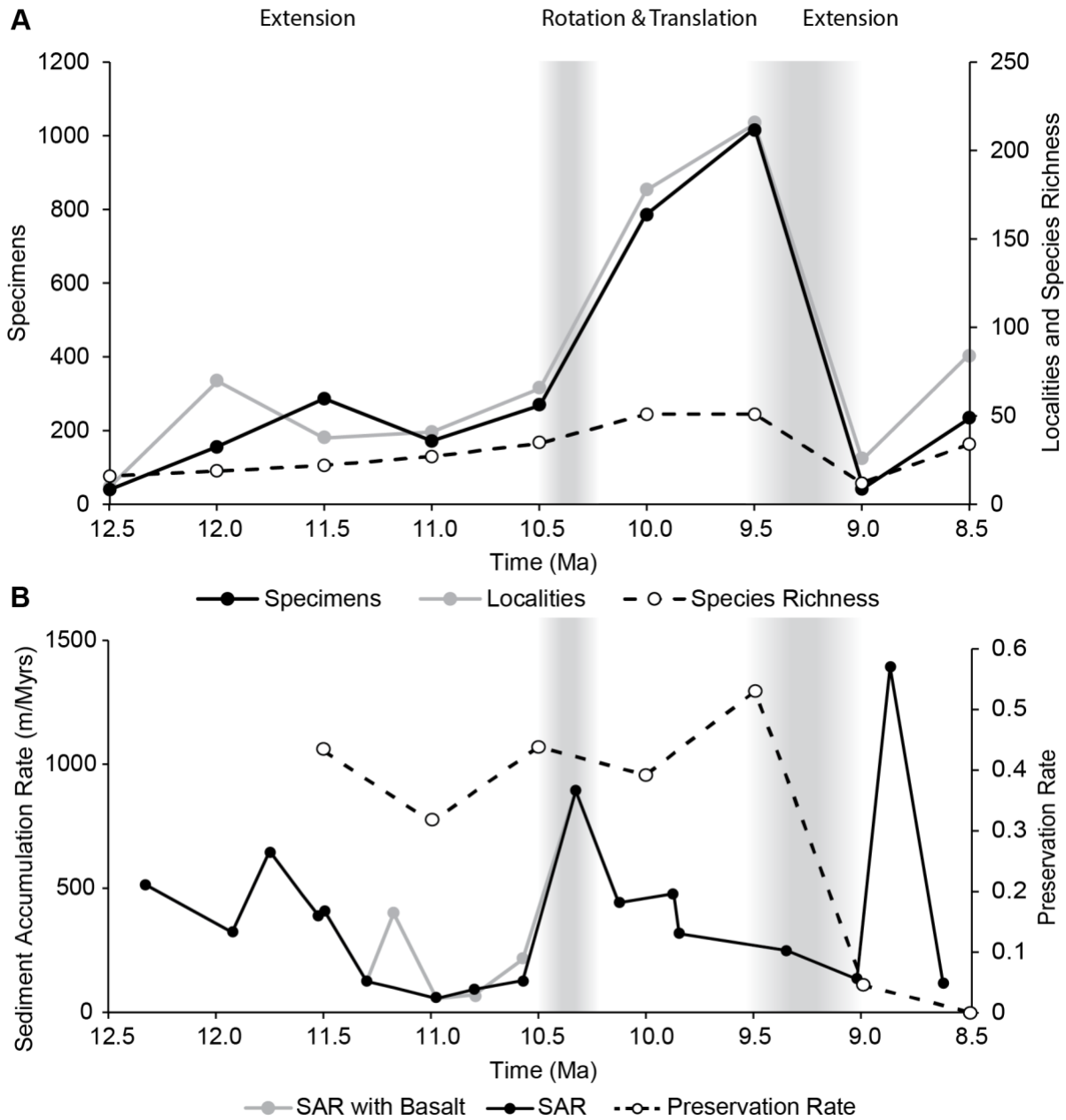


Figure 2.4: Patterns of fossil productivity and sediment accumulation in the Dove Spring Formation. A) Large mammal (>1 kg) fossil specimens, number of localities, and species richness based on raw observed occurrence data, excluding range-through taxa. Data for 0.5-million-year time bins are represented by points in the middle of each interval. Specimens recovered from the base of the section are represented by points at 12.5 Ma. B) Sediment accumulation rate (SAR) for the El Paso Basin. We removed a pair of basalt flows from our calculations to more accurately represent the basin's mode of sediment accumulation. As a result, rates were lower near 11.0 Ma and a moderate peak is no longer present. Tectonic episodes that began during the sequence are marked with grey zones to indicate uncertainty in the timing of their initiation.

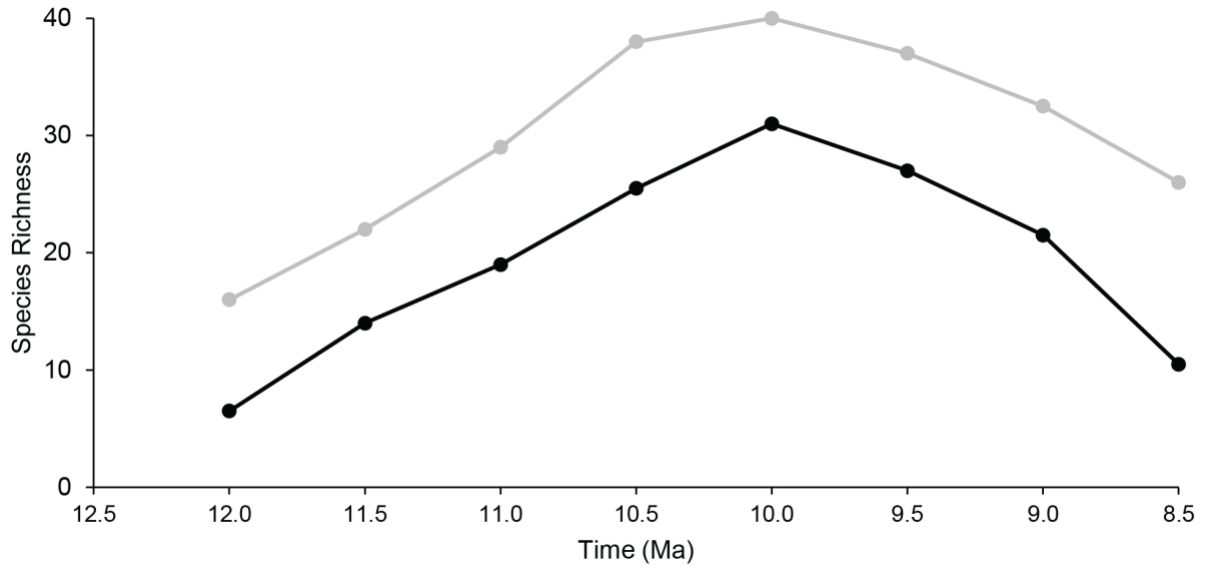


Figure 2.5: Standing richness of the Dove Spring Formation, excluding singletons due to their high dependence on preservation, resulting in a maximum species richness of 40, that is lower than the raw count (47). These plots incorporate range-through taxa and provide a better estimate of actual richness than the raw occurrence counts in Figure 4A. Both the observed and estimated fossil records follow a unimodal pattern.

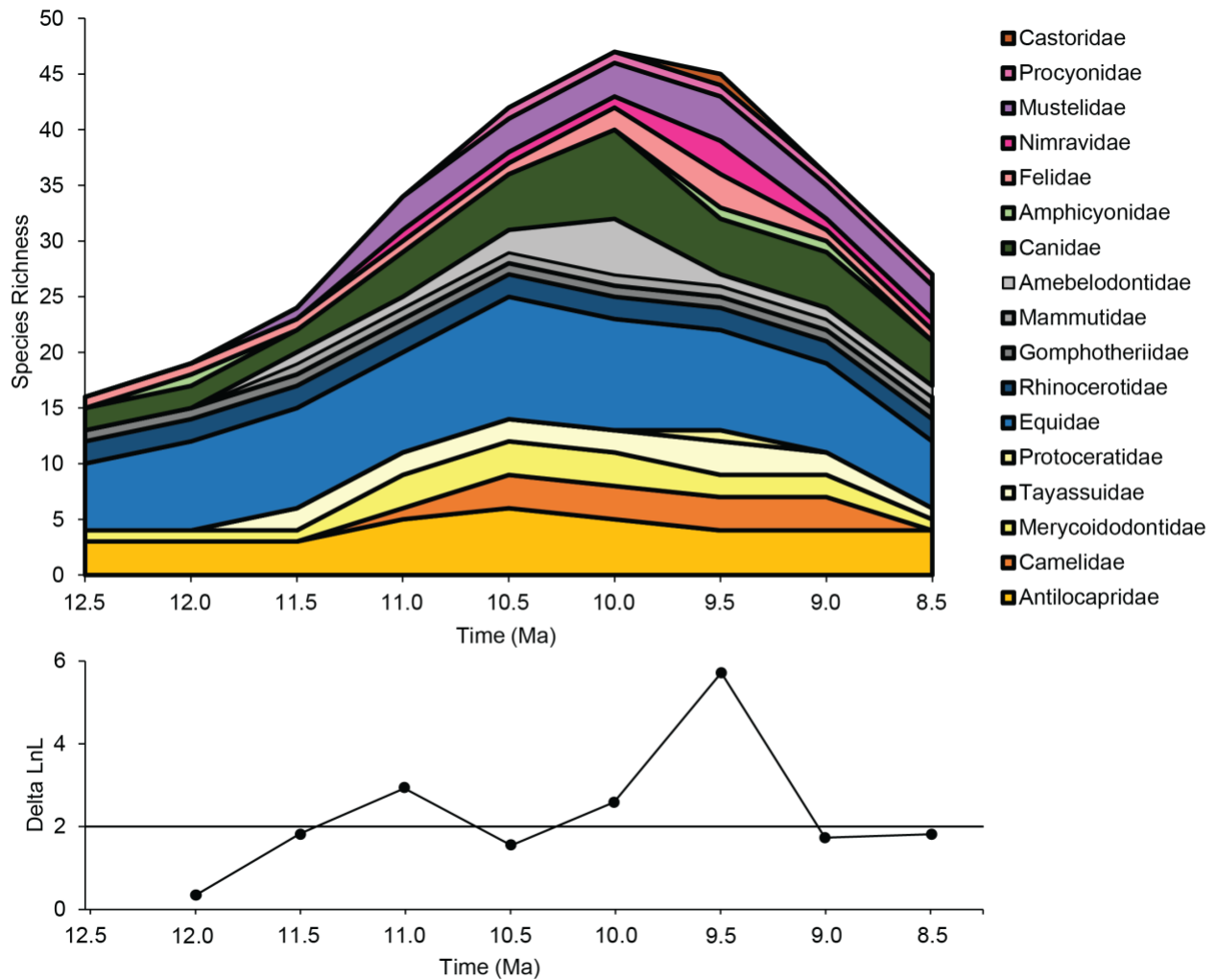


Figure 2.6: Taxonomic composition of large mammals in the Dove Spring Formation through time, including singletons. A) Stacked-richness of family-level species richness. B) Change in log-likelihood ratios (Delta LnL) of large-mammal assemblage composition. Values of 2.0 or greater indicate significant change in faunal composition for a given time interval compared to the previous interval. The 11.0 Ma peak is driven by two additional species each of Canidae, Merycoidodontidae and Mustelidae. The peak at 9.5 Ma is the result of a significant rise in nimravid species and sharp declines in canids and amebelodontid species.

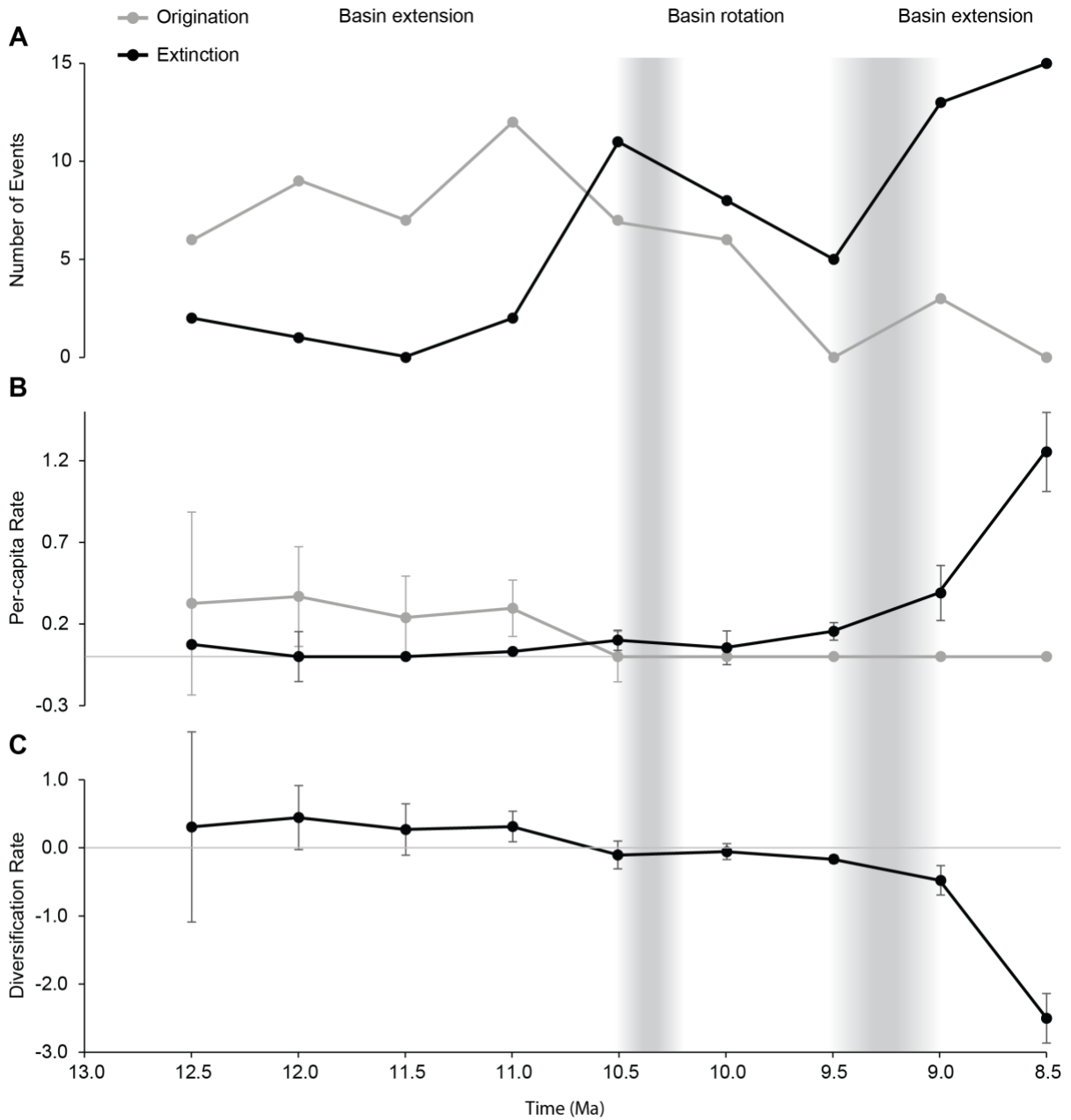


Figure 2.7: Diversification of large mammals based on estimated residence times. A) Originations (first appearances) and extinctions (last appearances) based on bottom- and top-boundary crossing taxa. B) Per-capita origination and extinction rates. C) Per-capita diversification rate. Tectonic episodes of basin rotation followed by extension are marked with grey zones to indicate uncertainty in the timing of their initiation. Confidence intervals are based on 1,000 bootstrap replicates of the dataset and are considered significant when they do not intersect zero (marked with a grey line).

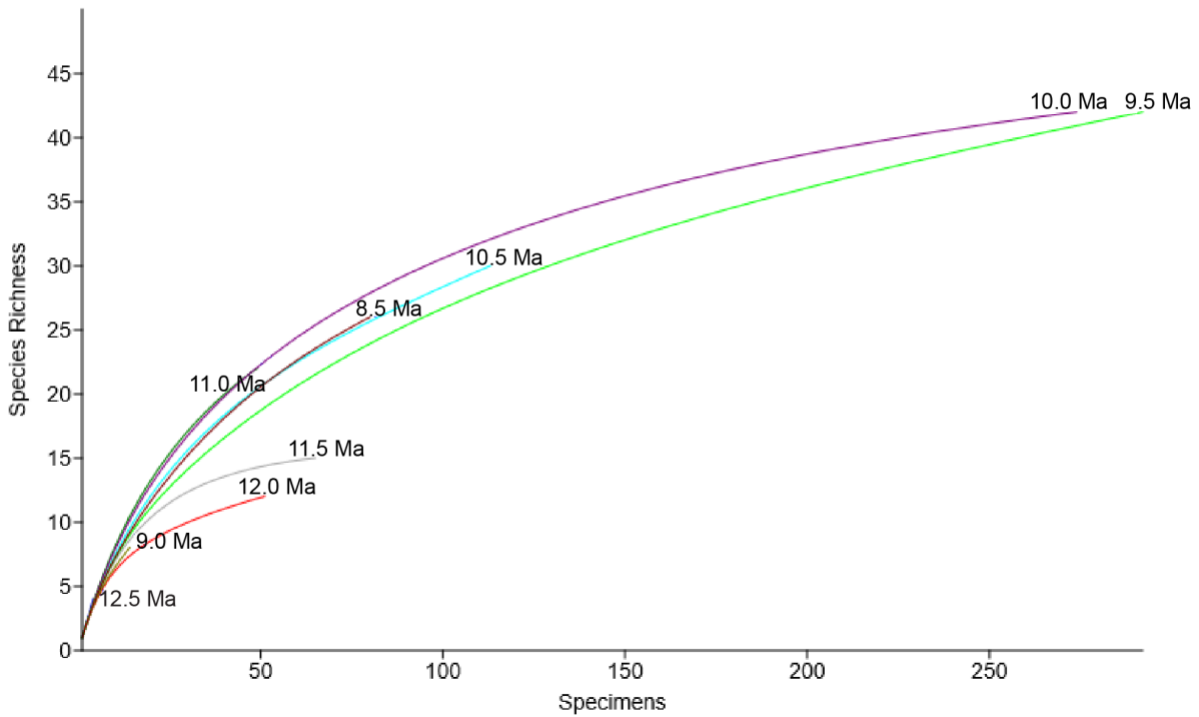


Figure 2.8: Sample-based rarefaction curves for 0.5-Myr time intervals within the Dove Spring Formation. Based on rarefaction curves that level off at much lower values of species richness, intervals 12.0 Ma and 11.5 Ma represent distinct faunas with lower species richness than intervals 11.0 Ma and younger, regardless of increased sampling. We used PAST: Paleontological Statistics version 4.09 for the rarefaction analysis.



Table 2.1: Large mammals of the Dove Spring Formation with observed and estimated first and last occurrences. Unassigned family-level designations marked with an asterisk were excluded from our diversification analyses because they span the entire formation and do not contribute meaningful information. Fossil horizons represent the number of half-million-year time bins from which any particular taxon has been recovered.

Group	Species	Obs. First Occ.	Obs. Last Occ.	Est. First Occ.	Est. Last Occ.	No. of Fossil Horizons
<b>Artiodactyla</b>						
Antilocapridae	Unassigned*	12.5	8.5			9
Antilocapridae	<i>Cosoryx</i> sp.	12.3	8.7	12.8	8.2	8
Antilocapridae	<i>Ilingoceros</i> sp.	8.5	8.5			1
Antilocapridae	<i>Merycodus</i> sp.	10.4	9.5	11.3	8.6	2
Antilocapridae	<i>Paracosoryx furlongi</i>	12.5	10.5	13.0	10.0	5
Antilocapridae	<i>Paracosoryx</i> sp.	12.0	11.0	13.0	10.5	4
Antilocapridae	<i>Plioceros</i> sp.	10.5	8.8	10.9	8.4	5
Antilocapridae	<i>Sphenophalos</i> sp.	10.9	8.5	11.5	7.9	5
Camelidae	Unassigned*	12.5	8.5			9
Camelidae	<i>Megatylopus</i> sp.	10.2	9.4	10.6	9.0	3
Camelidae	<i>Paracamelus</i> sp.	10.5	9.5	11.0	9.0	3
Camelidae	<i>Procamelus</i> sp.	11.0	9.8	11.4	9.4	4
Merycoidontidae	Unassigned*	12.5	8.5			8
Merycoidontidae	<i>Ticholeptus major</i>	10.6	10.4	10.8	10.2	2
Merycoidontidae	<i>Ustatochoerus californicus</i>	10.6	9.5	11.2	9.0	3
Merycoidontidae	<i>Ustatochoerus</i> sp.	12.5	8.7	13.3	7.9	6
Protoceratidae	<i>Leptoreodon</i> sp.	9.8	9.8			1
Tayassuidae	Unassigned	10.9	10.1	11.7	9.3	2
Tayassuidae	<i>Prosthennops</i> sp.	11.1	10.0	12.2	8.9	2
Tayassuidae	<i>Tayassu</i> sp.	9.9	9.9			1
<b>Perissodactyla</b>						
Equidae	Unassigned*	12.5	8.5			9
Equidae	<i>Cormohipparion occidentale</i>	11.9	9.5	12.5	8.9	5
Equidae	<i>Cormohipparion</i> sp.	11.9	9.5	12.5	8.9	5
Equidae	<i>Hipparion forcei</i>	11.7	8.5	12.2	8.0	7
Equidae	<i>Hipparion tehonense</i>	11.0	9.9	11.6	9.4	3
Equidae	<i>Hipparion</i> sp.	12.3	8.5	13.1	7.7	6
Equidae	<i>Hypohippus</i> sp.	10.5	10.4	10.6	10.3	2
Equidae	<i>Megahippus</i> sp.	12.5	12.4	12.6	12.3	2
Equidae	<i>Nannippus</i> sp.	10.5	10.5			1
Equidae	<i>Neohipparion</i> sp.	11.7	10.1	12.2	9.6	4
Equidae	<i>Pliohippus leardi</i>	11.0	8.5	11.6	7.9	5

Equidae	<i>Pliohippus tantalus</i>	12.4	9.5	13.0	8.9	6
Equidae	<i>Pliohippus tehonensis</i>	10.5	9.5	11.5	8.5	2
Equidae	<i>Pliohippus</i> sp.	12.4	8.0	13.5	6.9	5
Rhinocerotidae	Unassigned	11.9	8.5	12.8	7.7	6
Rhinocerotidae	<i>Aphelops</i> sp.	11.9	9.9	12.9	8.9	3
<b>Proboscidea</b>						
Amebelodontidae	<i>Amebelodon burnhami</i>	10.4	10.4			1
Amebelodontidae	<i>Amebelodon</i> sp.	11.0	10.5	11.5	10.0	2
Amebelodontidae	<i>Platybelodon</i> sp.	10.4	10.4			1
Amebelodontidae	<i>Serbelodon burnhami</i>	10.4	10.4			1
Amebelodontidae	<i>Serbelodon</i> sp.	10.2	8.8	10.9	8.1	3
Gomphotheriidae	Unassigned*	12.5	8.5			9
Gomphotheriidae	<i>Gomphotherium</i> sp.	12.3	8.5	12.8	8.0	8
Mammutidae	<i>Mammut</i> sp.	11.0	8.6	11.8	7.8	4
<b>Carnivora</b>						
Amphicyonidae	<i>Ischyrocyon</i> sp.	12	9.3	13.4	8.0	3
Canidae	Unassigned	12.0	8.8	12.6	8.2	6
Canidae (Borophaginae)	<i>Aelurodon aphobus</i>	10.4	10.4			1
Canidae (Borophaginae)	<i>Aelurodon</i> sp.	10.4	10.4			1
Canidae (Borophaginae)	<i>Tomarctus</i> sp.	11.0	9.6	12.4	8.2	2
Canidae	<i>Carpocyon webbi</i>	8.8	8.8			1
Canidae	<i>Epicyon haydeni</i>	10.5	9.7	10.9	9.3	3
Canidae	<i>Epicyon saevus</i>	12.0	8.8	12.8	8.0	5
Canidae	<i>Epicyon</i> sp.	10.3	9.6	11.0	8.9	2
Canidae	<i>Leotpcyon matthewi</i>	11.0	11.0			1
Canidae	<i>Leptocyon</i> sp.	11.3	8.8	12.6	7.6	3
Canidae	<i>Metalopex macconnelli</i>	9.7	8.5	10.9	7.3	2
Canidae	<i>Osteoborus diabloensis</i>	10.4	10.1			1
Canidae	<i>Osteoborus</i> sp.	9.7	8.8	10.6	7.9	2
Canidae	<i>Vulpes</i> sp.	8.3	8.3			1
Felidae	Unassigned	12.4	8.6	13.2	7.8	6
Felidae	<i>Ischyrosmilus</i> sp.	10.2	8.8	11.6	7.4	2
Felidae	<i>Pseudaelurus</i> sp.	9.8	9.5			1
Mustelidae	Unassigned	10.4	8.5	11.0	7.9	4
Mustelidae	<i>Martes</i> sp.	10.5	8.5	11.5	7.5	3
Mustelidae	<i>Martinogale</i> sp.	9.9	8.5	11.3	7.1	2
Mustelidae	<i>Mustela</i> sp.	9.9	9.9			1
Nimravidae	<i>Barbourofelis osborni</i>	9.5	9.5			1

Nimravidae	<i>Barbourofelis whitfordi</i>	9.7	9.7			1
Nimravidae	<i>Barbourofelis</i> sp.	10.4	9.5	11.3	8.6	2
Procyonidae	<i>Bassariscus</i> sp.	10.0	8.5	10.8	7.8	3

---

Table 2.2: Radiometric dates of prominent and laterally continuous ash layers within the Dove Spring Formation. All dates were updated with currently accepted radioactive decay constants. Sources of radiometric dates: <sup>(1)</sup> Evernden et al. (1964), <sup>(2)</sup> Cox and Diggles (1986), <sup>(3)</sup> Loomis and Burbank (1988), <sup>(4)</sup> Whistler and Burbank (1992), <sup>(5)</sup> Perkins et al. (1998), <sup>(6)</sup> Perkins and Nash (2002), <sup>(7)</sup> Smith et al. (2002), <sup>(8)</sup> Bonnicksen et al. (2007), <sup>(9)</sup> Whistler et al. (2009), <sup>(10)</sup> Knott et al. (2022).

Ash No.	Date (Ma)	Error ( $\pm$ Myr)	Radiometric System	Tephra Correlation	Date Using Updated Decay Constant (Ma)	Difference in Date (Myr)	Source
17	8.7945	0.1945		Monterey Fm.			10
16	8.5	0.15	Ar/Ar		8.52	0.02	4
15	8.4	1.8	FT		8.42	0.02	2
14	-	-					
13	-	-					
12	-	-					
11	9.7	0.2	Ar/Ar	Celetron 2	9.72	0.02	5, 6, 8
10	-	-					
9	10.2	0.2	Ar/Ar	OC3	10.22	0.02	5, 6, 8
8	10.6	0.2	Ar/Ar	OC2	10.62	0.02	5, 6, 8
7	10.4	1.6	FT		10.42	0.02	2
	10.5	0.25	Ar/Ar	Basalt	10.52	0.02	4
7	11.01	0.03	Ar/Ar	CPT XIII	11.03	0.02	5, 6, 8
6	10.5	0.25	Ar/Ar		10.52	0.02	4
5	11.2	0.1	Ar/Ar	CPT XII	11.23	0.03	5, 6, 8
4	11.64	0.05		Ammonia Tanks	11.67	0.03	5, 8
3	11.8	0.9	FT		11.83	0.03	3
3	11.83	0.05		Rainier Mesa	11.86	0.03	5, 8
2	11.7	0.2	Ar/Ar		11.55	-0.15	7
2	12.01	0.03	Ar/Ar	Ibex Hollow	12.04	0.03	5, 6, 8
1	10.3	-	K/Ar		10.32	0.02	1
1	12.15	0.04	Ar/Ar	CPT V	12.18	0.03	5, 8
0	15.1	0.5	K/Ar		15.13	0.03	2

Table 2.3: Taxon names corresponding to numbers in Figure 2.3.

1. *Ustatochoerus* sp.
2. Felidae
3. *Pliohippus* sp.
4. *Paracosoryx* sp.
5. *Paracosoryx furlongi*
6. *Hipparion* sp.
7. *Pliohippus tantalus*
8. Carnivora
9. *Aphelops* sp.
10. *Cosoryx* sp.
11. *Gomphotherium* sp.
12. Rhinocerotidae
13. Canidae
14. *Megahippus* sp.
15. *Cormohipparion occidentale*
16. *Cormohipparion* sp.
17. *Leptocyon* sp.
18. *Neohipparion* sp.
19. *Hipparion forcei*
20. *Prothennops* sp.
21. *Mammut* sp.
22. Tayassuidae
23. *Pliohippus leardi*
24. *Martes* sp.
25. *Amebelodon* sp.
26. *Hipparion tehonense*
27. *Sphenophalos* sp.
28. *Procamelus* sp.
29. *Merycodus* sp.
30. *Martinogale* sp.
31. *Ustatocheorus californicus*
32. Mustelidae
33. *Leptocyon matthewi*
34. *Epicyon* sp.
35. *Barbourofelis* sp.
36. *Plioceros* sp.
37. *Metalopex macconnelli*
38. *Serbelodon* sp.
39. *Epicyon haydeni*
40. *Ticholeptus major*
41. *Bassariscus* sp.

42. *Paracamelus* sp.
43. *Megatylopus* sp.
44. *Hypohippus* sp.
45. *Nannippus* sp.
46. *Serbelodon burnhami*
47. *Platybelodon* sp.
48. *Amebelodon burnhami*
49. *Aelurodon* sp.
50. *Aelurodon aphobus*
51. Machairodontinae
52. Ischyrosmilidae
53. *Tayassu* sp.
54. *Mustela* sp.
55. *Leptoreodon* sp.
56. *Pseudaelurus* sp.
57. *Barbourofelis whitfordi*
58. *Barbourofelis osborni*
59. *Carpocyon webbi*
60. *Illingoceros* sp.
61. *Vulpes* sp.

## Chapter 3

### **Stable Isotope Ecology of Miocene Ungulates in the Context of Tectonic History: Insights from the Dove Spring Formation, California, USA.**

#### Abstract

The Middle Miocene Climatic Transition (~14 Ma) was a period of extended cooling associated with the emergence of grasslands and an associated decline in the number of mammal species adapted to the forest biome. Isotopic measurements of carbon ( $\delta^{13}\text{C}$ ) and oxygen ( $\delta^{18}\text{O}$ ) from mammalian tooth enamel are powerful indicators of diet and moisture availability. Here we collected new enamel samples (n=153) from three common ungulate families (Antilocapridae, Camelidae, and Equidae) to examine the response of mammal communities to the tectonic history of the terrestrial Dove Spring Formation (12.5-8.5 Ma). We also added a temporal component to an existing isotopic dataset (n=89) to investigate correlations with the timing of tectonically-driven changes in the landscape. Three discrete tectonic episodes did not significantly affect the  $\delta^{13}\text{C}$  composition of dietary vegetation, suggesting that herbivores had consistent access to similar plant communities throughout the basin's four-million-year history. The diverse assemblage of mammals and vegetation has no exact modern analogue. The  $\delta^{18}\text{O}$  record from equids becomes subtly enriched over time and most closely tracks a regional signal observed in the nearby, marine Monterey Formation, with little to no correlation with the tectonic history of the basin. The  $\delta^{18}\text{O}$  record of antilocaprids and camelids exhibits more variability, likely due to their status as facultative drinkers that obtain the majority of their body water from dietary vegetation.

## 1 Introduction

The Mojave region during the Miocene was very different from today. The climate was cooler, wetter, and terrestrial mammals formed faunal assemblages unlike any observed in the modern world (Janis et al., 2000; Steinthorsdottir et al., 2021; Heusser et al., 2022). Significant environmental change is often met with ecological and evolutionary responses over geologic time (Axelrod, 1985; Anderson, 2006; Badgley et al., 2008; Blois and Hadly, 2009). This phenomenon is especially prevalent during the Miocene (23-5 Ma), an epoch characterized by massive changes in global climate, regional-scale tectonic episodes in North America, and the associated rapid and prolific diversification of terrestrial mammals (Barnosky and Carrasco, 2002; Janis et al., 2002; Badgley et al., 2008; Badgley and Finarelli, 2013; Badgley et al., 2014). The Middle Miocene Climatic Transition (MMCT) was an extended cooling interval that followed a ~3-Myr period of increased global temperatures and the diversification of many mammalian families that persist into the modern, such as antilocaprids, camelids, and equids (Zachos et al., 2001; Strömberg and McInerney, 2011; Smiley et al., 2017; Hyland et al., 2019). During the MMCT, North American grasslands emerged and expanded, with a corresponding decline of species adapted to the forest biome (Axelrod, 1985; Janis et al., 2000; Retallack, 2001; Janis et al., 2002; Chamberlain et al., 2014; Frigola et al., 2018).

Dramatically changing environmental conditions during the middle and late Miocene were principal factors in the diversification of many ungulate lineages (hoof mammals). Several North American ungulate families, including the Antilocapridae, Camelidae, and Equidae, developed ecological adaptations that led to their cosmopolitan distribution across the varied environments across the continent between 15 and 11 Ma, until a decline in species richness in the late Miocene (~11-5 Ma) (Webb, 1977; Marshall et al., 1982; Janis et al., 2000). These



adaptations included larger body sizes and longer limbs better suited for open habitats and greater hypsodonty to consume increasingly abrasive materials (Andrews and Evans, 1979; Grand, 1990; Jardine et al., 2012). Novel dietary preferences are ecological adaptations that developed alongside morphological changes (Cerling and Harris, 1999; Clementz and Koch, 2001; Perez-Barberia and Gordon, 2001; Schoeninger et al., 2002; Kohn, 2010; Kaiser et al., 2013). The goal of this study is to determine if tectonically-driven variation in topography and climate within a single basin correlates with changes in the dietary ecology of its mammal assemblages.

The fossil record provides an avenue to examine the response of mammal communities to changes in habitat types and resource availability through geologic time (Beever et al., 2003; Barnosky and Kraatz, 2007; Finarelli and Badgley, 2010; Badgley and Finarelli, 2013). Here we use stable isotope geochemistry to describe the dietary ecology of three ungulate families and test the hypothesis that changes in diet are linked to the local tectonic history. We used  $\delta^{13}\text{C}$  analysis of tooth enamel to determine the types of vegetation consumed by herbivores and  $\delta^{18}\text{O}$  analysis to investigate changes in moisture availability. Our hypothesis relies on the occurrence of significant changes in the types of vegetation consumed by herbivores in conjunction with the onset of tectonic episodes. If changes in dietary ecology occur regardless of tectonic activity, a link between herbivore diets and tectonic processes is unlikely. If such changes in dietary ecology are not observed, we would interpret a stable vegetation community.

## **2 Background**

### *2.1 Geologic setting*

The Dove Spring Formation preserves four million years of continental deposition and has high-resolution age control that allows us to track changes in faunal composition, tectonic setting, and herbivore dietary paleoecology to a resolution of at least 0.5 Myr. The Dove Spring Formation is located in the El Paso Basin of southern California's Mojave Region and has a continuous depositional record from 12.5 Ma to 8.5 Ma (Loomis and Burbank, 1988; Whistler and Burbank, 1992). The Dove Spring Formation is a primarily alluvial sequence of sediments with age constraint provided by 18 radiometrically dated ash layers (Loomis and Burbank, 1988; Whistler et al., 2009). Its stratigraphic record contains geologic evidence for three distinct tectonic intervals. These episodes include: 1) extension that began between 17-15 Ma and continued until approximately 10.0 Ma when (2) the basin was rotated and translated approximately 60 km westward along the Garlock fault (a major East-West trending, left-lateral strike-slip fault); 3) extension, subsidence, and a change in sediment source area around 9.0 Ma. The El Paso Mountains to the south provided an influx of sediments during much of the deposition of the Dove Spring Formation, but the sediment source area changed to the Sierra Nevada mountains late in the basin's depositional history (~9.0 Ma) (Loomis and Burbank, 1988).

Significant changes in topographic relief alter the moisture availability and drainage patterns within basins, which in turn affects plant communities (Axelrod, 1985; Gawthorpe and Leeder, 2000; Minnich et al., 2007; Smiley et al., 2017; Loughney et al., 2019). Well-developed paleosols, extensive soil carbonates, and silicified hardpan deposits (silcretes) are often the result of increases in the seasonality of temperature and a decline in moisture availability (Summerfield, 1983; Wynn, 2004; Breecker et al., 2009). Their presence throughout the upper two-thirds of the Dove Spring Formation has been interpreted as an indicator of a shift from

stream-dominated deposition towards more arid conditions (Loomis and Burbank, 1988; Whistler et al., 2009; Bowman et al., 2017; Liddy et al., 2018).

The nearby marine Monterey Formation (18-6 Ma) provides regional context for the climatic setting of the Dove Spring Formation (Flower and Kennett, 1993; Heusser et al., 2022; Knott et al., 2022). The Naples Beach section of the Monterey Formation is approximately 200 km southwest of the Sierra Nevada boundary with the El Paso Basin and has well-resolved oxygen isotope and pollen records. Oxygen isotope data from benthic foraminifera within the section match the global signal of cooling temperatures following the MCO (Flower and Kennett, 1993; Westerhold et al., 2020). Temperatures were relatively constant and moderate from ~13.0-10.5 Ma, and the pollen record indicates a shift in nearby coastal ecosystems from oak woodlands to beach scrub and chaparral during this time interval (Heusser et al., 2022). Global cooling resumed at 10.5 Ma and continues today (Westerhold et al., 2020). This cooling coincides with the expansion of pine forest communities within the Naples Beach section that eventually developed into a continuous coastal belt over the next two million years (Axelrod, 1977; Heusser et al., 2022). The intermittent presence of locally extinct plants with moderate moisture (mesophytic) requirements within the *Pinus*-dominated interval suggests shift towards a local climate with high summer temperatures, low precipitation (~140 mm/yr), and frequent, heavy fog by 7.5 Ma (Wahl, 2003; Heusser et al., 2022). The location of the Dove Spring Formation on the eastern side of the Sierra Nevada suggests the presence of a rain shadow, and the Monterey Formation is likely to exhibit a comparatively cooler and wetter environment. As the closest, contemporaneous record of climate and vegetation, the Monterey Formation provides some regional context for our interpretations.

Over 7,400 vertebrate fossils have been recovered from the Dove Spring Formation, at least 3,079 of which are large mammals (>1 kg). Ungulates (hoofed mammals) make up the largest proportion of this collection (Whistler and Burbank, 1992; Whistler et al., 2009). The relatively large and robust teeth of ungulates are useful for studies of paleoecology due to their common preservation and mineral composition that incorporates the isotopic signal of ingested vegetation. The fossil teeth of Antilocapridae (pronghorns), Camelidae (camels), and Equidae (horses) form the basis for our isotopic and morphological analyses because they are among the most abundant fossil remains in the collection and are often readily identifiable to the family or genus level.

## *2.2 Stable Isotope Paleoecology*

The carbon isotope composition of plants is determined by their photosynthetic pathway and is transferred to herbivores when consumed, making fossil teeth invaluable materials in the study of ecology in deep time (Quade et al., 1992; Cerling and Harris, 1999). Plants utilize one of three photosynthetic pathways: C<sub>3</sub>, C<sub>4</sub>, and Crassulacean Acid Metabolism (CAM). The dominant pathway in a flora is indicative of the environmental conditions where such plants are living (Ehleringer and Bjorkman, 1977; Tieszen et al., 1997). The C<sub>3</sub> pathway is utilized by most trees, shrubs, and cool-growing-season grasses yielding generally depleted  $\delta^{13}\text{C}$  values. Modern C<sub>3</sub> plants have a mean  $\delta^{13}\text{C}$  value of -27.0‰ and typically range between -22‰ to -35‰ (Quade et al., 1995; Ehleringer et al., 1997; Cerling et al., 2003; Kohn, 2010). The C<sub>4</sub> pathway is characteristic of plants adapted to arid conditions that are more water-efficient, particularly warm growing-season grasses (Ehleringer and Bjorkman, 1977; Ehleringer and Dawson, 1992; Pagani et al., 1999). Modern C<sub>4</sub> plants have a mean  $\delta^{13}\text{C}$  value of -13.0‰ and typically range between -9‰ to -19‰. CAM plants are typically restricted to xeric habitats, have intermediate values

between those of C<sub>3</sub> and C<sub>4</sub> plants, and are not a primary food source for most ungulates (Janis, 1988; Fox and Koch, 2003; Keeley and Rundel, 2003; Feranec and MacFadden, 2006). The  $\delta^{13}\text{C}$  values of plants are also influenced by the isotopic composition of atmospheric carbon dioxide, which varies through time (Farquhar et al., 1989). The  $\delta^{13}\text{C}_{\text{CO}_2}$  of the modern atmosphere has become more negative by about -1.5‰ over the past several hundred years, so interpretations of  $\delta^{13}\text{C}$  values must account for this offset (Friedli et al., 1986; Cerling and Harris, 1999; Tipple and Pagani, 2007).

Mammals incorporate the carbon isotopic value of consumed plants into their body tissues. The tooth enamel of large ungulate herbivores displays a consistent enrichment in  $\delta^{13}\text{C}$  values of approximately +14.0‰ from ingested vegetation due to biological fractionation (Cerling and Harris, 1999; Passey et al., 2002). Factoring in both the atmospheric composition of the middle- to late-Miocene and the fractionation of carbon isotopes in tooth enamel, herbivores that lived between 12.5 and 8.5 Ma and consumed a diet consisting exclusively of C<sub>3</sub> plants would have a  $\delta^{13}\text{C}$  value of -8.0‰ or less, while individuals consuming an entirely C<sub>4</sub> diet would have  $\delta^{13}\text{C}$  values of +2.0‰ or higher (Cerling and Harris, 1999; Passey et al., 2002; Feranec and Pagnac, 2013). By subtracting 14.5‰ from tooth enamel  $\delta^{13}\text{C}$  values, we can obtain dietary  $\delta^{13}\text{C}$  values that reflect the isotopic signature of the original vegetation consumed by herbivores. Variability of ~3.0‰ between individuals from the same population is common in both modern and fossil ungulate assemblages (Koch and Hoppe, 1998; Feranec, 2007; Bravo-Cuevas et al., 2017). Significant differences in mean  $\delta^{13}\text{C}$  values indicate resource partitioning among herbivores in modern ecosystems, suggesting that a similar pattern can be observed in fossil assemblages (Feranec, 2007).

By determining the primary carbon resources consumed by herbivores from a location, paleoenvironmental inferences about the dominant vegetation type are possible. Plants in closed-canopy habitats tend to have more depleted  $\delta^{13}\text{C}$  ratios while plants in open habitats are more enriched (Kohn, 2010; Cerling et al., 2011; Smiley et al., 2017). Due to the prevalence of  $\text{C}_3$  vegetation, forests and woodlands from a range of temperature and precipitation conditions exhibit more depleted mean and absolute  $\delta^{13}\text{C}$  values than grasslands or shrublands (Cerling et al., 1993; Wang et al., 1994; Cerling et al., 2011; Cotton et al., 2016; Blumenthal et al., 2017; Wang and Badgley, 2022).

The 4-million-year record of the Dove Spring Formation spans a time interval that potentially contains evidence for the northward expansion of the grassland ecoregion in North America during a period of dynamic tectonics. While  $\text{C}_4$  vegetation has been documented in older deposits south of the El Paso Basin, (Crowder Formation (~17 Ma), Cajon Valley Formation (16-15 Ma), and Barstow Formation (14.0-13.4 Ma)), a previous isotopic study of mammalian tooth enamel found that herbivores in the Dove Spring Formation did not consume  $\text{C}_4$  vegetation (Bowman et al., 2017; Smiley et al., 2017; Liddy et al., 2018; Loughney et al., 2019). By collecting additional samples and adding a temporal component, we investigate whether the  $\text{C}_3$  carbon resources consumed by herbivores reflect a shift from the regional woodland conditions recorded in the Monterey Formation towards a more arid-adapted and open-canopy ecosystem.

Oxygen isotopes are intrinsically tied to the hydrologic cycle and are used as indicators of past temperature and moisture conditions (Duplessy et al., 1970; Hays and Grossman, 1991; Bryant et al., 1994; Blumenthal et al., 2017). Measured as the ratio of heavy ( $^{18}\text{O}$ ) to light ( $^{16}\text{O}$ ) isotopes,  $\delta^{18}\text{O}$  is primarily controlled by temperature and is fractionated relative to ocean water

by a series of well-documented physical factors including latitude, continentality, annual precipitation, and elevation (Dansgaard, 1964; Rozanski et al., 1992; Schoeninger et al., 2002; Minnich et al., 2007; Tian et al., 2018). As latitude increases,  $\delta^{18}\text{O}$  values become more depleted (Dutton et al., 2005). With each 100 km of distance from the ocean, atmospheric  $\delta^{18}\text{O}$  values can be expected to decrease by about -2‰ (Dansgaard, 1964). The altitude effect relates to the variation of temperature with elevation and manifests as a decrease of  $\delta^{18}\text{O}$  values at higher elevations (Risi et al., 2008). The amount effect is the relationship between mean annual precipitation and isotopic fractionation: enriched  $\delta^{18}\text{O}$  values represent low rainfall and high evaporative potential; depleted  $\delta^{18}\text{O}$  values indicate high rainfall and low evaporative potential (Dansgaard, 1964; Risi et al., 2008). Oxygen is a complex isotopic system, but the magnitude of fractionation effects can be constrained by the selection of study site. The El Paso Basin is located within the mid-latitude Mojave region and its current location is only ~176 km from the nearest coast. Regional climate records from the Monterey Formation indicate a lack of freezing winter conditions during the middle to late Miocene (Flower and Kennett, 1993; Heusser et al., 2022). These collective fractionation parameters suggest that the primary control of vegetation  $\delta^{18}\text{O}$  in the Dove Spring Formation was mean annual precipitation, or the amount effect.

### *1.3 Ungulate Paleoecology*

Within the fossil record of the Dove Spring Formation, ungulates are the most abundant group in terms of specimens and species richness of large mammals recovered. We examined teeth from three families (Antilocapridae, Camelidae, and Equidae) because their teeth are abundant, readily identifiable to the family or genus, and useful for comparison among fossil localities within the Basin and Range region and elsewhere. We follow the taxonomy of Whistler et al. (2009) as it is the most recently reviewed. Our primary goal was to document ecological

attributes of ungulate lineages and interpret their history in relation to the El Paso Basin's tectonic history. If environmental conditions changed sufficiently enough to affect vegetation communities, this should be reflected in the isotopic values of the herbivores that inhabited the basin. Changes in mean  $\delta^{13}\text{C}$  values of tooth enamel for the whole assemblage of approximately 5‰ or greater would indicate significant differences in the vegetation consumed by herbivores, accounting for variability among individuals within assemblages (Hoppe et al., 2006; Feranec, 2007).

The Antilocapridae is an artiodactyl family endemic to North America that arose around 19 Ma and diversified in the late Miocene, with at least 13 genera present in North America during the time span of the Dove Spring Formation (Heffelfinger et al., 2002). The family developed gracile, long-legged skeletons relatively early in its evolutionary history (~18 Ma), and the sole modern descendant (*Antilocapra americana*) is well-adapted to open habitats (Heffelfinger et al., 2002; Semprebon and Rivals, 2007). Antilocaprids have exhibited hypsodont teeth from their earliest appearance, suggesting that these ruminants are capable of consuming abrasive vegetation (Semprebon and Rivals, 2007). However, extant antilocaprids are primarily browsers and strongly favor forbs and shrubs over grasses in the shrub-steppe, grassland, and desert biomes in which they are currently found, despite a high degree of hypsodonty that exceeds that of many obligate grazers such as modern bovids (Krueger, 1986; Rivals and Semprebon, 2006; Semprebon and Rivals, 2007). Based on micro- and mesowear analysis, fossil antilocaprids likely had similar diets, but an extensive isotopic study of the family over time has not yet been conducted (Janis, 1993; MacFadden, 1997; Janis, 2004; Feranec and MacFadden, 2006; Semprebon and Rivals, 2007). There are at least four genera of antilocaprid occur in the Dove Spring Formation, the most common of which are *Cosoryx* and *Paracosoryx*.



The Camelidae is an artiodactyl family that includes camels, llamas, vicunas, alpacas, and guanacos. Similar to the Antilocapridae, the Camelidae exhibit cursorial adaptations in their limbs from their first appearance in the late Eocene to early Oligocene (Honey et al., 1998; Semprebon and Rivals, 2010). North American fossil assemblages that include camelids are often interpreted as open, savanna-type habitats with an abundance of grasses, but the narrow muzzles, relatively small masseter muscles, and elongated necks to reach high leafy vegetation of the family suggest a specialization towards browsing behavior (Janis, 1988; Janis and Ehrhardt, 1988; Dompierre, 1995; Honey et al., 1998; Mendoza et al., 2002; Stromberg, 2004; Rybczynski et al., 2013; Morales-García et al., 2020). Modern camelid diets range from the browse-dominated diet of the Afro-Arabian *Camelus* to grass-dominated mixed feeding of the South American *Lama* (Gauthier-Pilters, 1971; Newman, 1984; Puig et al., 1997; Fraser, 1999). There are few isotopic studies that include North American camelids from the Miocene and most interpretations of their diet are based on microwear, mesowear or jaw morphology (Latorre et al., 1997; Feranec, 2003; Meachen, 2003; Feranec and MacFadden, 2006; Christianson, 2007; Semprebon and Rivals, 2010). The Dove Spring Formation contains at least four camelid species: *Aepycamelus* sp., *Hemiauchenia* sp., *Megatylopus* sp., and *Procamelus* sp., but diagnostic cranial material is relatively uncommon within the formation.

The Equidae is a family of perissodactyls that with a 55 million-year evolutionary history in North America and developed cursorial morphology during the Miocene. The Equidae of the Dove Spring Formation belong to two subfamilies: Anchitheriinae and Equinae (MacFadden and Hulbert, 1988; Hulbert, 1993). The Anchitheriinae was an older group of brachyodont, browsing horses that declined in prominence in North America from 17-14 Ma, and disappeared completely by 10 Ma (MacFadden and Hulbert, 1988; Hulbert, 1993; Eronen et al., 2010;

Semprebon et al., 2016). The Equinae first appeared in the early Miocene, diversified in the middle and late Miocene, then suffered several Late Cenozoic extinction events which led to the late Quaternary extinction of horses in North America (MacFadden and Hulbert, 1988; Hulbert, 1993; Semprebon et al., 2016). Horses first developed hypsodont cheek teeth by approximately 20 Ma, during which equid diversity increased from five genera in North America to at least thirteen (Hulbert, 1993; MacFadden and Cerling, 1994; Wang et al., 1994; Semprebon et al., 2016). A peak in hypsodont species diversity occurred between 10-9 Ma (Hulbert, 1993). The evolution of hypsodonty in equids reflects the ingestion of large amounts of abrasive material (such as soil and grasses) that accompanied a shift in feeding behavior towards grazing (Damuth and Janis, 2011). There are at least five genera of equids in the Dove Spring Formation within two subfamilies. The Equinae include: *Cormohipparion* sp., “*Dinohippus*” *leardi*, *Hipparion forcei*, *Hipparion techonense*, and *Pliohippus tantalus*. The Anchitheriinae are limited to *Megahippus* sp.

Most ungulates are obligate drinkers, meaning that they ingest water directly from streams or pools within their habitats (Kohn, 1996; Levin et al., 2006; Reid et al., 2019). The  $\delta^{18}\text{O}$  values of mammalian tooth enamel closely track the  $\delta^{18}\text{O}$  values of their drinking water and provide a record of the climatic conditions that affect the isotopic composition of meteoric water (Dansgaard, 1964; Rozanski et al., 1992). Obligate drinkers, such as equids, have  $\delta^{18}\text{O}$  values that follow local or regional trends, but some artiodactyls such as modern antilocaprids and camelids tend to have more enriched  $\delta^{18}\text{O}$  values due to their consumption of  $\delta^{18}\text{O}$ -enriched food such as leaves and fruit in environments where evaporation is greater (Kohn, 1996; Tutken et al., 2013). The  $\delta^{18}\text{O}$  enrichment of leaves is due to their sensitivity to evapotranspiration, and is more prominent away from the trunk and towards the leaf margin, where browsers consume

leaves (Levin et al., 2006; Barbour, 2007; Cernusak et al., 2022). Non-obligate or facultative drinking is an inherited trait observed in modern antilocaprids and camelids, suggesting that their ancestors possessed the ability to obtain most of their water through their diet (Gauthier-Pilters, 1971; Rivals and Semperebon, 2006; Semperebon and Rivals, 2010; Yann et al., 2013).

Isotopically, facultative drinkers tend to exhibit more enriched  $\delta^{18}\text{O}$  values than obligate drinkers due to decreasing their drinking water in arid conditions (Levin et al., 2006; Blumenthal et al., 2017). Our dataset provides an opportunity to test the hypothesis that Miocene antilocaprids and camelids were facultative drinkers. If these artiodactyl families possess this adaptation, they should exhibit enriched  $\delta^{18}\text{O}$  values with a pattern distinct from that of the equids.

### **3 Materials and Methods**

We were granted access by the Natural History Museum of Los Angeles County (NHM) to collect enamel powder from 153 teeth belonging to the Antilocapridae, Camelidae, and Equidae (Figure 3.1). We selected teeth representing four one-million year intervals of deposition: 12.5-11.5 Ma (Interval 1), 11.5-10.5 Ma (Interval 2), 10.5-9.5 Ma (Interval 3), and 9.5-8.5 (Interval 4). This approach allows us to establish mean isotopic values for each family and evaluate whether significant changes occur between subsequent one-million-year intervals. To maintain statistical robustness, we sampled individuals from each species of interest when possible, although in many cases identification was limited to the family level (Table 3.1).

#### *3.1 Sample Preparation and Stable Isotope Analysis*

Each tooth was drilled for at least 5 mg of enamel powder, with some larger specimens yielding more material. Each powder sample was treated according to the methods described in Koch et al. (1997). Samples were crushed with a mortar and pestle, then treated with 30%  $\text{H}_2\text{O}_2$

at 0.08 volume to weight, followed by 0.05 volume to weight of 0.1 M Ca-buffered acetic acid. We froze and then lyophilized each sample prior to analysis at the University of Michigan Stable Isotope Laboratory (SIL) on a Kiel IV Carbonate Device. All values were measured using the Vienna Pee Dee Belemnite (V-PDB) standard.

### *3.2 Statistical Analysis*

We used a series of parametric statistical tests (Student's t-tests) to compare results between subsequent one-million-year time intervals and investigate change in isotopic values over time. We also employed non-parametric methods (ANOVA and post-hoc Tukey-Kramer analysis) to compare time intervals. Included in our analysis of isotopic trends of the large mammal faunal assemblage are samples of 21 Gomphotheriidae (gomphotheres), 4 Merycoidodontidae (oreodonts), and 2 Rhinocerotidae (rhinoceros), all of which were analyzed by Bowman et al. (2017). We resampled 16 teeth that were previously examined by Bowman et al. (2017) to ensure that our results were consistent with previous work.

We applied 75% locally-estimated scatterplot smoothing (LOESS) to the data using PAST software v4.09 to examine variation in sample mean values over time. This non-parametric method of regression analysis fits a curve to our isotopic data and illustrates temporal trends better than a linear regression due to the variability of data and small sample size in some intervals. We used box-and-whisker plots to illustrate the isotopic range, median, and lower and upper quartiles for the whole assemblage and for individual ungulate families.

### *2.3 Morphological Characters*

We measured M/m1, M/m2 and M/m3 teeth from antilocaprids, camelids, and equids using vernier calipers. We measured crown height and width (buccal-lingual) of teeth to

calculate the hypsodonty index (HI) for each specimen by dividing the height by width. We classified taxa as brachydont ( $HI < 0.8$ ), mesodont ( $0.8 > HI < 1.2$ ), or hypsodont ( $HI = 1.2$ ) based on the classification schemes of Janis et al. (1998), Fortelius et al. (2002), and Janis (2008).

### **3 Results**

#### *3.1 Whole-assembly isotopic record*

We present the whole-assembly carbon isotopic record of the Dove Spring Formation in Figure 3.2, and we list data from individual teeth in Appendices 1 and 2. Herbivorous ungulates exhibit mean  $\delta^{13}C_{\text{enamel}}$  values of  $-9.23\text{‰}$ , with a standard deviation of  $1.30\text{‰}$  ( $n = 235$ ; Table 3.1). The isotopic range of  $\delta^{13}C_{\text{enamel}}$  in the assemblage is  $11.65\text{‰}$ , with a maximum value of  $-5.66\text{‰}$  and a minimum of  $-17.31\text{‰}$ . Whole-assembly oxygen isotopic data are presented in Figure 3.3, with data from individual teeth in Appendix 1. The mean  $\delta^{18}O_{\text{enamel}}$  for the assemblage is  $-6.51\text{‰}$ , with a standard deviation of  $1.76\text{‰}$  ( $n = 155$ ; Table 3.1). The isotopic range of  $\delta^{18}O_{\text{enamel}}$  is  $9.99\text{‰}$ , with a maximum of  $-0.62\text{‰}$ , and a minimum of  $-10.61\text{‰}$ . We resampled 16 teeth previously examined by Bowman et al. (2017), and our  $\delta^{13}C_{\text{enamel}}$  results were enriched by an average of  $+0.77\text{‰}$  compared to their published values. This variation is likely systematic due to slight differences in calibration of instrumentation and is small enough not to significantly affect our findings. Enamel  $\delta^{18}O$  values were not published by Bowman et al. (2017), so fewer specimens were available for inclusion here.

Our  $\delta^{13}C_{\text{enamel}}$  results exhibit two phases that roughly correspond with the basin's tectonic history: a pattern of depletion begins at the base of the sequence (12.5 Ma) followed by enrichment starting at 10.0 Ma. The early period of depletion corresponds with older basin

extension, while enrichment begins shortly after the start of basin rotation and translation and continues during the later period of extension. Our  $\delta^{18}\text{O}_{\text{enamel}}$  results show a gradual, modest enrichment that does not appear to correspond to the tectonic history of the basin.

### *3.2 Isotopic record of ungulate families*

Within individual ungulate families, more variation is apparent. The Antilocapridae and Camelidae exhibit variability in mean  $\delta^{13}\text{C}_{\text{enamel}}$  values with stronger signals of depletion than the Equidae (Figure 3.4). Most antilocaprid  $\delta^{13}\text{C}_{\text{enamel}}$  values fall within the range of 7.90‰ to 9.50‰, and nearly all species exhibit some depleted values lower than -10.00‰. Antilocaprid mean  $\delta^{18}\text{O}_{\text{enamel}}$  values become enriched by approximately +1.00‰ over the whole sequence, with wide isotopic ranges ( $\pm 6.00\%$ ) observed at 10.5 Ma and 8.5 Ma (Figure 3.5). Camelidae exhibit the highest magnitude of mean  $\delta^{13}\text{C}_{\text{enamel}}$  enrichment occurring after 9.5 Ma, with an increase of approximately +1.50‰. All members of the Camelidae have mean  $\delta^{13}\text{C}$  values lower than -9.50‰ (Figure 3.4). Camelid  $\delta^{18}\text{O}_{\text{enamel}}$  is the most variable of the families in this study, exhibiting marked enrichment (+2.00‰) at 10.3 Ma and 8.5 Ma, with a slight depletion (-0.50‰) at 9.5 Ma (Figure 3.5). Equids exhibit the most consistent mean  $\delta^{13}\text{C}_{\text{enamel}}$  values over the duration of the sequence, with a range of  $\pm 5.50\%$  (Figure 3.4). A slight depletion occurs in equids from 12.5 Ma to 9.7 Ma from approximately -8.00‰ to -9.00‰. Equid  $\delta^{18}\text{O}_{\text{enamel}}$  values exhibit even less variability than observed in carbon, with no significant trends (Figure 3.5). Antilocaprids and camelids exhibit wider ranges of wider  $\delta^{18}\text{O}_{\text{enamel}}$  values just before the episode of basin rotation and translation at ~10.5 Ma and just before extension resumes at ~9.5 Ma, whereas equids maintain a relatively narrow isotopic range during these tectonic intervals. The mean  $\delta^{18}\text{O}_{\text{enamel}}$  values for antilocaprids and camelids also vary more over time than those of the equids.

### 3.3 Hypsodonty Index

We took linear measurements of 123 ungulate cheek teeth with a focus on lower m1, m2, and upper M2 teeth (Figure 3.6A). None of the families displayed a statistically significant change in hypsodonty index (HI) over time, but there are subtle trends in antilocaprids and equids towards greater hypsodonty (Figure 3.6B). Camelids have the lowest HI values of the three families and all eight specimens classified as brachyodont ( $HI < 0.8$ ) belong to the Camelidae. Mesodont specimens ( $0.8 > HI < 1.2$ ) include seven camelids, two equids, and a single antilocaprid. The remaining 105 teeth are classified as hypsodont ( $HI > 1.2$ ) with a maximum HI of 4.88 and belong to antilocaprids and equids.

## 4 Discussion

The goal of this study was to evaluate the fossil ungulates from the Dove Spring Formation for ecological changes through time in relation to the tectonic history of the basin. I found only minor variation in the dietary  $\delta^{13}C$  and  $\delta^{18}O$  values of ungulates despite significant tectonic episodes that altered the relief of the El Paso Basin and its resulting topographic and hydrologic characteristics. My findings suggest that the environmental changes resulting from the basin's tectonic history were not the primary drivers of faunal change within the three ungulate groups documented. Along with the three ungulate families covered in this study, a diverse community of mammals that no longer exists inhabited the basin during the Miocene. Here I describe the isotopic signature of the assemblage as a whole and interpret isotopic variation over time in antilocaprids, camelids, and equids from the formation.

The habitats of the Dove Spring Formation supported mammal communities with high species richness in assemblages that no longer exist (i.e. multiple species of antilocaprids

occupying the same habitats as camelids, equids, and proboscideans). Conditions in this location were distinctive during the Miocene, with subtle variations that were isotopically most similar to the grassland-forest ecotonal boundaries observed between the modern Great Plains and Eastern Temperate Forest ecoregions of North America (Haveles et al., 2019).

#### *4.2 Whole-assembly Isotope Paleoecology*

Based on  $\delta^{13}\text{C}$  values, ungulates in the El Paso Basin consistently consumed similar carbon resources through time, with minor variation in response to tectonically driven changes in the basin's landscape (Figure 3.4). The regional  $\delta^{18}\text{O}$  record of Equidae indicates that temperatures and precipitation amounts remained relatively stable on the eastern side of the Sierra Nevada during the deposition of the Dove Spring Formation (Figure 3.7). Contemporaneous localities west of the Sierra Nevada exhibit  $\delta^{18}\text{O}$  values that are consistently and significantly enriched ( $p < 0.05$ ) between 10.0 and 5.0 Ma in comparison to those east of the mountain range.

The pattern of gradual depletion in ungulate  $\delta^{13}\text{C}$  values from the base of the sequence until approximately 10.5 Ma corresponds to the growth of plant communities supported by plentiful water resources, including a lake. This depletion occurs during an older episode of basin extension that began between 17 Ma and 15 Ma (Loomis and Burbank, 1988; Wernicke et al., 1996; Bahadori et al., 2018). The slight negative change in herbivore  $\delta^{13}\text{C}$  values within the Dove Spring Formation indicates that vegetation communities within the Dove Spring Formation did not always follow a regional trend towards increasing aridity (Figure 3.8). Conditions west of the Sierra Nevada became more arid during this interval, and pollen records from the Monterey Formation indicate a shift from oak woodlands to scrub-dominated vegetation along the California coast (Flower and Kennett, 1993; Heusser et al., 2022). Within the El Paso Basin, a



range of C<sub>3</sub> vegetation types was sustained by a relatively stable and moderate climate, as seen in the  $\delta^{18}\text{O}$  record from ungulate teeth (Figure 3.3). The  $\delta^{18}\text{O}$  record exhibits a more pronounced depletion ( $\sim 1.00\text{‰}$ ) than the regional signal from benthic foraminifera just before the onset of basin rotation and translation. This suggests that the local climate conditions within the El Paso basin were slightly cooler or wetter than the surrounding region between 12.5 and 10.5 Ma.

Lake sediments were absent after 10.5 Ma, suggesting that existing drainage networks were interrupted by the rotation and translation of the El Paso Basin approximately 60 km west along the Garlock fault. Between 10.5 and 10.0 Ma, all herbivores exhibit a narrower range of  $\delta^{13}\text{C}$  values, indicating that less variety of plants were available. An assemblage-wide enrichment in  $\delta^{13}\text{C}$  values began at approximately 10.0 Ma and suggests that habitats became more water-limited at this time.

$\delta^{13}\text{C}$  enrichment continued during a new episode of extension in the basin that began between 9.5 and 9.0 Ma. This interval represents an early stage of extension that promoted the development of new stream channels that transported coarse sediments from a new source area: the Sierra Nevada (Campos-Enriquez et al., 1999; Gawthorpe and Leeder, 2000). The  $\delta^{13}\text{C}$  values of the whole assemblage became more homogenous by 9.0 Ma, suggesting that ungulates consumed similar vegetation after tectonic processes altered the drainage characteristics of the basin (Figure 3.2).

The mean  $\delta^{18}\text{O}$  values for all mammal teeth from the Dove Spring Formation become gradually more enriched over time (net increase of  $0.88\text{‰}$ ; Figure 3.3). Regional climate data from benthic foraminifera in the Monterey Formation also display a trend of enrichment, although of a lower magnitude. There is little to no correlation with the tectonic history of the

basin, indicating that topographic changes did not significantly affect the temperature or precipitation characteristics of the El Paso Basin.

Tectonic processes did alter drainage networks and the available moisture for plant communities, but the changes in available vegetation were within the tolerance of most herbivorous species from the basin. Other factors, such as the preservation potential of sediments or dispersal of species throughout the greater Mojave region were likely responsible for the significant changes in species richness and faunal composition observed in the Dove Spring Formation.

#### *4.3 Isotope Paleoecology of Antilocaprid and Equid Genera*

We examined the  $\delta^{13}\text{C}$  values of several genera to determine whether intrafamily isotopic variation correlated with tectonic history. We tested the hypothesis that the primary driver for variability at this scale would be the appearance or disappearance of species. We identified two antilocaprid and three equid genera that occur throughout most of the sequence with sufficient numbers of available specimens ( $n \geq 2$ ) within most time intervals. Antilocapridae are here represented by *Paracosoryx* and *Cosoryx*, while equids are represented by *Cormohipparion*, *Hipparion*, and *Pliohippus*. Diagnostic material for camelids was too rare to identify enough specimens to the generic level for a similar comparison.

*Paracosoryx* first occurs at the base of the formation and exhibits a narrow  $\delta^{13}\text{C}$  range that is enriched relative to other ungulates before disappearing by 10.5 Ma (Figure 3.9). The genus co-occurred with the smaller *Cosoryx*, which exhibits both a longer residence time and a wider range of  $\delta^{13}\text{C}$  values. After the disappearance of *Paracosoryx*, *Cosoryx* displays a greater enrichment (+2.00‰) relative to all other ungulates at 10.0 Ma.

The three equid genera that we sampled have similar trends in mean values, although their isotopic ranges differ (Figure 3.10). *Cormohipparion* exhibits a relatively narrow range of intermediate  $\delta^{13}\text{C}$  values, with no significant changes throughout the sequence. This intermediate-sized genus has a low maximum hypsodonty index compared to other equids, suggesting that it was more limited in its ability to utilize grasses or other abrasive vegetation. *Cormohipparion* has been sampled as early as 12.0 Ma, but may have occurred alongside the other two equids at the base of the formation based on estimates of its residence time. Specimens younger than 9.5 Ma have not been recovered, but the species may have persisted in the basin until 9.0 Ma. *Hipparion* is found throughout the formation and contains the smallest equids recovered, but does have a greater range of body sizes than *Cormohipparion*. *Hipparion* also exhibits a wide isotopic range with a significant depletion and narrowing at Interval 3.1. The range of hypsodonty index values within the genus is variable, and the only mesodont equids in the formation belong to *Hipparion*. *Pliohippus* has a wide isotopic range and exhibits a variable mean  $\delta^{13}\text{C}$  signature through time, with four intervals that display significant differences from prior time intervals. The genus has the highest mean  $\delta^{13}\text{C}$  values among equids during all time intervals that it is present, with two exceptions. The first is a significant depletion during Interval 1.2, coinciding with the first occurrence of *Cormohipparion*. The second significant depletion occurs during Interval 3.1 when all taxa exhibit much narrower isotopic ranges. *Pliohippus* is the largest of the equids sampled and had the highest hypsodonty index. The large size and highly hypsodont teeth of *Pliohippus* gave it flexibility in selecting vegetation to consume and these results collectively suggest that the genus exhibited the greatest dietary plasticity of the equids in the formation.

The presence of discrete and dispersed ash deposits throughout the sequence may have had a minor influence the hypsodonty index of antilocaprids and equids, but no significant changes in hypsodonty index occurred (Figure 3.6). Camelids are generally meso- and brachyodont, but show no changes over time (Figure 3.6). The lack of significant trends in hypsodonty index indicate the absence of a selective pressure from dietary abrasiveness.

During the tectonic episode of basin rotation at 10.5 Ma, carbon resource usage by antilocaprids and equids became less variable relative to the rest of the sequence. As extension resumed,  $\delta^{13}\text{C}$  values in both families reflect the consumption of a wider variety of vegetation. The disappearance of the antilocaprid genus *Paracosoryx* precedes a significant enrichment ( $p < 0.05$ ) of 1.08‰ in the diet of *Cosoryx*. The signal of change in antilocaprid diets appears to be the result of changes in faunal composition rather than changes in resource consumption by existing species. Equids maintained similar diets to one another throughout the sequence, despite the arrival and disappearance of numerous species.

#### 4.3 Facultative Drinkers and $\delta^{18}\text{O}$

We observed changes in  $\delta^{18}\text{O}$  range of the Antilocapridae and Camelidae that may have ecological relevance (Figure 3.5). Mean  $\delta^{18}\text{O}$  values in equids are moderate throughout the sequence and fluctuate very little, on the order of  $\pm 1.50\text{‰}$ , whereas antilocaprids and camelids exhibit significant widening of their isotopic ranges (from  $\pm 2.00\text{‰}$  to  $\pm 4.00\text{‰}$ ) at 10.5 Ma and 9.0 Ma. Along with mean enrichment, these patterns suggest that the evaporative potential of the environment increased during the tectonic interval of rotation and translation. Existing channel networks were disrupted and became less reliable water sources, so artiodactyl species decreased their drinking water consumption and increased their food water intake. The absence of a highly enriched  $\delta^{18}\text{O}$  signal in equids indicates that a change in seasonality is unlikely. These findings

also indicate that equids and other obligate drinkers are more reliable indicators of environmental conditions, tracking atmospheric conditions more closely than facultative drinkers such as antilocaprids or camelids.

## **5 Conclusions**

We investigated the paleoecology of three herbivorous ungulate families in relation to the tectonic history of the Dove Spring Formation using stable isotopes of carbon and oxygen to test for changes in diet and climate conditions. While carbon and oxygen from the entire assemblage do exhibit minor variability from one tectonic episode to the next, the trends observed do not suggest drastic changes in vegetation availability or climate.  $\delta^{13}\text{C}$  is more variable than  $\delta^{18}\text{O}$ , but the weak correlation to changes in the basin's tectonic setting indicates that faunal change was not primarily a response to tectonically driven changes in vegetation. The  $\delta^{18}\text{O}$  record follows the regional trend of aridification observed in the coastal Monterey Formation. Two families (Antilocapridae and Camelidae) exhibit greater variability in  $\delta^{18}\text{O}$  during tectonically-active episodes between 10.5 and 8.5 Ma. Most of the  $\delta^{13}\text{C}$  variation within each ungulate family can be attributed to differences between genera and faunal change as species are replaced in the El Paso Basin. We acknowledge the possibility that ungulate diets included vegetation from outside the basin, particularly in genera with potentially large home ranges such as camelids and equids. An independent record of vegetation from soil carbonates would address this question by providing a primary source of carbon and oxygen isotopes that formed in-situ within paleosols.

A lack of change in hypsodonty across all taxa suggests that ecological pressure to change was minimal, despite a high amount of grit in the sequence in the form of dispersed volcanic ash.

Comparison with  $\delta^{13}\text{C}$  values from modern ecosystems suggests that the Dove Spring Formation supported diverse assemblages of large mammals within a relatively stable environment. The tectonic setting of the basin is primarily extensional, interrupted by a period of rotation and shear movement that placed it closer to the Sierra Nevada, after which incipient extension occurred near the top of the formation. Rotation and translation of the basin away from the El Paso Mountains interrupted drainage networks that supplied water to these ecosystems, creating a landscape of partially-fragmented closed-canopy and open habitats. Based on carbon isotope values, resource use among all three ungulate families was most similar during a period of basin rotation and translation away from its original sediment and hydrologic source area. A new period of extension followed, allowing the existing habitats to expand. Oxygen isotope data indicate a gradual decrease in precipitation and moisture availability, possibly facilitating greater evaporation potential within the basin.

The series of faunal assemblages within the Dove Spring Formation are no longer seen today and were supported by an ecosystem that has no modern analogue. Based on the consistent dietary ecology of ungulates, plant communities within this ecosystem were resilient and persisted during several significant episodes of tectonic activity and faunal change over the course of four million years. Rich fossil localities provide insight into the relationships between the physical environment, vegetation, and terrestrial organisms. In the case of the Dove Spring Formation, factors other than climate conditions and vegetation were responsible for changes in faunal composition and species richness. Further analyses of the history of depositional environments will yield information on the types of habitats available to mammals during each tectonic episode. A regional biogeographic approach may reveal patterns of dispersal among large mammals that coincide with faunal changes in the fossil record. These investigations

contribute to our understanding of the complex relationships between geological processes, climatic change, and ecological dynamics that shaped the history of mammal communities throughout the Mojave region.

### **Acknowledgments**

The authors thank Xiaoming Wang, Juliet Hook, and Sam McLeod of the Natural History Museum of Los Angeles County for access and assistance with fossil material in collections. We thank Brienne Catlin for her assistance in collecting samples of tooth enamel. We thank Sarah Katz and James Andrews for help with R programming. Naomi Levin for constructive discussions regarding the interpretation of isotopic results. This work was supported by Geological Society of America Grant #12905-20 and National Science Foundation Award #1949901 to FH and NSF Award 1813996 from the Integrated Earth Systems Program.

## References

- Anderson, R. C., 2006, Evolution and origin of the Central Grassland of North America: climate, fire, and mammalian grazers: *The Journal of the Torrey Botanical Society*, v. 133, no. 4, p. 626-647.
- Andrews, P. J. M. L., and Evans, E. M. N., 1979, Patterns of ecological diversity in fossil and modern mammalian faunas: *Biological Journal of the Linnean Society*, v. 11, p. 177-205.
- Axelrod, D., 1977, Outline history of California vegetation, *in* Barbour, M., and Major, J., eds., *Terrestrial vegetation of California*: New York, John Wiley & Sons, p. 139-194.
- Axelrod, D. I., 1985, Rise of the grassland biome, Central North America: *Botanical Review*, v. 51, no. 2, p. 163-201.
- Badgley, C., Barry, J. C., Morgan, M. E., Nelson, S. V., Behrensmeyer, A. K., Cerling, T. E., and Pilbeam, D., 2008, Ecological changes in Miocene mammalian record show impact of prolonged climatic forcing: *Proceedings of the National Academy of Sciences of the United States of America*, v. 105, no. 34, p. 12145-12149.
- Badgley, C., and Finarelli, J. A., 2013, Diversity dynamics of mammals in relation to tectonic and climatic history: comparison of three Neogene records from North America: *Paleobiology*, v. 39, no. 3, p. 373-399.
- Badgley, C., Smiley, T. M., and Finarelli, J. A., 2014, Great Basin mammal diversity in relation to landscape history: *Journal of Mammalogy*, v. 95, no. 6, p. 1090-1106.
- Bahadori, A., Holt, W. E., and Rasbury, E. T., 2018, Reconstruction modeling of crustal thickness of western North America since 36 Ma: *Geosphere*, v. 14, no. 3, p. 1207-1231.
- Barbour, M. M., 2007, Stable oxygen isotope composition of plant tissue: a review: *Funct Plant Biol*, v. 34, no. 2, p. 83-94.
- Barnosky, A. D., and Carrasco, M. A., 2002, Effects of Oligo-Miocene global climate changes on mammalian species richness in the northwestern quarter of the USA: *Evolutionary Ecology Research*, v. 4, p. 811-841.
- Barnosky, A. D., and Kraatz, B. P., 2007, The role of climatic change in the evolution of mammals: *BioScience*, v. 57, no. 6, p. 523-532.
- Beck, H. E., Zimmermann, N. E., McVicar, T. R., Vergopolan, N., Berg, A., and Wood, E. F., 2018, Present and future Koppen-Geiger climate classification maps at 1-km resolution: *Sci Data*, v. 5, p. 180214.
- Beever, E. A., Brussard, P. E., and Berger, J., 2003, Patterns of apparent extirpation among isolated populations of pikas (*Ochotona princeps*) in the Great Basin: *Journal of Mammalogy*, v. 84, p. 37-54.
- Blois, J. L., and Hadly, E. A., 2009, Mammalian response to Cenozoic climate change: *Annual Review of Earth and Planetary Sciences*, v. 37, p. 181-208.



- Blumenthal, S. A., Levin, N. E., Brown, F. H., Brugal, J. P., Chritz, K. L., Harris, J. M., Jehle, G. E., and Cerling, T. E., 2017, Aridity and hominin environments: *Proc Natl Acad Sci U S A*, v. 114, no. 28, p. 7331-7336.
- Bowman, C. N., Wang, Y., Wang, X., Takeuchi, G. T., Faull, M., Whistler, D. P., and Kish, S., 2017, Pieces of the puzzle: Lack of significant C4 in the late Miocene of southern California: *Palaeogeography, Palaeoclimatology, Palaeoecology*, v. 475, p. 70-79.
- Bravo-Cuevas, V. M., Rivals, F., and Priego-Vargas, J., 2017, Paleoecology ( $\delta^{13}\text{C}$  and  $\delta^{18}\text{O}$  stable isotopes analysis) of a mammalian assemblage from the late Pleistocene of Hidalgo, central Mexico and implications for a better understanding of environmental conditions in temperate North America ( $18^{\circ}$ – $36^{\circ}\text{N}$  Lat.): *Palaeogeography, Palaeoclimatology, Palaeoecology*, v. 485, p. 632-643.
- Breecker, D. O., Sharp, Z. D., and McFadden, L. D., 2009, Seasonal bias in the formation and stable isotopic composition of pedogenic carbonate in modern soils from central New Mexico, USA: *Geological Society of America Bulletin*, v. 121, no. 3-4, p. 630-640.
- Bryant, J. D., Froelich, P. N., Showers, W. J., and Genna, B. J., 1996, A tale of two quarries: Biologic and taphonomic signatures in the oxygen isotope composition of tooth enamel phosphate from Modern and Miocene equids: *Palaios*, v. 11, no. 4, p. 397-408.
- Bryant, J. D., Luz, B., and Froelich, P. N., 1994, Oxygen isotopic composition of fossil horse tooth phosphate as a record of continental paleoclimate: *Palaeogeography, Palaeoclimatology, Palaeoecology*, v. 107, p. 303-316.
- Campos-Enriquez, J. O., Ortega-Ramirez, J., Alatrliste-Vilchis, D., Cruz-Gatica, R., and Cabral-Cano, E., 1999, Relationship between extensional tectonic style and the paleoclimatic elements at Laguna El Fresnal, Chihuahua Desert, Mexico: *Geomorphology*, v. 28, p. 75-94.
- Cerling, T. E., and Harris, J. M., 1999, Carbon isotope fractionation between diet and bioapatite in ungulate mammals and implications for ecological and paleoecological studies: *Oecologia*, v. 120, p. 347-363.
- Cerling, T. E., Harris, J. M., and Passey, B. H., 2003, Diets of East African Bovidae based on stable isotope analysis: *Journal of Mammalogy*, v. 84, no. 2, p. 456-470.
- Cerling, T. E., Wang, Y., and Quade, J., 1993, Expansion of C4 ecosystems as an indicator of global ecological change in the late Miocene: *Nature*, v. 361, p. 344-345.
- Cerling, T. E., Wynn, J. G., Andanje, S. A., Bird, M. I., Korir, D. K., Levin, N. E., Mace, W., Macharia, A. N., Quade, J., and Remien, C. H., 2011, Woody cover and hominin environments in the past 6 million years: *Nature*, v. 476, no. 7358, p. 51-56.
- Cernusak, L. A., Barbeta, A., Bush, R. T., Eichstaedt, R., Ferrio, J. P., Flanagan, L. B., Gessler, A., Martín-Gómez, P., Hirl, R. T., Kahmen, A., Keitel, C., Lai, C. T., Munksgaard, N. C., Nelson, D. B., Ogée, J., Roden, J. S., Schnyder, H., Voelker, S. L., Wang, L., Stuart-Williams, H., Wingate, L., Yu, W., Zhao, L., and Cuntz, M., 2022, Do  $^2\text{H}$  and  $^{18}\text{O}$  in leaf water reflect environmental drivers differently?: *New Phytologist*, v. 235, no. 1, p. 41-51.

- Chamberlain, C. P., Winnick, M. J., Mix, H. T., Chamberlain, S. D., and Maher, K., 2014, The impact of neogene grassland expansion and aridification on the isotopic composition of continental precipitation: *Global Biogeochemical Cycles*, v. 28, p. 992-1004.
- Christianson, K. T., 2007,  $\delta^{13}\text{C}$  and  $\delta^{18}\text{O}$  analysis of Cenozoic Camelidae tooth enamel, Great Plains [Bachelor of Arts: Carleton College, 33 p.
- Clementz, M. T., and Koch, P. L., 2001, Differentiating aquatic mammal habitat and foraging ecology with stable isotopes in tooth enamel: *Oecologia*, v. 129, no. 3, p. 461-472.
- Cotton, J. M., Cerling, T. E., Hoppe, K. A., Mosier, T. M., and Still, C. J., 2016, Climate,  $\text{CO}_2$ , and the history of North American grasses since the Last Glacial Maximum: *Science Advances*, v. 2, no. e1501346.
- Crowley, B. E., Koch, P. L., and Davis, E. B., 2008, Stable isotope constraints on the elevation history of the Sierra Nevada Mountains, California: *Geological Society of America Bulletin*, v. 120, no. 5-6, p. 588-598.
- Damuth, J., and Janis, C. M., 2011, On the relationship between hypsodonty and feeding ecology in ungulate mammals, and its utility in palaeoecology: *Biol Rev Camb Philos Soc*, v. 86, no. 3, p. 733-758.
- Dansgaard, W., 1964, Stable isotopes in precipitation: *Tellus*, v. 16, p. 436-468.
- Dompierre, H., 1995, Observations on the diets of six late Cenozoic North American camelids: *Camelops, Hemiauchenia, Palaeolama, Procamelus, Alforjas, and Megatylopus*: University of Toronto, 209 p.
- Duplessy, J. C., Labeyrie, J., Lalou, C., and Nguyen, H. V., 1970, Continental climatic variations between 130,000 and 90,000 years BP: *Nature*, v. 226, p. 631-633.
- Dutton, A., Wilkinson, B. H., Welker, J. M., Bowen, G. J., and Lohmann, K. C., 2005, Spatial distribution and seasonal variation in  $^{18}\text{O}/^{16}\text{O}$  of modern precipitation and river water across the conterminous USA: *Hydrological Processes*, v. 19, no. 20, p. 4121-4146.
- Ehleringer, J., and Bjorkman, O., 1977, Quantum yields for  $\text{CO}_2$  uptake in  $\text{C}_3$  and  $\text{C}_4$  plants: *Plant Physiology*, v. 59, p. 86-90.
- Ehleringer, J. R., Cerling, T. E., and Helliker, B. R., 1997,  $\text{C}_4$  photosynthesis, atmospheric  $\text{CO}_2$ , and climate: *Oecologia*, v. 112, p. 285-299.
- Ehleringer, J. R., and Dawson, T. E., 1992, Water uptake by plants: perspectives from stable isotope composition: *Plant, Cell and Environment*, v. 15, p. 1073-1082.
- Eronen, J. T., Evans, A. R., Fortelius, M., and Jernvall, J., 2010, The impact of regional climate on the evolution of mammals: A case study using fossil horses: *Evolution*, v. 64, no. 2, p. 398-408.
- Farquhar, G. D., Ehleringer, J. R., and Hubick, K. T., 1989, Carbon isotope discrimination and photosynthesis: *Annual review of plant physiology and plant molecular biology*, v. 40, p. 503-537.

- Feranec, R. S., 2003, Stable isotopes, hypsodonty, and the paleodiet of *Hemiauchenia* (Mammalia: Camelidae): A morphological specialization creating ecological generalization: *Paleobiology*, v. 29, p. 230-242.
- , 2007, Stable carbon isotope values reveal evidence of resource partitioning among ungulates from modern C<sub>3</sub>-dominated ecosystems in North America: *Palaeogeography, Palaeoclimatology, Palaeoecology*, v. 252, no. 3-4, p. 575-585.
- Feranec, R. S., and MacFadden, B. J., 2006, Isotopic discrimination of resource partitioning among ungulates in C<sub>3</sub>-dominated communities from the Miocene of Florida and California: *Paleobiology*, v. 32, no. 2, p. 191-205.
- Feranec, R. S., and Pagnac, D., 2013, Stable carbon isotope evidence for the abundance of C<sub>4</sub> plants in the middle Miocene of southern California: *Palaeogeography, Palaeoclimatology, Palaeoecology*, v. 388, p. 42-47.
- Finarelli, J. A., and Badgley, C., 2010, Diversity dynamics of Miocene mammals in relation to the history of tectonism and climate: *Proceedings of the Royal Society B: Biological Sciences*, v. 277, p. 2721-2726.
- Flower, B. P., and Kennett, J. P., 1993, Relations between Monterey Formation deposition and middle Miocene global cooling: Naples Beach section, California: *Geology*, v. 21, p. 877-880.
- Fortelius, M., Eronen, J. T., Jernvall, J., Liu, L., Pushkina, D., Rinne, J., Tesakov, A., Vislobokova, I., Zhang, Z., and Zhou, L., 2002, Fossil mammals resolve regional patterns of Eurasian climate change over 20 million years: *Evolutionary Ecology Research*, v. 4, p. 1005-1016.
- Fox, D. L., and Koch, P. L., 2003, Tertiary history of C<sub>4</sub> biomass in the Great Plains, USA: *Geology*, v. 31, no. 9, p. 809-812.
- Fraser, M. D., 1999, A comparison of the diet composition of guanacos (*Lama guanicoe*) and sheep when grazing swards with different clover : grass ratios: *Small Ruminant Research*, v. 32, p. 231-241.
- Friedli, H., Lotscher, H., Oeschger, H., Siegenthaler, U., and Stauffer, B., 1986, Ice core record of the <sup>13</sup>C/<sup>12</sup>C ratio of atmospheric CO<sub>2</sub> in the past two centuries: *Nature*, v. 324, p. 1-2.
- Frigola, A., Prange, M., and Schulz, M., 2018, Boundary conditions for the Middle Miocene Climate Transition (MMCT v1.0): *Geoscientific Model Development*, v. 11, p. 1607-1626.
- Gauthier-Pilters, H., 1971, Behavior and ecology of camels in the Sahara, *in* Geist, V., and Walther, F., eds., IUCN, Volume 2: Calgary, Alberta, Canada, International Union for the Conservation of Nature and Natural Resources, p. 542-551.
- Gawthorpe, R. L., and Leeder, M. R., 2000, Tectono-sedimentary evolution of active extensional basins: *Basin Research*, v. 12, p. 195-218.

- Grand, T. I., 1990, The functional anatomy of body mass, *in* Damuth, J., and MacFadden, B. J., eds., *Body size in mammalian paleobiology: Estimation and biological implications*, Cambridge University Press.
- Haveles, A. W., Fox, D. L., and Fox-Dobbs, K., 2019, Carbon isoscapes of rodent diets in the Great Plains USA deviate from regional gradients in C4 grass abundance due to a preference for C3 plant resources: *Palaeogeography, Palaeoclimatology, Palaeoecology*, v. 527, p. 53-66.
- Hays, P. D., and Grossman, E. L., 1991, Oxygen isotopes in meteoric calcite cements as indicators of continental paleoclimate: *Geology*, v. 19, no. 5, p. 441-444.
- Heffelfinger, J. R., O'Gara, B. W., Janis, C. M., and Babb, R., 2002, A bestiary of ancestral antilocaprids: *Proceedings of the 20th Biennial Pronghorn Workshop*, p. 87-111.
- Heusser, L. E., Barron\*, J. A., Blake, G. H., and Nichols, J., 2022, Miocene terrestrial paleoclimates inferred from pollen in the Monterey Formation, Naples Coastal Bluffs section, California, *Understanding the Monterey Formation and Similar Biosiliceous Units across Space and Time*, p. 215-227.
- Honey, J. G., Harrison, J. A., Prothero, D. R., and Stevens, M. S., 1998, Camelidae, *in* Janis, C., Scott, K. M., and Jacobs, L. L., eds., *Evolution of Tertiary mammals of North America, Volume 1: Terrestrial Carnivores, Ungulates, and Ungulatelike Mammals*: Cambridge, Cambridge University Press, p. 439-462.
- Hulbert, R. C., 1993, Taxonomic evolution in North American Neogene horses (Subfamily Equinae): The rise and fall of an adaptive radiation: *Paleobiology*, v. 19, no. 2, p. 216-234.
- Hyland, E. G., Sheldon, N. D., Smith, S. Y., and Stromberg, C. A. E., 2019, Late Miocene rise and fall of C4 grasses in the western United States linked to aridification and uplift: *Geological Society of America Bulletin*, v. 131, no. 1/2, p. 224-234.
- Janis, C., 2004, The species richness of Miocene browsers, and implications for habitat type and primary productivity in the North American grassland biome: *Palaeogeography, Palaeoclimatology, Palaeoecology*, v. 207, no. 3-4, p. 371-398.
- Janis, C., 2008, An evolutionary history of browsing and grazing ungulates, *in* Gordon, I. J., and Prins, H. H. T., eds., *The ecology of browsing and grazing, Volume 195*: Berlin, Springer, p. 21-42.
- Janis, C. M., An estimation of tooth volume and hypsodonty indices in ungulate mammals, and the correlation of these factors with dietary preferences, *in* *Proceedings Teeth revisited: Proceedings of the VIIth International Symposium on Dental Morphology*, Paris, 1988, p. 367-387.
- Janis, C. M., 1993, Tertiary mammal evolution in the context of changing climates, vegetation, and tectonic events: *Annual Review of Ecology, Evolution, and Systematics*, v. 24, p. 467-500.

- Janis, C. M., Damuth, J., and Theodor, J. M., 2000, Miocene ungulates and terrestrial primary productivity: Where have all the browsers gone?: *Proceedings of the National Academy of Sciences of the United States of America*, v. 97, no. 14, p. 7899-7904.
- , 2002, The origins and evolution of the North American grassland biome: the story from the hoofed mammals: *Palaeogeography, Palaeoclimatology, Palaeoecology*, v. 177, p. 183-198.
- Janis, C. M., and Ehrhardt, D., 1988, Correlation of relative muzzle width and relative incisor width with dietary preference in ungulates: *Zoological Journal of the Linnean Society*, v. 92, no. 3, p. 267-284.
- Janis, C. M., Scott, K. M., and Jacobs, L. L., 1998, *Evolution of Tertiary mammals of North America*, 703 p.:
- Jardine, P. E., Janis, C. M., Sahney, S., and Benton, M. J., 2012, Grit not grass: Concordant patterns of early origin of hypsodonty in Great Plains ungulates and Glires: *Palaeogeography, Palaeoclimatology, Palaeoecology*, v. 365-366, p. 1-10.
- Kaiser, T. M., Müller, D. W. H., Fortelius, M., Schulz, E., Codron, D., and Clauss, M., 2013, Hypsodonty and tooth facet development in relation to diet and habitat in herbivorous ungulates: implications for understanding tooth wear: *Mammal Review*, v. 43, no. 1, p. 34-46.
- Keeley, J. E., and Rundel, P. W., 2003, Evolution of CAM and C4 carbon-concentrating mechanisms: *International Journal of Plant Sciences*, v. 164, no. S3, p. S55-S77.
- Knott, J. R., Sarna-Wojcicki, A. M., Barron, J. A., Wan, E., Heizler, L., and Martinez, P., 2022, Tephrochronology of the Miocene Monterey and Modelo Formations, California, *Understanding the Monterey Formation and Similar Biosiliceous Units across Space and Time*, p. 187-214.
- Koch, P. L., and Hoppe, K. A., 1998, The isotopic ecology of late Pleistocene mammals in North America (Part 1. Florida): *Chemical Geology*, v. 52, p. 119-138.
- Koch, P. L., Tuross, N., and Fogel, M. L., 1997, The effects of sample treatment and diagenesis on the isotopic integrity of carbonate in biogenic hydroxylapatite: *Journal of Archaeological Science*, v. 24, no. 417-429.
- Kohn, M. J., 1996, Predicting animal  $\delta^{18}\text{O}$ : Accounting for diet and physiological adaptation: *Geochimica et Cosmochimica Acta*, v. 60, no. 23, p. 4811-4829.
- Kohn, M. J., 2010, Carbon isotope compositions of terrestrial C3 plants as indicators of (paleo)ecology and (paleo)climate: *Proc Natl Acad Sci U S A*, v. 107, no. 46, p. 19691-19695.
- Krueger, K., 1986, Feeding relationships among bison, pronghorn, and prairie dogs: An experimental analysis: *67*, v. 3, no. 760-770.
- Latorre, C., Quade, J., and McIntosh, W. C., 1997, Expansion of C4 grasses and global change in the late Miocene: Stable isotope evidence from the Americas: *Earth and Planetary Science Letters*, v. 146, p. 83-96.

- Levin, N. E., Cerling, T. E., Passey, B. H., Harris, J. M., and Ehleringer, J. R., 2006, A stable isotope aridity index for terrestrial environments: *Proceedings of the National Academy of Sciences of the United States of America*, v. 103, no. 30, p. 11201-11205.
- Liddy, H. M., Feakins, S. J., Corsetti, F. A., Sage, R., Dengler, N., Whistler, D. P., Takeuchi, G. T., Faull, M., and Wang, X., 2018, Photosynthetic pathway of grass fossils from the upper Miocene Dove Spring Formation, Mojave Desert, California: *Palaeogeography, Palaeoclimatology; Palaeoecology*, v. 490, p. 131-140.
- Loomis, D. P., and Burbank, D. W., 1988, The stratigraphic evolution of the El Paso basin, southern California: Implications for the Miocene development of the Garlock fault and uplift of the Sierra Nevada: *Geological Society of America Bulletin*, v. 100, p. 12-28.
- Loughney, K. M., Hren, M. T., Smith, S. Y., and Pappas, J. L., 2019, Vegetation and habitat change in southern California through the Middle Miocene Climatic Optimum: Paleoenvironmental records from the Barstow Formation, Mojave Desert, USA: *GSA Bulletin*.
- MacFadden, B. J., 1997, Origin and evolution of the grazing guild in new world terrestrial mammals: *Trends in Ecology & Evolution*, v. 12, no. 5, p. 182-187.
- MacFadden, B. J., and Cerling, T. E., 1994, Fossil horses, carbon isotopes and global change: *Trends in Ecology & Evolution*, v. 9, no. 12, p. 481-486.
- MacFadden, B. J., and Hulbert, R. C., 1988, Explosive speciation at the base of the adaptive radiation of Miocene grazing horses: *Nature*, v. 336, p. 466-468.
- Maguire, K. C., 2015, Dietary niche stability of equids across the mid-Miocene Climatic Optimum in Oregon, USA: *Palaeogeography, Palaeoclimatology, Palaeoecology*, v. 426, p. 297-307.
- Marshall, L. G., Webb, S. D., Sepkoski, J. J., and Raup, D. M., 1982, Mammalian evolution and the Great American Interchange: *Science*, v. 215, no. 4538, p. 1351-1357.
- Meachen, J. A., 2003, A new species of *Hemiauchenia* (Camelidae: Lamini) from the Plio-Pleistocene of Florida [Master of Science: University of Florida, 67 p.
- Mendoza, M., Janis, C. M., and Palmqvist, P., 2002, Characterizing complex craniodental patterns related to feeding behaviour in ungulates: a multivariate approach: *Journal of Zoology*, v. 258, no. 2, p. 223-246.
- Minnich, R. A., Keeler-Wolf, T., and Schoenherr, A. A., 2007, Climate, Paleoclimate, and Paleovegetation, in Barbour, M., ed., *Terrestrial Vegetation of California*, University of California Press, p. 43-70.
- Morales-García, N. M., Säilä, L. K., and Janis, C. M., 2020, The Neogene Savannas of North America: A Retrospective Analysis on Artiodactyl Faunas: *Frontiers in Earth Science*, v. 8.
- Newman, D. M. R., 1984, The feeds and feeding habits of Old and New World camels, in Cockrill, W. R., ed., *The Camelid: An all-purpose animal*: Uppsala, Scandinavian Institute of African Studies, p. 250-292.

- Olson, D. M., Dinerstein, E., Wikramanayake, E. D., Burgess, N. D., Powell, G. V. N., Underwood, E. C., D'Amico, J. A., Itoua, I., Strand, H. E., Morrison, J. C., Loucks, C. J., Allnutt, T. F., Ricketts, T. H., Kura, Y., Lamoreux, J. F., Wettengel, W. W., Hedao, P., and Kassem, K. R., 2001, Terrestrial ecoregions of the world: A new map of life on earth: *BioScience*, v. 51, no. 11, p. 933-938.
- Pagani, M., Freeman, K. H., and Arthur, M. A., 1999, Late Miocene atmospheric CO<sub>2</sub> concentrations and the expansion of C4 grasses: *Science*, v. 285, no. 5429, p. 876-879.
- Passey, B. H., Cerling, T. E., Perkins, M. E., Voorhies, M. R., Harris, J. M., and Tucker, S. T., 2002, Environmental change in the Great Plains: An isotopic record from fossil horses: *The Journal of Geology*, v. 110, p. 123-140.
- Peel, M. C., Finlayson, B. L., and McMahon, T. A., 2007, Updated world map of Köppen-Geiger climate classification: *Hydrology and Earth System Sciences*, v. 11, no. 5, p. 1633-1644.
- Perez-Barberia, F. J., and Gordon, I. J., 2001, Relationships between oral morphology and feeding style in the Ungulata: a phylogenetically controlled evaluation: *Proc Biol Sci*, v. 268, no. 1471, p. 1023-1032.
- Puig, S., Videla, F., and Cona, M. I., 1997, Diet and abundance of the guanaco (*Lama guanicoe* Muller 1776) and food availability in northern Patagonia, Argentina: *Journal of Arid Environments*, v. 34, p. 215-224.
- Putman, R. J., 1996, Ungulates in temperate forest ecosystems: Perspectives and recommendations for future research: *Forest Ecology and Management*, v. 88, p. 205-214.
- Quade, J., Cerling, T. E., Andrews, P., and Alpagut, B., 1995, Paleodietary reconstruction of Miocene faunas from Pasalar, Turkey using stable carbon and oxygen isotopes of fossil tooth enamel: *Journal of Human Evolution*, v. 28, p. 373-384.
- Quade, J., Cerling, T. E., Barry, J. C., Morgan, M. E., Pilbeam, D. R., Chivas, A. R., Lee-Thopr, J. A., and Merwe, N. J. v. d., 1992, A 16-Ma record of paleodiet using carbon and oxygen isotopes in fossil teeth from Pakistan: *Chemical Geology*, v. 94, p. 183-192.
- Reid, R. E. B., Jones, M., Brandt, S., Bunn, H., and Marshall, F., 2019, Oxygen isotope analyses of ungulate tooth enamel confirm low seasonality of rainfall contributed to the African Humid Period in Somalia: *Palaeogeography, Palaeoclimatology, Palaeoecology*, v. 534.
- Retallack, G. J., 2001, Cenozoic expansion of grasslands and climatic cooling: *Journal of Geology*, v. 109, p. 407-426.
- Risi, C., Bony, S., and Vimeux, F., 2008, Influence of convective processes on the isotopic composition ( $\delta^{18}\text{O}$  and  $\delta\text{D}$ ) of precipitation and water vapor in the tropics: 2. Physical interpretation of the amount effect: *Journal of Geophysical Research*, v. 113, no. D19.
- Rivals, F., and Semprebon, G. M., 2006, A comparison of dietary habits of a large sample of the Pleistocene Pronghorn *Stockoceros onusrosagris* from the Papago Springs Cave in Arizona to the modern *Antilocapra americana*: *Journal of Vertebrate Paleontology*, v. 26, p. 495-500.

- Rozanski, K., Araguas-Araguas, L., and Gonfiantini, R., 1992, Relation between long-term trends of oxygen-18 isotope composition of precipitation and climate: *Science*, v. 258, p. 981-985.
- Rybczynski, N., Gosse, J. C., Harington, C. R., Wogelius, R. A., Hidy, A. J., and Buckley, M., 2013, Mid-Pliocene warm-period deposits in the High Arctic yield insight into camel evolution: *Nat Commun*, v. 4, p. 1550.
- Schoeninger, M. J., Kohn, M. J., and Valley, J. W., 2002, Tooth oxygen isotope ratios as paleoclimate monitors in arid ecosystems: *Biogeochemical approaches to paleodietary analysis*, p. 117-140.
- Semprebon, G. M., and Rivals, F., 2007, Was grass more prevalent in the pronghorn past? An assessment of the dietary adaptations of Miocene to Recent Antilocapridae (Mammalia: Artiodactyla): *Palaeogeography, Palaeoclimatology; Palaeoecology*, v. 253, p. 332-347.
- , 2010, Trends in the paleodietary habits of fossil camels from the Tertiary and Quaternary of North America: *Palaeogeography, Palaeoclimatology, Palaeoecology*, v. 295, no. 1-2, p. 131-145.
- Semprebon, G. M., Rivals, F., Solounias, N., and Jr., R. C. H., 2016, Paleodietary reconstruction of fossil horses from the Eocene through Pleistocene of North America: *Palaeogeography, Palaeoclimatology; Palaeoecology*, v. 442, p. 110-127.
- Smiley, T. M., Hyland, E. G., Cotton, J. M., and Reynolds, R. E., 2017, Evidence of early C4 grasses, habitat heterogeneity, and faunal response during the Miocene Climatic Optimum in the Mojave Region: *Palaeogeography, Palaeoclimatology; Palaeoecology*, v. 490, p. 415-430.
- Steinthorsdottir, M., Coxall, H. K., de Boer, A. M., Huber, M., Barbolini, N., Bradshaw, C. D., Burls, N. J., Feakins, S. J., Gasson, E., Henderiks, J., Holbourn, A. E., Kiel, S., Kohn, M. J., Knorr, G., Kürschner, W. M., Lear, C. H., Liebrand, D., Lunt, D. J., Mörs, T., Pearson, P. N., Pound, M. J., Stoll, H., and Strömberg, C. A. E., 2021, The Miocene: The Future of the Past: *Paleoceanography and Paleoclimatology*, v. 36, no. 4.
- Stromberg, C. A. E., 2004, Using phytolith assemblages to reconstruct the origin and spread of grass-dominated habitats in the great plains of North America during the late Eocene to early Miocene: *Palaeogeography, Palaeoclimatology, Palaeoecology*, v. 207, no. 3-4, p. 239-275.
- Strömberg, C. A. E., and McInerney, F. A., 2011, The Neogene transition from C3 to C4 grasslands in North America: assemblage analysis of fossil phytoliths: *Paleobiology*, v. 37, no. 1, p. 50-71.
- Summerfield, M. A., 1983, Silcrete as a palaeoclimatic indicator: evidence from southern Africa: *Palaeogeography, Palaeoclimatology, Palaeoecology*, v. 41, no. 1-2, p. 65-79.
- Tian, C., Wang, L., Kaseke, K. F., and Bird, B. W., 2018, Stable isotope compositions ( $\delta(2)H$ ,  $\delta(18)O$  and  $\delta(17)O$ ) of rainfall and snowfall in the central United States: *Sci Rep*, v. 8, no. 1, p. 6712.



- Tieszen, L. L., Reed, B. C., Bliss, N. B., Wylie, B. K., and DeJong, D. D., 1997, N<sub>2</sub>O and C<sub>3</sub> and C<sub>4</sub> production, and Distributions in Great Plains Grassland Land Cover Classes: Ecological Applications, v. 7, no. 1, p. 59-78.
- Tipple, B. J., and Pagani, M., 2007, The early origins of terrestrial C<sub>4</sub> photosynthesis: Annual Review of Earth and Planetary Sciences, v. 35, p. 435-461.
- Tutken, T., Kaiser, T. M., Vennemann, T., and Merceron, G., 2013, Opportunistic feeding strategy for the earliest old world hypsodont equids: evidence from stable isotope and dental wear proxies: PLoS One, v. 8, no. 9, p. e74463.
- Wahl, E. R., 2003, Assigning climate values to modern pollen surface sample sites and validating modern analog climate reconstructions in the southern California region: Madroño, v. 50, no. 4, p. 271-285.
- Wang, B., and Badgley, C., 2022, Carbon-isotope composition of artiodactyl tooth enamel and its implications for paleodiets: Frontiers in Ecology and Evolution, v. 10.
- Wang, Y., Cerling, T. E., and MacFadden, B. J., 1994, Fossil horses and carbon isotopes: new evidence for Cenozoic dietary, habitat, and ecosystem changes in North America: Palaeogeography, Palaeoclimatology, Palaeoecology, v. 107, p. 269-279.
- Webb, S. D., 1977, A history of savanna vertebrates in the new world. Part I: North America: Annual Review of Ecology and Systematics, v. 8, p. 355-380.
- Wernicke, B., Clayton, R., Ducea, M., Jones, C. H., Park, S., Ruppert, S., Saleeby, J., Snow, J. K., Squires, L., Fliedner, M., Jiracek, G., Keller, R., Klemperer, S., Luetgert, J., Malin, P., Miller, K., Mooney, W., Oliver, H., and Phinney, R., 1996, Origin of high mountains in the continents: The Southern Sierra Nevada: Science, v. 271, no. 5246, p. 190-193.
- Westerhold, T., Marwan, N., Drury, A. J., Liebrand, D., Agnini, C., Anagnostou, E., Barnet, J. S. K., Bohaty, S. M., De Vleeschouwer, D., Florindo, F., Frederichs, T., Hodell, D. A., Holbourn, A. E., Kroon, D., Lauretano, V., Littler, K., Lourens, L. J., Lyle, M., Pälike, H., Röhl, U., Tian, J., Wilkens, R. H., Wilson, P. A., and Zachos, J. C., 2020, An astronomically dated record of Earth's climate and its predictability over the last 66 million years: Science, v. 369, no. 6509, p. 1383-1387.
- Whistler, D. P., and Burbank, D. W., 1992, Miocene biostratigraphy and biochronology of the Dove Spring Formation, Mojave Desert, California, and characterization of the Clarendonian mammal age (late Miocene) in California: Geological Society of America Bulletin, v. 104, p. 644-658.
- Whistler, D. P., Tedford, R. H., Takeuchi, G. T., Wang, X., Tseng, Z. J., and Perkins, M. E., 2009, Revised Miocene biostratigraphy and biochronology of the Dove Spring Formation, Mojave Desert, California: Museum of Northern Arizona Bulletin, v. 65, p. 331-362.
- Wynn, J. G., 2004, Influence of Plio-Pleistocene aridification on human evolution: evidence from paleosols of the Turkana Basin, Kenya: Am J Phys Anthropol, v. 123, no. 2, p. 106-118.

Yann, L. T., DeSantis, L. R. G., Haupt, R. J., Romer, J. L., Corapi, S. E., and Ettenson, D. J., 2013, The application of an oxygen isotope aridity index to terrestrial paleoenvironmental reconstructions in Pleistocene North America: *Paleobiology*, v. 39, no. 4, p. 576-590.

Zachos, J., Pagani, M., Sloan, L., Thomas, E., and Billups, K., 2001, Trends, rhythms, and aberrations in global climate 65 Ma to Present: *Science*, v. 292, no. 5517, p. 686-693.

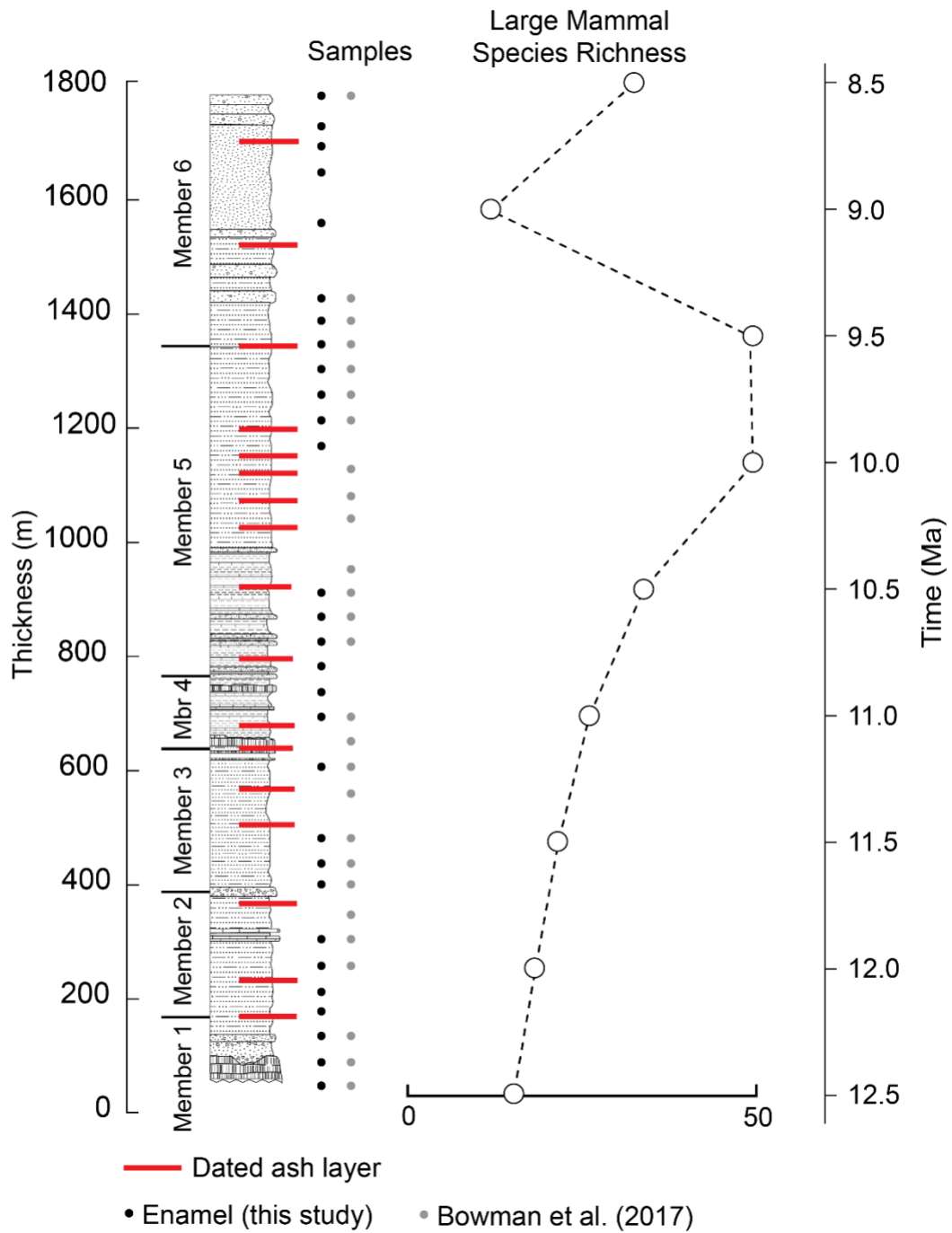


Figure 3.1: Composite stratigraphic column for the Dove Spring Formation showing stratigraphic position of samples. Species richness includes family-, genus-, and species-level designations.

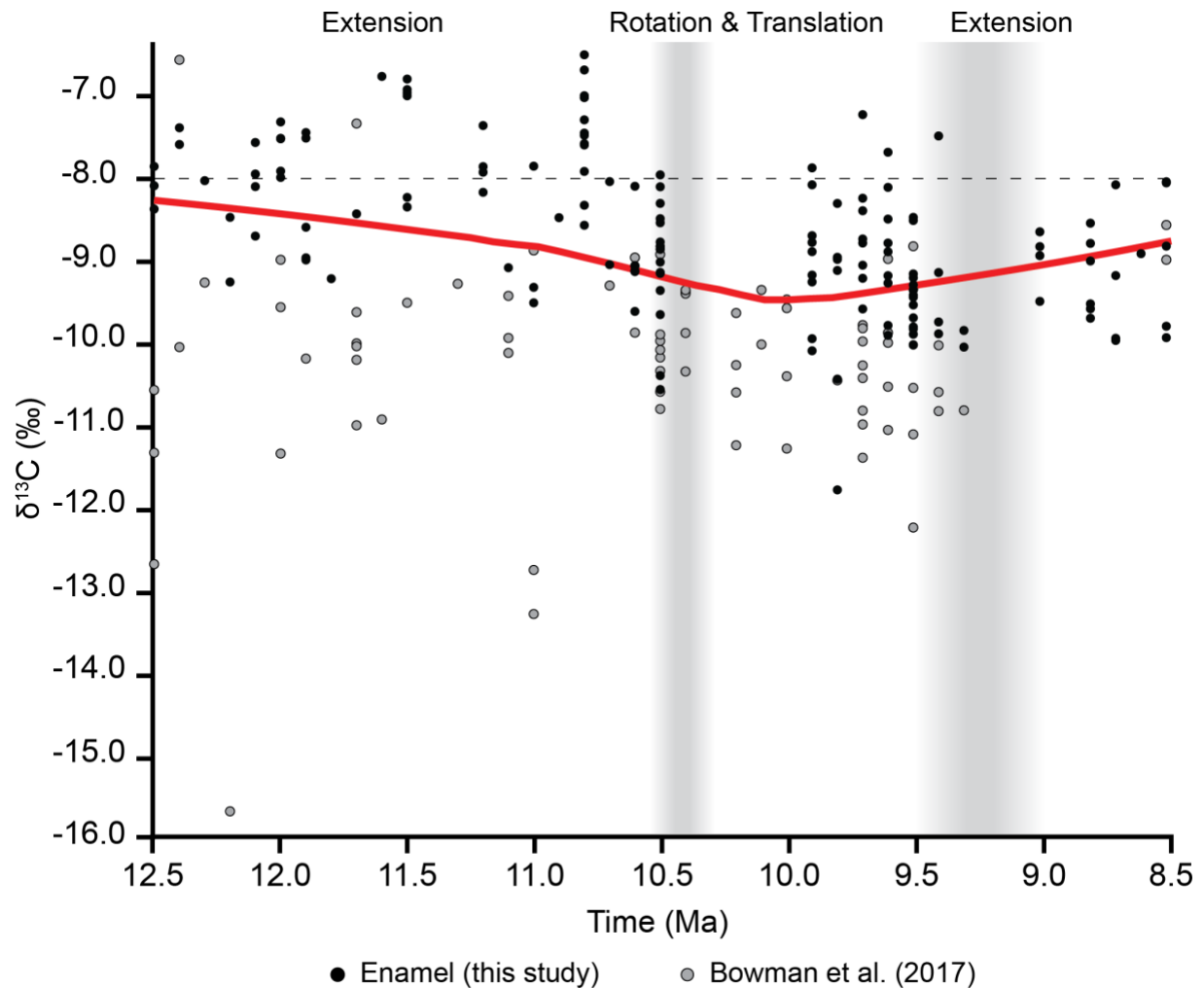


Figure 3.2:  $\delta^{13}\text{C}$  values for tooth enamel in the Dove Spring Formation. Plot includes tooth enamel  $\delta^{13}\text{C}$  data from Bowman et al. (2017; grey dots). Individuals below  $-8.0\text{‰}$  (indicated by dotted line) represent pure  $\text{C}_3$  feeders, with those above representing mixed feeders. While variation does correspond with the tectonic history of the basin, the isotopic range of each time interval is within the range observed in populations.  $\delta^{13}\text{C}$  values became more depleted as older extension progressed, with an enrichment trend beginning at 10.0 Ma lagging behind an episode of basin rotation and translation that began no later than 10.3 Ma. Depleted outliers at 12.5, 11.0, and 9.5 Ma belong to the Gomphotheriidae. Tectonic episode boundaries are marked with grey zones to indicate uncertainty in the timing of their initiation.

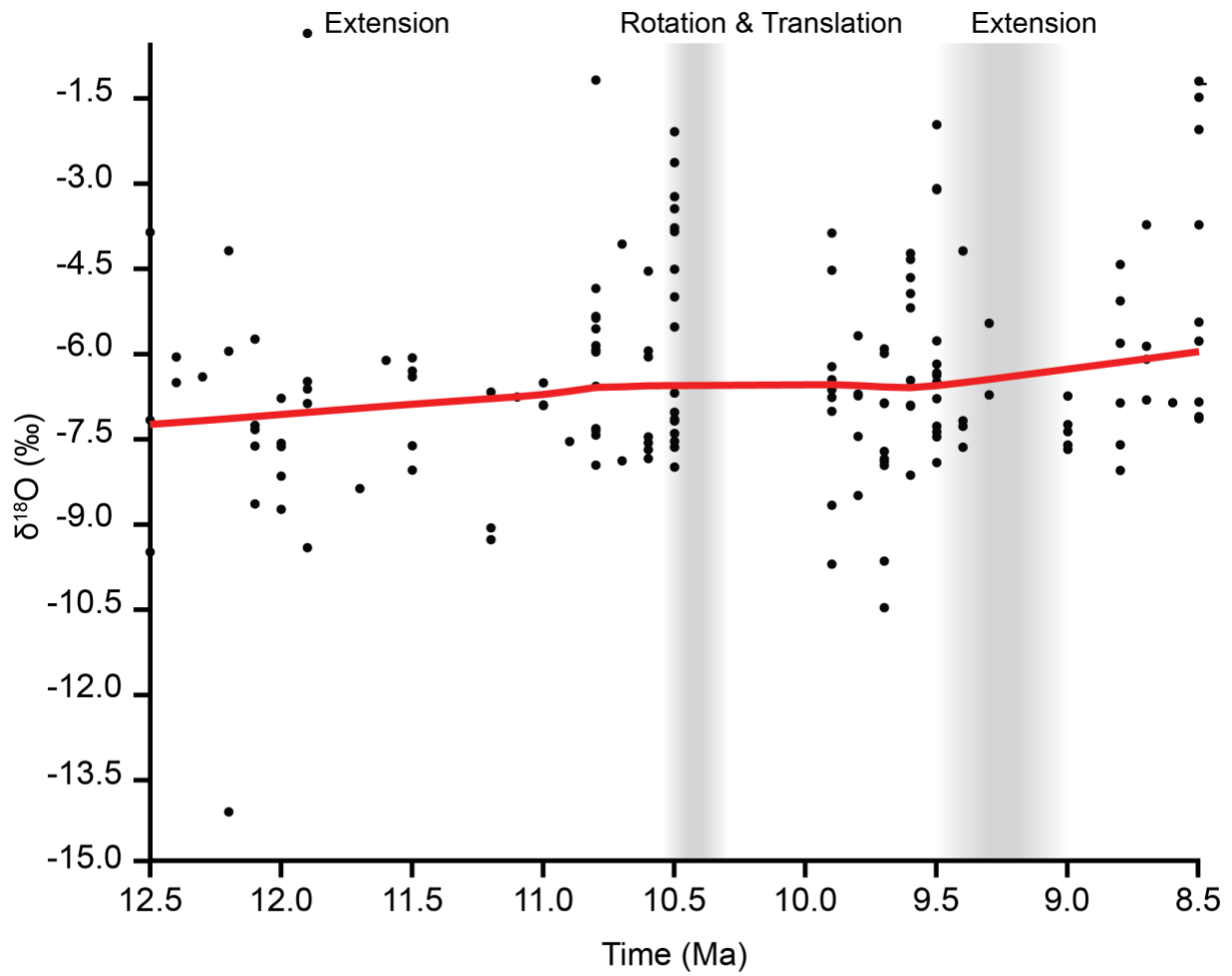


Figure 3.3:  $\delta^{18}\text{O}$  values for ungulates in the Dove Spring Formation become gradually more enriched over time. No significant changes occur over time, but a minor depletion coincides with basin rotation and translation. Wide isotopic ranges at approximately 10.5 Ma and 9.5 Ma are driven by values observed in Antilocapridae and Camelidae. Tectonic episode boundaries are marked with grey zones to indicate uncertainty in the timing of their initiation.

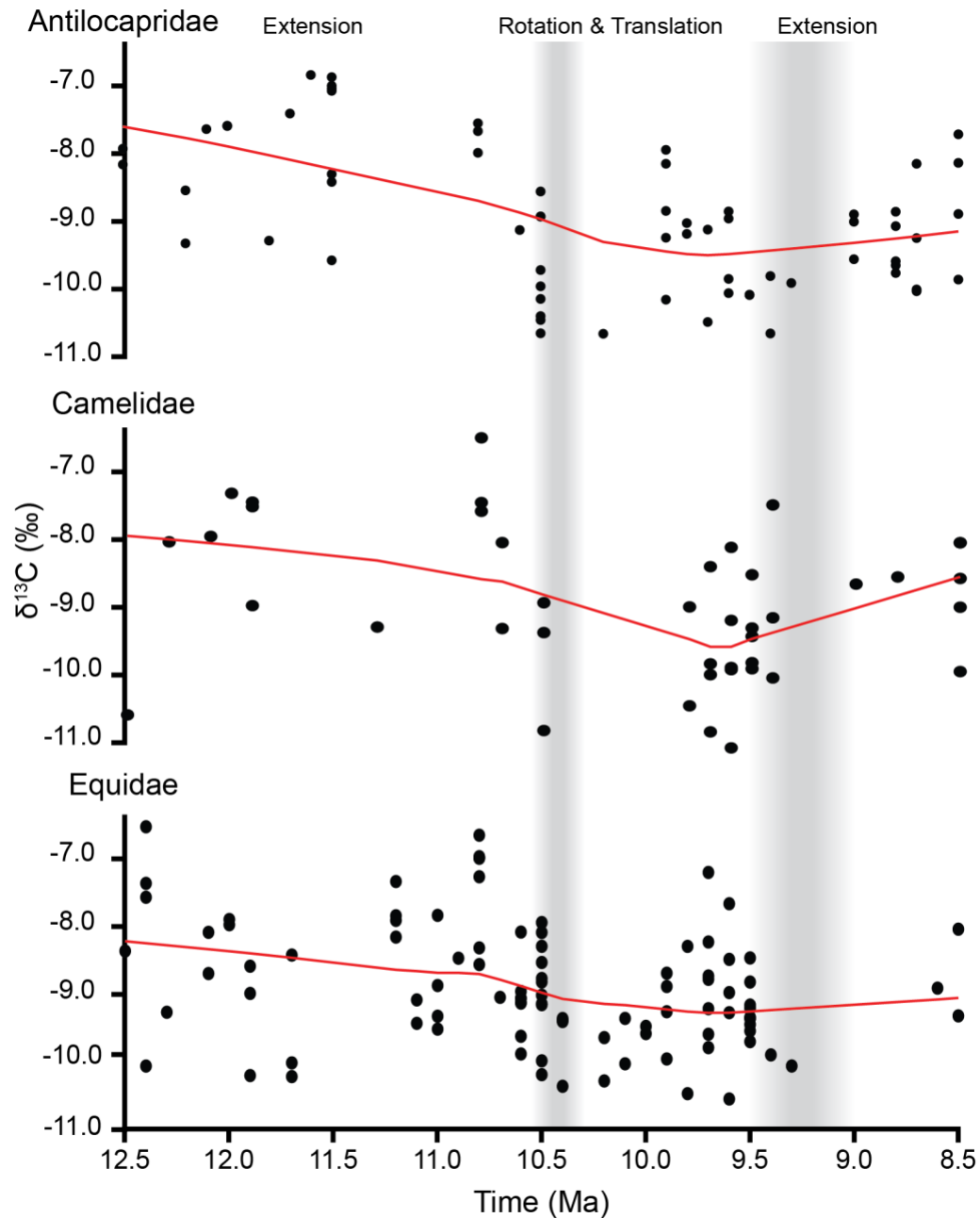


Figure 3.4:  $\delta^{13}\text{C}$  results for three ungulate families in the Dove Spring Formation. All three families exhibit a similar pattern of early depletion followed by enrichment near 9.7 Ma. Mean isotopic variation at any point is within the range of expected variation within individuals of a single population ( $< 2.0\text{‰}$ ), suggesting that these variations were within the tolerance of ungulates from the basin. Tectonic episode boundaries are marked with grey zones to indicate uncertainty in the timing of their initiation.

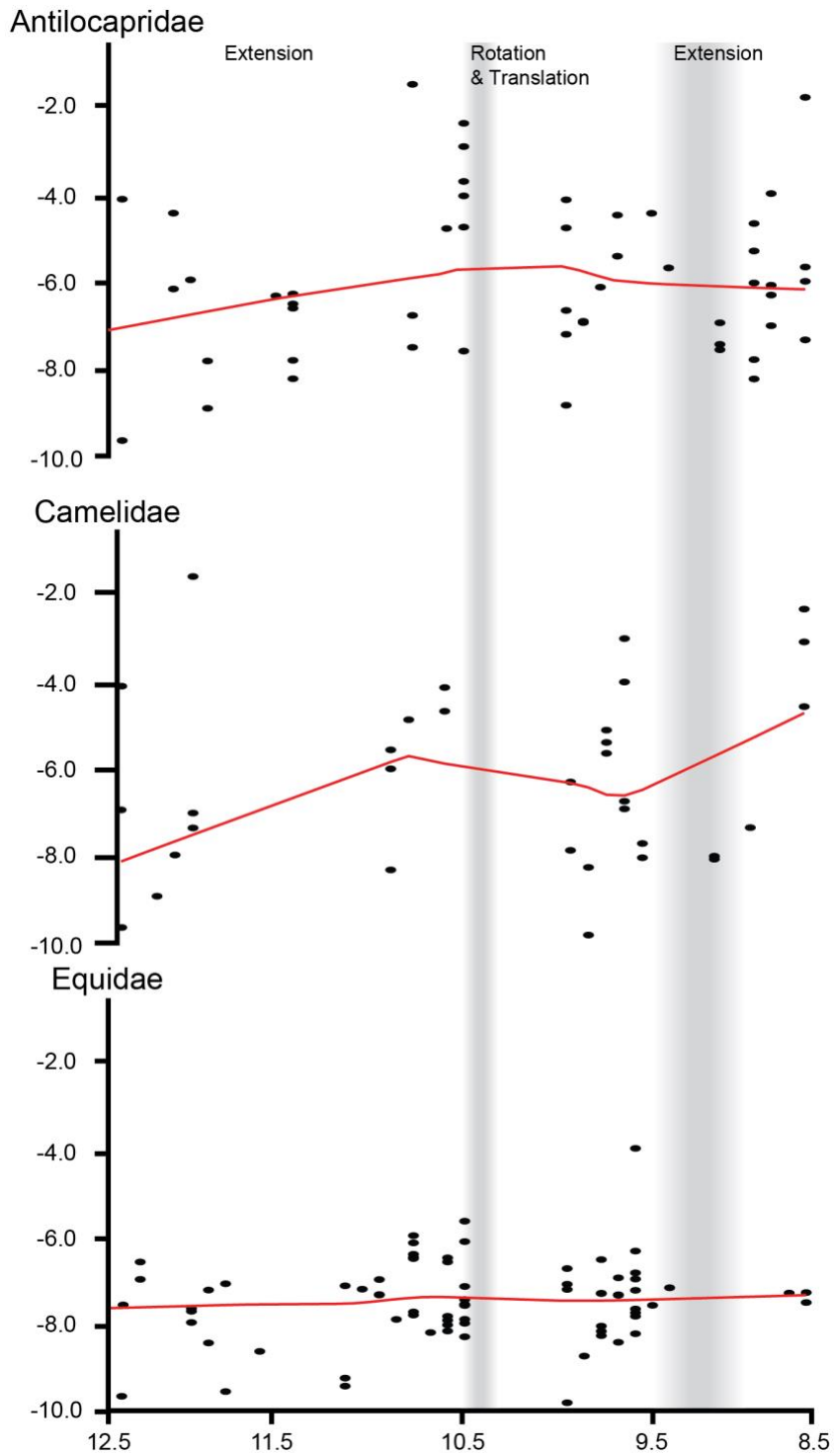


Figure 3.5:  $\delta^{18}\text{O}$  values for ungulate families from the Dove Spring Formation. Higher variability in Antilocapridae and Camelidae is likely the result of the families' status as facultative drinkers that do not have a biological requirement to consume meteoric water directly. Tectonic episode boundaries are marked with grey zones to indicate uncertainty in the timing of their initiation.

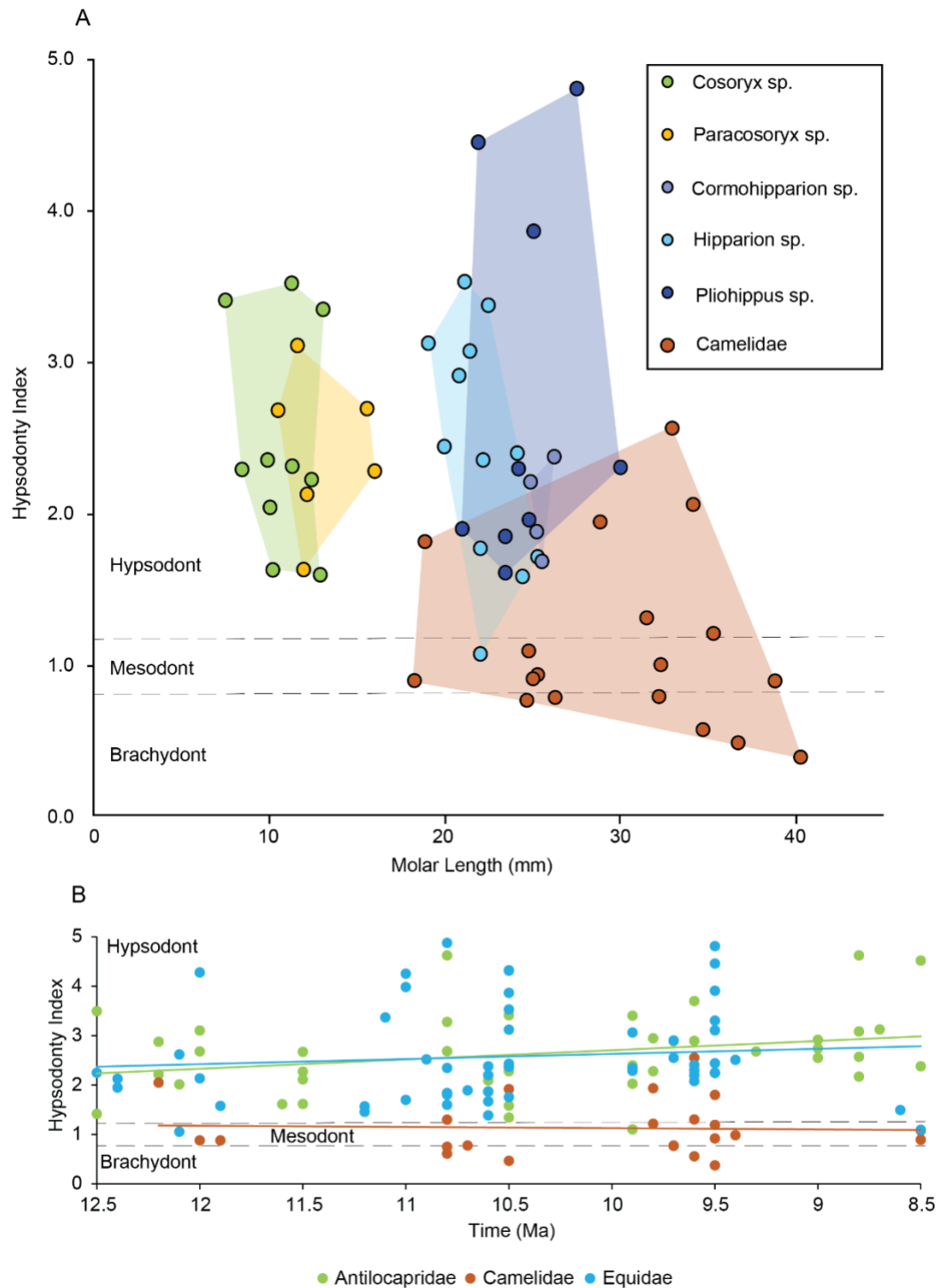


Figure 3.6 Linear measurements of ungulate teeth. A) Molar size as an indicator of body size vs. hypsodonty index (HI) for ungulate genera of the Dove Spring Formation. Antilocaprids are consistently the smallest ungulates in the assemblage and exhibit moderate HI. Camelids occupy the greatest range of body size and are the only family to exhibit brachydont dentition. Equids have a wide range of HI values (though most are hypsodont) and have medium to large body sizes. B) Hypsodonty index over time. No significant trends were observed, although a slight trend towards higher hypsodonty is present in both the Antilocapridae and Equidae.



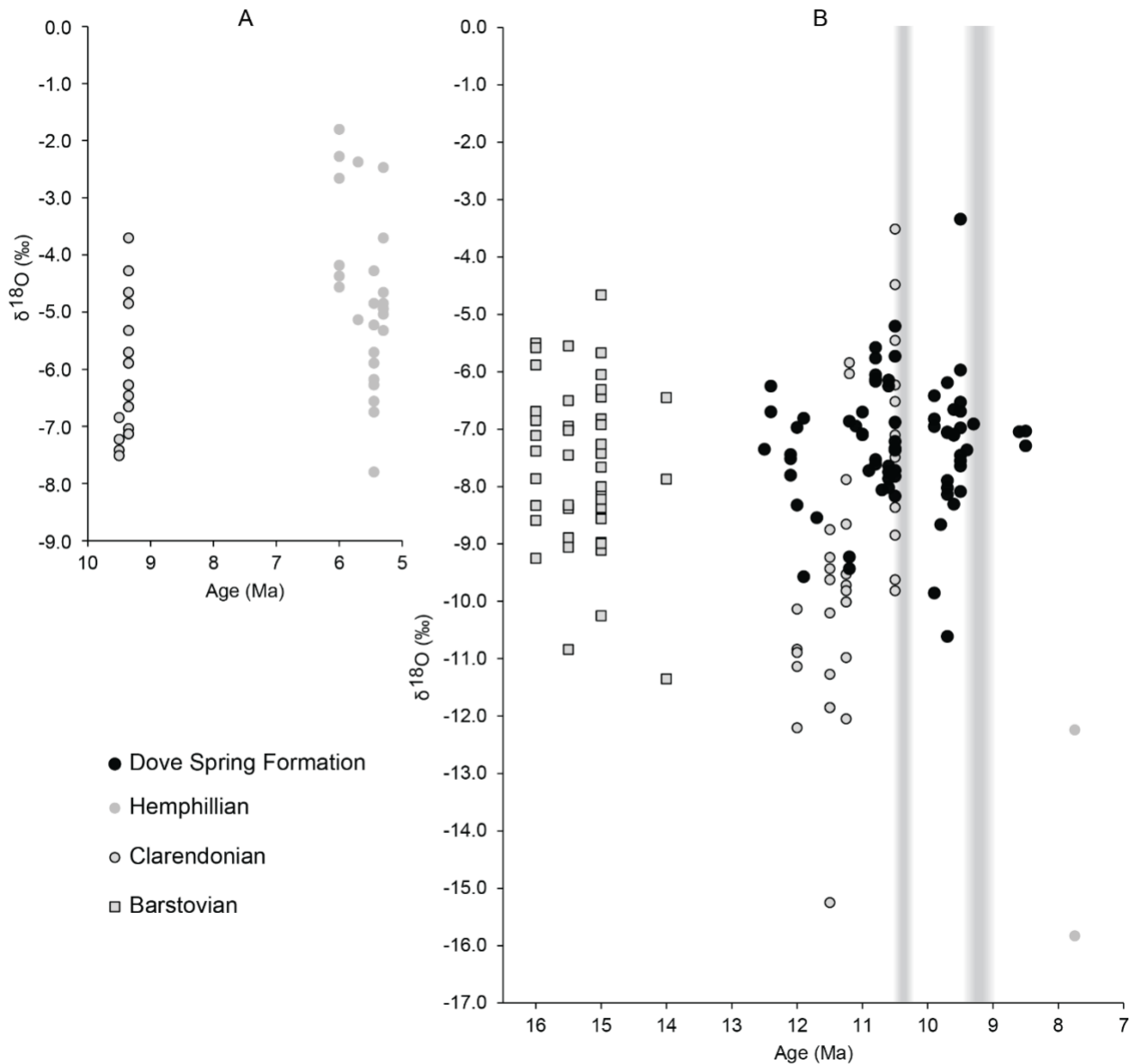


Figure 3.7: Equid  $\delta^{18}\text{O}$  values from the Dove Spring Formation and other regions, organized by position relative to the Sierra Nevada and North American Land Mammal Age, with age estimates based on MioMap and FaunMap databases. A) Localities west of the Sierra Nevada; B) Localities east of the Sierra Nevada. Equids from the Dove Spring Formation exhibit  $\delta^{18}\text{O}$  values that are significantly more depleted than contemporaneous individuals (10.0 to 9.0 Ma) found west of the Sierra Nevada during ( $p < 0.05$ ). Barstovian data from Oregon (16-14 Ma) are from Maguire (2015). Clarendonian data from Nebraska (12 Ma) are from Bryant et al. (1996). Clarendonian and Hemphillian data are from Crowley et al. (2008) and represent California, Nevada, and North Dakota. Tectonic episode boundaries in the Dove Spring Formation are marked with grey zones.

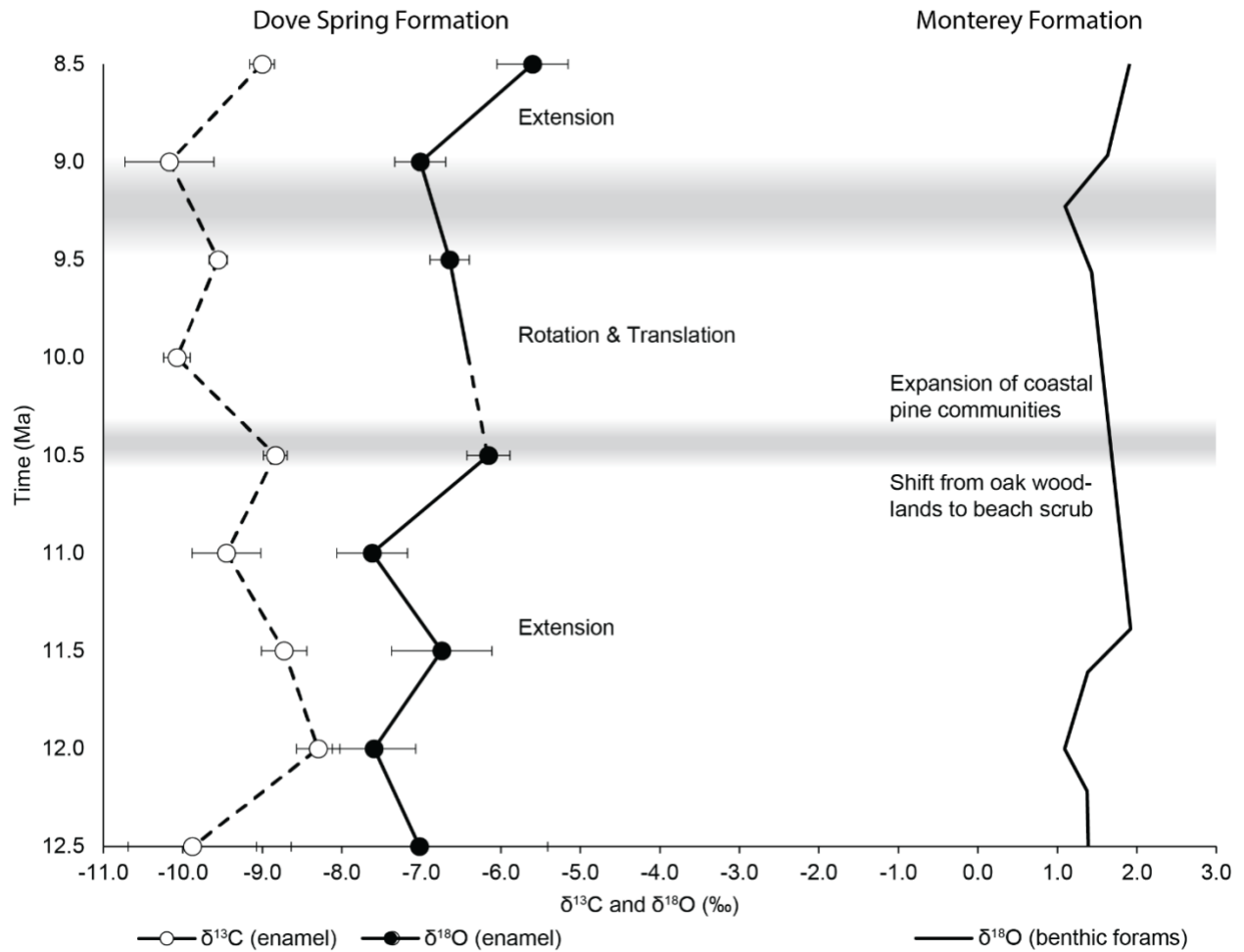


Figure 3.8: Comparison of terrestrial Dove Spring Formation whole assemblage tooth enamel isotopic record with the marine Monterey Formation. Monterey  $\delta^{18}\text{O}$  record is sourced from benthic foraminifera (*Bolivina advena*). Tectonic episode boundaries are marked with grey zones to indicate uncertainty in the timing of their initiation. Vegetation patterns within the Monterey Formation are based on palynological analysis by Heusser et al. (2022).  $\delta^{18}\text{O}$  data is not available for the Dove Spring Formation between 10.5 and 10.0 Ma.

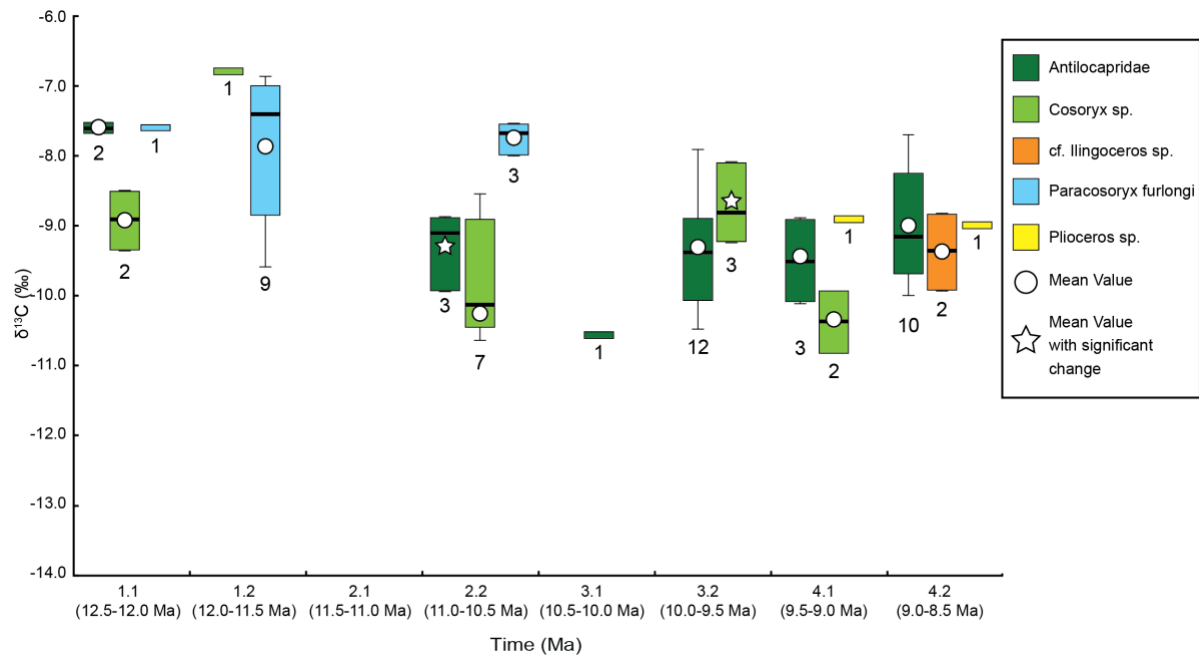


Figure 3.9: Box and whisker plots illustrating  $\delta^{13}\text{C}$  values of individual lineages within the Antilocapridae. *Paracosoryx* typically exhibits the most enriched values of all antilocaprids, and when it no longer appears in the fossil record ( $< 10.5$  Ma), *Cosoryx* exhibits significantly enriched values for approximately 0.5 Myr. Sample sizes for each 0.5-Myr time bin are indicated by numbers underneath each plot.

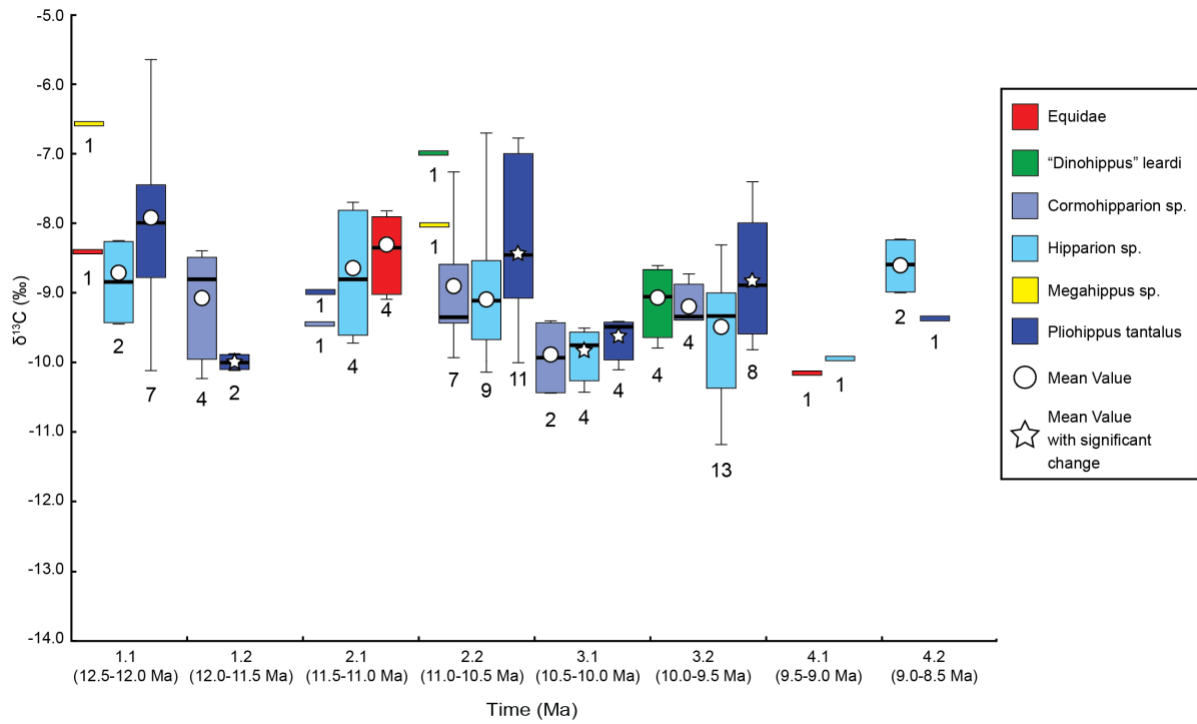


Figure 3.10: Box and whisker plots illustrating  $\delta^{13}\text{C}$  values of individual genera within the Equidae. Isotopic range across all equid species narrows at 10.5 Ma, suggesting convergence on similar resources.

Table 3.1: Whole-assemblage enamel  $\delta^{13}\text{C}$  and  $\delta^{18}\text{O}$  values in the Dove Spring Formation, organized by 0.5-Myr time intervals and 1-Myr time bins. Abbreviations: n = number of specimens; SD = standard deviation.

Time Interval (Ma)	n	$\delta^{13}\text{C}$ ‰ V-PDB						$\delta^{18}\text{O}$ ‰ V-PDB						
		Mean	SD	Max	Min	Range	Net Change	n	Mean	SD	Max	Min	Range	Net Change
8.5	22	-9.00	0.72	-7.73	-10.03	2.30	1.17	20	-5.60	2.00	-1.45	-8.22	6.77	1.41
9.0	15	-10.17	2.16	-7.57	-17.31	9.74	-0.62	11	-7.01	1.07	-4.41	-7.86	3.45	-0.37
9.5	67	-9.55	0.96	-7.32	-12.28	4.97	0.53	45	-6.64	1.66	-2.21	-10.61	8.40	-0.49
10.0	15	-10.07	0.65	-9.42	-11.33	1.90	-1.24	-						
10.5	51	-8.84	1.06	-6.60	-10.85	4.26	0.62	42	-6.16	1.76	-1.43	-8.17	6.73	1.46
11.0	15	-9.45	1.68	-7.45	-13.32	5.87	-0.73	7	-7.62	1.18	-6.70	-9.43	2.73	-0.87
11.5	23	-8.73	1.37	-6.86	-11.05	4.19	-0.43	12	-6.75	2.19	-0.62	-9.57	8.95	0.41
12.0	21	-8.30	1.24	-5.66	-11.39	5.73	1.58	15	-7.16	1.20	-4.40	-8.90	4.50	-0.13
12.5	6	-9.88	1.98	-7.94	-12.72	4.79		3	-7.02	2.80	-4.08	-9.64	5.56	
Interval 4	37	-9.48	1.57	-7.57	-17.31	9.74	0.17	31	-6.10	1.84	-1.45	-8.22	6.77	0.54
Interval 3	82	-9.64	0.93	-7.32	-12.28	4.97	-0.67	45	-6.64	1.66	-2.21	-10.61	8.40	-0.28
Interval 2	66	-8.98	1.24	-6.60	-13.32	6.73	-0.29	49	-6.37	1.76	-1.43	-9.43	8.00	0.61
Interval 1	50	-8.69	1.45	-5.66	-12.72	7.06		30	-6.98	1.76	-0.62	-9.64	9.03	

Table 3.2: Tooth enamel bulk samples with  $\delta^{13}\text{C}$  and  $\delta^{18}\text{O}$  values collected by Hardy (this study) and measured at the University of Michigan Stable Isotope Laboratory.

Sample ID	Family	Species	Age	$\delta^{13}\text{C}$ (VPDB)	$\delta^{18}\text{O}$ (VPDB)
FH.21.001	Antilocapridae		12.1	-7.65	-5.94
FH.21.002	Equidae	Hipparion sp.	12.1	-8.18	-7.80
FH.21.003	Equidae	Pliohippus sp.	12.1	-5.66	-7.44
FH.21.004	Antilocapridae	Cosoryx sp.	12.2	-8.55	-6.15
FH.21.005	Antilocapridae		12.0	-7.60	-7.81
FH.21.010	Equidae		12.5	-8.45	-7.35
FH.21.011	Antilocapridae		12.5	-8.17	-4.08
FH.21.012	Antilocapridae		12.5	-7.94	-9.64
FH.21.015	Equidae	Pliohippus sp.	12.0	-8.07	-8.32
FH.21.017	Camelidae		12.1	-8.03	-8.81
FH.21.018	Equidae	Pliohippus sp.	12.1	-8.78	-7.51
FH.21.020	Camelidae		12.3	-8.11	-6.60
FH.21.021	Camelidae		12.0	-7.40	-7.75
FH.21.022	Equidae	Pliohippus sp.	12.0	-7.99	-6.97
FH.21.023	Antilocapridae	Cosoryx sp.	12.2	-9.33	-4.40
FH.21.024	Antilocapridae	Paracosoryx furlongi	12.0	-7.61	-8.90
FH.21.025	Camelidae		12.2	-15.69	-14.17
FH.21.027	Equidae	Pliohippus sp.	12.4	-7.67	-6.25
FH.21.028	Antilocapridae	Paracosoryx sp.	11.5	-7.05	-6.49
FH.21.029	Antilocapridae	Paracosoryx sp.	11.5	-7.09	-6.27
FH.21.030	Antilocapridae	Paracosoryx sp.	11.5	-7.01	-7.80
FH.21.031	Antilocapridae	Paracosoryx sp.	11.5	-8.31	-6.59
FH.21.032	Antilocapridae	Paracosoryx sp.	11.5	-6.89	-8.22
FH.21.033	Antilocapridae	Cosoryx sp.	11.6	-6.86	-6.31
FH.21.036	Camelidae		11.9	-7.60	-7.06
FH.21.037	Camelidae		11.9	-9.04	-6.68
FH.21.038	Camelidae		11.9	-7.53	-0.62
FH.21.041	Equidae	Cormohipparion sp.	11.9	-8.67	-9.57
FH.21.043	Equidae	Cormohipparion occidentale	11.7	-8.51	-8.54
FH.21.044	Equidae	Cormohipparion occidentale	11.9	-9.06	-6.81
FH.21.045	Equidae	Neohipparion sp.	11.2	-8.01	-9.22
FH.21.046	Equidae	Neohipparion sp.	11.2	-8.25	-9.43
FH.21.047	Equidae	Hipparion sp.	11.0	-9.58	-7.10
FH.21.048	Equidae	Hipparion forcei	11.1	-9.16	-6.95
FH.21.049	Equidae	Hipparion tehonense	11.0	-7.93	-7.08
FH.21.050	Equidae	Hipparion forcei	11.2	-7.45	-6.86
FH.21.051	Equidae	Pliohippus tantalus	12.4	-7.47	-6.70
FH.21.052	Equidae	Pliohippus leardi	10.8	-7.11	-7.61
FH.21.053	Equidae	Pliohippus tehonensis	10.8	-6.78	-6.05
FH.21.054	Equidae	Cormohipparion sp.	10.6	-9.19	-6.14
FH.21.055	Equidae	Cormohipparion sp.	10.5	-8.38	-7.35
FH.21.056	Equidae	Cormohipparion sp.	10.6	-9.20	-8.02
FH.21.057	Equidae	Cormohipparion sp.	10.5	-8.90	-6.88

FH.21.058	Equidae	Cormohipparion occidentale	10.8	-7.09	-7.53
FH.21.059	Equidae	Cormohipparion occidentale	10.6	-9.68	-7.86
FH.21.060	Equidae	Cormohipparion occidentale	10.6	-9.13	-6.25
FH.21.061	Equidae	Pliohippus tantalus	10.7	-9.12	-8.06
FH.21.062	Equidae	Pliohippus tantalus	10.8	-7.11	-5.57
FH.21.063	Equidae	Pliohippus tantalus	10.8	-8.65	-6.16
FH.21.064	Equidae	Pliohippus tantalus	10.8	-7.38	-6.13
FH.21.065	Equidae	Pliohippus tantalus	10.5	-8.85	-7.72
FH.21.066	Equidae	Pliohippus sp.	10.5	-8.18	-7.21
FH.21.068	Equidae	Pliohippus sp.	10.6	-9.13	-7.74
FH.21.069	Equidae	Pliohippus sp.	10.8	-8.40	-5.76
FH.21.070	Equidae	Hipparion sp.	10.5	-9.22	-7.82
FH.21.071	Equidae	Hipparion sp.	10.5	-8.62	-7.36
FH.21.072	Equidae	Hipparion sp.	10.5	-9.09	-7.35
FH.21.073	Equidae	Hipparion forcei	10.6	-8.18	-7.64
FH.21.074	Equidae	Hypohippus sp.	10.5	-8.04	-5.20
FH.21.075	Equidae	Hipparion forcei	10.9	-8.55	-7.72
FH.21.076	Equidae	Hipparion forcei	10.5	-9.21	-8.17
FH.21.077	Equidae	Hipparion forcei	10.5	-10.24	-7.33
FH.21.078	Equidae	Hipparion forcei	10.5	-10.04	-5.73
FH.21.079	Equidae	Hipparion sp.	9.9	-10.01	-9.86
FH.21.080	Equidae	Hipparion sp.	9.8	-8.38	-8.66
FH.21.081	Equidae	Hipparion sp.	9.9	-9.33	-6.95
FH.21.082	Equidae	Hipparion forcei	9.7	-9.84	-7.89
FH.21.083	Equidae	Pliohippus sp.	9.5	-9.60	-6.98
FH.21.085	Equidae	Cormohipparion occidentale	9.5	-9.42	-7.45
FH.21.086	Equidae	Pliohippus leardi	9.7	-8.86	-6.19
FH.21.087	Equidae	Hipparion forcei	9.7	-9.28	-8.14
FH.21.088	Equidae	Pliohippus tantalus	9.5	-9.41	-6.53
FH.21.089	Equidae	Pliohippus leardi	9.6	-8.57	-7.10
FH.21.090	Equidae	Pliohippus leardi	9.5	-9.28	-6.69
FH.21.091	Equidae	Pliohippus leardi	9.7	-9.65	-7.06
FH.21.092	Equidae	Pliohippus sp.	9.7	-7.32	-10.61
FH.21.093	Equidae	Pliohippus sp.	9.9	-8.77	-6.82
FH.21.094	Equidae	Hipparion forcei	9.6	-9.05	-8.31
FH.21.095	Equidae	Pliohippus tantalus	9.6	-7.77	-6.66
FH.21.096	Equidae	Pliohippus sp.	9.5	-8.55	-3.34
FH.21.097	Equidae	Hipparion forcei	9.5	-9.23	-7.64
FH.21.098	Equidae	Hipparion sp.	9.5	-9.51	-5.97
FH.21.099	Equidae	Pliohippus sp.	9.5	-9.76	-7.55
FH.21.100	Equidae	Hipparion forcei	9.7	-8.32	-7.05
FH.21.101	Equidae	Cormohipparion sp.	9.6	-9.34	-7.09
FH.21.102	Equidae	Cormohipparion sp.	9.7	-8.81	-8.02
FH.21.103	Equidae	Cormohipparion sp.	9.5	-9.42	-8.09
FH.21.104	Equidae	Hipparion tehonense	9.9	-8.96	-6.42
FH.21.105	Equidae	Nannippus sp.	11.0	-9.39	-6.70
FH.21.106	Antilocapridae		10.6	-9.13	-4.76
FH.21.107	Antilocapridae	Merycodus sp.	9.6	-9.85	-4.45
FH.21.108	Camelidae		10.5	-8.99	-3.46

FH.21.109	Camelidae		10.8	-7.54	-5.06
FH.21.110	Antilocapridae		9.9	-7.96	-8.83
FH.21.111	Antilocapridae	Merycodus sp.	9.9	-10.15	-4.74
FH.21.112	Camelidae	Paracamelus	10.5	-9.43	-4.07
FH.21.113	Camelidae	Paracamelus sp.	9.5	-9.96	-3.32
FH.21.115	Camelidae	Procamelus sp.	9.8	-11.83	-5.88
FH.21.116	Camelidae	Procamelus sp.	9.8	-9.06	-7.63
FH.21.117	Camelidae		9.5	-9.87	-6.37
FH.21.118	Antilocapridae		9.8	-9.19	-6.90
FH.21.119	Antilocapridae		9.8	-9.03	-6.93
FH.21.120	Camelidae		10.7	-8.12	-4.29
FH.21.122	Antilocapridae		10.5	-8.93	-7.58
FH.21.123	Antilocapridae		9.7	-9.13	-6.11
FH.21.124	Antilocapridae		9.6	-8.86	-5.39
FH.21.125	Camelidae		9.6	-8.19	-5.15
FH.21.126	Camelidae		9.6	-9.25	-4.55
FH.21.127	Antilocapridae	Cosoryx sp.	10.5	-8.57	-4.00
FH.21.129	Camelidae		9.5	-9.36	-6.57
FH.21.130	Antilocapridae	Cosoryx sp.	10.5	-10.65	-2.33
FH.21.131	Antilocapridae	Cosoryx sp.	10.5	-9.72	-2.87
FH.21.132	Antilocapridae	Cosoryx sp.	10.5	-8.93	-3.67
FH.21.133	Antilocapridae	Cosoryx sp.	10.5	-10.14	-4.72
FH.21.134	Camelidae		9.6	-9.97	-4.87
FH.21.135	Antilocapridae	Paracosoryx furlongi	10.8	-8.00	-6.76
FH.21.136	Antilocapridae	Paracosoryx furlongi	10.8	-7.68	-1.43
FH.21.137	Antilocapridae	Paracosoryx furlongi	10.8	-7.56	-7.50
FH.21.138	Camelidae		10.8	-7.66	-5.54
FH.21.139	Camelidae		10.8	-6.60	-8.13
FH.21.140	Camelidae		9.5	-8.59	-2.21
FH.21.141	Antilocapridae	Cosoryx sp.	9.9	-8.16	-7.20
FH.21.142	Antilocapridae	Cosoryx sp.	9.9	-8.85	-6.65
FH.21.143	Camelidae		9.7	-8.47	-8.07
FH.21.144	Antilocapridae	Cosoryx sp.	9.9	-9.24	-4.09
FH.21.151	Equidae	Hipparion sp.	8.6	-8.99	-7.05
FH.21.152	Antilocapridae		8.7	-8.16	-7.00
FH.21.153	Equidae	Hipparion sp.	8.5	-8.13	-7.03
FH.21.154	Camelidae		8.8	-8.62	-7.05
FH.21.155	Antilocapridae		8.8	-8.86	-8.22
FH.21.156	Antilocapridae		8.8	-9.59	-4.64
FH.21.157	Camelidae		9.0	-17.31	-7.78
FH.21.158	Antilocapridae		8.3	-7.73	-7.32
FH.21.159	Camelidae		8.2	-8.12	-3.95
FH.21.160	Antilocapridae		8.2	-8.15	-5.64
FH.21.161	Antilocapridae		8.8	-9.76	-7.78
FH.21.162	Antilocapridae		8.8	-9.65	-6.01
FH.21.163	Camelidae		9.4	-7.57	-7.82
FH.21.164	Antilocapridae	Plioceros sp.	8.8	-9.07	-5.27
FH.21.165	Antilocapridae		8.7	-10.00	-6.06
FH.21.167	Camelidae		8.5	-10.00	-1.45



FH.21.168	Camelidae		8.5	-8.12	-2.29
FH.21.169	Equidae	Pliohippus sp.	8.0	-9.39	-7.29
FH.21.170	Camelidae		9.0	-8.72	-7.86
FH.21.171	Antilocapridae	Plioceros sp.	9.0	-8.90	-7.43
FH.21.172	Antilocapridae	Cosoryx sp.	9.4	-9.81	-4.41
FH.21.173	Camelidae		9.4	-9.21	-7.46
FH.21.174	Antilocapridae		9.3	-9.91	-5.66
FH.21.175	Equidae		9.3	-10.11	-6.91
FH.21.176	Antilocapridae	Illingoceros sp.	8.5	-9.86	-1.73
FH.21.177	Antilocapridae	Illingoceros sp.	8.5	-8.90	-5.97
FH.21.179	Antilocapridae	Cosoryx sp.	8.7	-10.03	-3.95
FH.21.180	Antilocapridae	Cosoryx sp.	8.7	-9.25	-6.29
FH.21.182	Antilocapridae	Sphenophalos sp.	9.0	-9.56	-6.93
FH.21.183	Antilocapridae	Sphenophalos sp.	9.0	-9.01	-7.55
FH.21.185	Equidae	Hipparion forcei	9.4	-9.95	-7.36

Table 3.3: Tooth enamel bulk samples with  $\delta^{13}\text{C}$  values collected and measured by Bowman et al. (2017).

Sample ID	Family	Species	Age	$\delta^{13}\text{C}$ (VPDB)
DSF-01	Camelidae		8.5	-8.64
DSF-02	Merycoidodontidae	Merychys sp.	11.6	-10.98
DSF-03 (01-13)	Camelidae		8.5	-9.06
DSF-04	Antilocapridae	Cosoryx sp.	10.5	-10.40
DSF-05	Antilocapridae	Cosoryx sp.	10.5	-10.45
DSF-06	Camelidae		11.3	-9.35
DSF-07	Equidae	Cormohipparion sp.	10.4	-10.40
DSF-08 (01-09)	Equidae	Pliohippus sp.	10.1	-10.08
DSF-14	Antilocapridae	Cosoryx sp.	9.4	-10.65
DSF-15	Equidae	Pliohippus tantalus	9.5	-8.90
DSF-16	Gomphotheriidae		11.0	-12.79
DSF-17	Equidae	Hipparion forcei	10.2	-9.70
DSF-18	Gomphotheriidae		9.3	-10.87
DSF-19	Gomphotheriidae		11.0	-13.32
DSF-20	Antilocapridae		10.2	-10.65
DSF-21	Camelidae		9.6	-11.11
DSF-22	Gomphotheriidae	Gomphotherium sp.	10.0	-10.46
DSF-23	Gomphotheriidae	Gomphotherium sp.	11.1	-10.00
DSF-24	Equidae	Hipparion forcei	10.2	-10.33
DSF-25	Camelidae		9.7	-9.88
DSF-26	Gomphotheriidae	Gomphotherium sp.	9.7	-11.44
DSF-27	Gomphotheriidae	Gomphotherium sp.	10.2	-11.29
DSF-28 (01-12)	Equidae	Hipparion forcei	9.6	-10.59
DSF-29	Equidae	Megahippus sp.	12.4	-6.66
DSF-30	Equidae	Pliohippus tantalus	11.7	-10.06
DSF-31	Camelidae		10.5	-10.85
DSF-32	Equidae	Pliohippus tantalus	10.0	-9.54
DSF-33 (01-18)	Gomphotheriidae		10.0	-11.33
DSF-34	Equidae	Pliohippus tantalus	10.4	-9.45
DSF-35 (01-13)	Equidae	Pliohippus tantalus	10.4	-9.47
DSF-36	Equidae	Pliohippus tantalus	11.9	-10.25
DSF-37	Equidae	Pliohippus tantalus	11.0	-8.95
DSF-39 (01-14)	Equidae	Hipparion forcei	9.5	-11.16
DSF-41	Merycoidodontidae	Merychys sp.	11.7	-9.69
DSF-42 (01-14)	Equidae	Pliohippus tantalus	10.6	-9.94
DSF-43	Gomphotheriidae	Gomphotherium sp.	12.0	-11.39
DSF-44 (01-06)	Antilocapridae	Paracosoryx furlongi	11.8	-9.29
DSF-45	Gomphotheriidae	Gomphotherium sp.	9.7	-11.04
DSF-46	Gomphotheriidae		12.0	-9.63
DSF-47	Camelidae		9.7	-10.04
DSF-48 (01-06)	Antilocapridae	Paracosoryx furlongi	11.5	-8.43
DSF-49	Antilocapridae	Paracosoryx furlongi	11.5	-9.58
DSF-50	Antilocapridae	Paracosoryx furlongi	11.7	-7.42
DSF-51	Equidae	Hipparion forcei	9.8	-10.51

DSF-52	Equidae	Pliohippus tantalus	12.4	-10.11
DSF-53 (01-16)	Equidae	Hipparion forcei	10.4	-9.42
DSF-54 (01-14)	Equidae	Hipparion forcei	10.0	-9.64
DSF-56	Equidae	Hipparion forcei	10.6	-9.03
DSF-58 (01-05)	Camelidae		10.7	-9.37
DSF-59	Gomphotheriidae		9.5	-9.89
DSF-60	Camelidae		12.5	-10.63
DSF-61	Gomphotheriidae		12.5	-11.38
DSF-62	Gomphotheriidae	Gomphotherium sp.	12.5	-12.72
DSF-63	Equidae	Hipparion forcei	12.3	-9.33
DSF-64 (01-19)	Gomphotheriidae	Gomphotherium sp.	10.5	-10.62
DSF-65 (01-10)	Merycoidodontidae	Merychys sp.	9.7	-10.33
DSF-66	Antilocapridae		9.7	-10.48
DSF-67	Antilocapridae		10.5	-9.96
DSF-69	Gomphotheriidae		11.1	-10.18
DSF-70	Camelidae		9.6	-9.94
DSF-71	Antilocapridae		9.6	-8.96
DSF-72	Antilocapridae		9.6	-10.06
DSF-73	Camelidae		9.4	-10.09
DSF-74	Gomphotheriidae		9.4	-10.88
DSF-75	Gomphotheriidae		9.5	-10.60
DSF-76	Equidae		11.2	-7.94
DSF-78	Gomphotheriidae		12.0	-9.06
DSF-79	Gomphotheriidae		9.5	-12.28
DSF-80	Camelidae	Procamelus sp.	9.8	-10.49
DSF-81	Antilocapridae		9.5	-10.09
DSF-82	Antilocapridae		9.5	-10.08
DSF-83	Camelidae		9.5	-9.48
DSF-84 (01-20)	Rhinocerotidae	Teleoceras meridianum	11.7	-11.05
DSF-85	Merycoidodontidae	Merychys major major	10.5	-8.90
DSF-86	Gomphotheriidae	Amebelodon burnhami	10.4	-9.94
DSF-87 (01-10)	Camelidae		9.7	-10.87
DSF-88	Equidae	Cormohipparion sp.	11.7	-10.26
DSF-89	Equidae	Cormohipparion sp.	10.1	-9.42
DSF-90 (01-14)	Rhinocerotidae	Aphelops sp.	11.7	-10.10
DSF-91	Equidae	Cormohipparion sp.	11.1	-9.49

Table 3.4: Published equid tooth enamel  $\delta^{18}\text{O}$  values shown in Figure 3.7.

Sample ID	NALMA	Taxon	Age	$\delta^{18}\text{O}$ (VPDB)	Side	Location
<b>Crowley et al. (2008)</b>						
UCMP 153872	Hemphillian	Pliohippus sp.	5.30	-4.9	West	California
UCMP 153873	Hemphillian	Pliohippus edensis	5.30	-5.0	West	California
UCMP 153874	Hemphillian	Pliohippus edensis	5.30	-5.1	West	California
UCMP 153875	Hemphillian	Pliohippus edensis	5.30	-5.0	West	California
UCMP 153888	Hemphillian	Pliohippus edensis	5.30	-4.7	West	California
UCMP 153889	Hemphillian	Pliohippus edensis	5.30	-2.4	West	California
UCMP 153890	Hemphillian	Pliohippus edensis	5.30	-3.7	West	California
UCMP 29783	Hemphillian	Pliohippus edensis	5.30	-5.4	West	California
UCMP 320025	Hemphillian	Dinohippus	5.45	-6.2	West	California
UCMP 320012	Hemphillian	Dinohippus leidymanus	5.45	-7.9	West	California
UCMP 320049	Hemphillian	Dinohippus leidymanus	5.45	-6.3	West	California
UCMP 320016	Hemphillian	Dinohippus leidymanus	5.45	-6.8	West	California
UCMP 320020	Hemphillian	Dinohippus leidymanus	5.45	-5.7	West	California
UCMP 320043	Hemphillian	Dinohippus leidymanus	5.45	-4.3	West	California
UCMP 320044	Hemphillian	Dinohippus leidymanus	5.45	-6.6	West	California
UCMP 320056	Hemphillian	Dinohippus leidymanus	5.45	-4.9	West	California
UCMP 320059	Hemphillian	Dinohippus leidymanus	5.45	-5.3	West	California
UCMP 153933	Hemphillian	Dinohippus leidymanus	5.45	-5.9	West	California
UCMP 153884	Hemphillian	Pliohippus sp.	5.70	-2.3	West	California
UCMP 153918	Hemphillian	Pliohippus sp.	5.70	-5.2	West	California
UCMP 153881	Hemphillian	Pliohippus sp.	6.00	-4.2	West	California
UCMP 153882	Hemphillian	Pliohippus sp.	6.00	-2.6	West	California
UCMP 153883	Hemphillian	Pliohippus sp.	6.00	-2.3	West	California
UCMP 57790	Hemphillian	Pliohippus sp.	6.00	-4.4	West	California
UCMP 33058	Hemphillian	Pliohippus sp.	6.00	-1.8	West	California
UCMP 22937	Hemphillian	Pliohippus sp.	6.00	-4.6	West	California
N/A	Clarendonian	Pliohippus sp.	9.35	-7.1	West	California
N/A	Clarendonian	Pliohippus sp.	9.35	-6.3	West	California
UCMP 49752	Clarendonian	Pliohippus sp.	9.35	-4.7	West	California
UCMP 34622	Clarendonian	Pliohippus sp.	9.35	-4.3	West	California
UCMP 33541	Clarendonian	Pliohippus sp.	9.35	-3.7	West	California
UCMP 33530	Clarendonian	Pliohippus sp.	9.35	-7.2	West	California
UCMP 158218	Clarendonian	Pliohippus sp.	9.35	-5.9	West	California
UCMP 34836	Clarendonian	Nannippus sp.	9.35	-5.9	West	California
UCMP 64740	Clarendonian	Hipparion sp.	9.35	-6.7	West	California
UCMP 34603	Clarendonian	Hipparion sp.	9.35	-6.7	West	California
UCMP 58542	Clarendonian	Hipparion sp.	9.35	-5.7	West	California
UCMP 94794	Clarendonian	Hipparion sp.	9.35	-7.2	West	California
UCMP 131660	Clarendonian	Hipparion sp.	9.35	-4.9	West	California
UCMP 131663	Clarendonian	Hipparion forcei	9.35	-5.4	West	California
UCMP 58264	Clarendonian	Hipparion forcei	9.35	-6.5	West	California
UCMP 128154	Clarendonian	Hipparion forcei	9.35	-6.3	West	California
UCMP 34568	Clarendonian	Hipparion sp.	9.50	-7.5	West	California

UCMP 153928	Clarendonian	Hipparion sp.	9.50	-7.6	West	California
UCMP 34266	Clarendonian	Nannippus?	9.50	-6.9	West	California
UCMP 35275	Clarendonian	Nannippus sp.	9.50	-7.3	West	California
UCMP 70378	Hemphillian	Equidae	7.75	-12.2	East	North Dakota
UCMP 22126	Hemphillian	Neohipparion sp.	7.75	-14.4	East	North Dakota
UCMP 313147	Clarendonian	Hipparion mohavensis	10.50	-4.5	East	California
UCMP 313222	Clarendonian	Hipparion sp.	10.50	-9.6	East	California
UCMP 153927	Clarendonian	Pliohippus fairbanksi	10.50	-8.4	East	California
UCMP 313242	Clarendonian	Pliohippus sp.	10.50	-7.5	East	California
UCMP 153938	Clarendonian	Pliohippus sp.	10.50	-6.5	East	California
UCMP 313088	Clarendonian	Pliohippus sp.	10.50	-8.4	East	California
UCMP 313146	Clarendonian	Pliohippus tantalus	10.50	-5.5	East	California
UCMP 313221	Clarendonian	Pliohippus sp.	10.50	-6.9	East	California
UCMP 19443	Clarendonian	Pliohippus sp.	10.50	-3.5	East	California
UCMP 37141	Clarendonian	Hipparion sp.	10.50	-7.3	East	California
UCMP 44715	Clarendonian	Pliohippus sp.	10.50	-8.8	East	Nevada
UCMP 153867	Clarendonian	Hipparion tehonense	10.50	-6.2	East	Nevada
UCMP 153868	Clarendonian	Hipparion tehonense	10.50	-7.1	East	Nevada
UCMP 153887	Clarendonian	Hipparion sp.	10.50	-9.8	East	Nevada
UCMP 153865	Clarendonian	Hipparion tehonense	11.20	-6.0	East	Nevada
UCMP 153866	Clarendonian	Hipparion tehonense	11.20	-5.8	East	Nevada
UCMP 153912	Clarendonian	Equidae	11.25	-7.9	East	Nevada
UCMP 153904	Clarendonian	Neohipparion sp.	11.25	-10.0	East	Nevada
UCMP 153911	Clarendonian	Neohipparion sp.	11.25	-8.7	East	Nevada
UCMP 153913	Clarendonian	Neohipparion sp.	11.25	-9.7	East	Nevada
UCMP 153876	Clarendonian	Neohipparion sp.	11.25	-12.0	East	Nevada
UCMP 153877	Clarendonian	Neohipparion sp.	11.25	-9.5	East	Nevada
UCMP 153878	Clarendonian	Neohipparion sp.	11.25	-11.0	East	Nevada
UCMP 153879	Clarendonian	Neohipparion sp.	11.25	-9.8	East	Nevada
UCMP 153880	Clarendonian	Neohipparion sp.	11.25	-10.0	East	Nevada
UCMP 33916	Clarendonian	Neohipparion sp.	11.50	-15.2	East	Nevada
UCMP 153906	Clarendonian	Neohipparion sp.	11.50	-11.9	East	Nevada
UCMP 153903	Clarendonian	Neohipparion sp.	11.50	-11.3	East	Nevada
UCMP 153917	Clarendonian	Neohipparion sp.	11.50	-9.6	East	Nevada
UCMP 29664	Clarendonian	Neohipparion sp.	11.50	-10.2	East	Nevada
UCMP 153906	Clarendonian	Neohipparion sp.	11.50	-11.9	East	Nevada
UCMP 153909	Clarendonian	Neohipparion sp.	11.50	-9.2	East	Nevada
UCMP 153915	Clarendonian	Neohipparion sp.	11.50	-8.7	East	Nevada
UCMP 153905	Clarendonian	Pliohippus sp.	11.50	-9.4	East	Nevada
<b>Maguire (2015)</b>						
JODA 16555	Early Barstovian	Archaeohippus sp.	15.50	-7.0	East	Oregon
UCMP 26643	Early Barstovian	Archaeohippus sp.	15.50	-7.5	East	Oregon
UCMP 1689A	Early Barstovian	Archaeohippus sp.	15.50	-6.5	East	Oregon
UCMP 1689B	Early Barstovian	Archaeohippus sp.	15.5	-7.0	East	Oregon
UCMP 41203	Early Barstovian	Archaeohippus sp.	15.5	-5.6	East	Oregon
UCMP 1701	Early Barstovian	Desmatippus sp.	15.5	-10.8	East	Oregon

JODA 4211	Early Barstovian	Parahippus sp.	15.5	-8.4	East	Oregon
JODA 2410	Early Barstovian	Parahippus sp.	15.5	-9.1	East	Oregon
JODA 2416	Early Barstovian	Parahippus sp.	15.5	-8.3	East	Oregon
UCMP 40240	Early Barstovian	Parahippus sp.	15.5	-8.9	East	Oregon
JODA 4269	Early Barstovian	aff. Acritohippus	16	-6.7	East	Oregon
JODA 4276	Early Barstovian	aff. Acritohippus	16	-8.3	East	Oregon
JODA 4277	Early Barstovian	aff. Acritohippus	16	-9.3	East	Oregon
JODA 3334	Early Barstovian	aff. Acritohippus	16	-5.9	East	Oregon
JODA 8894	Early Barstovian	aff. Acritohippus	16	-7.9	East	Oregon
JODA 16565	Early Barstovian	aff. Acritohippus	16	-7.4	East	Oregon
JODA 10309	Early Barstovian	aff. Acritohippus	16	-7.1	East	Oregon
JODA 10310	Early Barstovian	aff. Acritohippus	16	-6.7	East	Oregon
JODA 8570	Early Barstovian	aff. Acritohippus	16	-5.5	East	Oregon
JODA 14943	Early Barstovian	aff. Acritohippus	16	-8.6	East	Oregon
UCMP 39111	Early Barstovian	aff. Acritohippus	16	-5.5	East	Oregon
UCMP 41202	Early Barstovian	aff. Acritohippus	16	-6.9	East	Oregon
JODA 14950	Early Barstovian	aff. Acritohippus	16	-5.6	East	Oregon
JODA 1113	Late Barstovian	aff. Acritohippus	15	-8.6	East	Oregon
JODA 6286	Late Barstovian	aff. Acritohippus	15	-6.1	East	Oregon
JODA 6300	Late Barstovian	aff. Acritohippus	15	-8.2	East	Oregon
JODA 16551	Late Barstovian	aff. Acritohippus	15	-7.7	East	Oregon
JODA 6277	Late Barstovian	aff. Acritohippus	15	-6.8	East	Oregon
JODA 4213	Late Barstovian	aff. Acritohippus	15	-4.7	East	Oregon
JODA 6622	Late Barstovian	aff. Acritohippus	15	-6.8	East	Oregon
JODA 7575	Late Barstovian	aff. Acritohippus	15	-8.4	East	Oregon
JODA 16558	Late Barstovian	aff. Acritohippus	15	-9.0	East	Oregon
JODA 16559	Late Barstovian	aff. Acritohippus	15	-9.1	East	Oregon
JODA 16564	Late Barstovian	aff. Acritohippus	15	-7.4	East	Oregon
JODA 16546	Late Barstovian	aff. Acritohippus	15	-10.3	East	Oregon
JODA 4294	Late Barstovian	aff. Acritohippus	15	-6.9	East	Oregon
JODA 4246	Late Barstovian	aff. Acritohippus	15	-8.4	East	Oregon
JODA 4252	Late Barstovian	aff. Acritohippus	15	-6.4	East	Oregon
JODA 12050	Late Barstovian	aff. Acritohippus	15	-7.3	East	Oregon
JODA 14945	Late Barstovian	aff. Acritohippus	15	-8.0	East	Oregon
JODA 14948	Late Barstovian	aff. Acritohippus	15	-6.4	East	Oregon
UCMP 40322	Late Barstovian	aff. Acritohippus	15	-9.0	East	Oregon
UCMP 40322	Late Barstovian	aff. Acritohippus	15	-8.2	East	Oregon
UCMP 39296	Late Barstovian	aff. Acritohippus	15	-6.3	East	Oregon
UCMP 39296	Late Barstovian	aff. Acritohippus	15	-5.7	East	Oregon
JODA 10026	Late Barstovian	aff. Acritohippus	14	-11.4	East	Oregon
JODA 6350	Late Barstovian	aff. Acritohippus	14	-6.5	East	Oregon
JODA 3333	Late Barstovian	aff. Acritohippus	14	-7.9	East	Oregon

**Bryant et al. (1996)**

F:AM 110562	Clarendonian	"Merychippus" primus	12.0	-10.8	East	Nebraska
F:AM 110456	Clarendonian	"Merychippus" primus	12.0	-11.1	East	Nebraska
F:AM 110470	Clarendonian	"Merychippus" primus	12.0	-10.9	East	Nebraska
F:AM 110496	Clarendonian	"Merychippus" primus	12.0	-12.2	East	Nebraska
F:AM 110961	Clarendonian	"Merychippus" primus	12.0	-10.1	East	Nebraska

## Chapter 4

### Facies Analysis of Depositional Environments at Multiple Scales in the Dove Spring Formation, Southern California

#### Introduction

Tectonic processes play a crucial role in determining topographic gradients within landscapes, affecting temperatures and rainfall amounts, which in turn influence various geomorphic processes such as sediment production, erosion, transport, and deposition (Beatley, 1975; Miall, 1985; Bridge, 2003). The resulting depositional environments of sedimentary basins have varying potential to bury and preserve organisms. Reconstructions of past conditions allow for assessments of the quality of the fossil record. By examining depositional environments in a particular stratigraphic record, I aim to understand the processes that govern the availability of life habitats for terrestrial organisms as well as the depositional environments that preserve their fossil remains (Holland, 2016; Loughney et al., 2021).

Interpretations of faunal history rely on the fossil record, which is inherently incomplete due to the rare nature of fossilization. The conditions leading to fossil preservation are dependent on accommodation space, sediment supply, and position on the landscape, all of which are governed at the basin scale by tectonic processes (Behrensmeier, 1987, 1988; Kidwell and Holland, 2002; Bridge, 2003). Continental basins collect sediments through alluvial and lacustrine depositional systems, providing habitats and resources for terrestrial and aquatic organisms, (Gawthorpe and Leeder, 2000; Loughney and Badgley, 2020).

The dynamic tectonic setting of the Mojave region has led to a complex landscape with elevational gradients that affect sediment accumulation rates and depositional characteristics (Smiley, 2018; Loughney et al., 2021). I investigated the variety and sequence of depositional settings in a terrestrial basin as they relate to tectonic history and changes in mammalian species richness. I conducted a series of lithofacies analyses within the Dove Spring Formation with the following goals: 1) to determine the geographic and temporal distribution of major facies associations; 2) to evaluate facies changes in relation to the tectonic history of the El Paso Basin; 3) to describe the depositional environments of highly productive fossil localities; and 4) to test the hypothesis that the history of faunal change is related to changes in the distribution of facies associations through time. If faunal change is primarily a function of sampling, fossil productivity will positive correlate with the areal exposure of depositional environments that serve as life habitats for large mammals and preserve their remains. If a negative correlation is observed, faunal change is more likely to be driven by other factors, such as competition, predation, or displacement by new species.

## **2 Geological Background**

Located in the El Paso Basin of southern California, the Dove Spring Formation is an 1800 m-thick sequence of alluvial and lacustrine sediments, and at least 18 laterally continuous ash layers that provide age control to a resolution for individual strata of 500 kyr (Loomis and Burbank, 1988; Whistler and Burbank, 1992; Whistler et al., 2009). The formation is highly fossiliferous, with over 7400 vertebrate fossils documented from more than 750 localities that represent a variety of depositional environments. The high frequency of fossil recovery and a well-documented geochronology make it an ideal study location to examine the relationship between tectonic history, depositional environments, and fossil preservation. The Dove Spring



Formation spans late Clarendonian (12.5-10.3 Ma) to early Hemphillian (10.3-8.5 Ma) North American Land Mammal Ages; these time intervals exhibit decreasing species richness in ungulate taxa at the continental scale (Woodburne, 1987, 2004; Janis et al., 2000). In the Dove Spring Formation, large mammals (body mass >1 kg) show an early increase in species richness with long residence times until 11.0 Ma, followed by a decline in the number of species through the end of the sequence (Hardy and Badgley, in review). While some aspects of this pattern represent authentic faunal change, the variable fossil productivity of depositional environments may be the primary contributing factor to observed changes in species richness and faunal composition (Holland et al., 2022).

Structurally, the fault-bound El Paso Basin exhibits characteristics of both extensional and shear movement. The interval recorded by the Dove Spring Formation (12.5–8.5 Ma) contains lithological, structural, and sedimentological evidence for three tectonic episodes (Loomis and Burbank, 1988). The first tectonic episode is a period of extension that began between 17 and 15 Ma and continued through the early stages of deposition of the Dove Spring Formation and represents a period of basin growth that generated accommodation space and allowed for the development of mature southeast-to-northwest drainage networks that transported sediments from the El Paso Mountains into the basin (Figure 4.1). Coarse-grained sandstones and conglomerates containing volcanic cobbles are common lithologies observed in this part of the sequence.

Episode 2 began as early as 10.5 Ma with the initiation of shear movement as the Garlock fault to the south accommodated slip between the Walker Lane belt to the north and the Eastern California Shear Zone to the south. During this episode, the distribution of up to 64 km of movement along the Garlock fault caused the El Paso Basin to rotate and translate westward and

closer to the Sierra Nevada Mountains. The tectonic changes during this interval interrupted existing drainage channels and generated a spike in sediment accumulation rate from 100 to 900 mm/yr between 10.5 and 10.3 Ma (Figure 4.2).

In the third episode, extension once again became the dominant tectonic process between 9.5 and 9.0 Ma, based on cut strata and progressively less rotated beds younger than 10.0 Ma (Loomis and Burbank, 1988). Sediments deposited during this episode include coarser material with distinctive clast composition that indicates the Sierra Nevada Mountains to the west as the primary sediment source by 9.0 Ma. Additionally, the drainage pattern of the basin shifted to a northwest-to-southeast direction, based on paleocurrent studies by Loomis and Burbank (1988). The increasing presence of coarse sediments suggests the presence of stream channels similar to those that formed during the earlier phase of extension of Episode 1 (Miall, 1985; Gawthorpe and Leeder, 2000).

Observations and models of extensional basins provide the framework to interpret the history of depositional environments within the El Paso Basin (Miall, 1985; Leeder and Gawthorpe, 1987; Gawthorpe and Leeder, 2000; Bridge, 2003). These authors identify three major stages of deposition in extensional terrestrial basins: 1) Initiation stage wherein normal faulting allows alluvial fans from the sediment source area to accumulate and prograde towards the depositional center of the basin, potentially forming lakes; 2) Interaction and linkage stage during which accommodation space grows as faults continue to develop, allowing channels to propagate and form drainage networks that fill lakes and generate floodplains; 3) Through-going drainage stage, during which continued faulting promotes the development of a large channel belt that runs parallel to the footwall of the main normal fault, supplying sediment to channel margin deposits and floodplains throughout the basin. In general, rates of sediment accumulation

are high during phases of extension as basins increase in area (Bridge and Leeder, 1979; Bridge, 2003; Woolderink et al., 2022). Conversely, deposition rates are low and basin growth stagnates during late-stage extension or quiescent phases (Jackson, 1999; Bridge, 2003).

The suitability of life habitats for terrestrial mammals and their preservation potential vary in part due to topographic gradients and water supply. Terrestrial mammals rely on environments with fresh water and vegetation resources that provide both food for herbivores and shelter from weather conditions or predators (Mayor et al., 2009). Floodplains and channel margins often provide both of these necessities and accumulate sediments and vertebrate remains, making the floodplains that form during Stage 2 of extensional basin development ideal locations to preserve fossils (Eberth et al., 2007; Loughney and Badgley, 2017). While active channels provide water resources and supply sediments that could bury and preserve vertebrate remains, they are unsuitable life habitats for most terrestrial mammals.

Two processes by which terrestrial vertebrate remains may become fossilized in alluvial systems involve fluvial transport or in-situ accumulation, both of which involve preservational biases (Behrensmeyer, 1978). Large mammals (>1 kg) are more likely to be concentrated in channel deposits than microvertebrates due to their more durable skeletal elements that resist obliteration during transport (Kidwell and Flessa, 1996; Arribas and Palmqvist, 1998). Floodplain and channel margin deposits serve as life habitats for most mammals and are more likely to concentrate specimens of all sizes, although small mammals are often underrepresented in fossil assemblages due to taphonomic biases against their preservation (Kidwell and Flessa, 1996; Caledo, 2016).

Fossils within the Dove Spring Formation include small to large mammals, reptiles, three birds, and a single fish belonging to Cyprinodontidae (Whistler et al., 2009). Large mammals are

the most commonly recovered fossils, representing at least 3700 of approximately 7200 fossil specimens. Small mammals are the next most common fossils. Patterns of species richness in the sequence suggest that a strong sampling effect may be a primary control on the record of faunal change. Here I investigate changes in lithofacies to determine if fossil productivity varies in conjunction with depositional environments governed by tectonic processes.

### **3 Methods**

To describe broad trends in the lithofacies of the Dove Spring Formation, I measured 19 stratigraphic sections at the meter scale using a Jacob's staff and Brunton geologic compass (Figure 4.1). I also measured 48 additional stratigraphic sections at the decimeter scale to document detailed facies analysis at individual fossil localities. Nearly every decimeter-scale section (45/48) corresponds to a fossil locality, and I prioritized the 30 localities with the highest number of catalogued specimens (Table 4.1). Each section was georeferenced on site using a Garmin inReach Mini 2 Satellite Communicator and Apple iPad Air (4th generation) running Esri Field Maps software (v 23.1.0). I placed localities into temporal context using a combination of aerial photographs, topographic maps, field notes, and GPS coordinates provided by prior collectors to tie into meter-scale sections. Most stratigraphic intervals within the Dove Spring Formation are supported by robust age control based on a series of at least 18 laterally continuous ash deposits with radiometric dates and tephrochronologic correlations. Magnetostratigraphic correlations to the Geomagnetic Time Scale were also performed in the sequence by Loomis and Burbank (1988), providing another timescale when primary radiometric dates are unavailable.

While measuring meter-scale stratigraphic sections for exposed outcrops, I documented dominant lithologies, average color, and sharp contacts between units (Table 4.2). I grouped

facies with similar lithological and stratigraphic relationships into a series of three macrofacies associations based on methods developed by (Reading, 1986). For decimeter-scale stratigraphic sections, I dug trenches to expose fresh surfaces and documented variations in lithology, color, sedimentary structure, post-depositional features, and contacts between individual beds. I grouped the results into eight microfacies associations that are the basis for inferring the depositional environments for individual fossil localities. My interpretations are based on the established relationships found in alluvial systems and published examples of terrestrial basins (Mitchell and Reading, 1978; Reading, 1986; Behrensmeier, 1987; Leeder et al., 1998; Bridge, 2003).

To estimate the surface exposure of each depositional facies, I mapped their geographic extent with the nearest measured stratigraphic section using the North American Datum of 1983 (NAD 83) in ArcGIS Pro 2.7.0. I then compiled the numbers of localities and specimens found within the mapped extent of each macrofacies to determine fossil productivity for each of the major depositional settings. These estimates are based on mapped and measured portions of the Dove Spring Formation associated with existing fossil localities, and I acknowledge that considerable outcrop area remains to be investigated.

## **4 Results**

I used meter-scale stratigraphic sections to describe three major facies associations that occur throughout the Dove Spring Formation. Decimeter-scale sections provide higher resolution for the variation within each of macrofacies as a basis for interpretation of the depositional environments found at individual fossil localities. Below I describe facies associations at both the meter and decimeter scales. I then present the distribution of fossil localities in relation to macro- and microfacies associations.

## 4.1 Macrofacies

Nineteen stratigraphic sections measured at the meter scale are the basis for my interpretations of three facies associations that occur throughout the El Paso Basin (Figure 4.3). These descriptions represent broad-scale patterns in lithological characteristics associated with the major depositional environments within an alluvial system (Table 4.2).

Macrofacies Association 1: FA 1 is dominated by medium- to coarse-grained sandstones and conglomerates that occur in two general expressions. Thick sequences of approximately 20-50 m are laterally extensive for up to 1.4 km and tend to be well-sorted. These thick sequences feature prominent parallel bedding, crossbedding, and ripple marks. Thin sequences of approximately 10-20 m are often associated with coarsening-upward sequences that have sharp, undulating basal contacts with finer material. Thin sequences exhibit poor sorting and are typically highly bioturbated, with abundant root casts, and occasional parallel bedding or crossbedding. I interpret the thick sequences to represent deep channel deposits, similar in configuration to the modern Mississippi River or the thick sandstones of the Late Cretaceous Mesa Verde Group in Prince Canyon, Utah (Penland and Suter, 1989; Olsen et al., 1995). These sequences are most prevalent early and late in the sequence, coinciding with episodes of extensional tectonics. Thin sequences represent smaller channels that occur primarily in the middle of the sequence, during a period of shear tectonic movement.

Macrofacies Association 2: FA 2 primarily consists of fine-grained sandstones, siltstones, and clayey siltstones, typically in fining-upward sequences 30 to 200 m thick, with individual beds of 20-50 m. Sequences within this facies association commonly feature parallel or laminated bedding and occasionally exhibit blocky fracture. Carbonate rind surfaces, dispersed ash, and root casts are common. Fining upward sequences within FA2 occur above both incised

and gradational basal contacts with silt to medium-grained sandstones. FA2 extends laterally approximately 5 km across much of the lower part of the formation but is restricted to the western portion of the basin after 10.5 Ma and the tectonic interval of rotation and translation. This westward restriction accompanies a similar pattern observed in FA1. FA2 is almost always positioned stratigraphically above or close to sequences of FA1. I interpret FA2 to represent channel margin deposits and proximal floodplains. Fining-upward sequences from medium-grained sandstone to siltstone have been interpreted as channel and bar deposits by Reading (1986). The pattern of “stacked” channel margin deposits observed between 10.0 and 9.0 Ma suggests fluctuations in sediment supply and water discharge, leading to laterally extensive marginal deposits as stream channels are overwritten (Bridge and Leeder, 1979).

Marls of interbedded carbonate and silcretes also occasionally occur within this facies association, and are limited in their lateral extent (< 20 m). These beds are highly indurated, with prominent laminated bedding in a minor siltstone component that contains occasional siliceous root casts and veins of silicate interbeds. The marlstone component of FA2 ranges from approximately 10-30 m thick, and represents oxbow lake or pond deposits.

Macrofacies Association 3: FA 3 consists of siltstones with varying amounts of clay content; these sequences range from 20-570 m thick, with individual beds of 10 to 150 m. Beds of FA3 are often well-indurated with blocky fracture and occasionally exhibit faint parallel bedding. Ripple marks, mudcracks, and petrified tree stumps are uncommon features but are well-preserved where they occur. Discontinuous carbonate layers and root casts occur throughout this facies association. Dispersed ash and gypsum are common features within claystones. Siltstones may contain silcretes layers and are often capped by medium- to coarse-grained sandstones. FA3 represents distal floodplain deposits, which first occur after 11.7 Ma. This

facies association becomes more common by 11.5 Ma, when exposures are found throughout the basin. The Early-Middle Miocene Santa Cruz Formation in Patagonia, Argentina exhibits a similarly floodplain-dominated sequence of depositional environments that developed near a low-gradient fluvial system (Cuitiño et al., 2021).

Based on their areal extent and proximity to water resources, the near-channel environments of FA2 and the floodplains of FA3 were suitable life habitats for a wide variety of terrestrial mammals. These macrofacies associations represent areas on the landscape where sediments accumulate, contributing to the preservation of fossil remains. While channel deposits of FA1 transport sediments with the potential to preserve fossils, they are not suitable life habitats for most mammals.

## **4.2 Microfacies**

The 48 stratigraphic sections measured at the decimeter-scale were the basis for recognizing five microfacies associations in the Dove Spring Formation (Figure 4.4; Table 4.3). These microfacies associations include subclasses of channel and floodplain deposits as well as ponds and crevasse splays. These categories provide additional detail about the variability across the landscape in terms of the kinds of depositional environments associated with fossil localities.

Microfacies Association 1: The medium- to coarse-grained sandstone facies of FA1a is similar to what is observed at the meter scale, with additional variation in bed thickness (Figure 4.4A). FA1a is laterally extensive up to 1.4 km and occurs in beds ranging in thickness between 2.0 and 7.0 m of well-sorted sandstones with prominent parallel bedding and occasional crossbedding or ripple marks. The beds of FA1a represent channel deposits and are prevalent at the base of the formation before 11.5 Ma; after that time, beds of FA1b become more common.



FA1a reappears near the top of the sequence, after 9.0 Ma, and contains distinctive lithologies sourced from the Sierra Nevada. FA1a is often interbedded with FA2 and FA5, and rare occurrences of FA4 are limited in their vertical expression.

Beds of FA1b are poorly sorted sandstones, with rare faint to prominent crossbedding, and typically exhibit considerable bioturbation (Figure 4.4B). Undulating basal contacts with siltstones are common and root casts are usually associated within blocky, indurated fining-upward sequences. The beds of FA1b are typically 0.6-1.6 m in thickness, and coarsen upward from fine-grained sediments, grading over approximately 0.2 m. FA1b represents small, potentially ephemeral channel deposits that are often interbedded with units of FA2 and FA3. These small channels are initially common in the eastern part of the basin, but shift westward at 11.0 Ma, preceding the timing of basin rotation and translation along the Garlock fault by approximately 0.5 Myr.

Microfacies Association 2: Clayey siltstone, siltstone, and fine-grained sandstones make up the majority of deposits in FA2 (Figure 4.4C). Siltstone beds are typically 1.5 m thick and exhibit blocky fracture with faint laminated bedding. Occasional beds of medium-grained sandstone are present throughout the finer-grained facies. Carbonate rind surfaces and dispersed ash and carbonate are common in all facies. Root casts are common in FA2, although the expression varies based on position within the section: units older than 11.0 Ma contain small siliceous root casts (~5-10 mm diameter), while units younger than 11.0 Ma contain large root casts (up to 30 mm diameter) that are either siliceous or carbonaceous in composition. FA2 represents channel margin deposits, interbedded with thin beds of FA3 and FA5. Found throughout the sequence, the westward migration of FA2 is also visible at the microfacies scale. This microfacies occasionally crops out as interbeds with FA1b.

Microfacies Association 3: FA3 at the macrofacies scale represents floodplain deposits, and at the decimeter scale, three distinct expressions among the siltstones and claystones are discernable (Figure 4.4D, E, F). The facies categorized as FA3 are differentiated primarily by sedimentary and post-depositional structures; bedding, pedogenic features, and the presence of carbonate or clay content. Color also plays an important role in the differentiation of this facies, with most dominant lithologies displaying one of three shades of tan.

FA3a most commonly contains buff tan (5 Y 7/2) clayey siltstones that exhibit blocky fracture and faint to no bedding (Figure 4.4D). Ripple marks are relatively common within the siltstone units of this facies. Root casts are uncommon and limited to blocky clay and siltstone units, suggesting overbank or waning flood deposits. Units classified as FA3a range from 1-4 m thick and are not found prior to 11.0 Ma. Zones of dispersed ash and gypsum commonly occur within claystones, indicating wetting and drying stages of a well-drained, floodplain-dominated landscape.

FA3b consists of greyish tan (10 YR 6/2) claystone to siltstone interbedded with abundant discontinuous carbonate layers and occasional zones of dispersed ash (Figure 4.4E). Faint to prominent parallel or laminated bedding is common in well-indurated silty claystone units. Carbonaceous or siliceous root casts (5-10 mm diameter) are also common within these claystone units. Interbeds of buff tan (5 Y 7/2) siltstones are uncommon and associated with silcrete layers. Units of FA3b are generally no more than 1-2 m thick. Units of FA3b are not found prior to 11.0 Ma and represent arid floodplain deposits with relatively high potential evaporation.

FA3c primarily consists of siltstones often capped by poorly sorted, highly bioturbated, medium- to coarse-grained sandstones (Figure 4.4F). Root casts are abundant and thin carbonate

surfaces are common within well- to poorly indurated clayey siltstones that are typically 1.3 to 2.1 meters thick. Mud cracks and faint parallel bedding are uncommon but occur throughout the facies association. FA3c represents poorly-drained floodplain deposits. Alternating clay and silt layers with similar combinations of pedogenic features and plant fossils have been observed in the Miocene Tagay Formation of Olkhon Island in Eastern Siberia (Daxner-Höck et al., 2022). The modern Nylsvlei wetland in the Northern Province of South Africa is an example of a modern wetland system within a semi-arid region, containing abundant clay layers, this system is supported primarily by sheetflow (Tooth et al., 2012).

Microfacies Association 4: FA4 is limited in its vertical and lateral exposure throughout most of the formation (Figure 4.4G). This facies association is dominated by alternating beds of highly indurated marlstone and silcrete. A highly indurated siltstone component is present and exhibits prominent laminated bedding, with siliceous root casts and occasional veins of silicate minerals. Several thin units of FA4 occur associated with FA2 and FA3, and an approximately 30 m thick marlstone and silcrete sequence crops out in the easternmost extent of the formation. FA4 represents standing water and pond deposits.

Microfacies Association 5: Facies within FA5 are primarily medium- to coarse-grained sandstone with massive bedding, interbedded within outcrops of all other facies associations (Figure 4.4). Medium-grained sandstones often have well-defined crossbedding. Both of these expressions have thin beds (0.3-1.0 m) and represent crevasse splay deposits.

### **4.3 Distribution of fossil localities and specimens**

At least 750 fossil localities in the Dove Spring Formation have been documented by the Natural History Museum of Los Angeles County. I established the macrofacies associations for

623 of these localities by considering their stratigraphic position and geographic location (Table 4.4). Approximately half (300) of the localities with macrofacies coverage are located within the spatial distribution of floodplain sequences (FA3), while channel sequences (FA1) hold the fewest localities (126). Channel margin sequences (FA2) yielded the highest total number of specimens (3320), which includes microvertebrates recovered from screenwashed sites. When microvertebrates are removed from consideration, more specimens are recovered from FA3 (1373), followed by FA2 (660).

Fossil productivity for large mammals does not fully correlate with changes in the distribution of depositional environments (Table 4.4). While FA1 increased in area between episodes 1 and 2, fossil productivity dropped by nearly 50% and continued to decrease through the top of the formation. FA2 also increased in area between episodes 1 and 2, and fossil productivity increased dramatically in conjunction with this change. FA2 then decreased in area during episode 3, but fossil productivity continued to increase moderately. Fossil productivity in FA3 is highest during episode 2, despite the greatest area of floodplain sequences occurring during episode 3. When considering all species from the assemblage as a whole, the same trends are observed, although at higher magnitudes of localities and specimens. The shift from the extensional tectonic setting of episode 1 to the shearing movement of episode 2 contributes to the greatest changes in fossil productivity observed in the sequence. However, the area of any given macrofacies association is not a strong predictor of fossil productivity.

I classified the microfacies association for 30 productive fossil localities (with at least 10 specimens) plus an additional 15 localities with varying productivity (Table 4.1, Table 4.5). Within this scheme, 19 localities occur within subclasses of FA3, most of them occurring within FA3b. Subclasses of FA1 hold the next most localities (16) and FA1b has the same number (9)

as FA3b. Twelve localities are found in FA2. Only one locality is found in FA4, and none in FA5. Among these microfacies associations, fossils specimens are distributed unevenly. FA1 subclasses contain the most fossil specimens, followed by the three subclasses of FA3. When viewed individually, FA1b holds the most fossils, then FA2. If microvertebrate sites are removed from consideration, FA1a contains the greatest number of large mammal specimens and FA3b contains the next most. Overall, FA3 and its subclasses contain the most large mammal specimens. FA4 contains only three plant fossils and no vertebrates.

FA2 and FA3 represent life habitats for terrestrial mammals at both the meter- and decimeter-scale as well as depositional environments with good preservation potential for fossil remains. The greatest concentration of fossil specimens occurs in the middle of the sequence and the western part of the basin. These localities are dated between 10.5 and 9.5 Ma and were deposited during the rotational tectonic episode of the El Paso Basin. Sediment accumulation rates during this tectonic interval were high at 10.5 Ma and decreased rapidly through 9.0 Ma (Figure 4.2).

## **5 Discussion**

Facies associations within the Dove Spring Formation represent a series of alluvial depositional environments that vary in their vertical and lateral extent, and are primarily determined by the local tectonic setting. As new tectonic intervals occurred, the El Paso Basin's topography and position on the landscape changed over time, leading to changes in the dominant facies. Here I present interpretations of facies associations as they relate to the basin's tectonic history. This is followed by a discussion of variability in microfacies associations and fossil productivity. I conclude with a discussion of faunal change in the context of depositional environments.

## 5.1 Macrofacies and tectonic episodes

A period of older tectonic extension began between 17 and 15 Ma and continued during the early stages of deposition in the Dove Spring Formation. This extensional period facilitated basin growth and an increase in accommodation space for sediments (Gawthorpe and Leeder, 2000; Bridge, 2003). The large channels of FA1 are most commonly found near the base of the sequence, indicating that extensive drainage networks formed as subsidence and expansion progressed. The parallel orientation of the major channel belt of FA1 to the El Paso Mountains is consistent with normal faults near this stratigraphic level, suggesting that it represents a series of axial channels that ran along the basin margin southeast. The only other facies association commonly found early in the sequence is FA2, a series of channel-margin deposits. This configuration suggests that the lower Dove Spring Formation represents a large, main channel belt that formed during late-stage extension. Based on the areal extent of their outcrops, these channels were laterally extensive and provided plentiful water resources for vegetation and fauna.

At 11.7 Ma, subsidence and basin growth decreased. Sediment accumulation rate reached its minimum at 11.0 Ma, which coincided with the final appearance of large channels that flowed from the El Paso Mountains. As sediment accumulation and preservation rates approached their minima, the depositional center of the basin shifted from east to west based on paleocurrent directions from Loomis and Burbank (1988) and the landscape positions of FA1 and FA2. The large channels of FA1 and channel margin deposits of FA2 remained prominent in the western part of the basin, while the floodplain deposits of FA3 are the primary outcrops in the eastern part. Additionally, channel margin deposits of FA2 are absent from the eastern side of the basin after 11.7 Ma and only the small channels of FA1 are present.

The extensional tectonic setting of the Dove Spring Formation was interrupted by a period of rotation and translation along the Garlock Fault that began by 10.3 Ma. The large channels of FA1 were no longer present in the basin by the start of this tectonic episode and few channel margin deposits (FA2) gave way to the extensive floodplain deposits of FA3. Existing drainage networks were disrupted by shearing movement that may have cut off channels from their source areas (Bridge and Leeder, 1979; Dokka and Macaluso, 2001). Shear movement in place of extension also had the potential to decrease the slope of the main channel belt, which would encourage avulsion and facilitate the development of laterally extensive floodplains (Bridge, 2003). The prominence of FA3 during this tectonic episodes suggests that this was the case. These deposits became the primary source for the majority of fossil specimens recovered from the formation. As shear movement progressed, variation across the landscape manifested as a series of channel margin sequences associated with small channels throughout the basin. The main channel belt of the basin continued to shift and had migrated eastward by approximately 1 km by 9.8 Ma.

Shear movement subsided and extension resumed by 9.0 Ma, leading to the reappearance of large channels associated with FA1. These channels transported sediments from the Sierra Nevada, which became the new source area at this time. Floodplains of FA3 became less common, and the uppermost 250 meters of the sequence were dominated by FA1 (channels) and FA2 (channel margin deposits), with channel belts that extend across a greater proportion of the basin than during the episode of shear movement (Figure 4.1; Figure 4.3). This redevelopment of channels aligns with stage 1 of Gawthorpe and Leeder (2000), wherein channels transport sediments towards the center of the basin as normal faults tilt and generate additional accommodation space.

While all three macrofacies associations occur throughout the Dove Spring Formation, differences in their areal extent likely contribute to the uneven distribution of fossil localities. FA3 has an outcrop area of approximately 6.8 km<sup>2</sup>, FA2 has approximately 4.1 km<sup>2</sup>, and FA1 has approximately 2.5 km<sup>2</sup>. The average numbers of localities and specimens per area for the total assemblage do not fully correlate with changes in areal extent of macrofacies associations (Table 4.4). For example, FA3 continuously increases in area up-section, but the highest fossil productivity in terms of both localities and specimens occurs during tectonic episode 2. The areal expression of FA3 during this interval is intermediate compared to those of episodes 1 and 3. Exposure areas of FA2 are greatest in extent during episode 2, but the highest numbers of localities and specimens occur during episode 3. When considering only large mammals, patterns of fossil productivity are similar, but FA3 within tectonic episode 2 contains the greatest fossil productivity. These trends indicate that fossil productivity is not entirely a function of changes in area in the dominant macrofacies sequences. Additional data about microfacies associations are necessary to investigate patterns of landscape variation within these macrofacies sequences that contribute to patterns of preservation.

## **5.2 Microfacies and fossil localities**

Stratigraphic sections measured at the decimeter scale document the variation of depositional environments across the landscape. Analysis of these microfacies associations also allow for interpretations of changes in fossil productivity through the sequence. In addition to the three major macrofacies associations described above, microfacies associations allow for the differentiation of crevasse splays, pond deposits, and three distinct expressions of floodplains. Pond deposits (FA4) are rare in the Dove Spring Formation and do not often preserve vertebrate fossil specimens. Crevasse splay deposits (FA5) are found as interbeds within other microfacies



associations, and there are no localities where this is the primary depositional environment. The majority of highly productive fossil localities are located near the middle of the sequence, within laterally extensive floodplain deposits of macrofacies association FA3 (Figure 4.1).

The three kinds of floodplain deposits (FA3a, FA3b, Fa3c) contain the majority (n=19) of highly productive fossil localities (Table 4.5). These microfacies associations represent life habitats that also have the potential to preserve remains. Localities in FA3 collectively hold a total of 682 specimens, 377 of which belong to large mammals. The preservational nature of these expressions is not uniform. FA3a (well-drained floodplains) and FA3b (arid floodplains) contain similar numbers of total specimens, less than half of which are large mammals. Conversely, nearly all specimens recovered from FA3c (poorly drained floodplains) belong to large mammals. Aerial exposure in FA3a and FA3b may have led to greater weathering or disarticulation of deceased large mammals by surface processes (transport or breakdown by scavengers), but additional data on the wear stage of bone elements is necessary to confirm this hypothesis.

Channels of FA1 are the next most common for productive localities ( $n \geq 15$ ), with FA1b holding the most total specimens (Table 4.5). However, the majority of these specimens (n=836) are disarticulated microvertebrates recovered by screenwashing. Large mammal remains make up a significant proportion of the specimens in FA1a, suggesting that large channels transported and preserved robust bone elements, while obliterating or scattering smaller bone elements belonging to rodents and other microvertebrates (Badgley, 1986; Behrensmeier, 1988). Several highly productive localities occur in channel sequences near the base of the sequence, indicating that channels had the potential to transport or concentrate the remains of mammals, despite being unsuitable life habitats. Channel margin and levee sequences of FA2 contain 12 highly

productive localities, holding roughly the same number (~n=100) of large mammal specimens as FA1b, FA3a, and FA3c.

### **5.3 Landscape heterogeneity within macrofacies associations**

In Figure 4.5, I present a series of microstratigraphic sections to illustrate heterogeneity across 900 meters of the paleo landscape. This series was measured with an average distance of 150 m between sections and most were located within macrofacies association FA3 (floodplain deposits). In addition to several sandstone layers and fining upward sequences that are useful for correlation, Ash Tra9 ( $10.2 \pm 0.2$  Ma) is well exposed and serves as a marker bed across the landscape, forming a measurable unit (0.5 m) near the center of the lateral transect (Figure 4.2, Figure 4.5). From west to east, the sections represent expressions of FA2, FA3a, FA3b, and FA1b. The westernmost section (22.28) represents a channel margin and levee sequence and contains NHM locality 3422 within a coarsening upward sequence from silt to fine sandstone. Section 22.27 ~125 m to the east represents a well-drained floodplain deposit (FA3a) with fossil horizon NHM 5719 within a fining-upward sequence from silt to silty clay, representing a transition from levee to the floodplain. Root casts are abundant in both sections 22.28 and 22.27, but are mostly absent in the subsequent three sections (22.18, 22.17, and 22.16).

Three sections (22.18, 22.17, and 22.16; Figure 4.5) cover approximately 354 m to the east and represent deposits belonging to microfacies association FA3b (arid floodplains). The absence of vertebrate fossils and root casts suggests that fresh water and vegetation may have been uncommon, resulting in life habitats that were less desirable to mammals.

Section 21.04 is 118m east of section 22.16 and also represents FA3b, with fossil horizon NHM 3436 within a fining upward sequence from medium- to fine-grained sandstone that

contains parallel bedding and ripple marks, indicating its position close to the channel margin (Figure 4.5). The easternmost section (22.29) primarily consists of medium-grained sandstone outcrops of FA1, indicating that channel deposits are dominant at both the meter and decimeter scales. Fossil horizon NHM 3445 is within sandstone that fines and coarsens several times over approximately 3 m of stratigraphic thickness. NHM 3445 represents a fossil assemblage that may have been transported by a small stream channel, accumulated during a period of channel abandonment, or concentrated by carnivores.

Collectively, the sections described here indicate that over a distance of less than one kilometer, variation in the landscape is expressed at multiple scales. Two macrofacies associations (FA1 and FA3) are present within the area, and four microfacies associations (FA2, FA3a, FA3b, and FA1b) were documented. Individual fossil horizons within each facies association are found within distinctive lithofacies that represent channel and levee deposits (Table 4.6). All 64 of the fossil specimens recovered from these sections are large mammals, and the lack of microvertebrates suggests that differential preservation may have affected sampling. The absence of fossil horizons within FA3b may suggest that arid floodplains did not provide sufficient water or vegetation resources to consistently attract mammals.

I compared the distribution of cranial versus postcranial elements from the four sections mentioned above to other highly productive, contemporaneous (within 0.25 Myr) localities that have associated microstratigraphic sections (Table 4.6). Within the correlated transect, diagnostic cranial elements (jaws, skulls, and teeth) of large mammals were approximately evenly distributed within gradational channel margin units and one fine-grained sandstone representing a small channel. In the six contemporaneous

localities, I found that fossil horizons from gradational beds within channel sequences preserved the highest frequency of diagnostic cranial elements (jaws, skulls, and teeth). Fine-grained sandstones from a large channel in section 22.02 (NHM 1553; Appendix Figure 9) preserved mostly large mammal specimens, half of which were cranial elements or teeth. In contrast, the fossil horizon of section 21.05 (NHM 3444) represents a levee deposit that preserved numerous microvertebrate specimens, but less than a third of which were cranial elements or teeth. Species richness was highest within channel deposits, but these likely represent time-averaged deposits with taphonomic biases to preserve robust or highly mineralized bone elements (Behrensmeyer et al., 2000).

#### **5.4 Depositional environments and faunal change**

The basin's tectonic setting and landscape evolution played important roles in the development of depositional environments. During the early extensional episode near the base of the sequence, large channels (FA1a) are the most common setting for highly productive fossil localities. Within this macrofacies association, fining-upward sequences were the primary lithofacies of fossil horizons, as they represent channel margin environments that served as life habitats with high fossil productivity. From approximately 12.5 to 10.5 Ma, new species occurred with increasing frequency as the El Paso Basin grew in area and additional habitat space was generated. Fossil preservation early in the sequence is concentrated in the eastern part of the basin and most recoveries are bone elements from large mammals. A decrease in sediment accumulation rate at 11.7 Ma coincides with a decline in the number of localities and the first appearance of floodplain sediments within the basin's stratigraphic record.

Once the basin began to rotate and move westward along the Garlock fault by 10.3 Ma, fossil preservation most commonly occurred in channel margin and floodplain deposits, with

more variability in the depositional environments of fossil horizons. The middle part of the sequence contains the three types of floodplains (FA3a, FA3b, and FA3c), channel margin deposits (FA2), and small channels (FA1b), with interbedded crevasse splays (FA5) as flooding events took place. While large channels (FA1a) were absent after 10.7 Ma, landscape heterogeneity provided diverse habitats and plentiful water resources for terrestrial mammals. A stratigraphically persistent lake (Section 22.39, Appendix Figure 47), was present in the extreme northeastern part of the basin at 10.4 Ma, but its significant distance (> 4.5 km) from the rest of the correlated stratigraphic record and a lack of vertebrate fossils limits further interpretation of its spatial and stratigraphic relationship to other depositional environments.

The predominance of channel margin or levee deposits that preserve fossils near 10.2 Ma indicates that small channels were active throughout the broader floodplains that dominated the landscape during this period of the El Paso Basin's depositional history. The shear tectonic movement during this interval disrupted existing channel networks and generated suitable habitat space for mammals of multiple size categories. Bone elements were often preserved in floodplain sequences in close proximity to the main channel belt. Preservation in stream channels was less common than in the life habitats of floodplains, but diagnostic specimens from a greater variety of species were concentrated in channel deposits. Species richness and the number of localities peaked at 10.0 Ma, followed by a switch towards extinction as the primary driver of significant faunal change.

Extension resumed as early as 9.5 Ma, but the landscape expression of this change in tectonic regime is most prominent about 0.5 Myr later. Although the life habitats of floodplains were still common, species richness and the number of specimens declined until approximately 9.0 Ma. A sharp increase in the sediment accumulation rate at 8.8 Ma coincides with the

presence of new large channels that extended beyond the confines of the main channel belt (Figure 4.2). The number of localities and specimens localities increased slightly through the end of the Dove Spring Formation's depositional history.

## **6 Conclusion**

I documented the facies associations and depositional environments within the El Paso Basin in the context of its tectonic history. The Dove Spring Formation is dominated by alluvial facies that represent a series of depositional environments associated with channels and floodplains, with variation at several scales (decimeter to meter). Three major tectonic episodes act as large-scale controls on the landscape expression of these environments: late-stage extension, shear movement, and incipient extension. During both extensional episodes, macrofacies associations primarily represent large channels and few proximal floodplain deposits, consistent with observations and depositional models of other extensional basins (Leeder and Gawthorpe, 1987; Gawthorpe and Leeder, 2000; Loughney and Badgley, 2017). As shear movement became the primary tectonic process, the earlier channel belt was disrupted and smaller channels promoted the development of extensive floodplains. This change in depositional setting manifests at finer scales in patterns of depositional environments and fossil preservation.

Within the broad scheme of these macrofacies, landscape heterogeneity is present at the decimeter-scale. I described microfacies associations that represent two subclasses of channels (small and large), and three kinds of floodplains. The depositional environments for 47 of the most highly productive fossil localities were examined in detail, revealing that while floodplain deposits are associated with more localities, channel sequences yield more specimens and higher species richness – especially for large mammals. Overall, fining-upward sequences within

floodplains represent the majority of productive fossil horizons, indicating that life habitats near stream channels have the highest preservation potential for terrestrial vertebrates.

The history of tectonically-influenced depositional environments within the Dove Spring Formation contributed a sampling effect on the fossil record. Changes in species richness are often directly correlated with the number of localities. However, change in the prevalence of depositional environments is not a strong predictor of fossil productivity. The interactions between tectonic history, depositional environments, and faunal change are most prominent once shear movement began midway through the sequence. Extinction became the dominant process of faunal change even though floodplains were most common during this interval and formed life habitats for mammals. When extension resumed near the top of the formation, large channel sequences and their associated depositional environments reappeared, contributing to increases in species richness and the number of localities. These insights help to refine interpretations of the impact of tectonic processes on depositional environments, fossil preservation, and faunal change.

#### Acknowledgments

I thank Dave Whistler and Xiaoming Wang for their guidance and previous work on the Dove Spring Formation, which has been fundamental in providing the background necessary for my analyses. I thank Sam McLeod and Juliet Hook of the Natural History Museum of Los Angeles County, who provided me with aerial photographs, topographic maps, field notebooks, and access to the NHM museum database. I thank Ethan VanValkenburg, Wes Johnston, Mairin Balisi, and Brandon Agcopra for their assistance in field data collection. The California Department of State Parks has been a gracious host during my field expeditions and I would like to extend my gratitude to Jacqueline Boyster, Ranger Damion Laughlin and Ranger Mark Faull

in particular. I thank the Bureau of Land Management for work permits and access to parts of the field site. This project was funded in part by the Rackham Graduate School and the Department of Earth and Environmental Sciences at the University of Michigan.



## References

- Arribas, A., and Palmqvist, P., 1998, Taphonomy and palaeoecology of an assemblages of large mammals; Hyaenid activity in the lower Pleistocene site at Venta Micena (Orce, Guadix Basin, Granada, Spain): *Geobios*, v. 31, p. 3-47.
- Badgley, C., 1986, Counting individuals in mammalian fossil assemblages from fluvial environments: *Palaios*, v. 1, no. 3, p. 328-338.
- Beatley, J. C., 1975, Climates and vegetation pattern across the Mojave/Great Basin Desert transition of southern Nevada: *The American Midland Naturalist*, v. 93, no. 1, p. 53-70.
- Behrensmeyer, A. K., 1978, Taphonomic and ecologic information from bone weathering: *Paleobiology*, v. 4, no. 2, p. 150-162.
- Behrensmeyer, A. K., 1987, Miocene fluvial facies and vertebrate taphonomy in northern Pakistan: *Recent Developments in Fluvial Sedimentology*, v. Society of Economic Paleontologists and Mineralogists Recent Developments in Fluvial Sedimentology, no. SP39, p. 169-176.
- , 1988, Vertebrate preservation in fluvial channels: *Palaeogeography, Palaeoclimatology, Palaeoecology*, v. 63, p. 183-199.
- Behrensmeyer, A. K., Kidwell, S. M., and Gastaldo, R. A., 2000, Taphonomy and paleobiology: *Paleobiology*, v. 26, no. 4, p. 103-147.
- Bridge, J. S., 2003, *Rivers and Floodplains*, Blackwell Science, 491 p.:
- Bridge, J. S., and Leeder, M. R., 1979, A simulation model of alluvial stratigraphy: *Sedimentology*, v. 26, p. 617-644.
- Calede, J. J., 2016, Comparative Taphonomy of the Mammalian Remains from the Cabbage Patch Beds of Western Montana (Renova Formation, Arikareean): *Contrasting Depositional Environments and Specimen Preservation: Palaios*, v. 31, no. 11, p. 497-515.
- Cuitiño, J. I., Sol Raigemborn, M., Susana Bargo, M., Vizcaíno, S. F., Muñoz, N. A., Kohn, M. J., and Kay, R. F., 2021, Insights on the controls on floodplain-dominated fluvial successions: a perspective from the Early–Middle Miocene Santa Cruz Formation in Río Chalía (Patagonia, Argentina): *Journal of the Geological Society*, v. 178, no. 4.
- Daxner-Höck, G., Mörs, T., Kazansky, A. Y., Matasova, G. G., Ivanova, V. V., Shchetnikov, A. A., Filinov, I. A., Voyta, L., and Erbajeva, M. A., 2022, A synthesis of fauna, palaeoenvironments and stratigraphy of the Miocene Tagay locality (Olkhon Island, Lake Baikal, Eastern Siberia): *Palaeobiodiversity and Palaeoenvironments*, v. 102, no. 4, p. 969-983.

- Dokka, R. K., and Macaluso, K. Y., 2001, Topographic effects of the Eastern California Shear Zone in the Mojave Desert: *Journal of Geophysical Research: Solid Earth*, v. 106, no. B12, p. 30625-30644.
- Eberth, D. A., Shannon, M., and Noland, B. G., 2007, A bonebeds database: Classification, biases and patterns of occurrence, *in* Rogers, R. R., Eberth, D. A., and Fiorillo, A. R., eds., *Bonebeds: Genesis, analysis, and paleobiological significance*: Chicago, University of Chicago Press, p. 103-220.
- Gawthorpe, R. L., and Leeder, M. R., 2000, Tectono-sedimentary evolution of active extensional basins: *Basin Research*, v. 12, p. 195-218.
- Holland, S. M., 2016, The non-uniformity of fossil preservation: *Philosophical Transactions of the Royal Society B: Biological Sciences*, v. 371, p. 11.
- Holland, S. M., Loughney, K. M., and Cone, M., 2022, Preferential preservation of low-elevation biotas in the nonmarine fossil record: *Geology*, v. 51, no. 1, p. 111-114.
- Jackson, J., 1999, Fault death: A perspective from actively deforming regions: *Journal of Structural Geology*, v. 21, p. 1003-1010.
- Janis, C. M., Damuth, J., and Theodor, J. M., 2000, Miocene ungulates and terrestrial primary productivity: Where have all the browsers gone?: *Proceedings of the National Academy of Sciences of the United States of America*, v. 97, no. 14, p. 7899-7904.
- Kidwell, S. M., and Flessa, K. W., 1996, The quality of the fossil record: Populations, species, and communities: *Annual Review of Earth and Planetary Sciences*, v. 24, p. 433-464.
- Kidwell, S. M., and Holland, S. M., 2002, The quality of the fossil record: Implications for evolutionary analyses: *Annual Review of Ecology, Evolution, and Systematics*, v. 33, p. 561-588.
- Leeder, M. R., and Gawthorpe, R. L., 1987, Sedimentary models for extensional tilt-block/half-graben basins: *Geological Society, London, Special Publications*, v. 28, no. 1, p. 139-152.
- Leeder, M. R., Harris, T., and Kirkby, M. J., 1998, Sediment supply and climate change: implications for basin stratigraphy: *Basin Research*, v. 10, p. 7-18.
- Loomis, D. P., and Burbank, D. W., 1988, The stratigraphic evolution of the El Paso basin, southern California: Implications for the Miocene development of the Garlock fault and uplift of the Sierra Nevada: *Geological Society of America Bulletin*, v. 100, p. 12-28.
- Loughney, K. M., and Badgley, C., 2017, Facies, environments, and fossil preservation in the Barstow Formation, Mojave Desert, California: *Palaios*, v. 32, p. 396-412.
- , 2020, The Influence of Depositional Environment and Basin History on the Taphonomy of Mammalian Assemblages from the Barstow Formation (Middle Miocene), California: *Palaios*, v. 35, no. 4, p. 175-190.
- Loughney, K. M., Badgley, C., Bahadori, A., Holt, W. E., and Rasbury, E. T., 2021, Tectonic influence on Cenozoic mammal richness and sedimentation history of the Basin and Range, western North America: *Science Advances*, v. 7, p. 13.

- Mayor, S. J., Schneider, D. C., Schaefer, J. A., and Mahoney, S. P., 2009, Habitat selection at multiple scales: *Écoscience*, v. 16, no. 2, p. 238-247.
- Miall, A. D., 1985, Architectural-element analysis: A new method of facies analysis applied to fluvial deposits: *Earth-Science Reviews*, v. 22, p. 261-308.
- Mitchell, A. H. G., and Reading, H. G., 1978, Sedimentation and tectonics, *in* Reading, H. G., ed., *Sedimentary environments and facies*: New York, Elsevier, p. 557.
- Olsen, T., Steel, R., Hogseth, K., Skar, T., and Roe, S. L., 1995, Sequential architecture in a fluvial succession; sequence stratigraphy in the Upper Cretaceous Mesaverde Group, Prince Canyon, Utah: *Journal of Sedimentary Research*, v. 65, no. 265-280.
- Penland, S., and Suter, J. R., 1989, The geomorphology of the Mississippi River Chenier Plain: *Marine Geology*, v. 90, p. 231-258.
- Reading, H. G., 1986, Facies, *in* Reading, H. G., ed., *Sedimentary Environments and Facies*, Department of Earth Sciences University of Oxford, p. 4-19.
- Smiley, T. M., 2018, Detecting diversification rates in relation to preservation and tectonic history from simulated fossil records: *Paleobiology*, v. 44, no. 1, p. 1-24.
- Tooth, S., McCarthy, T. S., Hancox, P. J., Brandt, D., Buckley, K., Nortje, E., and McQuade, S., 2012, The geomorphology of the Nyl River and floodplain in the semi-arid Northern Province, South Africa: *South African Geographical Journal*, v. 84, no. 2, p. 226-237.
- Whistler, D. P., and Burbank, D. W., 1992, Miocene biostratigraphy and biochronology of the Dove Spring Formation, Mojave Desert, California, and characterization of the Clarendonian mammal age (late Miocene) in California: *Geological Society of America Bulletin*, v. 104, p. 644-658.
- Whistler, D. P., Tedford, R. H., Takeuchi, G. T., Wang, X., Tseng, Z. J., and Perkins, M. E., 2009, Revised Miocene biostratigraphy and biochronology of the Dove Spring Formation, Mojave Desert, California: *Museum of Northern Arizona Bulletin*, v. 65, p. 331-362.
- Woodburne, M. O., 1987, *Cenozoic mammals of North America*, University of California Press, 336 p.:
- , 2004, *Late Cretaceous and Cenozoic mammals of North America: Biostratigraphy and geochronology*, Columbia University Press, 376 p.:
- Woolderink, H. A. G., Weisscher, S. A. H., Kleinhans, M. G., Kasse, C., and van Balen, R. T., 2022, Modelling the effects of normal faulting on alluvial river meandering: *Earth Surf Process Landf*, v. 47, no. 5, p. 1252-1270.

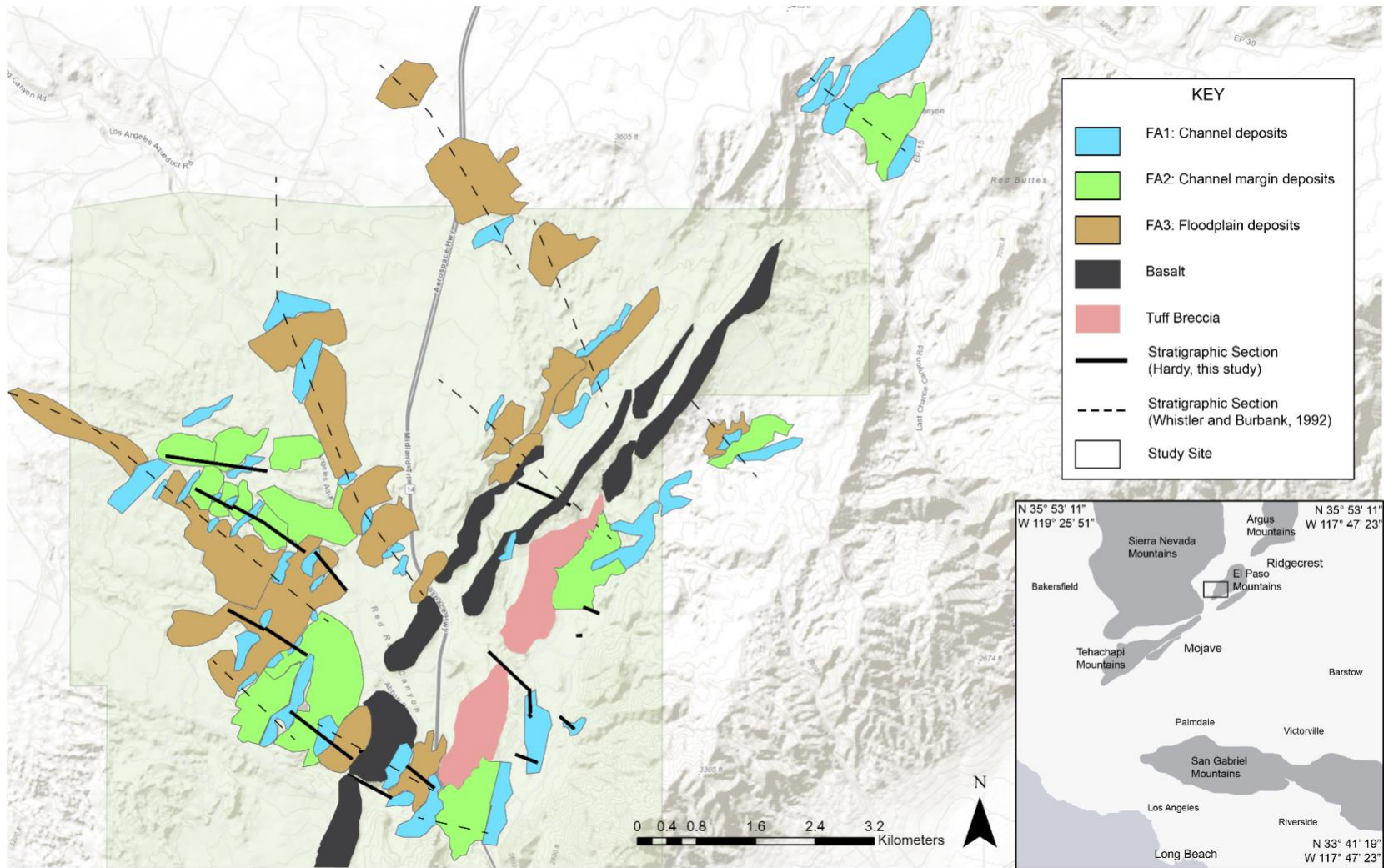


Figure 4.1: Location map of the Dove Spring Formation. Colored polygons represent macrofacies associations. Fossil localities are not shown due to the sensitive nature of the resource.

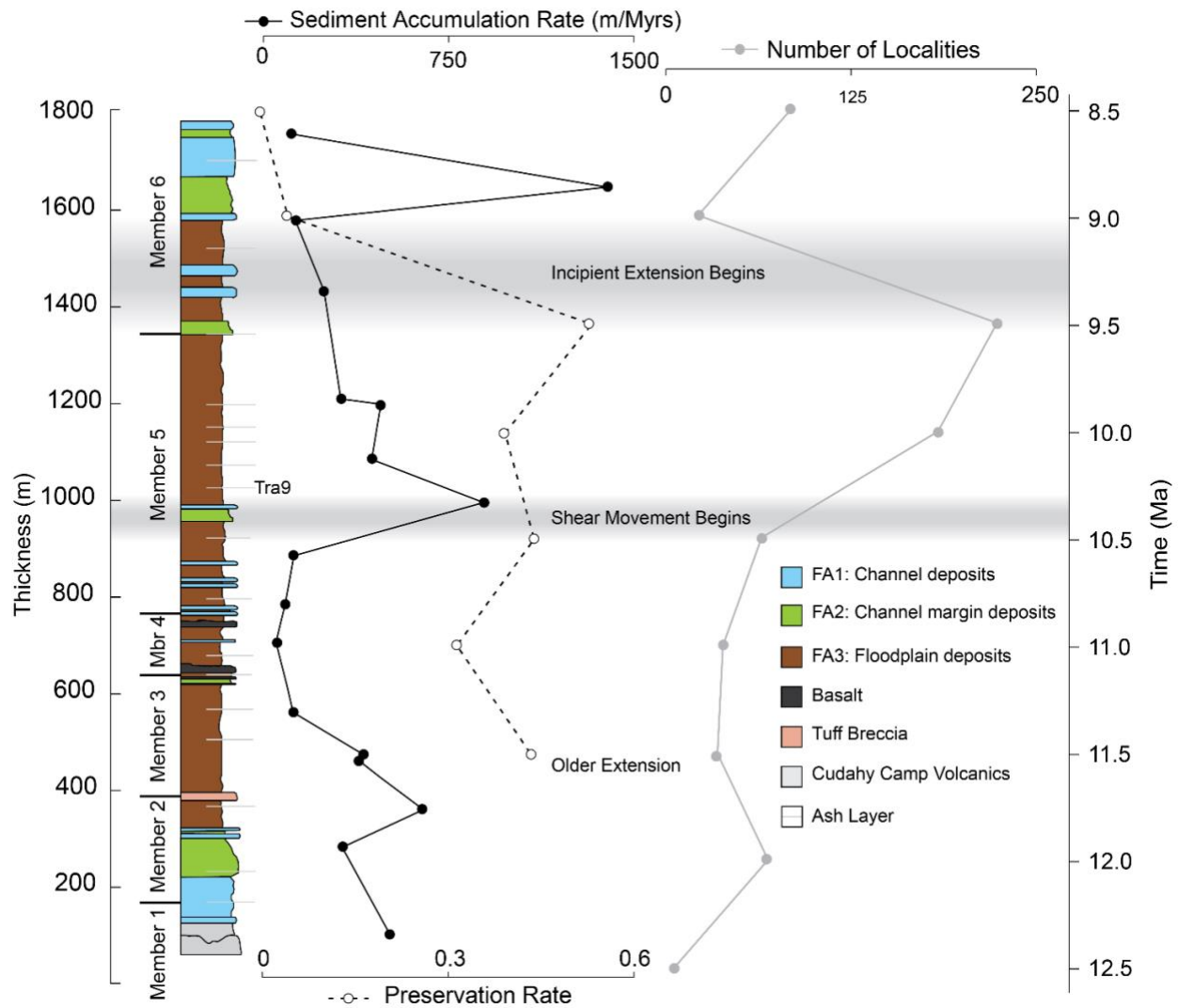


Figure 4.2: Composite lithostratigraphy of the Dove Spring Formation with dominant macrofacies associations for each member. Sediment accumulation and preservation rates are included with number of localities to illustrate changes in fossil productivity. Tectonic episodes are marked with grey zones to indicate uncertainty in the timing of their initiation. Radiometrically dated ash Tra9 ( $10.2 \pm 0.2$  Ma) is associated with a lateral transect presented in Figure 4.5. Stratigraphic column modified from Whistler et al. (2009).

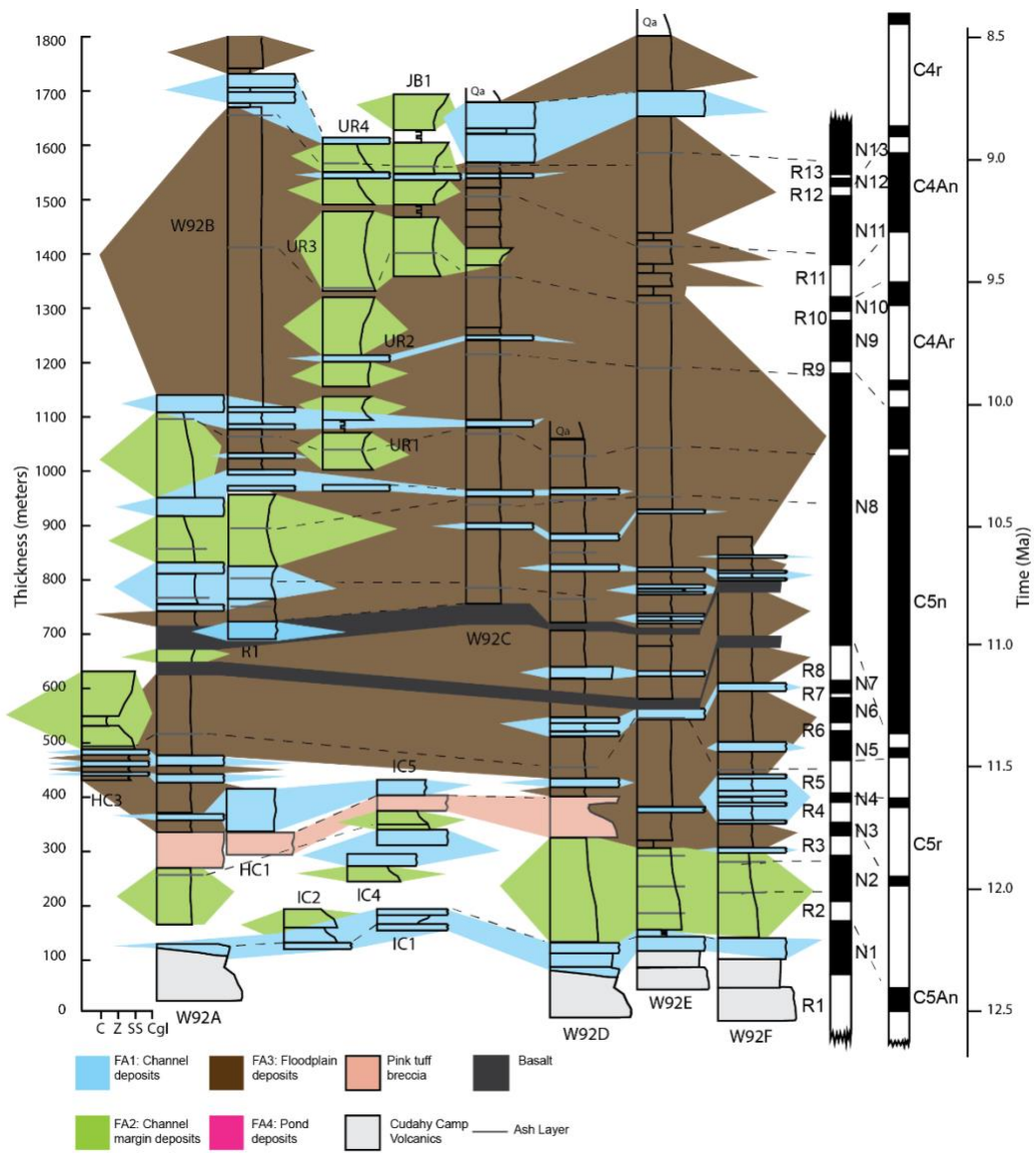


Figure 4.3: Fence diagram illustrating correlations of macrofacies associations throughout meter-scale stratigraphic sections. Columns labelled W92 modified from Whistler and Burbank (1992).



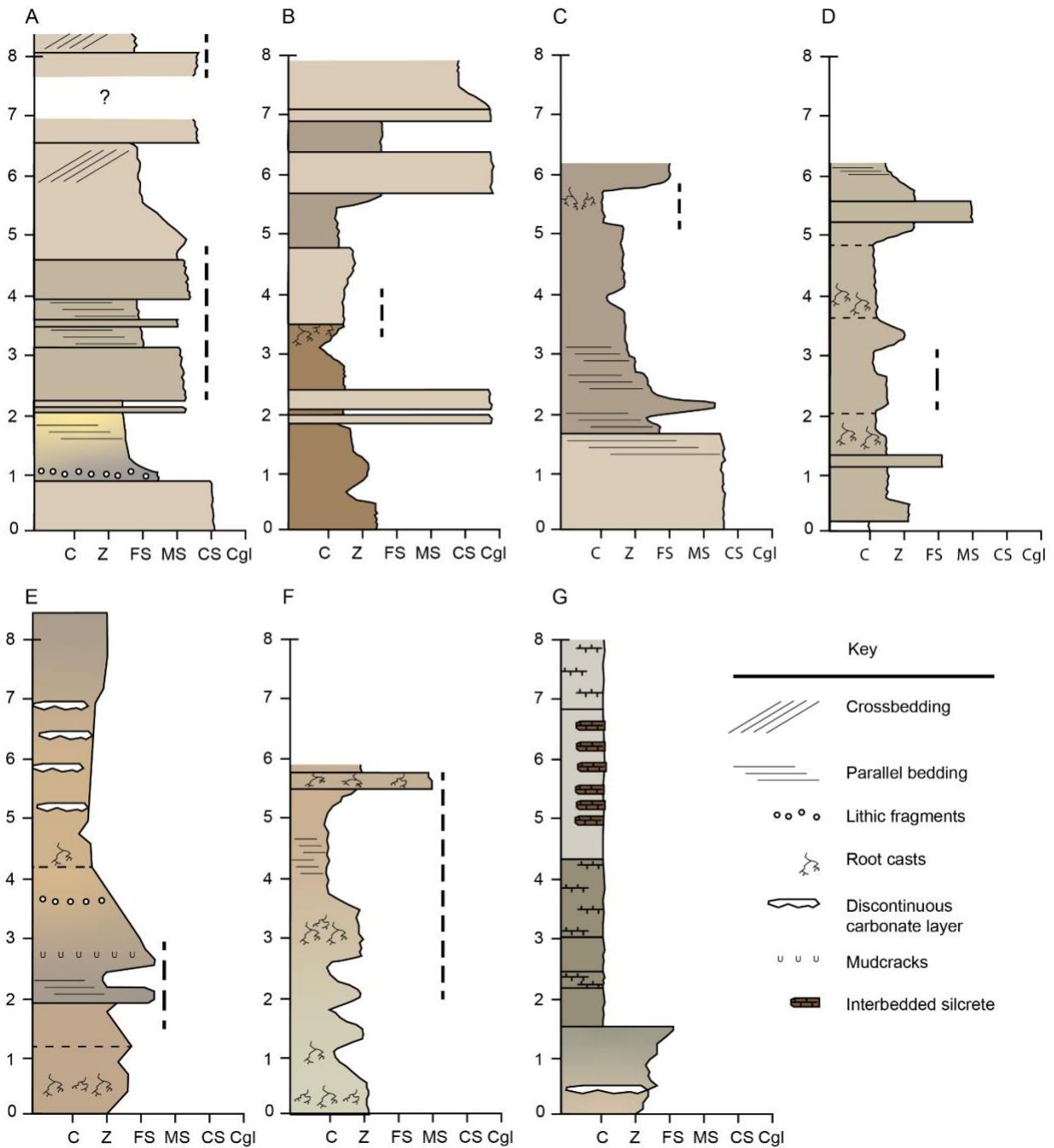


Figure 4.4: Representative stratigraphic columns for each microfacies association. A) FA1a, large channels; B) FA1b, small channels; C) FA2, channel margin and levee deposits; D) FA3a, well-drained floodplains; E) FA3b, floodplains and playa lake deposits; F) FA3c poorly-drained floodplains; G) FA4, pond or lake deposits. FA5 represents crevasse splays which are found interbedded within other microfacies associations.

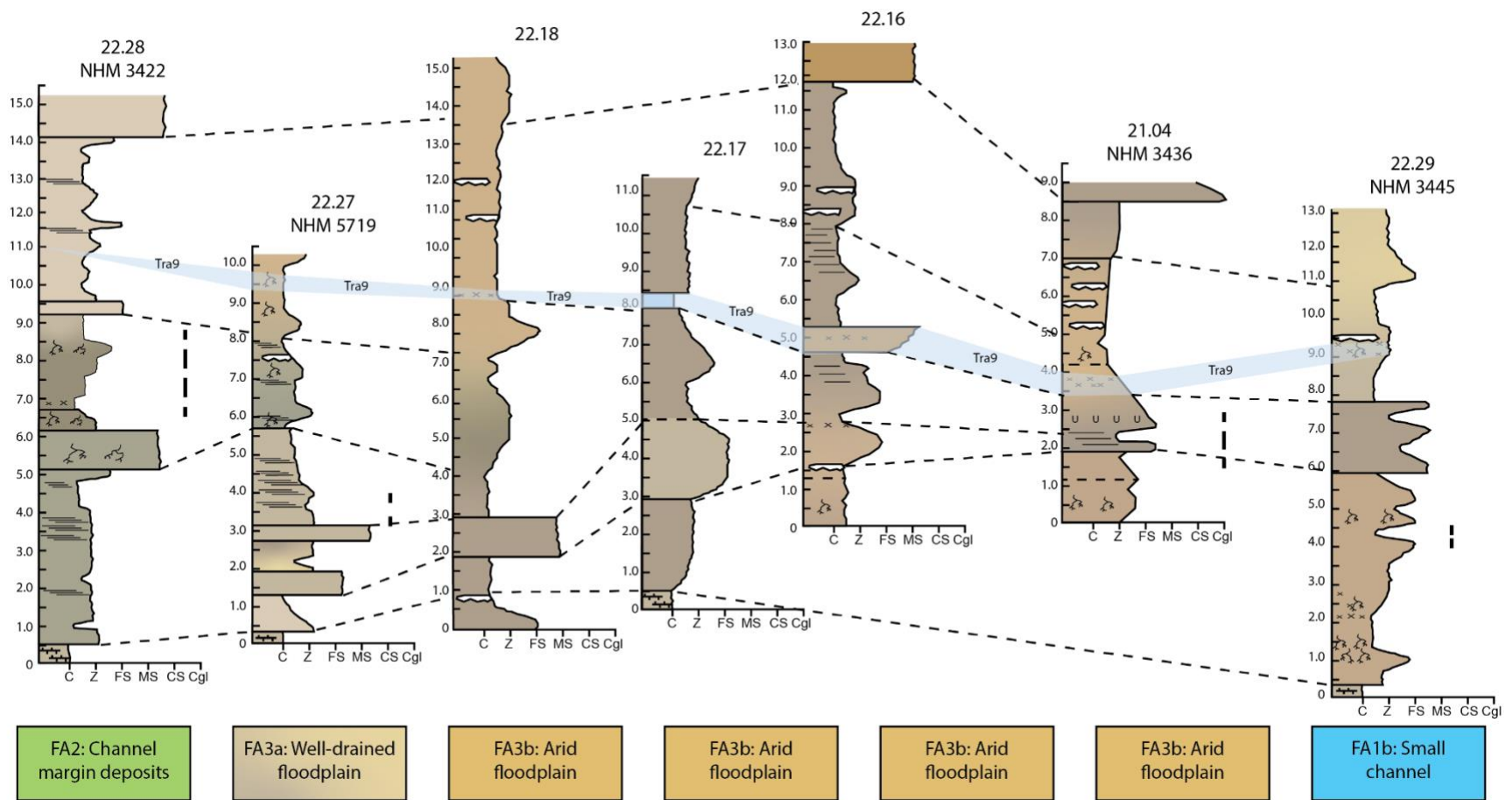


Figure 4.5: Correlation of microstratigraphic sections illustrating landscape heterogeneity and fossil horizons within each microfacies sequence. Tra9 is a radiometrically dated ( $\text{Ar}/\text{Ar}$   $10.2 \pm 0.2$  Ma) ash layer that is correlative throughout the area due to its distinctive blue-grey coloration. Fossil horizons are denoted by vertical dotted lines next to the stratigraphic sections. Numbers refer to field designations of sections. NHM locality numbers are presented when documented fossil horizons were located within sections.



Table 4.1: Highly productive fossil localities of the Dove Spring Formation with age, number of specimens, macro- and microfacies associations for localities, and interpretation of fossil horizon depositional environment based on lithofacies. In some cases, we were unable to locate evidence for specific fossil horizons in the field (marked unknown).

NHM Locality Number	Age (Ma)	Number of Specimens	Large Mammal Specimens	Macro FA	Micro FA	Fossil Horizon Depositional Environment
3472	9.9	22	21	3	2	Channel margin
3436	10.0	4	4	3	3b	Channel margin
3444	10.1	155	8	1	1b	Channel margin
3447	9.8	203	16	2	2	Poorly-drained floodplain
3621	9.6	2	2	2	1b	Small channel
3420	10.1	58	58	3	3b	Arid floodplain
1553	10.4	84	65	1	1a	Large channel
1741	11.7	48	48	1	1a	Channel margin
6375	9.9	172	13	3	3a	Well-drained floodplain
1108	11.9	102	100	1	1a	Channel margin
3662	12.5	56	12	1	1a	Well-drained floodplain
5718	8.5	65	31	1	1b	Well-drained floodplain
4702	8.5	657	4	2	1b	Channel margin
6380	8.5	74	19	3	3b	Arid floodplain
5669	8.5	5	5	3	2	Channel margin
6923	8.5	1	1	3	2	Unknown
6141	12.5	7	2	1	1a	Channel margin
6620	12.5	8	8	1	1a	Channel margin
4651	8.5	2	2	3	2	Channel margin
5693	8.5	2	0	3	1b	Channel margin
5719	10.1	10	10	3	3a	Channel margin
5976	10.1	10	0	3	3b	Unknown
3416	12.0	13	13	1	2	Channel margin
3679	12.0	9	8	1	1a	Channel margin
3531	9.5	53	40	3	3c	Unknown
3532	9.5	13	13	3	3a	Well-drained floodplain
3556	9.8	44	44	3	3b	Channel margin
7356	9.7	7	7	3	3a	Well-drained floodplain
3580	9.5	139	21	3	2	Channel margin
3665	9.6	7	7	3	2	Channel margin
3422	10.2	14	14	3	2	Channel margin
3668	9.9	14	0	1	2	Channel margin
3445	10.2	36	36	1	1b	Small channel
4639	10.9	30	3	3	3b	Poorly-drained floodplain
5094	10.9	66	27	3	3b	Poorly-drained floodplain
1414	11.0	74	74	3	3a	Well-drained floodplain

3598	10.4	6	6	3	3a	Channel margin
3415	10.2	38	38	3	3c	Channel margin
1739	12.4	5	5	1	2	Channel margin
7543	8.8	1	1	2	3c	Poorly-drained floodplain
1105	9.6	18	16	3	3c	Poorly-drained floodplain
7466	8.8	3	3	3	3a	Well-drained floodplain
4640	10.6	2	2	3	1b	Poorly-drained floodplain
CIT 510	10.6	3	3	2	1b	Poorly-drained floodplain
8019	10.4	3	0	1	4	Unknown
6397	8.7	1	1	3	2	Oxbow lake/pond
3589	8.8	1	1	3	3c	Poorly-drained floodplain

---

Table 4.2: Descriptions of facies within each macrofacies association (FA).

FA	Primary lithologies	Sedimentary structures	Sequence Thickness	Spatial relationships	Interpretation
1	Medium- to coarse-grained sandstone; yellow tan (10 YR 8/2), buff tan (5 YR 7/2), greyish tan (10 YR 6/2)	Prominent parallel bedding, ripple marks, crossbedding	20-50 m	Beds are very thick, well-sorted	Laterally extensive, large channel deposits
	Medium- to coarse-grained sandstones and conglomerates; greyish tan (10 YR 6/2), fine- to medium- grained sandstone, amber tan (10 YR 5/4)	Poor sorting, highly bioturbated, root casts, occasional parallel and cross-bedding	10-20 m	Coarsen upwards from fine-grained sediments, sharp undulating contacts with finer material	Small channel deposits
2	Fine-grained sandstones, siltstones and clayey siltstones; greyish tan (10 YR 6/2)	Indurated units, blocky fracture, faint laminated bedding, carbonate rind surfaces, dispersed ash and carbonate, siliceous root casts (5-10 mm) in older units (> 11.0 Ma); carbonate root casts (5-10 mm) in younger units (> 11.0 Ma)	30-200 m	Fining upwards from incised base or gradational contacts with fine-to medium-grained sediments	Channel margin and levee deposits
	Marlstone, beige (5 Y 8/1), siltstone greyish tan (10 Y 6/2)	Highly indurated, prominent laminated bedding in siltstone, siliceous root casts	10-30 m	Veins of silcrete interbedded within carbonate	Pond deposits
3	Clayey siltstone, buff tan (5 Y 7/2), siltstone to claystone, greyish tan (10 YR 6/2), siltstone, orange tan (10 YR 7/4)	Blocky fracture, faint to prominent parallel or laminated bedding or massive, ripple marks common, root casts, discontinuous carbonate layers, uncommon mudcracks, petrified tree stumps	20-570 m	Dispersed ash and gypsum common within claystones, interbeds of buff tan (5 Y 7/2) siltstones associated with silcrete layers, often capped by medium- to coarse-grained sandstones	Floodplain deposits

Table 4.3: Descriptions of facies within each high-resolution microfacies association (FA).

Fossil Horizon FA	Primary lithologies	Sedimentary structures	Bed thickness	Spatial relationships	Interpretation	
1	a	Medium- to coarse-grained sandstone; yellow tan (10 YR 8/2), buff tan (5 YR 7/2)	Prominent parallel bedding, ripple marks, crossbedding	2.0-7.0 m	Beds are very thick, well-sorted	Laterally extensive, large channel deposits
	b	Medium- to coarse-grained sandstones and conglomerates; greyish tan (10 YR 6/2), buff tan (10 YR 7/2)	Poor sorting, highly bioturbated, root casts, faint to prominent crossbedding	0.6-1.6 m	Coarsen upwards from fine-grained sediments, or grade over < 0.2 m, undulating basal contacts with siltstones	Small channel deposits
2	Fine-grained sandstones, buff tan (5 YR 7/2), amber tan (10 YR 5/4), siltstones and clayey siltstones; greyish tan (10 YR 6/2)	Indurated units, blocky fracture, faint laminated bedding, carbonate rind surfaces, dispersed ash and carbonate, siliceous root casts in older units (> 11.0 Ma); carbonate root casts in younger units (> 11.0 Ma)	0.5-1.5 m	Fining upwards from incised base or gradational contacts with fine- to medium-grained sediments	Channel margin and levee deposits	
3	a	Clayey siltstone, buff tan (5 Y 7/2)	Blocky fracture, faint bedding or massive, ripple marks common, root casts uncommon and limited to blocky clay and siltstone units	1.0-4.0 m	Dispersed ash and evaporites common within claystones	Floodplain deposits, well-drained
	b	Siltstone to claystone, greyish tan (10 YR 6/2)	Abundant discontinuous carbonate layers, dispersed ash, evaporite minerals, faint to prominent parallel or laminated bedding, root casts common in claystones, petrified tree stumps	1.0-2.5 m	Interbeds of buff tan (5 Y 7/2) siltstones associated with silcrete layers, carbonate interbeds and discontinuous surfaces	Floodplain deposits, arid
	c	Siltstone, orange tan (10 YR 7/4)	Root casts, faint parallel bedding, uncommon mudcracks, thin carbonate layers	1.3-2.1 m	Often capped by medium- to coarse-grained sandstones	Floodplain deposits, poorly drained
4	Marlstone, beige (5 Y 8/1), siltstone greyish tan (10 Y 6/2)	Highly indurated, prominent laminated bedding in siltstone, siliceous root casts	7.0-8.25 m	Veins of silcrete interbedded within carbonate	Pond deposits	
5	Coarse-grained sandstone; yellow tan (10 YR 8/2), medium-grained sandstone; buff tan (5 Y 7/2)	Well-defined crossbedding, massive	0.3-1.0 m	Interbedded within finer sediments	Crevasse splay deposits	

Table 4.4: Distribution of fossil localities and specimens within macrofacies sequences and comparison with localities only containing large mammals. Based on meter-scale stratigraphic columns.

Tectonic Episode	Macrofacies Sequence and Time Interval	Localities	Specimens	Area (km <sup>2</sup> )	Localities per km <sup>2</sup>	Specimens per km <sup>2</sup>
<b>Large Mammals</b>						
Episode 3 (9.4 to 8.5 Ma)	Floodplains	83	539	3.46	24	156
	Channel margins	56	357	1.27	44	280
	Channels	16	118	0.72	22	164
Episode 2 (10.4 to 9.5 Ma)	Floodplains	92	599	2.01	46	298
	Channel margins	45	296	1.75	26	170
	Channels	26	146	0.91	29	161
Episode 1 (12.5 to 10.5 Ma)	Floodplains	42	235	1.34	31	175
	Channel Margins	3	7	1.07	3	7
	Channels	37	378	0.83	45	455
<b>All Fossil Specimens</b>						
Episode 3 (9.4 to 8.5 Ma)	Floodplains	114	784	3.46	33	227
	Channel margins	102	1970	1.27	80	1546
	Channels	23	181	0.72	32	252
Episode 2 (10.4 to 9.5 Ma)	Floodplains	134	852	2.01	67	424
	Channel margins	86	1342	1.75	49	769
	Channels	42	257	0.91	46	282
Episode 1 (12.5 to 10.5 Ma)	Floodplains	52	261	1.34	39	195
	Channel margins	9	8	1.07	8	7
	Channels	61	454	0.83	73	547

Table 4.5: Distribution of fossil localities and specimens among microfacies associations, based on decimeter-scale microstratigraphic columns.

Micro FA	No. of localities	Percent of total localities	No. of specimens	Percent of total specimens	Large mammal specimens	Life habitat for large mammals?
1a	7	14.9	314	13.4	245	No
b	8	17.0	922	39.3	86	No
2	12	25.5	426	18.2	106	Yes
3a	6	12.8	272	11.6	113	Yes
b	8	17.0	299	12.7	168	Yes
c	5	10.6	111	4.7	96	Yes
4	1	2.1	3	0.1	0	No
5	0	0.0	0	0.0	0	Yes

Table 4.6: Comparison of bone elements recovered from 10.2 Ma lateral transect (upper four rows) and contemporaneous localities (bottom rows).

NHM Locality	Age (Ma)	Micro FA	Fossil Horizon Depositional Environment	No. of Specimens	Large Mammal Specimens	Large Mammal Cranial Elements	Microvertebrate Cranial Elements
3422	10.2	2	Channel margin	14	14	6	0
5719	10.2	3a	Channel margin	10	10	6	0
3436	10.2	3b	Channel margin	4	4	2	0
3445	10.2	1b	Small channel	36	36	5	0
3420	10.1	3b	Floodplain	58	58	23	0
3415	10.2	3c	Channel margin	38	38	15	0
3444	10.1	1b	Channel margin	155	8	7	38
3598	10.4	3a	Channel margin	6	6	5	0
1553	10.4	1a	Large channel	84	65	30	6
8019	10.4	4	Unknown	3	0	0	0

Table 4.7: List of localities and specimens from NHM database for 10.2 Ma lateral section correlation in Table 4.6.

NHM Locality	Taxon	Fossil Element	NHM Specimen No.
1553	<i>Aelurodon</i>	Tooth: C frag	4166
1553	<i>Aelurodon aphobus</i>	Tooth: /p4-m2	4165
1553	<i>Alluvisorex chasseur</i>	Dentary frag w teeth	4264
1553	<i>Alluvisorex chasseur</i>	Dentary frag w teeth	4265
1553	<i>Amebelodon burnhami</i>	Tooth: M3/	59701
1553	Antilocapridae	Astragalus	59558
1553	Antilocapridae	Metapodial dist	59559
1553	Antilocapridae	Patella	59557
1553	Antilocapridae	Sesamoid	59560
1553	Antilocapridae	Tooth: M3/	59554
1553	Antilocapridae	Tooth: Tooth frag	59555
1553	Antilocapridae	Tooth: Tooth frag	59556
1553	Camelidae	Astragalus	59710
1553	Camelidae	Calcaneum	59551
1553	Camelidae	Calcaneum	59711
1553	Camelidae	Dentary frag ?	4145
1553	Camelidae	Dentary w p4-m2	4160
1553	Camelidae	Dentary w p4-m3	4159
1553	Camelidae	Femur incompl	4137
1553	Camelidae	Innominate acetabulum	59708
1553	Camelidae	Maxilla w P3-M3	4158
1553	Camelidae	Metapodial	4141
1553	Camelidae	Metapodial	4148
1553	Camelidae	Metapodial dist	4152
1553	Camelidae	Metatarsal Prox	59552
1553	Camelidae	Phalanx	4149
1553	Camelidae	Phalanx dist	4151
1553	Camelidae	Phalanx Medial	59553
1553	Camelidae	Radioulna dist	4130
1553	Camelidae	Scapula frag	59707
1553	Camelidae	Tibia prox	4150
1553	Camelidae	Tooth: /i3	59706
1553	Camelidae	Tooth: /p4	4161
1553	Camelidae	Tooth: M frag	4125
1553	Camelidae	Tooth: M1/	4163
1553	Camelidae	Unciform	59709
1553	Canidae	Metacarpal dist	146041
1553	Canidae	Tooth: /i + c	4172
1553	Canidae	Tooth: C	4157



1553	Carnivora	Phalanx dist	4171
1553	Carnivora	Tooth: /i	150881
1553	Carnivora	Tooth: /i3	150879
1553	Carnivora	Tooth: /i3	150880
1553	Carnivora	Tooth: /p2	150882
1553	Carnivora	Vertebra Caudal	59698
1553	<i>Cormohipparion</i> sp.	Tooth: P2-M3/ Maxilla frag w P4-M2 + P4-M1	148928
1553	<i>Epicyon haydeni</i>	Dentary w dp3-m1	143519
1553	<i>Epicyon saevus</i>	Dentary w dp3-m1	59697
1553	Equidae	Tooth: /cheek tooth frag	59704
1553	Equidae	Tooth: /i2	59702
1553	Equidae	Tooth: Cheek Tooth frag	59703
1553	<i>Gerrhonotus</i> sp.	Dentary	151258
1553	<i>Gerrhonotus</i> sp.	Dentary	151259
1553	<i>Gerrhonotus</i> sp.	Dentary	151260
1553	<i>Gerrhonotus</i> sp.	Frontal	151262
1553	<i>Gerrhonotus</i> sp.	Frontal	151263
1553	<i>Gerrhonotus</i> sp.	Frontal	151264
1553	<i>Gerrhonotus</i> sp.	Frontal	151265
1553	<i>Gerrhonotus</i> sp.	Maxilla	151251
1553	<i>Gerrhonotus</i> sp.	Maxilla	151252
1553	<i>Gerrhonotus</i> sp.	Maxilla	151253
1553	<i>Gerrhonotus</i> sp.	Maxilla	151254
1553	<i>Gerrhonotus</i> sp.	Maxilla	151255
1553	<i>Gerrhonotus</i> sp.	Maxilla	151256
1553	<i>Gerrhonotus</i> sp.	Maxilla	151257
1553	<i>Gerrhonotus</i> sp.	Premaxilla	151261
1553	<i>Gerrhonotus</i> sp.	Quadrate	151266
1553	Gomphotheriidae	Tooth: M frag	59700
1553	Mammalia	Femur dist	59563
1553	Mammalia	Patella	59564
1553	Mammalia	Ulna prox	59561
1553	Mammalia	Vertebra Cervical	59562
1553	<i>Merycodus</i> sp.	Maxilla w Teeth	4162
1553	Merycoidodontidae	Maxilla frag + M1-M3	4170
1553	Mustelidae	Dentary frag	4173
1553	<i>Neohipparion</i> sp.	Tooth: /cheek tooth	59699
1553	<i>Osteoborus diabloensis</i>	Dentary w p3-m1 + p4	4167
3415	Antilocapridae	Calcaneum frag	59809
3415	Antilocapridae	Calcaneum frag	59810
3415	Antilocapridae	Dentary w dp2-m1	59806
3415	Antilocapridae	Dentary w dp3-m1	59808
3415	Antilocapridae	Dentary w p4-m2	59807
3415	Antilocapridae	Phalanx Prox Prox	59811

3415	Antilocapridae	Tooth: /m1+m2	59805
3415	Antilocapridae	Tooth: /p4	59804
3415	Camelidae	Astragalus frag	144473
3415	Camelidae	Bone frags	3635
3415	Camelidae	Calcaneum incompl	59800
3415	Camelidae	Metapodial dist	59801
3415	Camelidae	Metapodial dist	59802
3415	Camelidae	Phalanx Prox	59803
3415	Camelidae	Vertebra Cervical	59799
3415	Canidae	Phalanx Medial	59791
3415	Canidae	Tooth: /i3	59790
3415	Canidae	Ulna prox	59792
3415	Carnivora	Tooth: P	59793
3415	Equidae	Tooth: /cheek tooth frags	59796
3415	Equidae	Tooth: Cheek Tooth/ frags	59795
3415	Equidae	Tooth: I	59798
3415	Felidae	Humerus incompl	3643
3415	Gomphotheriidae	Tooth: Tooth frag	59794
3415	<i>Hipparion</i> sp.	Metapodial dist + Phalanx	3642
3415	<i>Hipparion</i> sp.	Tibia dist + Astragalus	3639
3415	<i>Hipparion</i> sp.	Tooth: /i2-i3 + I2-I3/	59797
3415	<i>Hipparion forcei</i>	Dentary frag + teeth	3637
3415	<i>Hipparion tehonense</i>	Tooth: Teeth	3634
3415	<i>Ischyrosmilus</i> sp.	Humerus dist	3641
3415	Machairodontinae	Humerus dist	59789
3415	Mammalia	Tooth: Tooth frags	59812
3415	<i>Paracamelus</i> sp.	Metapodial + Vertebra	3640
3415	<i>Pliohippus tantalus</i>	Bone frags	3636
3415	<i>Procamelus</i> sp.	Carpal ?	3645
3415	<i>Procamelus</i> sp.	Dentary frag	3644
3415	<i>Procamelus</i> sp.	Podial	3638
3415	Testudinata	Carapace frag	59788
3420	Antilocapridae	Astragalus	59875
3420	Antilocapridae	Astragalus	148197
3420	Antilocapridae	Calcaneum	59876
3420	Antilocapridae	Dentary frag w p2-p4	59866
3420	Antilocapridae	Dentary frags	59867
3420	Antilocapridae	Dentary w dp2-m2	59862
3420	Antilocapridae	Dentary w m1-m2	59865
3420	Antilocapridae	Dentary w m3	59864
3420	Antilocapridae	Femur prox	59873
3420	Antilocapridae	Fibula	59874
3420	Antilocapridae	Humerus dist	146038
3420	Antilocapridae	Humerus dist	148198
3420	Antilocapridae	Metacarpal prox	59877

3420	Antilocapridae	Metapodial dist	59878
3420	Antilocapridae	Phalanx dist	59881
3420	Antilocapridae	Phalanx Prox	59879
3420	Antilocapridae	Phalanx Ungual	59880
3420	Antilocapridae	Radius prox	59871
3420	Antilocapridae	Rib mid frag	59872
3420	Antilocapridae	Tooth: /m3	152685
3420	Antilocapridae	Tooth: root	59863
3420	Antilocapridae	Tooth: Tooth frag	59882
3420	Antilocapridae	Tooth: Tooth frags	59868
3420	Antilocapridae	Vertebra Lumbar frag	59870
3420	Antilocapridae	Vertebra Thoracic prox	59869
3420	Camelidae	Bone frags	143947
3420	Camelidae	Cuneiform	59859
3420	Camelidae	Dentary ant w i1-c	59853
3420	Camelidae	Navicular	59858
3420	Camelidae	Phalanx Prox Prox	59860
3420	Camelidae	Radioulna prox	59857
3420	Camelidae	Tooth: Cheek Tooth frags	59852
3420	Camelidae	Vertebra Cervical frag	59855
3420	Camelidae	Vertebra Cervical frag	59856
3420	Camelidae	Vertebra Lumbar frag	59854
3420	Carnivora	Maxilla frag w C	59843
3420	Equidae	Astragalus	144081
3420	Equidae	Astragalus frag	59849
3420	Equidae	Cuboid	59847
3420	Equidae	Metacarpal	144073
3420	Equidae	Pes Centrale	148201
3420	Equidae	Phalanx dist frag	59850
3420	Equidae	Tooth: Cheek Teeth frags	59846
3420	Gomphotheriidae	Tooth: Tooth frag	59841
3420	<i>Hipparion</i> sp.	Calcaneum frag	59848
3420	<i>Hipparion</i> sp.	Tooth: /i + tooth frag	146248
3420	<i>Hipparion</i> sp.	Tooth: Cheek Tooth/	59845
3420	<i>Hipparion</i> sp.	Tooth: Cheek Tooth/ frag	59844
3420	<i>Hipparion forcei</i>	Tooth: /m1	146037
3420	<i>Hipparion forcei</i>	Tooth: M/	143950
3420	<i>Hypolagus</i> sp.	Tibia dist	148199
3420	<i>Leptocyon</i> sp.	Dentary frag	59842
3420	<i>Pliohippus</i> sp.	Tooth: L M1/	143948
3420	<i>Pliohippus</i> sp.	Tooth: L M3/	143949
3420	Tayassuidae	Dentary ant w c root	59851
3420	Testudinidae	Carapace frag	148200
3420	Testudininae	Carapace frags	146292
3422	Camelidae	Astragalus	59893

3422	Camelidae	Astragalus	59904
3422	Camelidae	Astragalus	132675
3422	Camelidae	Astragalus	148184
3422	Camelidae	Cuboid	143999
3422	Camelidae	Cuneiform frag	59894
3422	Equidae	Scapula frag	59898
3422	<i>Hipparion</i> sp.	Tooth: M1/ -or- P4/	59897
3422	<i>Hipparion</i> sp.	Tooth: M2/	148903
3422	<i>Hipparion forcei</i>	Tooth: /cheek tooth frags	59895
3422	<i>Hipparion forcei</i>	Tooth: /m2	59896
3422	<i>Hipparion forcei</i>	Tooth: P/	148904
3422	<i>Merycodus</i> sp.	Dentary frag w m1+m3	4285
3422	<i>Pliohippus</i> sp.	Metapodial dist frag	59899
3436	Camelidae	Bone frags	148190
3436	Gomphotherium	Tooth: tooth frags	146060
3436	<i>Hipparion</i> sp.	Calcaneum	59972
3436	<i>Plioceros</i> sp.	Tooth: /m2 frag + M1/	146059
3444	Agamidae	Dentary	151280
3444	<i>Alluvisorex chasseur</i>	Dentary w teeth	118970
3444	Antilocapridae	Dentary w i2+p2+p4-m3	59991
3444	Antilocapridae	Dentary w p2-m3	59990
3444	Antilocapridae	Tooth: P4-M1/	59992
3444	Camelidae	Tibia dist	59989
3444	Camelidae	Tooth: /i2	59988
3444	Camelidae	Tooth: Cheek Tooth	59987
3444	Camelidae	Tooth: Cheek Tooth frag	59986
3444	<i>Copemys</i> sp.	Dentary w m1-m3	124790
3444	<i>Copemys</i> sp.	Dentary w m1-m3	124910
3444	<i>Copemys</i> sp.	Tooth: /m1	124791
3444	<i>Copemys</i> sp.	Tooth: /m1	124792
3444	<i>Copemys</i> sp.	Tooth: /m1	124793
3444	<i>Copemys</i> sp.	Tooth: /m1	124794
3444	<i>Copemys</i> sp.	Tooth: /m1	124911
3444	<i>Copemys</i> sp.	Tooth: /m2	125060
3444	<i>Copemys</i> sp.	Tooth: /m2	125061
3444	<i>Copemys</i> sp.	Tooth: /m2	125062
3444	<i>Copemys</i> sp.	Tooth: /m2	125063
3444	<i>Copemys</i> sp.	Tooth: /m2	125064
3444	<i>Copemys</i> sp.	Tooth: /m2	125066
3444	<i>Copemys</i> sp.	Tooth: /m3	125065
3444	<i>Copemys</i> sp.	Tooth: M1/	125408
3444	<i>Copemys</i> sp.	Tooth: M1/	125409
3444	<i>Copemys</i> sp.	Tooth: M1/	125410
3444	<i>Copemys</i> sp.	Tooth: M1/	125411
3444	<i>Copemys</i> sp.	Tooth: M1/	125412

3444	<i>Copemys</i> sp.	Tooth: M1/	125413
3444	<i>Copemys</i> sp.	Tooth: M1/	125414
3444	<i>Copemys</i> sp.	Tooth: M1/	125415
3444	Cricetidae	Tooth: /m1	125171
3444	Cricetidae	Tooth: /m3	125169
3444	Cricetidae	Tooth: /m3	125170
3444	Cricetidae	Tooth: /m3	125172
3444	Cricetidae	Tooth: /m3	125173
3444	Cricetidae	Tooth: M1/ + /m2	125652
3444	Cricetidae	Tooth: M1-M3/	125651
3444	Cricetidae	Tooth: M2/	125710
3444	Cricetidae	Tooth: M2/	125711
3444	Cricetidae	Tooth: M2/	125712
3444	Cricetidae	Tooth: M2/	125713
3444	Cricetidae	Tooth: M3/	125935
3444	Cricetidae	Tooth: M3/	125936
3444	Cricetidae	Tooth: M3/	125937
3444	<i>Gerrhonotus</i> sp.	Dentary	127551
3444	<i>Gerrhonotus</i> sp.	Dentary	127552
3444	<i>Gerrhonotus</i> sp.	Dentary	127553
3444	<i>Gerrhonotus</i> sp.	Dentary	127554
3444	<i>Gerrhonotus</i> sp.	Dentary	127555
3444	<i>Gerrhonotus</i> sp.	Maxilla	127544
3444	<i>Gerrhonotus</i> sp.	Maxilla	127545
3444	<i>Gerrhonotus</i> sp.	Maxilla	127546
3444	<i>Gerrhonotus</i> sp.	Maxilla	127557
3444	<i>Gerrhonotus</i> sp.	Maxilla	127558
3444	<i>Gerrhonotus</i> sp.	Maxilla	127559
3444	<i>Gerrhonotus</i> sp.	Maxilla	127560
3444	<i>Gerrhonotus</i> sp.	Maxilla	127561
3444	<i>Gerrhonotus</i> sp.	Maxilla	127562
3444	<i>Gerrhonotus</i> sp.	Skull Frontal	127549
3444	<i>Gerrhonotus</i> sp.	Skull Frontal	127550
3444	<i>Gerrhonotus</i> sp.	Skull Pterygoid	127547
3444	<i>Gerrhonotus</i> sp.	Skull Pterygoid	127548
3444	<i>Hesperolagomys</i> sp.	Tooth: M/	152965
3444	<i>Hypolagus</i> sp.	Tooth: M3/	126806
3444	Iguanidae	Dentary	151312
3444	Iguanidae	Dentary	151313
3444	Iguanidae	Dentary	151314
3444	Iguanidae	Dentary	151315
3444	Iguanidae	Dentary	151316
3444	Iguanidae	Dentary	151317
3444	Iguanidae	Maxilla	151302
3444	Iguanidae	Maxilla	151303

3444	Iguanidae	Maxilla	151304
3444	Iguanidae	Maxilla	151305
3444	Iguanidae	Maxilla	151306
3444	Iguanidae	Maxilla	151307
3444	Iguanidae	Maxilla	151308
3444	Iguanidae	Maxilla	151309
3444	Iguanidae	Maxilla	151310
3444	Iguanidae	Maxilla	151311
3444	<i>Parapliosaccomys</i> sp.	Tooth:	126801
3444	<i>Parapliosaccomys</i> sp.	Tooth:	126802
3444	<i>Parapliosaccomys</i> sp.	Tooth:	126803
3444	<i>Parapliosaccomys</i> sp.	Tooth:	126805
3444	<i>Parapliosaccomys</i> sp.	Tooth:	126807
3444	<i>Parapliosaccomys</i> sp.	Tooth:	126808
3444	<i>Parapliosaccomys</i> sp.	Tooth:	126809
3444	<i>Parapliosaccomys</i> sp.	Tooth:	126810
3444	<i>Parapliosaccomys</i> sp.	Tooth:	126811
3444	<i>Parapliosaccomys</i> sp.	Tooth:	126812
3444	<i>Parapliosaccomys</i> sp.	Tooth:	126814
3444	<i>Parapliosaccomys</i> sp.	Tooth:	126815
3444	<i>Parapliosaccomys</i> sp.	Tooth:	126818
3444	<i>Parapliosaccomys</i> sp.	Tooth:	126819
3444	<i>Parapliosaccomys</i> sp.	Tooth:	126820
3444	<i>Parapliosaccomys</i> sp.	Tooth:	126821
3444	<i>Parapliosaccomys</i> sp.	Tooth:	126822
3444	<i>Parapliosaccomys</i> sp.	Tooth:	126823
3444	<i>Parapliosaccomys</i> sp.	Tooth:	126824
3444	<i>Parapliosaccomys</i> sp.	Tooth:	126825
3444	<i>Parapliosaccomys</i> sp.	Tooth:	126826
3444	<i>Parapliosaccomys</i> sp.	Tooth:	126827
3444	<i>Parapliosaccomys</i> sp.	Tooth:	126828
3444	<i>Parapliosaccomys</i> sp.	Tooth:	126830
3444	<i>Parapliosaccomys</i> sp.	Tooth:	126831
3444	<i>Parapliosaccomys</i> sp.	Tooth: /p4	126817
3444	<i>Parapliosaccomys</i> sp.	Tooth: /p4	126829
3444	<i>Parapliosaccomys</i> sp.	Tooth: P4/	126804
3444	<i>Parapliosaccomys</i> sp.	Tooth: P4/	126816
3444	<i>Perognathus</i> sp.	Tooth:	126862
3444	<i>Perognathus</i> sp.	Tooth: /m1	126858
3444	<i>Perognathus</i> sp.	Tooth: /m2	126859
3444	<i>Perognathus</i> sp.	Tooth: /m3	126860
3444	<i>Perognathus</i> sp.	Tooth: /p4	126847
3444	<i>Perognathus</i> sp.	Tooth: /p4-m1	126846
3444	<i>Perognathus</i> sp.	Tooth: /tooth	126861
3444	<i>Perognathus</i> sp.	Tooth: M1/	126848

3444	<i>Perognathus</i> sp.	Tooth: M1/	126849
3444	<i>Perognathus</i> sp.	Tooth: M1/	126850
3444	<i>Perognathus</i> sp.	Tooth: M2/	126851
3444	<i>Perognathus</i> sp.	Tooth: M2/	126852
3444	<i>Perognathus</i> sp.	Tooth: M2/	126853
3444	<i>Perognathus</i> sp.	Tooth: M2/	126854
3444	<i>Perognathus</i> sp.	Tooth: M2/	126855
3444	<i>Perognathus</i> sp.	Tooth: M3/	126856
3444	<i>Perognathus</i> sp.	Tooth: M3/	126857
3444	<i>Phelosacomys</i> sp.	Tooth:	126813
3444	Xantusia	Dentary	127446
3444	Xantusia	Dentary	127447
3444	Xantusia	Dentary	127448
3444	Xantusia	Dentary	127449
3444	Xantusia	Dentary	127450
3444	Xantusia	Dentary	127451
3444	Xantusia	Dentary	127452
3444	Xantusia	Dentary	127453
3444	Xantusia	Dentary	127454
3444	Xantusia	Dentary	127455
3444	Xantusia	Maxilla	127430
3444	Xantusia	Maxilla	127431
3444	Xantusia	Maxilla	127432
3444	Xantusia	Maxilla	127433
3444	Xantusia	Maxilla	127434
3444	Xantusia	Maxilla	127435
3444	Xantusia	Maxilla	127436
3444	Xantusia	Maxilla	127437
3444	Xantusia	Maxilla	127438
3444	Xantusia	Maxilla	127439
3444	Xantusia	Maxilla	127440
3444	Xantusia	Maxilla	127441
3444	Xantusia	Maxilla	127442
3444	Xantusia	Maxilla	127443
3444	Xantusia	Maxilla	127444
3444	Xantusia	Maxilla	127445
3444	Xantusia	Premaxilla	127429
3445	Antilocapridae	Astragalus frag	60017
3445	Antilocapridae	Calcaneum frag	60022
3445	Antilocapridae	Cuboid	60002
3445	Antilocapridae	Endocuneiform	60019
3445	Antilocapridae	Endocuneiform	60020
3445	Antilocapridae	Femur incompl	60009
3445	Antilocapridae	Femur incompl	60010
3445	Antilocapridae	Femur prox	60006

3445	Antilocapridae	Femur prox	60007
3445	Antilocapridae	Femur prox	60008
3445	Antilocapridae	Innominate acetabulum frag	60003
3445	Antilocapridae	Innominate acetabulum frag	60004
3445	Antilocapridae	Innominate acetabulum frag	60005
3445	Antilocapridae	Magnum + Trapezoid	60021
3445	Antilocapridae	Maxilla w dP4-M1	59997
3445	Antilocapridae	Metapodial dist	60025
3445	Antilocapridae	Metapodial dist	60026
3445	Antilocapridae	Patella	60011
3445	Antilocapridae	Patella	60012
3445	Antilocapridae	Patella	60013
3445	Antilocapridae	Patella	60014
3445	Antilocapridae	Patella	60015
3445	Antilocapridae	Phalanx Prox	60024
3445	Antilocapridae	Phalanx Prox dist	60027
3445	Antilocapridae	Phalanx Prox dist	60028
3445	Antilocapridae	Radioulna dist	60001
3445	Antilocapridae	Sesamoid	60023
3445	Antilocapridae	Tibia dist	60016
3445	Antilocapridae	Tooth: /i2	59998
3445	Antilocapridae	Tooth: Tooth frags	59999
3445	Antilocapridae	Unciform frag	60018
3445	Antilocapridae	Vertebra Cervical frag	60000
3445	Camelidae	Radioulna prox	59996
3445	Camelidae	Scapula frag	59995
3445	Equidae	Tooth: I incompl	59994
3445	Equidae	Tooth: I3/	59993
3598	Camelidae	Calcaneum frag	60545
3598	<i>Cormohipparion occidentale</i>	Tooth: P4/	55684
3598	Gomphotheriidae	Tooth: root	60542
3598	Gomphotheriidae	Tooth: Tusk frag	60541
3598	<i>Hipparion</i> sp.	Tooth: Cheek Teeth frags	60543
3598	Tayassuidae	Radioulna prox	60544
5719	Antilocapridae	Calcaneum	147512
5719	Antilocapridae	Dentary frag	146186
5719	Antilocapridae	Radius + Metacarpal II+III	146184
5719	Antilocapridae	Tibia dist	147508
5719	Antilocapridae	Tooth: /m3	147511
5719	Antilocapridae	Tooth: M2/	147510
5719	Camelidae	Scaphoid	147509
5719	Camelidae	Tooth: P4-M2/	146185
5719	<i>Cormohipparion</i> sp.	Tooth: M1/ frag	146183
5719	<i>Hipparion tehonense</i>	Dentary w p3-m2	140734
8019	Poaceae	shoots	160024



8019 Poaceae  
8019 Poaceae

shoots  
shoots

160025  
160026

## Chapter 5

### **Faunal Change and Paleocology in the Context of Landscape History**

Terrestrial basins throughout the Basin and Range province record a history of topographic change driven by tectonic processes. By integrating a high-resolution stratigraphic record with extensive fossil data from a single basin, I placed faunal change and paleocology into context with landscape history. This allowed me to investigate correlations between faunal change and periods of tectonic activity through the use of faunal analysis, stable isotope paleocology, facies analysis, and interpretation of depositional environments.

I reviewed the geochronology of the Dove Spring Formation using updated radiometric decay constants to establish a temporal framework for evaluating the hypothesis that faunal change related to tectonic history. This work provided context for the spatial and stratigraphic distribution of fossil localities in relation to changes in the tectonic setting. Evidence for temporal boundaries of tectonic episodes is limited by erosion, weathering, and current exposure. Tectonic processes occur over the course of thousands of years, so we allowed for uncertainty of up to 0.25 Myr in my estimates of their timing. The fossil record is influenced by preservation rates that vary with depositional environments, so I used estimates of residence times based on confidence intervals and average stratigraphic gap between occurrences of lineages to provide a more realistic chronology of faunal history. By examining these datasets in conjunction with one another I acknowledged the uncertainty around the timing of changes. The primary test for a causal link between tectonic episodes and faunal change is the timing of these events. When faunal change coincided with or closely followed tectonic activity, it provided support for the

hypothesis of a link between datasets. When faunal change occurred at times different from changes in tectonic activity, it suggested that other factors, such as regional climate change or biotic processes were responsible. By investigating the patterns that occur when tectonic, depositional, and faunal events coincide, we approach a more complete understanding of the interactions between the physical environment and the distribution and evolution of mammals.

I recognized two major phases of faunal change that coincide with the Dove Spring Formation's tectonic history. The accumulation of large mammal species early on is associated with tectonic extension and growth in basin area. This early pattern may represent the generation of additional habitat space or the expansion of dispersal corridors, both of which could facilitate immigration or geographic range shifts to the El Paso Basin. Species loss is the dominant pattern later on and coincides with shear movement. As the basin moved further away from its original source area, drainage networks and water supply were altered or interrupted, potentially resulting in the decline in species richness of large mammals. Sediment supply was also disrupted by shearing, which manifests as a decrease in fossil productivity in the later part of the sequence. Preservation rates were moderate throughout most of the basin's history but decrease significantly after the initiation of a new stage of extension late in the sequence. The presence of numerous, chronically rare lineages such as carnivores during intervals with significant per-capita extinction rates indicates that some of the observed faunal changes were genuine despite low fossil productivity. These findings support a link between tectonic processes and the mammalian community and prompted two new hypotheses that formed the basis for my subsequent research.

In the first scenario, faunal change is driven by ecological changes that result from tectonic alteration of topographic climate and vegetation gradients. In this case, significant

changes in dietary ecology would coincide with episodes of tectonic activity. An alternative hypothesis suggests that apparent faunal change is driven by changes in the fossil productivity of basin sediments. In this case, changes in fossil productivity would occur without significant ecological change and community composition would remain relatively stable throughout the sequence. I used stable isotope analysis to investigate the dietary paleoecology of large mammals and address the first hypotheses. I then applied facies analysis to infer depositional environments in relation to fossil productivity and address the second hypothesis. Here I present my findings in context with the major tectonic episodes that were drivers of landscape evolution during the deposition of the Dove Spring Formation.

### **Older Extension (12.5 Ma to ~10.3 Ma)**

North-south extension beginning between 17 and 15 Ma facilitated subsidence in the El Paso Basin that accommodated the deposition of the early Dove Spring Formation (Loomis and Burbank, 1988). The prevalence of laterally extensive and deep stream channels between 12.5 and 11.7 Ma indicates that extension must have continued in order to generate extensive drainage networks and accommodation space for sediments as the basin continued to grow in area and develop into the “through-going fault stage” of Gawthorpe and Leeder (2000). Sediment accumulation rates indicate that basin growth and subsidence began to slow between 11.7 and 11.0 Ma, at which point large channels no longer appeared. Large channels represented by macrofacies association FA1 were most common near the base of the sequence, with an extensive channel belt that likely ran along the basin margin with the El Paso Mountains to the south. Microfacies associations revealed that depositional environments during this interval were predominantly stream channel and channel-margin deposits, and floodplain deposits were either rare or exposed outside of the main study area. The channel-dominated landscape supplied ample

water resources to vegetation and herbivores, but preservation of life habitats for terrestrial mammals was uncommon until approximately 11.7 Ma or outside of the exposed area.

Fossil productivity of large mammals during the older extensional episode was moderate (~30 localities/km<sup>2</sup> for both channels and floodplains) and relatively constant until the onset of shearing at 10.3 Ma. The presence of significant rates of origination and high log-likelihood ratios of change are evidence for changes in species richness and faunal composition that are not simply the result of sampling. Origination was the primary process of faunal change during early extension in the formation. New species continually appeared and early arrivals exhibited residence times of 1.5-2.0 Myr. The first significant peak in per-capita origination rate occurred at 11.0 Ma, coinciding with a significant change in faunal composition as several new species of canids, mustelids, and merycoidodontids appeared. The majority of species are found elsewhere in the region prior to their first occurrences in the Dove Spring Formation, suggesting that most of the new additions were the result of immigration events, rather than in-situ speciation. The gradual accumulation of species is likely driven by the generation of additional habitat space and environmental gradients that allowed for increasing numbers of species to coexist (Kisel et al., 2011). The expansion of floodplains at 11.0 Ma indicates a change in environmental gradient that facilitated the expansion of life habitats for large mammals.

$\delta^{13}\text{C}$  values of mammalian tooth enamel exhibit gradual depletion between 12.5 and 10.5 Ma, suggesting that habitats with an abundance of C<sub>3</sub> vegetation supported the increasingly diverse assemblage of mammals. The  $\delta^{18}\text{O}$  record from ungulate teeth suggests that a range of C<sub>3</sub> vegetation types was sustained by a moderate climate that was slightly wetter than other nearby Basin and Range sequences (Chapin, 2008; Heusser et al., 2022).

### **Shear Movement (~10.3 Ma to ~9.5 Ma)**

The extensional tectonic setting of the Dove Spring Formation was interrupted by a period of shear movement that began by 10.3 Ma and continued until around 9.5 Ma (Loomis and Burbank, 1988). During this interval, the El Paso Basin was rotated approximately 15° counterclockwise and translated westward along the Garlock fault (Loomis and Burbank, 1988). The basin's geometry was altered, causing changes in water availability and sediment supply. Existing drainage networks were disrupted by strike-slip movement that may have cut them off from their source areas (Bridge and Leeder, 1979; Dokka and Macaluso, 2001). Sediment accumulation rates dropped steadily after 10.4 Ma, decreasing through this tectonic interval. The slope of the main channel belt decreased during this interval and facilitated the development of extensive floodplain deposits represented by FA3, which were the primary source for the majority of fossil specimens.

The expansion of floodplain deposits and an increase in fossil productivity within the floodplain macrofacies association suggest that environmental conditions were conducive to preservation within life habitats for terrestrial mammals. This interval yielded the highest species richness and the majority of fossil specimens. However, origination rates became non-significant and extinction became the dominant process of faunal change. The highest magnitude of change in faunal composition occurred between 10.0 and 9.5 Ma due to species loss across several families. This coincides with an increase in the number of localities, indicating that species loss occurred despite high sampling.

The range of  $\delta^{13}\text{C}$  values of ungulate herbivores narrowed between 10.5 and 10.0 Ma, indicating the consumption of less variety of carbon resources.  $\delta^{13}\text{C}$  values became enriched across all species at approximately 10.0 Ma, suggesting that habitats became slightly more water-limited, but within the threshold of tolerance for most species within the basin.  $\delta^{18}\text{O}$  values

remained relatively stable in obligate drinkers such as equids through this interval, indicating that precipitation amounts were similar to those of the prior tectonic interval. However, two artiodactyl families (Antilocapridae and Camelidae) exhibit a greater range and enrichment in  $\delta^{18}\text{O}$  values during this interval. These animals may have obtained a significant portion of their body water through the leaves in their diet, and such an enrichment is associated with changes in the evaporation potential of the environment (Levin et al., 2006). This would suggest a trend towards aridification, which aligns with the regional signal observed in the isotopic and palynological records of the nearby marine Monterey Formation (Flower and Kennett, 1993; Heusser et al., 2022). Along with the decreased availability of precipitation, the disruption of channel networks may have encouraged the development of additional open-canopy habitats based on the pattern of enrichment in  $\delta^{13}\text{C}$  values that continued through the top of the sequence.

### **Incipient Extension (~9.5 to 8.5 Ma)**

Shear movement in the Dove Spring Formation subsided and extension resumed around 9.5 Ma. By 8.8 Ma, a sharp increase in sediment accumulation rate coincides with the basin-wide replacement of floodplains represented by FA3 by channel belts of FA1. This tectonic episode represents an incipient stage of basin extension and the development of new, large channels that transported coarse sediments from a source in the Sierra Nevada. This pattern aligns with models and observations of extensional basins in which channels transport sediments towards the center of the basin as newly-activated normal faults generate additional accommodation space (Gawthorpe and Leeder, 2000). Fewer depositional environments were suitable life habitats for terrestrial mammals and preservation rate decreased to its lowest level during this interval.

Per-capita extinction rates continued to rise through the end of the sequence, which may have been related to the minor disruption of pre-existing vegetation or a decrease in fossil

productivity. However, rare species account for 14 out of 35 species within the channel sequences at the top of the formation. Species richness, specimen recovery, and the number of localities modestly increased at the end of the Dove Spring Formation's depositional history, preserved in channel margin and floodplain horizons within the channel-dominated sequences. The presence of numerous rare taxa and several new species during this interval indicates authentic faunal change that is not just related to sampling.

$\delta^{13}\text{C}$  values in all taxa became less variable by 9.0 Ma and a subtle trend of enrichment continued through the end of the sequence. This indicates that herbivores consumed similar vegetation even after tectonic processes altered the drainage characteristics of the basin.  $\delta^{18}\text{O}$  values continued their trend of enrichment, following a regional trend of gradual aridification. While slight climatic changes did occur in conjunction with the basin's tectonic history, significant variations in the ecological diversity of herbivores were not observed. The Dove Spring Formation thus represents a relatively stable, non-analogue environment that persisted for at least four million years.

## **Conclusion**

The tectonic history of terrestrial basins has significant impacts on mammal communities over the span of millions of years. Topographic changes influence climatic conditions that determine vegetation resource gradients as well as depositional environments that have the potential to preserve fossil remains. The vegetation resources of the Dove Spring Formations remained relatively stable for four million years. Based on regional climate data and a potential increase in evaporation documented by  $\delta^{18}\text{O}$  values in two ungulate families, the basin may have become slightly more arid over time. However, changes in the dietary ecology of ungulates were not major contributing factors to faunal change in the large mammal assemblages.



Amphicyonids, camelids, felids, tayassuids, and nimravidids all exhibit greater species loss near the end of the sequence than the remaining families of large mammals, suggesting that other processes, such as dispersal into other regions may be responsible for the extinction or extirpation of many species from the basin.

Tectonic processes had a substantive effect on the distribution of depositional environments within the Dove Spring Formation. The resulting changes in fossil productivity of basin sediments influenced the fossil record by preserving variable frequencies of localities and species. However, the areal extent of depositional environments was not a strong predictor of fossil productivity. The greatest numbers of localities and specimens per area occurred during the shearing tectonic episode. The appearance of chronically rare taxa during intervals with low preservation indicates that some faunal changes occurred despite declining fossil productivity. The tectonic history of the basin had a greater influence on the distribution of life habitats and environments of preservation than it did on vegetation and climatic gradients. Investigations of patterns in fossil productivity yield insight into environmental controls on the fossil record and allow for more complete interpretations of the interconnected history of tectonic processes and terrestrial mammals.

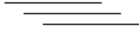

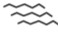

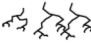


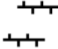
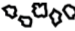

## References

- Bridge, J. S., and Leeder, M. R., 1979, A simulation model of alluvial stratigraphy: *Sedimentology*, v. 26, p. 617-644.
- Chapin, C. E., 2008, Interplay of oceanographic and paleoclimate events with tectonism during middle to late Miocene sedimentation across the southwestern USA: *Geosphere*, v. 4, p. 976-991.
- Dokka, R. K., and Macaluso, K. Y., 2001, Topographic effects of the Eastern California Shear Zone in the Mojave Desert: *Journal of Geophysical Research: Solid Earth*, v. 106, no. B12, p. 30625-30644.
- Flower, B. P., and Kennett, J. P., 1993, Relations between Monterey Formation deposition and middle Miocene global cooling: Naples Beach section, California: *Geology*, v. 21, p. 877-880.
- Gawthorpe, R. L., and Leeder, M. R., 2000, Tectono-sedimentary evolution of active extensional basins: *Basin Research*, v. 12, p. 195-218.
- Heusser, L. E., Barron\*, J. A., Blake, G. H., and Nichols, J., 2022, Miocene terrestrial paleoclimates inferred from pollen in the Monterey Formation, Naples Coastal Bluffs section, California, *Understanding the Monterey Formation and Similar Biosiliceous Units across Space and Time*, p. 215-227.
- Kisel, Y., McInnes, L., Toomey, N. H., and Orme, C. D., 2011, How diversification rates and diversity limits combine to create large-scale species-area relationships: *Philos Trans R Soc Lond B Biol Sci*, v. 366, no. 1577, p. 2514-2525.
- Levin, N. E., Cerling, T. E., Passey, B. H., Harris, J. M., and Ehleringer, J. R., 2006, A stable isotope aridity index for terrestrial environments: *Proceedings of the National Academy of Sciences of the United States of America*, v. 103, no. 30, p. 11201-11205.
- Loomis, D. P., and Burbank, D. W., 1988, The stratigraphic evolution of the El Paso basin, southern California: Implications for the Miocene development of the Garlock fault and uplift of the Sierra Nevada: *Geological Society of America Bulletin*, v. 100, p. 12-28.

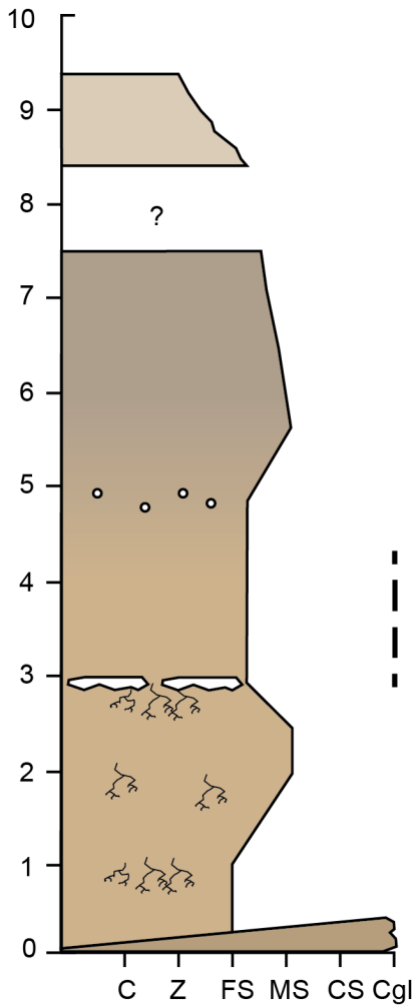
## **Appendix**

### **Stratigraphic Sections of Highly Productive Fossil Localities in the Dove Spring Formation**

Here I present a series of microstratigraphic sections measured at the decimeter scale within the Dove Spring Formation. I focused on highly productive fossil localities to investigate patterns in fossil preservation and depositional environments within microfacies associations. Each entry includes: stratigraphic section number, the closest associated Natural History Museum of Los Angeles County (NHM) locality number; approximate stratigraphic position within the Dove Spring Formation; age; number of fossil specimens recovered; number of large vertebrate (>1 kg) fossil specimens; lithofacies of the primary fossiliferous horizon; classification of the locality's depositional environment; and noteworthy features. Vertical scale is presented in meters, horizontal scale indicates grain size (C = claystone, Z = siltstone, FS = fine-grained sandstone, MS = medium-grained sandstone, CS = coarse-grained sandstone, Cgl = conglomerate).

	Parallel bedding
	Crossbedding
	Ripple Marks
	Mudcracks
	Root casts
	Discontinuous carbonate layer
	Interbedded silcrete
	Carbonate
	Lithic fragments
	Dispersed Ash

Appendix Figure 1: Key to symbols used to denote sedimentary structures and other features within stratigraphic sections.



Appendix Figure 2: Section 21.01

NHM locality number: 3436

Approximate stratigraphic position: 715 m

Age: 10.1 Ma

Number of specimens: 4

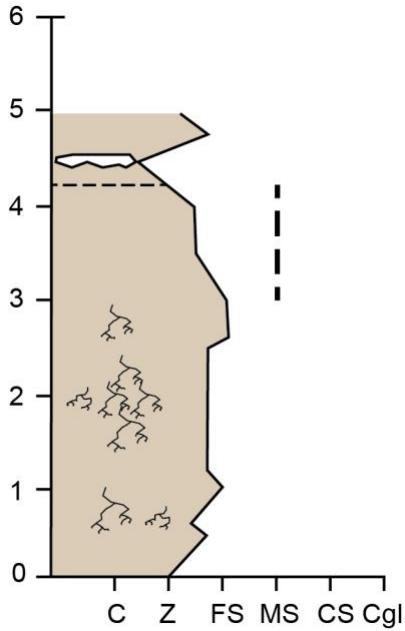
Number of large mammal specimens: 4

Primary fossil horizon: Fine-grained sandstone

Classification of depositional environment: Small channel

Notes: Abundant carbonaceous root casts and discontinuous carbonate surfaces within fine-grained sandstone; clay content is variable from absent to moderately blocky fracture; sparse carbonate nodules just below contact with clayey siltstone.

Dusted white surfaces appear in upper M sandstone, ash drapes and continuous ash layers also present.



Appendix Figure 3: Section 21.02

NHM locality number: 3472

Approximate stratigraphic position: 1020 m

Age: 9.9 Ma

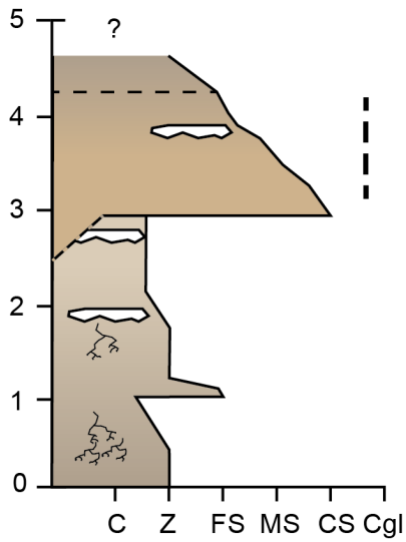
Number of specimens: 22

Number of large mammal specimens: 21

Primary fossil horizon: Gradational sequence, fine-grained sandstone to silty sandstone

Classification of depositional environment: Channel margin

Notes: Siliceous root casts common throughout sandy siltstone; fissile to indurated beds.



Appendix Figure 4: Section 21.03

NHM locality number: 3533

Approximate stratigraphic position: 1020 m

Age: 9.5 Ma

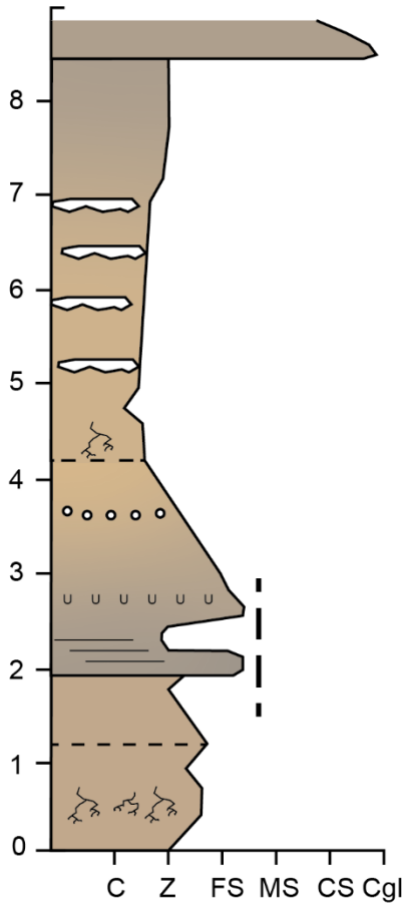
Number of specimens: 71

Number of large mammal specimens: 21

Primary fossil horizon: Gradational sequence, coarse- to fine-grained sandstone

Classification of depositional environment: Channel margin

Notes: Massive sandstone incises into siltstone; prominent siliceous root casts throughout siltstone.



Appendix Figure 5: Section 21.04

NHM locality number: 3436

Approximate stratigraphic position: 730 m

Age: 10.2 Ma

Number of specimens: 4

Number of large mammal specimens: 4

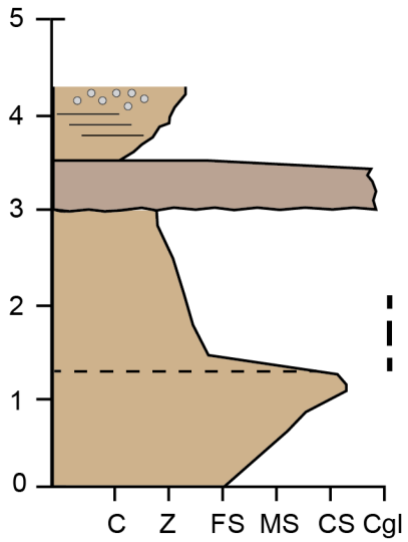
Primary fossil horizon: Gradational sequence, fine-grained sandstone to siltstone

Classification of depositional environment: Arid floodplain

Notes: Root casts and discontinuous carbonate surfaces within siltstones; mudcracks in thick gradational sequence.

This section is laterally continuous with sections 22.28, 22.27, 22.18, 22.17, 22.16, and 22.29.





Appendix Figure 6: Section: 21.05

NHM locality number: 3444

Approximate stratigraphic position: 400 m

Age: 10.1 Ma

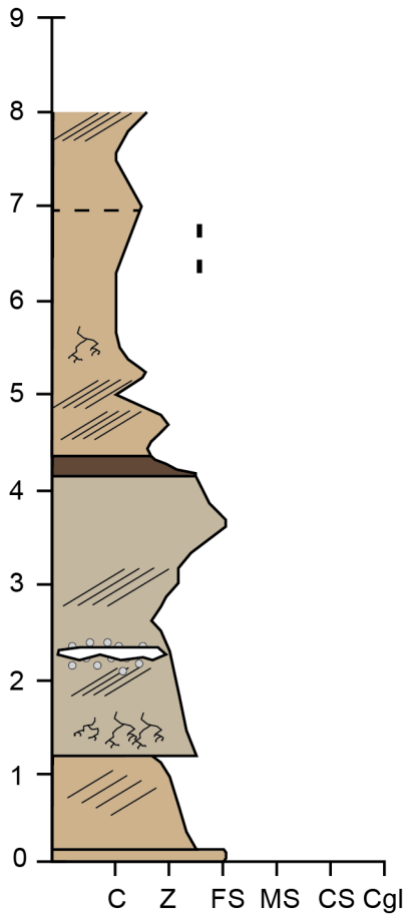
Number of specimens: 155

Number of large mammal specimens: 8

Primary fossil horizon: Fine-grained sandstone

Classification of depositional environment: Channel margin

Notes: Conglomerate clasts range 2-40 mm; laminated bedding prominent in gradational sequence at top of section; dispersed ash reworked into sandy siltstone.



Appendix Figure 7: Section 21.06

NHM locality number: 3447

Approximate stratigraphic position: 725 m

Age: 9.8 Ma

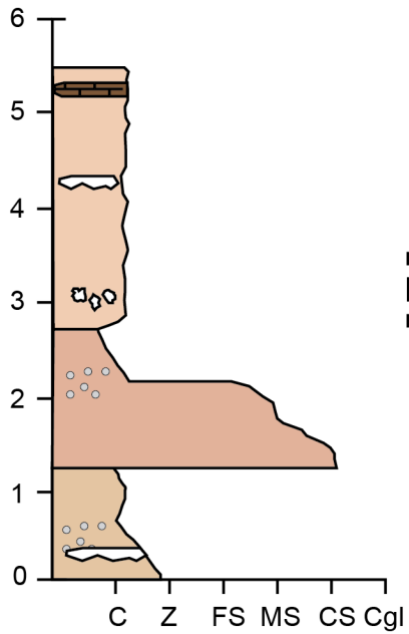
Number of specimens: 203

Number of large mammal specimens: 16

Primary fossil horizon: Clayey siltstone

Classification of depositional environment: Channel margin

Notes: Siliceous root casts within sandy silt; thin, faint crossbedding and carbonate surfaces in siltstone. Organic-rich layer at transition between greyish tan (10 YR 6/2) and buff tan (10 YR 7/2) units.



Appendix Figure 8: Section 22.01

NHM locality number: 3420

Approximate stratigraphic position: 715 m

Age: 10.1 Ma

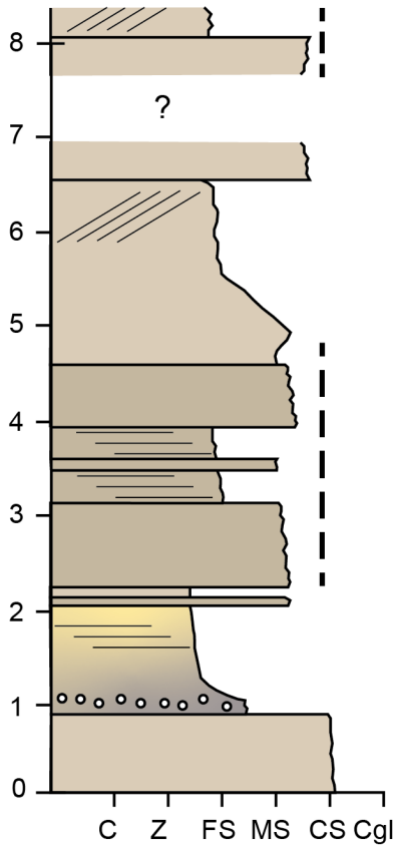
Number of specimens: 58

Number of large mammal specimens: 58

Primary fossil horizon: Siltstone

Classification of depositional environment: Arid floodplain

Notes: Discontinuous carbonate layers and carbonate clasts within lower siltstone; dispersed ash within claystone; discontinuous carbonate layers, carbonate clasts, and thin, continuous silcrete within upper siltstone.



Appendix Figure 9: Section 22.02

NHM locality number: 1553

Approximate stratigraphic position: 650 m

Age: 10.4 Ma

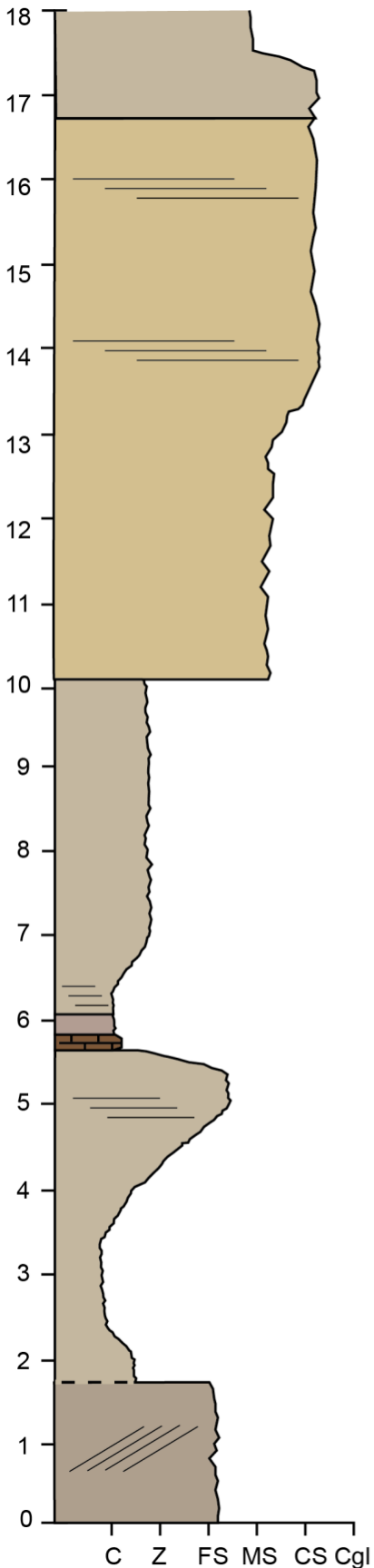
Number of specimens: 84

Number of large mammal specimens: 65

Primary fossil horizon: Coarse- and fine-grained sandstone

Classification of depositional environment: Large channel

Notes: Prominent laminated bedding in fine-grained sandstone; carbonate clasts at base of lower gradational sequence from medium- to fine-grained sandstone.



Appendix Figure 10: Section 22.03

NHM locality number: 1741

Approximate stratigraphic position: 400 m

Age: 11.7 Ma

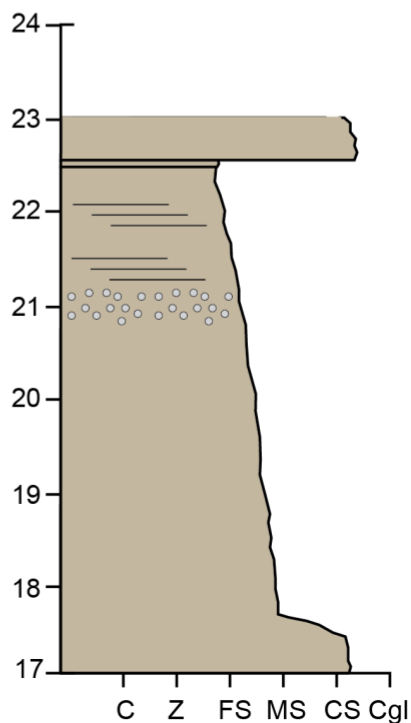
Number of specimens: 48

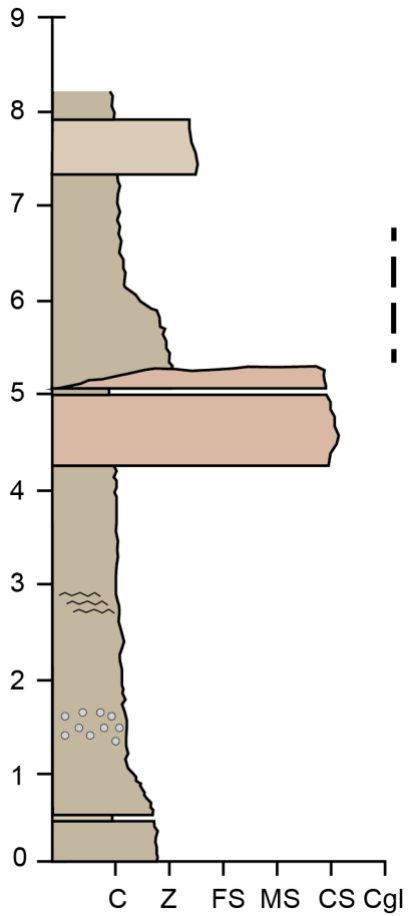
Number of large mammal specimens: 48

Primary fossil horizon: Gradational sequence, medium- to fine-grained sandstone

Classification of depositional environment: Large channel

Notes: Faint to prominent crossbedding in lower fine-grained sandstone; laminated bedding in fine-grained sandstones; dispersed ash heavily concentrated in upper fine-grained sandstone, below prominent laminated beds.





Appendix Figure 11: Section 22.04

NHM locality number: 6375

Approximate stratigraphic position: 725 m

Age: 9.9 Ma

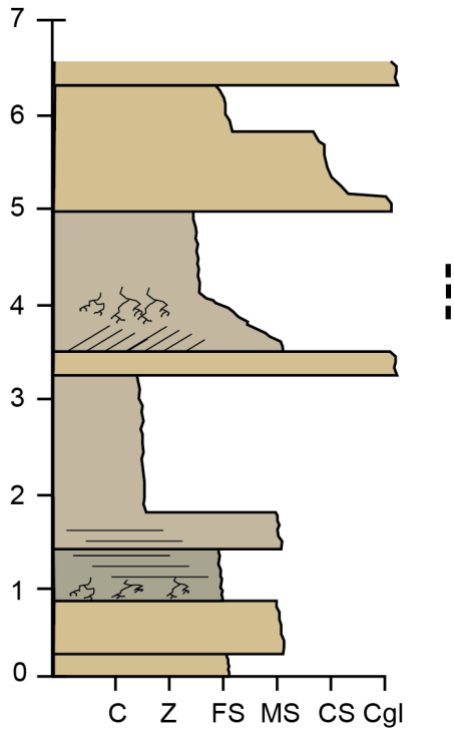
Number of specimens: 172

Number of large mammal specimens: 13

Primary fossil horizon: Clayey siltstone

Classification of depositional environment: Well-drained floodplain

Notes: Ripple marks, blocky fracture, dispersed ash within claystone; bioturbation and carbonate throughout coarse-grained sandstone; carbonate absent from upper siltstone.



Appendix Figure 12: Section 22.05

NHM locality number: 1108

Approximate stratigraphic position: 240 m

Age: 11.9 Ma

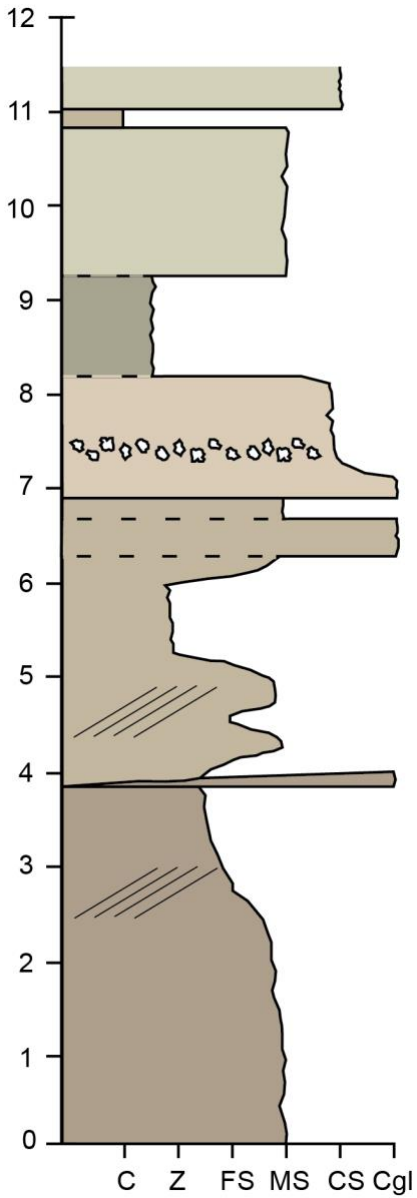
Number of specimens: 102

Number of large mammal specimens: 100

Primary fossil horizon: Gradational sequence, medium-to fine-grained sandstone

Classification of depositional environment: Channel margin

Notes: Laminated bedding and abundant small root casts (5-10 mm diameter) in fine sandstone unit; crossbedding and large root casts (20 mm diameter) in medium-grained sandstone unit, just above conglomerate layer.



Appendix Figure 13: Section 22.06

NHM locality number: 3662

Approximate stratigraphic position: 200 m

Age: 12.5

Number of specimens: 56

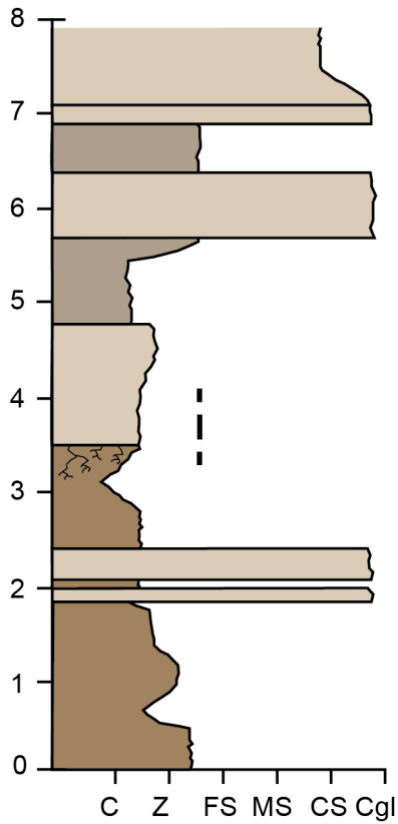
Number of large mammal specimens: 12

Primary fossil horizon: Siltstone

Classification of depositional environment: Large channel

Notes: Poorly sorted, coarse-grained layers associated with crevasse splay deposits; gradational sequences ~30 cm thick; chert and blocky fracture common in siltstone and clay units.





Appendix Figure 14: Section 22.07

NHM locality number: 5718

Approximate stratigraphic position: 1400 m

Age: 8.5 Ma

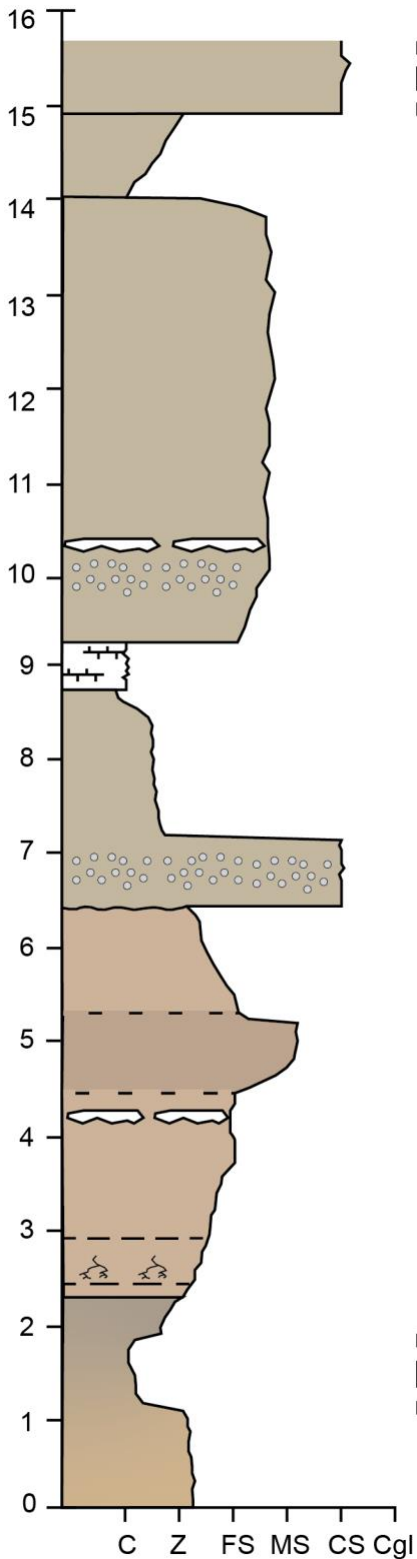
Number of specimens: 65

Number of large mammal specimens: 31

Primary fossil horizon: Siltstone

Classification of depositional environment: Small channel

Notes: Poor sorting throughout section, some cobbles present in lowest siltstone; root casts and extensive bioturbated surface at ~3.3m; weak bedding at 5m in siltstone layer.



Appendix Figure 15: Section 22.08

NHM locality number: 4702

Approximate stratigraphic position: 1250 m

Age: 8.5 Ma

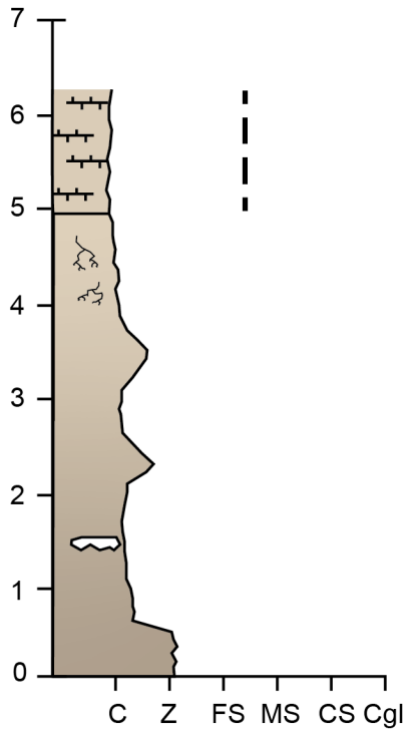
Number of specimens: 657

Number of large mammal specimens: 4

Primary fossil horizon: Coarse-grained sandstone

Classification of depositional environment: Large channel

Notes: Carbonate and root casts within blocky, highly indurated gradational sequence ~3 m; dispersed ash common; undulating basal contact of coarse-grained sandstone to siltstone at 6.3 m.



Appendix Figure 16: Section 22.09a

NHM locality number: 6397

Approximate stratigraphic position: 1225 m

Age: 8.7 Ma

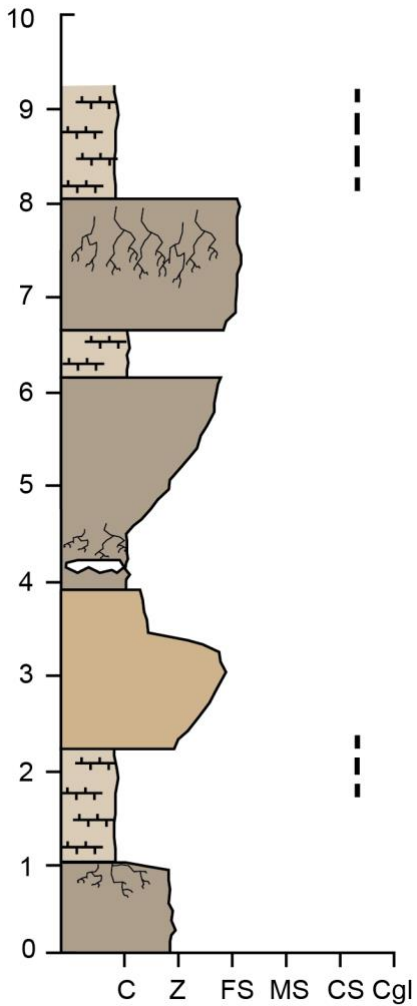
Number of specimens: 1

Number of large mammal specimens: 1

Primary fossil horizon: Marlstone

Classification of depositional environment: Oxbow lake/pond deposit

Notes: Carbonate rind surfaces and dispersed carbonate, blocky fracture, and faint bedding throughout indurated lower siltstone and clayey silt; Siliceous root casts and blocky fracture in well-indurated, upper claystone.



Appendix Figure 17: Section 22.09b

NHM locality number: 3589

Approximate stratigraphic position: 1225 m

Age: 8.8 Ma

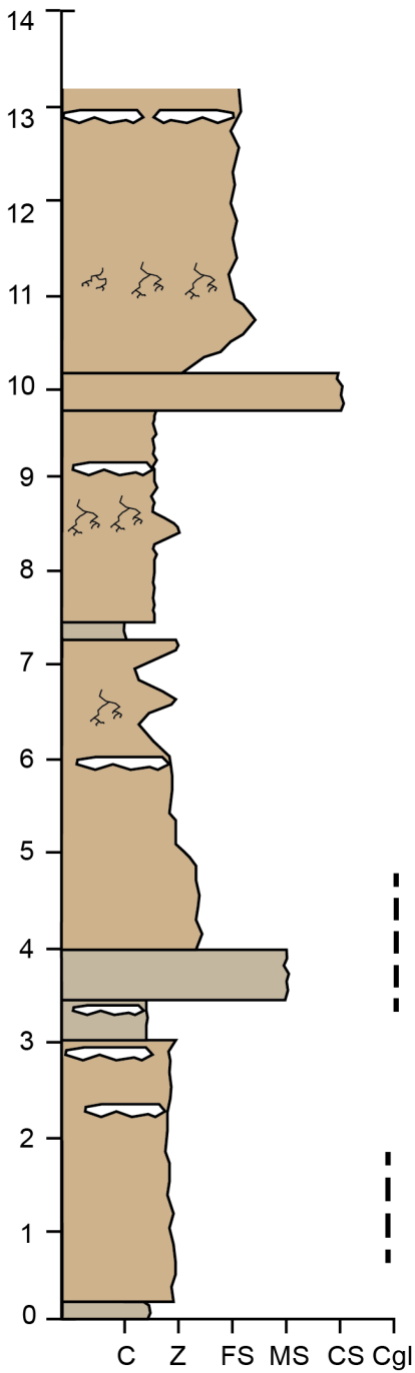
Number of specimens: 1

Number of large mammal specimens: 1

Primary fossil horizon: Marlstone

Classification of depositional environment: Poorly-drained floodplain

Notes: Root casts commonly directly underneath carbonate layers; root-rich layers are well-indurated with no bedding; discontinuous carbonate layers within claystone at 4ml alternating carbonate- and silicate-rich layers.



Appendix Figure 18: Section 22.10

NHM locality number: 6380

Approximate stratigraphic position: 1500 m

Age: 8.5 Ma

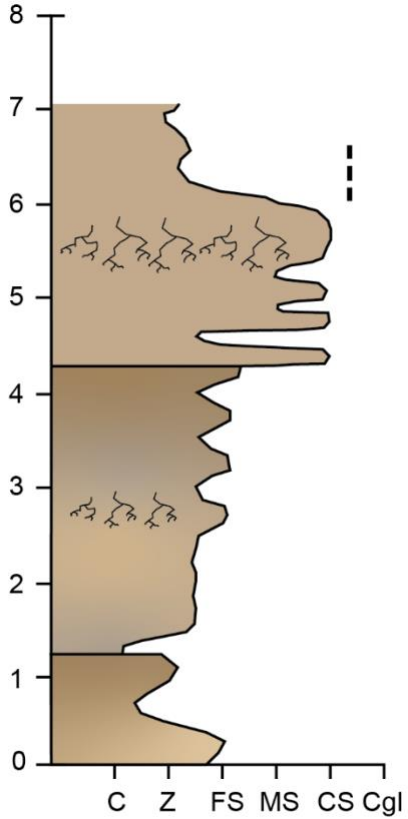
Number of specimens: 74

Number of large mammal specimens: 19

Primary fossil horizon: Siltstone

Classification of depositional environment: Arid floodplain

Notes: Discontinuous carbonate layers throughout section; faint bedding within siltstones; root casts and thin carbonate surfaces within claystones.



Appendix Figure 19: Section 22.11

NHM locality number: 5669

Approximate stratigraphic position: 1750 m

Age: 8.5 Ma

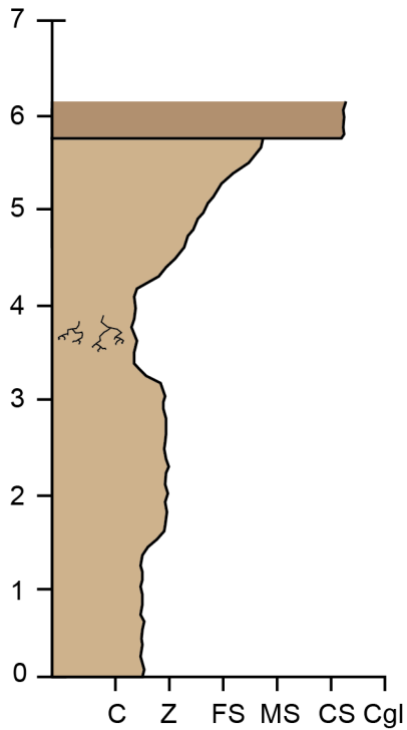
Number of specimens: 5

Number of large mammal specimens: 5

Primary fossil horizon: Siltstone

Classification of depositional environment: Channel margin

Notes: Blocky fracture throughout siltstone and sandy silt; carbonate root casts common in siltstones and within indurated sandstone ledge.



Appendix Figure 20: Section 22.12

NHM locality number: 6923

Approximate stratigraphic position: 1700 m

Age: 8.5 Ma

Number of specimens: 1

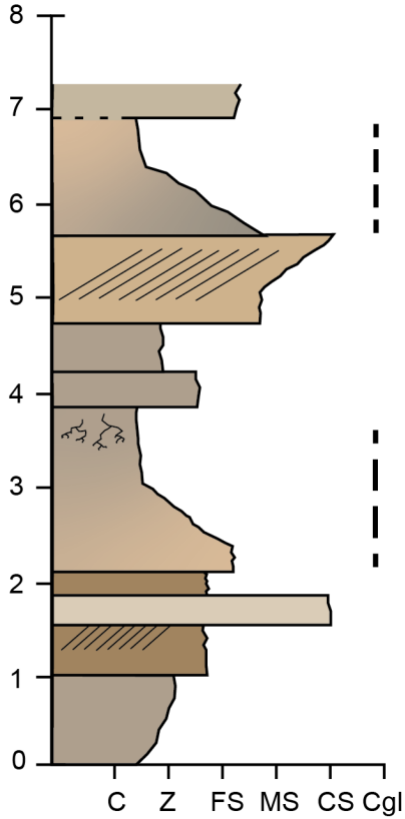
Number of large mammal specimens: 1

Primary fossil horizon: Unknown

Classification of depositional environment: Channel margin

Notes: Alternation between well-indurated and poorly-indurated clayey siltstones; carbonaceous root casts common within clayey siltstone at 4m; capped by poorly sorted, coarse-grained sandstone.

Fossil horizon was not located.



Appendix Figure 21: Section 22.13

NHM locality number: 6141

Approximate stratigraphic position: 160 m

Age: 12.5 Ma

Number of specimens: 8

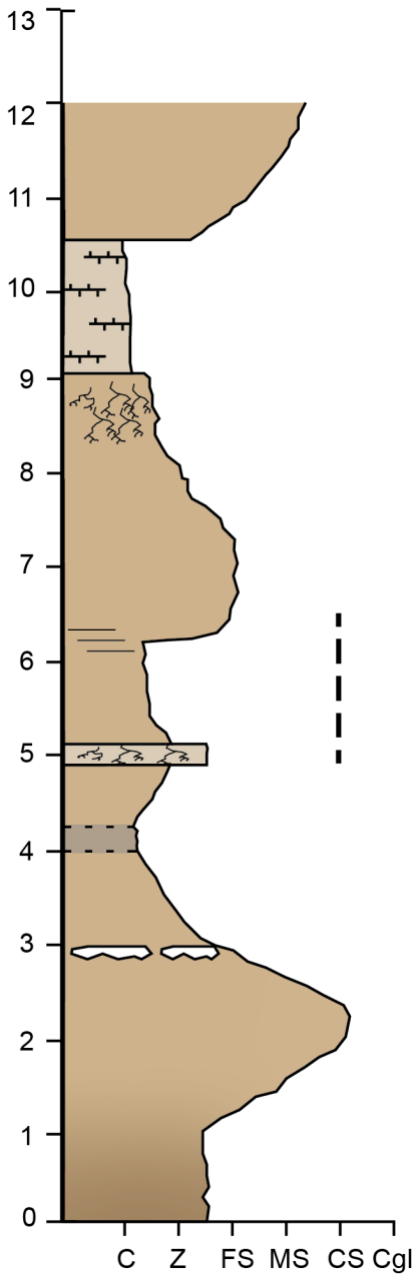
Number of large mammal specimens: 8

Primary fossil horizon: Gradational sequence, fine-grained sandstone to clayey siltstone

Classification of depositional environment: Large channel

Notes: Sandstones ~1m thick with well-defined crossbedding; small, siliceous root casts (5-10 mm diameter) common in fine-grained sediments above sandstones.





Appendix Figure 22: Section 22.14

NHM locality number: 5693

Approximate stratigraphic position: 1500 m

Age: 8.5

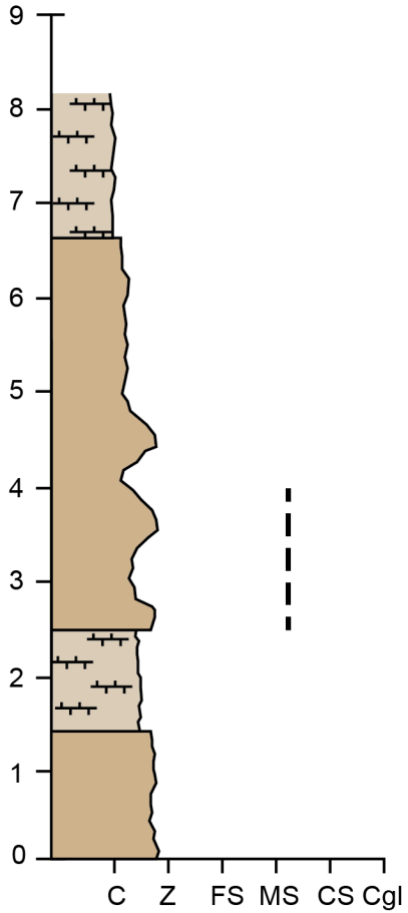
Number of specimens: 2

Number of large mammal specimens: 0

Primary fossil horizon: Siltstone

Classification of depositional environment: Small channel

Notes: Root casts common in upper siltstone; dusted white carbonate surfaces within gradational sequences; abundant carbonate root casts within crevasse splay deposit at 5m; carbonate unit from 9-10.75m is continuous and well-indurated.



Appendix Figure 23: Section 22.15

NHM locality number: 3588

Approximate stratigraphic position: 1450 m

Age: 8.8 Ma

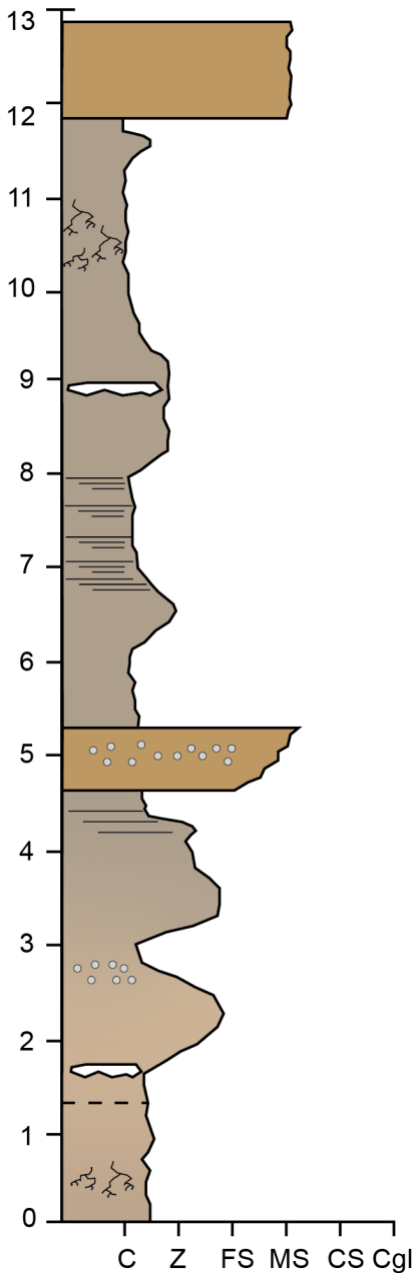
Number of specimens: 2

Number of large mammal specimens: 2

Primary fossil horizon: Siltstone and clayey siltstone

Classification of depositional environment: Arid floodplain

Notes: Alternation between blocky fracture to poorly-indurated siltstones; well-indurated claystones contain carbonate.



Appendix Figure 24: Section 22.16

NHM locality number: N/A

Approximate stratigraphic position: 730 m

Age: 10.2 Ma

Number of specimens: N/A

Number of large mammal specimens: N/A

Primary fossil horizon: N/A

Classification of depositional environment: Arid floodplain

Notes: Small root casts (5-10 mm diameter) within indurated silty claystone; laminated bedding throughout silty claystone; disperse ash in gradational sequence at 2.6 m; discontinuous carbonate layers within silty claystones; tree stumps and dispersed ash within beige (5 Y 8/1) sandstone.

This section does not contain a fossiliferous horizon. It is laterally continuous with sections 22.28, 22.27,

Appendix Figure 25: Section 22.17

NHM locality number: 5976

Approximate stratigraphic position: 730 m

Age: 10.2 Ma

Number of specimens: 10

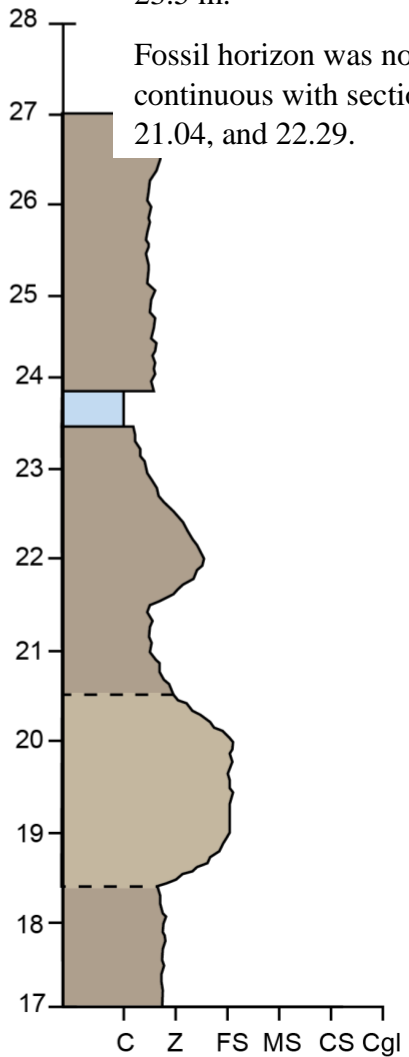
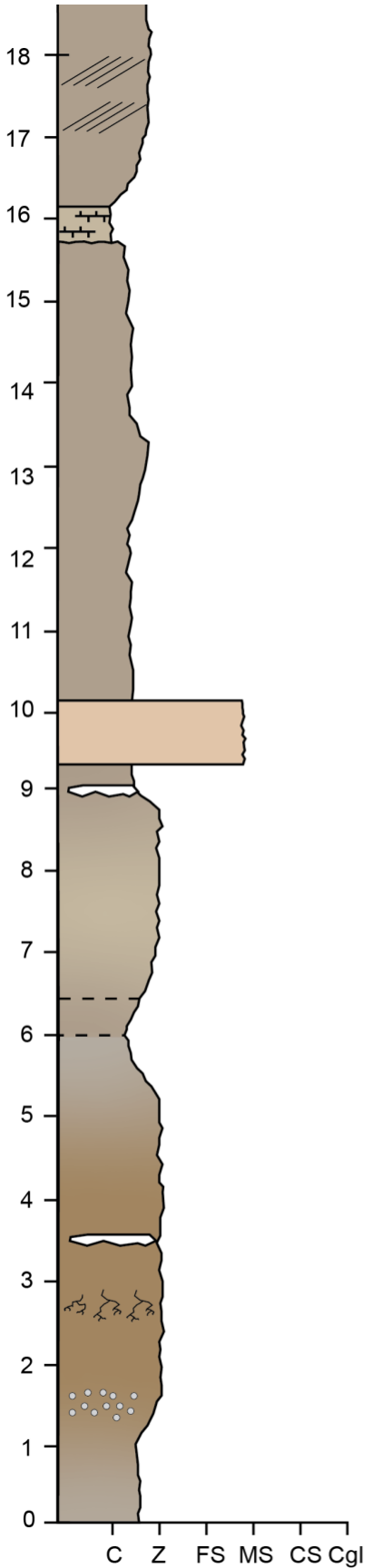
Number of large mammal specimens: 0

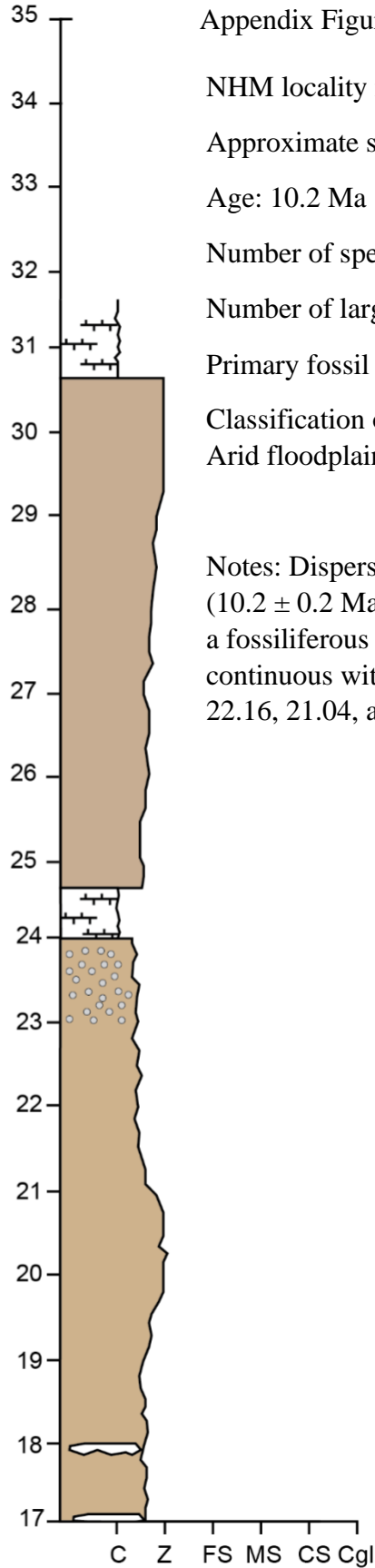
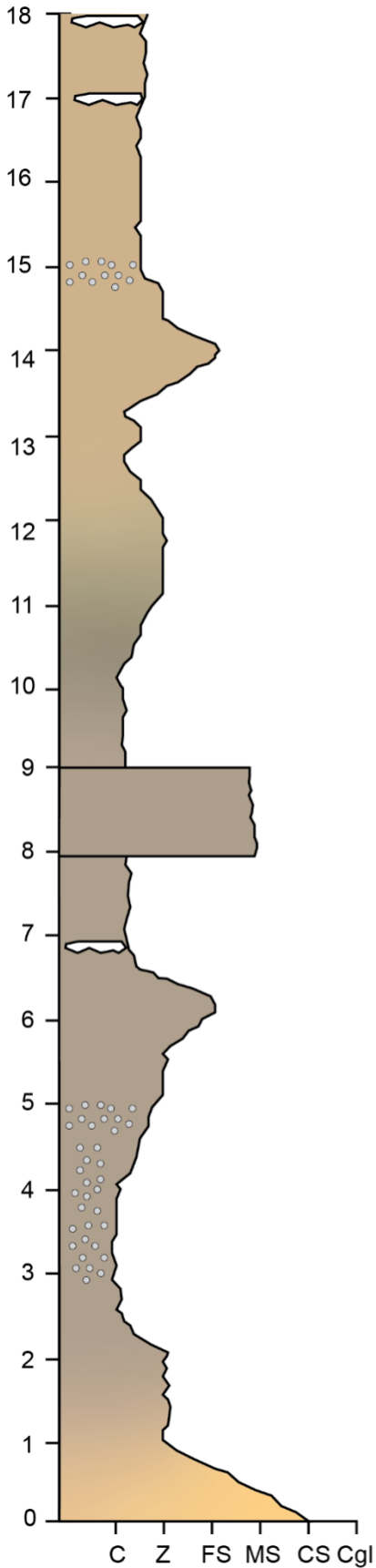
Primary fossil horizon: Unknown

Classification of depositional environment: Arid floodplain

Notes: Ash Tra9 ( $10.2 \pm 0.2$  Ma) forms a thick bed at 23.5 m.

Fossil horizon was not located. This section is laterally continuous with sections 22.28, 22.27, 22.18, 22.16, 21.04, and 22.29.





Appendix Figure 26: Section 22.18

NHM locality number: N/A

Approximate stratigraphic position: 730 m

Age: 10.2 Ma

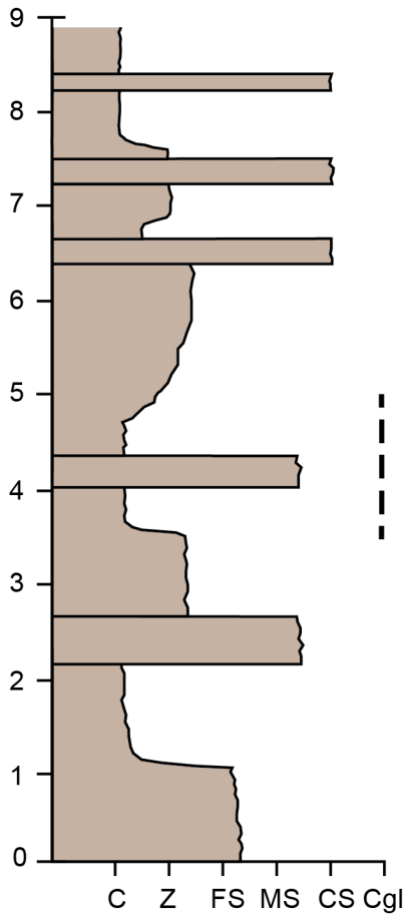
Number of specimens: N/A

Number of large mammal specimens: N/A

Primary fossil horizon: N/A

Classification of depositional environment:  
Arid floodplain

Notes: Dispersed ash correlates with Tra9 (10.2 ± 0.2 Ma). This section does not contain a fossiliferous horizon. It is laterally continuous with sections 22.28, 22.27, 22.17, 22.16, 21.04, and 22.29.



Appendix Figure 27: Section 22.19

NHM locality number: 3416

Approximate stratigraphic position: 230 m

Age: 12.0 Ma

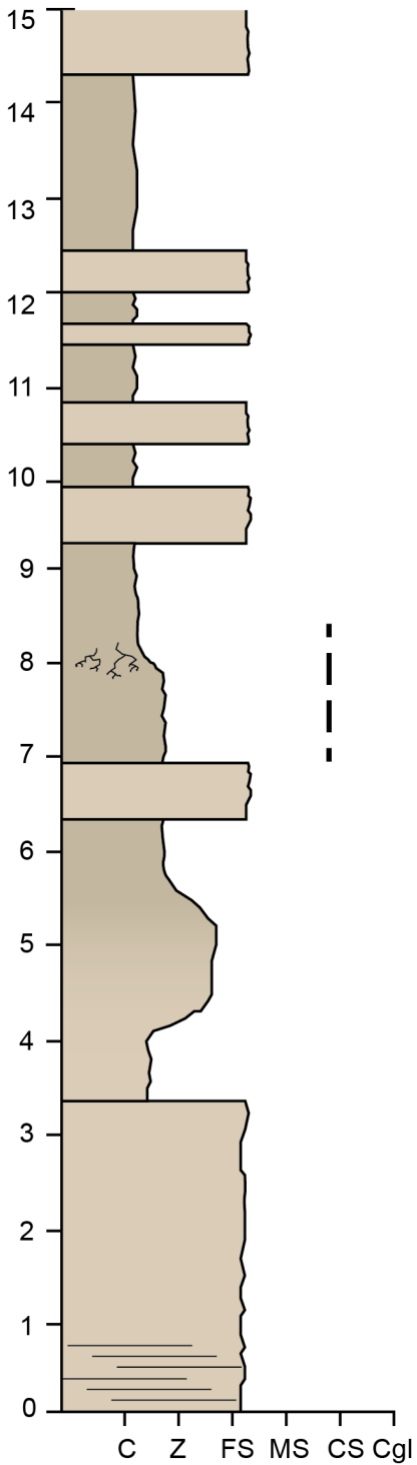
Number of specimens: 13

Number of large mammal specimens: 13

Primary fossil horizon: Silty claystone

Classification of depositional environment: Channel margin

Notes: Blocky fracture in silty clays; fining-upward sequences appear above coarse-grained sandstones.



Appendix Figure 28: Section 22.20

NHM locality number: 3679

Approximate stratigraphic position: 250 m

Age: 12.0 Ma

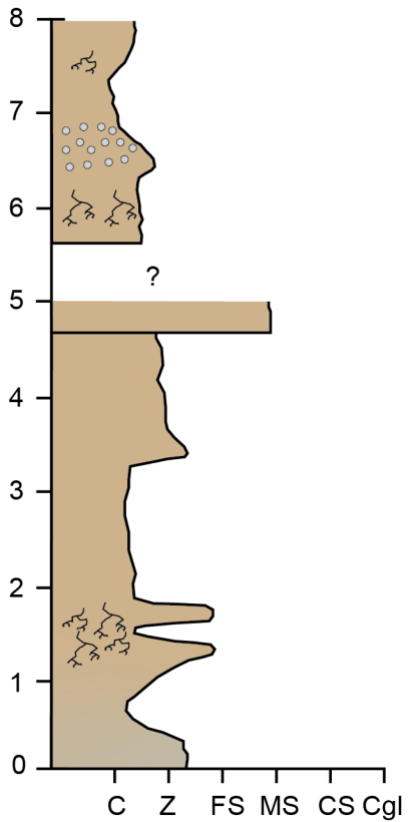
Number of specimens: 9

Number of large mammal specimens: 8

Primary fossil horizon: Siltstone and clayey siltstone

Classification of depositional environment: Channel margin

Notes: Laminated sandstone only present at base of section; fining upward sequences occur in poorly-indurated siltstones; root casts only occur in a single horizon (8m).



Appendix Figure 29: Section 22.21

NHM locality number: 3531

Approximate stratigraphic position: 1030 m

Age: 9.5 Ma

Number of specimens: 53

Number of large mammal specimens: 40

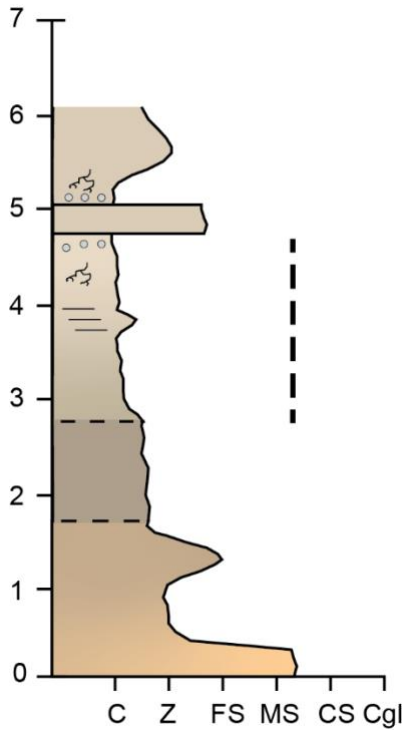
Primary fossil horizon: Unknown

Classification of depositional environment: Poorly-drained floodplain

Notes: Abundant siliceous root casts in claystone and crevasse splay deposits; sandstones are poorly sorted, weakly indurated, and massive; siltstones have blocky fracture; discontinuous white surfaces present in siltstones (evaporite or ash).

Fossil horizon was not located.





Appendix Figure 30: Section 22.22

NHM locality number: 3532

Approximate stratigraphic position: 1050 m

Age: 9.5 Ma

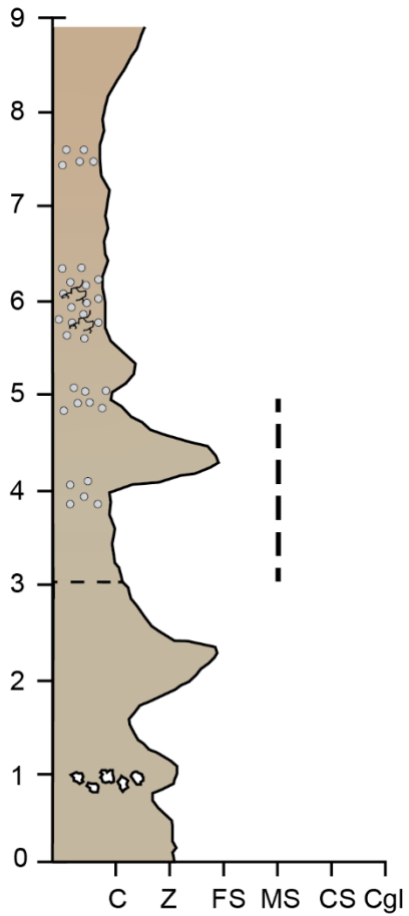
Number of specimens: 13

Number of large mammal specimens: 13

Primary fossil horizon: Silty claystone

Classification of depositional environment: Well-drained floodplain

Notes: Weak bedding and poor sorting throughout section; faint laminated bedding in silty clay; thin, discontinuous white surfaces in silty clay; abundant very small root casts (2-5 mm diameter) in zone of dispersed ash.



Appendix Figure 31: Section 22.33

NHM locality number: 3556

Approximate stratigraphic position: 775 m

Age: 9.8 Ma

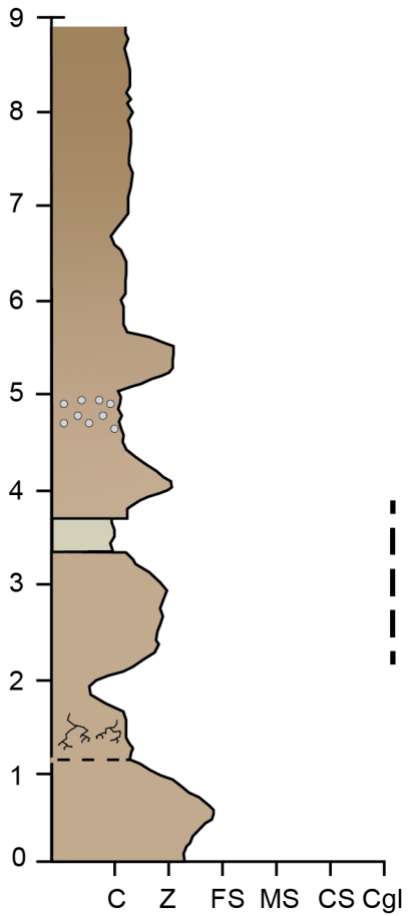
Number of specimens: 44

Number of large mammal specimens: 44

Primary fossil horizon: Claystone and fine-grained sandstone

Classification of depositional environment: Well-drained floodplain

Notes: Clayey siltstone exhibits faint bedding, blocky fracture and contains abundant dispersed ash; fine-grained sandstones are poorly sorted, with discontinuous white surfaces (evaporite or ash).



Appendix Figure 32: Section 22.24

NHM locality number: 7356

Approximate stratigraphic position: 775 m

Age: 9.7 Ma

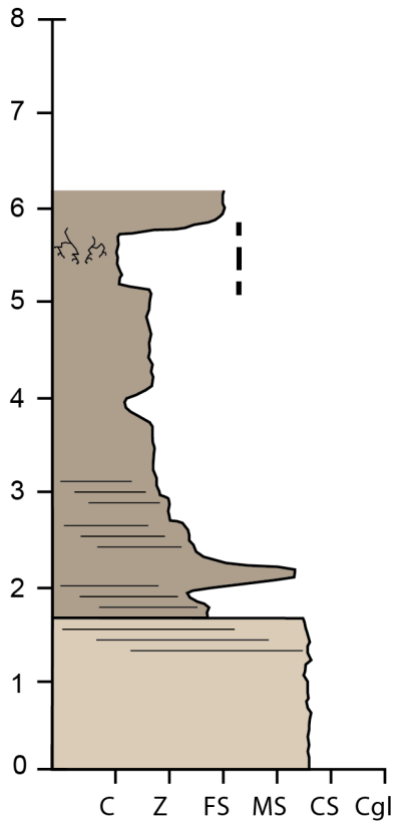
Number of specimens: 7

Number of large mammal specimens: 7

Primary fossil horizon: Siltstone, thick ash deposit

Classification of depositional environment: Well-drained floodplain

Notes: Siliceous root casts and evaporite or ash within clayey siltstone; ash forms distinct bed at 3.5 m; dispersed ash and discontinuous white surfaces common throughout upper clayey siltstone.



Appendix Figure 33: Section 22.25

NHM locality number: 3580

Approximate stratigraphic position: 850 m

Age: 9.5 Ma

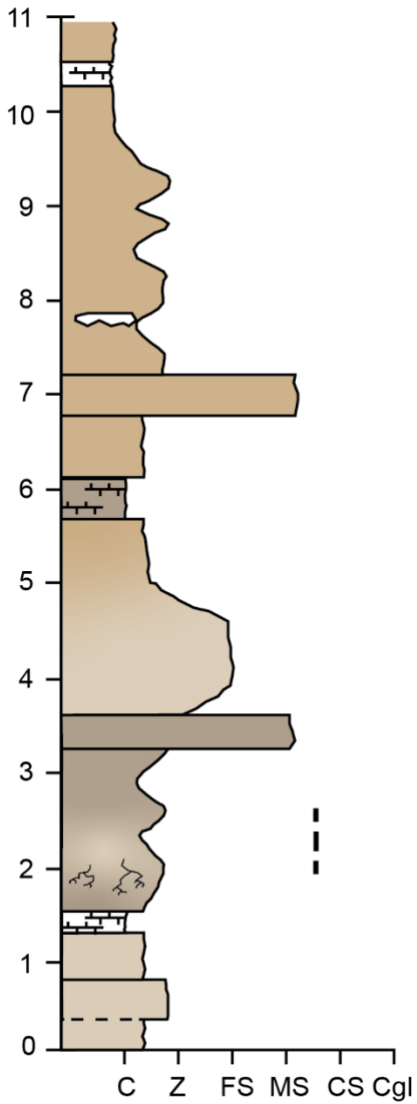
Number of specimens: 139

Number of large mammal specimens: 21

Primary fossil horizon: Silty claystone

Classification of depositional environment: Channel margin

Notes: Prominent bedding throughout lower 3.5m, interbedded with massive fine-grained sandstone; blocky fracture, clay matrix, and carbonaceous root casts in siltstone.



Appendix Figure 34: Section 22.26

NHM locality number: 3665

Approximate stratigraphic position: 1000 m

Age: 9.6 Ma

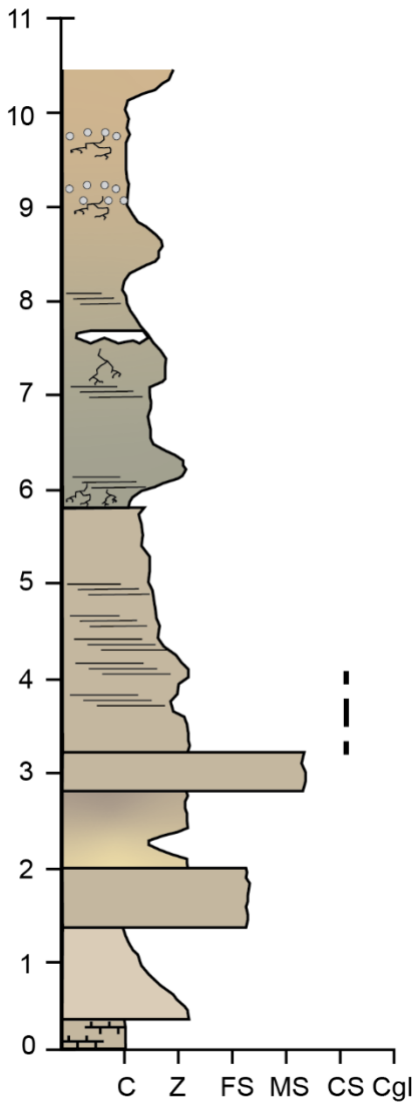
Number of specimens: 7

Number of large mammal specimens: 7

Primary fossil horizon: Siltstone

Classification of depositional environment: Channel margin

Notes: Lower siltstone contains abundant siliceous root casts; carbonate appears above 6.5 m; sandstones are well-indurated and form ledges; carbonate units are continuous and form cap layers; discontinuous carbonate layers within upper siltstones are 2-5 cm thick.



Appendix Figure 35: Section 22.27

NHM locality number: 3422

Approximate stratigraphic position: 730 m

Age: 10.2 Ma

Number of specimens: 14

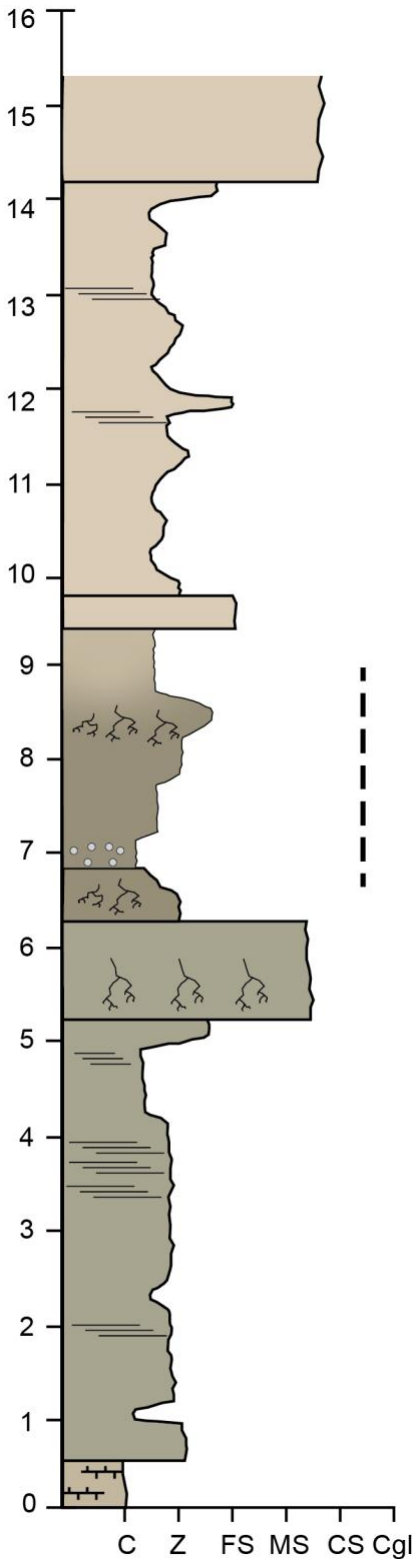
Number of large mammal specimens: 14

Primary fossil horizon: Siltstone

Classification of depositional environment: Channel margin

Notes: Laminated bedding within lower siltstone, abundant siliceous root casts and dispersed ash within upper siltstone; base of section is very resistant continuous carbonate unit.

This section is laterally continuous with sections 22.28, 22.18, 22.17, 22.16, 21.04 and 22.29.



Appendix Figure 36: Section 22.28

NHM locality number: 3668

Approximate stratigraphic position: 730 m

Age: 9.9 Ma

Number of specimens: 14

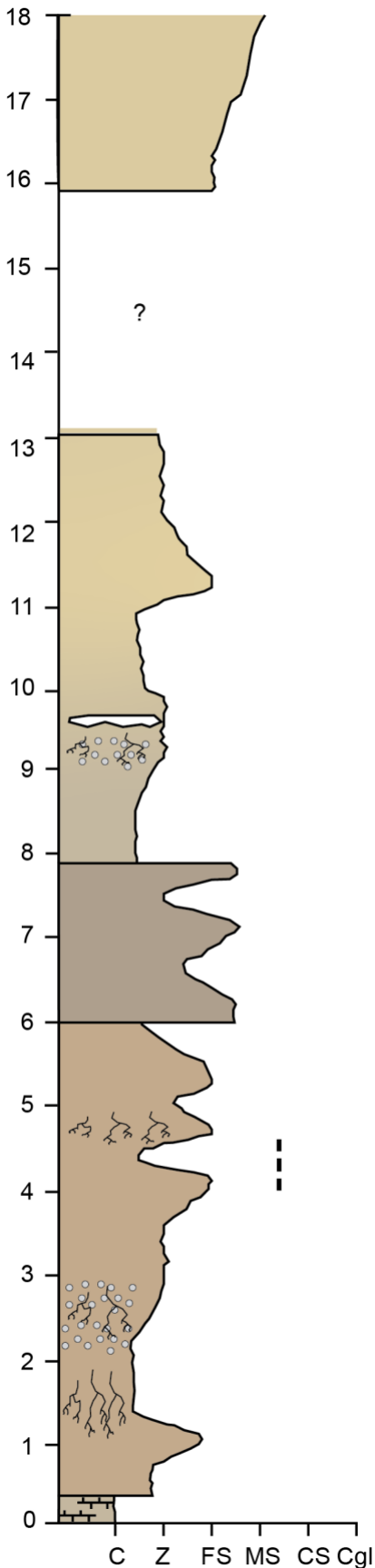
Number of large mammal specimens: 0

Primary fossil horizon: Gradational sequence from siltstone to fine-grained sandstone

Classification of depositional environment: Channel margin

Notes: Faint bedding throughout lower siltstone and claystone; small root casts (5-10 mm diameter) within siltstone; large root casts (30-50 mm diameter) in upper siltstone; sandstones poorly sorted, contain subangular clasts, poorly indurated.

This section is laterally continuous with sections 22.27, 22.18, 22.17, 22.16, 21.04 and 22.29.



Appendix Figure 37: Section 22.29

NHM locality number: 3445

Approximate stratigraphic position: 730 m

Age: 10.2 Ma

Number of specimens: 36

Number of large mammal specimens: 36

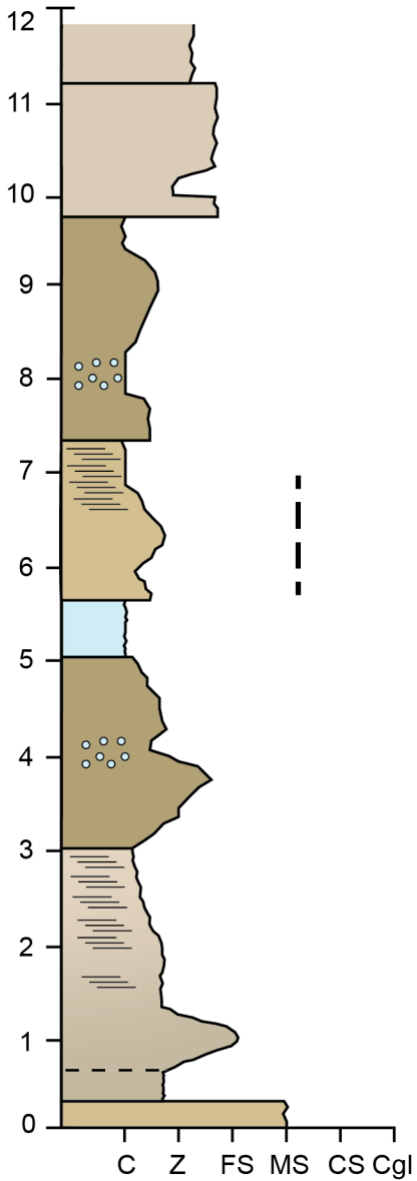
Primary fossil horizon: Clayey siltstone

Classification of depositional environment: Small channel

Notes: Abundant small root casts (5-10 mm diameter) and dispersed ash within lower siltstones; Discontinuous carbonate surfaces intermixed with root casts and dispersed ash in upper siltstones.

This section is laterally continuous with sections 22.28, 22.27, 22.18, 22.17, 22.16, and 21.04.





Appendix Figure 38: Section 22.30

NHM locality number: 5094

Approximate stratigraphic position: 610 m

Age: 10.9 Ma

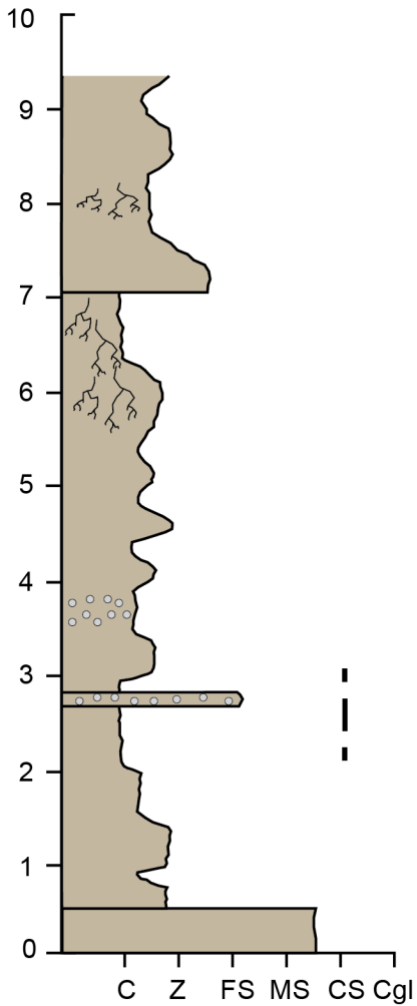
Number of specimens: 66

Number of large mammal specimens: 27

Primary fossil horizon: Siltstone to claystone

Classification of depositional environment: Poorly-drained floodplain

Notes: Prominent laminated bedding and blocky fracture within silty claystones. Ash layer at 5.1 m forms 0.5 m-thick continuous unit.



Appendix Figure 39: Section 22.31

NHM locality number: 1414

Approximate stratigraphic position: 565 m

Age: 11.0 Ma

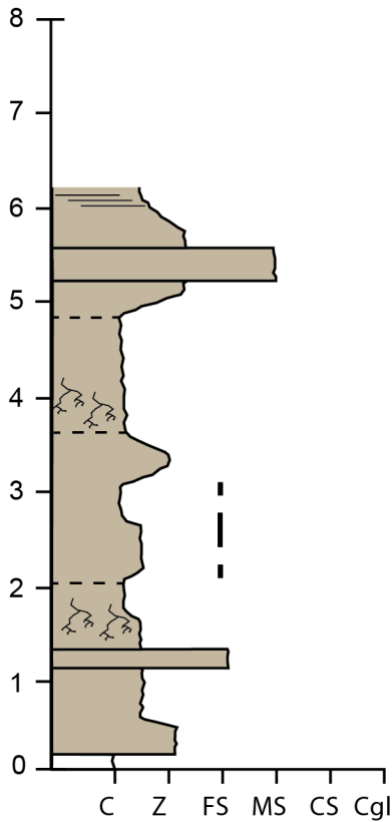
Number of specimens: 74

Number of large mammal specimens: 74

Primary fossil horizon: Claystone

Classification of depositional environment: Well-drained floodplain

Notes: Abundant root casts and prominent bedding within upper blocky clay and siltstone units; weak bedding and dispersed ash within siltstones.



Appendix Figure 40: Section 22.32

NHM locality number: 3598

Approximate stratigraphic position: 675 m

Age: 10.4 Ma

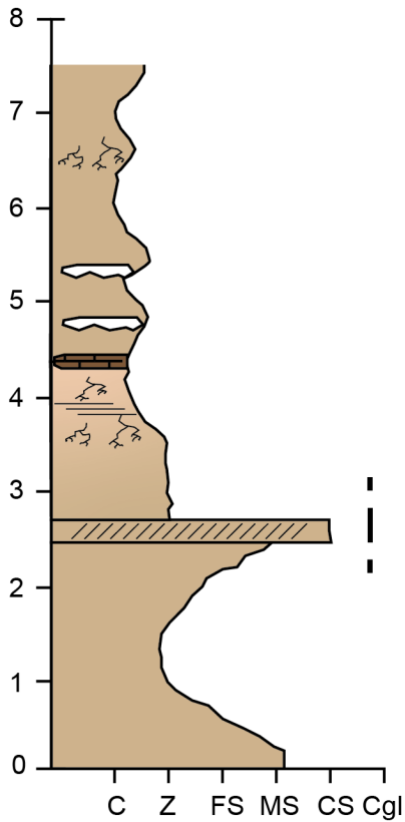
Number of specimens: 6

Number of large mammal specimens: 6

Primary fossil horizon: Gradational sequence from siltstone to claystone

Classification of depositional environment: Well-drained floodplain

Notes: Faint laminated bedding and abundant, siliceous root casts in gradational sequences; faint ash dispersed throughout lower crevasse splay deposit.



Appendix Figure 41: Section 22.33

NHM locality number: 3415

Approximate stratigraphic position: 600 m

Age: 10.2 Ma

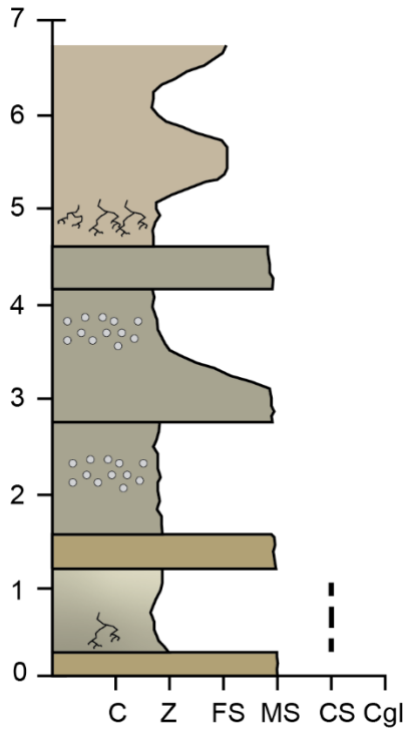
Number of specimens: 38

Number of large mammal specimens: 38

Primary fossil horizon: Siltstone, medium- to coarse-grained sandstone

Classification of depositional environment: Poorly-drained floodplain

Notes: Prominent laminated bedding and abundant siliceous root casts within silty claystone units; localized silcrete beneath several discontinuous carbonate layers; carbonaceous root casts in upper section; poor sorting in gradational sequences.



Appendix Figure 42: Section 22.34

NHM locality number: 1739

Approximate stratigraphic position: 250 m

Age: 12.4 Ma

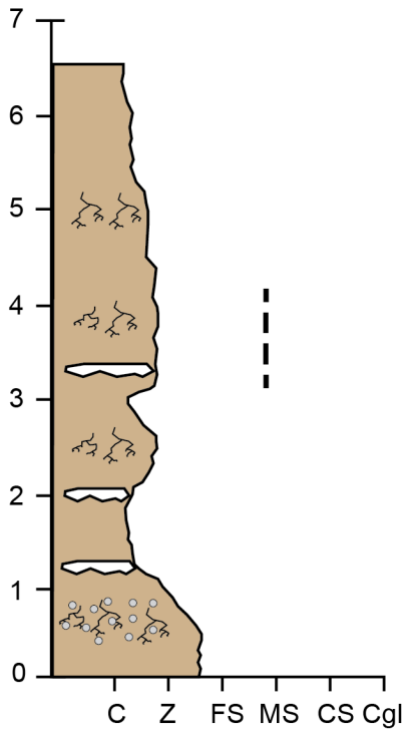
Number of specimens: 5

Number of large mammal specimens: 5

Primary fossil horizon: Siltstone

Classification of depositional environment: Channel margin

Notes: Well-indurated sandstones in upper section for ridges; fining-upward gradational sequences contain small, siliceous root casts (5-10 mm diameter).



Appendix Figure 43: Section 22.35

NHM locality number: 7543

Approximate stratigraphic position: 1125 m

Age: 8.8 Ma

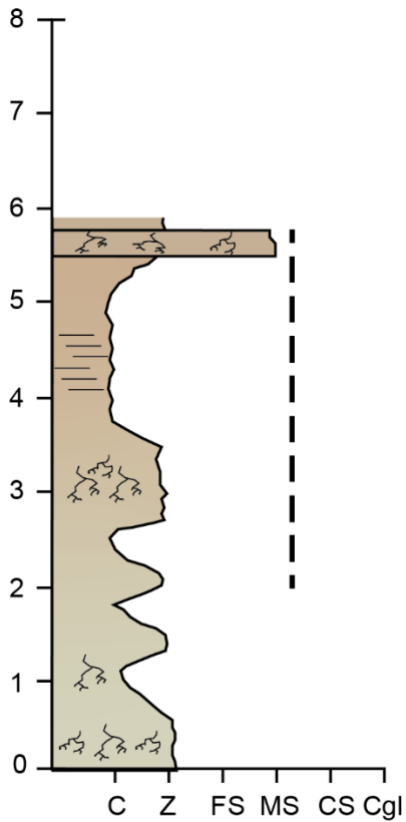
Number of specimens: 1

Number of large mammal specimens: 1

Primary fossil horizon: Siltstone

Classification of depositional environment: Poorly-drained floodplain

Notes: Abundant small siliceous root casts (5-10 mm diameter) throughout indurated beds with blocky fracture; large siliceous root casts (25 mm diameter) at 2.5 m; dispersed ash common in lowest sandy siltstone unit.



Appendix Figure 44: Section 22.36

NHM locality number: 1105

Approximate stratigraphic position: 900 m

Age: 9.6 Ma

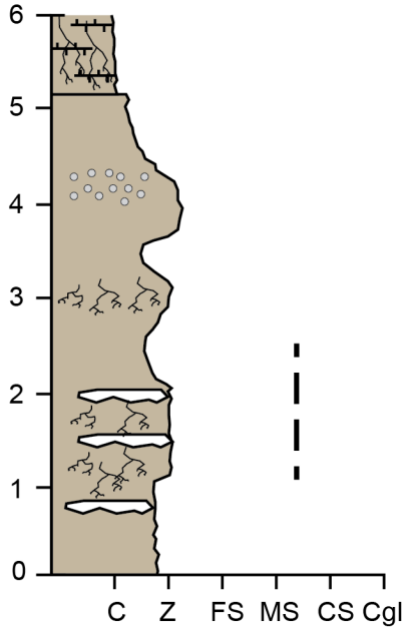
Number of specimens: 18

Number of large mammal specimens: 16

Primary fossil horizon: Siltstone to claystone

Classification of depositional environment: Poorly-drained floodplain

Notes: Abundant root casts ranging from 2-10 mm diameter throughout section; prominent laminated bedding and dispersed carbonate in upper clayey siltstone; carbonaceous root casts within upper medium-grained sandstone.



Appendix Figure 45: Section 22.37

NHM locality number: 7466

Approximate stratigraphic position: 1225 m

Age: 8.8 Ma

Number of specimens: 3

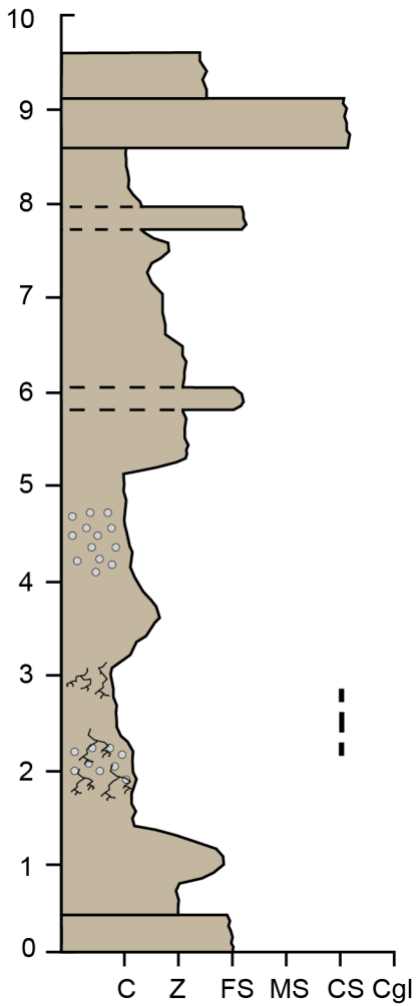
Number of large mammal specimens: 3

Primary fossil horizon: Siltstone

Classification of depositional environment: Well-drained floodplain

Notes: Abundant carbonaceous root casts interbedded with discontinuous carbonate surfaces in lower 2 m; root casts less common from 2-5 m; dispersed ash within sandy siltstone; highly indurated carbonate cap layer contains very large root casts at top of section.





Appendix Figure 46: Section 22.38

NHM locality number: 4640

Approximate stratigraphic position: 650 m

Age: 10.6 Ma

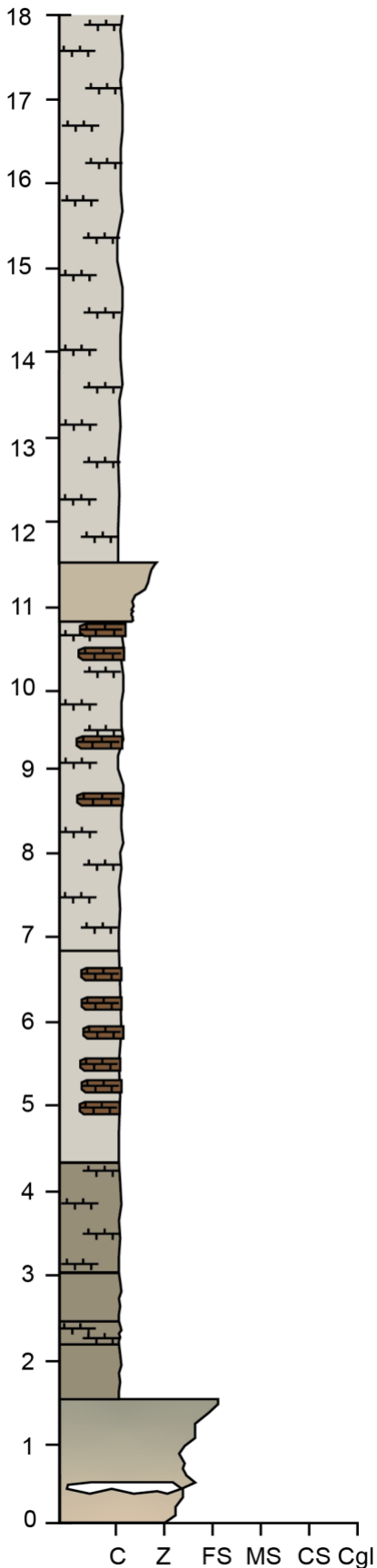
Number of specimens: 2

Number of large mammal specimens: 2

Primary fossil horizon: Claystone

Classification of depositional environment: Small channel

Notes: Abundant, small root casts (5-10 mm diameter) and dispersed ash within clayey siltstone that exhibit blocky fracture; crevasse splays form resistant beds.



Appendix Figure 47: Section 22.39

NHM locality number: 8019

Approximate stratigraphic position: 900 m

Age: 10.4 Ma

Number of specimens: 3

Number of large mammal specimens: 0

Primary fossil horizon: Unknown

Classification of depositional environment: Pond or lake deposits

Notes: Highly indurated and continuous, prominent silcretes and carbonates interbedded throughout.